STRUCTURE AND SALT TECTONICS OF MESSINIAN EVAPORITES IN THE CILICIA BASIN, EASTERN MEDITERRANEAN

COLLEEN BRIDGE

Structure and Salt Tectonics of Messinian Evaporites in the Cilicia Basin, Eastern Mediterranean

by

A thesis submitted to the School of Graduate Studies

in partial fulfilment of the requirements for the degree of

Master of Science

Earth Science Department

Memorial University of Newfoundland

January 2004

ABSTRACT

During the Oligocene to late Miocene, the Cilicia Basin evolved as a foreland basin in front of the Taurus Mountains thrust front. Over time, the regional eastern Mediterranean tectonics, the continual subsidence of the Cilicia Basin and the rapid progradational loading of the evaporite unit by sediments from the northeast end of the Cilicia Basin (the Adana Basin) have resulted in the development of three tectonic domains within the basin.

A particular type of faulting and salt tectonism characterizes each tectonic domain. The inner domain consists of salt rollers that have their distribution and lateral extent controlled by the presence of extensional growth faults at the progradational listric fault fan. The boundary domain is a zone of larger salt walls that accumulated and rose partially due to the progradational loading of evaporites, which squeezed the evaporites to the west, to the central portion of the basin. The outer domain contains a series of thrusted and non-thrusted salt anticlines and salt pillows that have arisen as a result of regional north-south contraction in the eastern Mediterranean.

Within the Cilicia Basin it is possible to delineate four major tectonic systems each system sharing a common purpose. They are:

A) The Basin-Forming Tectonic System – those faults responsible for the formation of the basin

B) Intra-Salt Gravitational Gliding Tectonic System – faults within the evaporite unit which record the change from a south tilted basin to a north tilting basin

C) Convergent Fold and Thrust Belt Tectonic System - composed of the salt structures and faults which coincide with the hypothesized presence of a basin central extensional fault near the central part of the Cilicia Basin, which acts as a buttress to southward moving sediments

D) Supra-Salt Gravitational Gliding Tectonic System - records extension related to delta progradation from the northeastern portion of the basin and the resultant contraction at the toe of the gravitationally controlled tectonic system

The migration of evaporites in the Cilicia Basin is dynamically linked to the tectonic elements internal to the basin but are also strongly linked to large-scale regional tectonic activity of the Eastern Mediterranean.

ACKNOWLEDGEMENTS

This thesis is dedicated to everyone who has ever taught me something, be it teaching me my first words, teaching me the true meaning of friendship or teaching me how to look at rocks as more than something to walk on. Your encouragement, companionship and confidence in me have been, and will continue to be, one of the most important things in my life. Without all of you this thesis would have been impossible.

Thanks for the help and assistance of all of the professors and staff at the Earth Sciences Department at Memorial University, you made that place feel like my second home! Financial support from the departments of Earth Sciences and Graduate Studies at Memorial University as well as from the Atlantic Accord Career Development Program is gratefully acknowledged.

Academic support from my thesis supervisory committee, Ali Aksu, Tom Calon and Jeremy Hall is greatly appreciated and forever remembered. I couldn't have found a better source of information and technical assistance anywhere. Their constant support allowed me to get through the tough times and let me see that there is (finally) some light at the end of the tunnel. I couldn't thank you enough.

I'd particularly like to thank Ali Aksu who so many years ago (I'm afraid to think of how many) offered me an honours thesis project and changed my world forever. Boss, because of you I've had some of the greatest years of my life! Your jokes, great conversations and amazing personality have made it all bearable and will be an inspiration to me for many years to come.

Last, but definately not least, I'd like to thank my family who provided countless rides to and from the university at all hours, who listened to all my worries and troubles,who constantly supported me in anything I did and who have always showed me who I could be and helped me to be that person. You guys are the best!

LIST OF FIGURES

1. INTRODUCTION

The Cilicia Basin is nestled between the southern coast of Turkey and the northern coast of Cyprus in the Eastern Mediterranean Sea (Fig. 1-1). It holds an upper Miocene (Messinian) evaporite sequence that has been influenced by the Miocene to Recent tectonic activity in the region. Two tectonic events, of particular importance to the Cilicia Basin, are i) a protracted episode of regional north-south shortening associated with the collision of Eurasia and Africa, and ii) more local tectonic activity in basinal areas related to gravitational collapse above a regional salt detachment. Located in an area of complex, active micro plate tectonics, the Cilicia Basin provides an ideal site for the study of salt tectonics.

The Messinian evaporite sequence that is found in the Cilicia Basin also lies beneath the seafloor of the entire Mediterranean Sea. Despite this fact, little work has been completed on the salt tectonics of the Mediterranean Basin and much less has been completed on the salt tectonics of the Cilicia Basin. Most previous studies in the Mediterranean region focused on the processes leading to deposition of evaporites rather than the changes that have occurred since then (eg. Hsü et al., 1973, Ryan et al., 1973, Ben-Avraham et al., 1995, Clauzon et al., 1996). However, some preliminary studies reporting on the structural, salt tectonic and sedimentological activity within the Eastern Mediterranean Basins since evaporite deposition have been completed by authors such as Mulder (1973), Mulder et al. (1975) and Woodside (1976, 1977). These reports attempt to place structural, salt tectonic and sedimentological observations made during various seismic surveys into the regional and tectonic framework of the Eastern Mediterranean.

Despite the scarcity of works on the salt tectonics of the Eastern Mediterranean, a great deal of literature exists on topics such as factors which initiate salt tectonics, the behaviour of evaporites under various sedimentary and tectonic stresses (extension and compression, gravitational loading, etc.), and the relationship existing between these stresses and the geometry and styles of diapirism. This information will be applied to the Cilicia Basin evaporites in an attempt to understand the salt tectonic history of the basin.

1.1 Plate Tectonic Setting

The easternmost Mediterranean Sea is located in a critical area of complex plate interactions where a pervasive collision of the Eurasian and African plates (via the Syrian-Arabian Microplate) has been taking place for the last ~ 5 Ma (Fig. 1-2). The plate convergence, which ultimately caused this continent-continent collision, began in the Cretaceous and continued into the Pliocene and Quaternary. The Aegean-Anatolian Microplate plays an important role in shaping the architecture of this collisional margin as it becomes rotated, wedged and squeezed while escaping westward from the converging larger plates. The boundaries between the various plates and microplates constitute the principal tectonic elements of the Eastern Mediterranean region. These plate boundaries are the North Anatolian Fault Zone, the East Anatolian Fault Zone, the Cyprean Arc and associated arc segments and the Dead Sea Fault Zone (Fig. 1-2). Movements occurring at the plate boundaries, along these major fault zones, are responsible for the complex collisional tectonics of the region.

The initial collision of the Eurasian and African Plates occurred via the Syrian-

Arabian Microplate (Fig. 1-2). The Syrian-Arabian Microplate is not a part of the African Plate but rather meets the African Plate along a major sinistral fault zone, the Dead Sea Fault Zone. Invertebrate paleontology established that the first connection between Eurasia and Africa occurred at the Bitlis Suture via the Syrian-Arabian Microplate in the Burdigalian (Görür et al., 1998). After this collision, the Syrian-Arabian Microplate and African Plate continued to move northward, increasing the region of plate contact.

The eventual collision between the Syrian-Arabian and Aegean-Anatolian microplates occurred at the Bitlis-Zagros suture in southeastern Turkey (Fig. 1-3). The collision between these two microplates initiated the westward escape of the Aegean-Anatolian Microplate along the East Anatolian and North Anatolian Fault Zones. The westward movement of the Aegean-Anatolian Microplate was accompanied by a counter-clockwise rotational spin, which was likely established because of the influence of the curved trace of the North Anatolian Fault Zone on the rhombohedral Aegean-Anatolian Microplate (Şengör et al., 1985). The East Anatolian Fault Zone, the more southerly of the two fault zones allowing the tectonic escape of the Aegean-Anatolian Microplate, is a sinistral transtensional fault zone that forms the plate boundary between the Syrian-Arabian and Aegean-Anatolian microplates. This fault zone terminates at a complex triple point junction where it connects with the Dead Sea Fault Zone and Amanos Fault; a segment of the Cyprean Arc system (Perinçek and Çemen, 1990) (Fig. 1-3).

While the Syrian-Arabian Microplate collides with the Eurasian Plate, the African Plate subducts beneath the southern margin of the southwestward moving Aegean-Anatolian Microplate. This collision occurs along a large approximately west-east

trending arc complex consisting of, from west to east: the Hellenic Arc, the Pliny-Strabo Trench, the Florence Rise and Cyprean Arc (subduction arcs), the West Tartus Ridge, the Nahir El Kebir Fault, the Amik Transfer Zone and the Amanos Fault. The eastern portion of this subduction arc complex has a clearly arcuate trace until it reaches the Florence Rise. West of the Florence Rise, in the region of the Anaximaxander Seamounts, the Pliny-Strabo Trench offsets the remainder of the arc complex to a position just southeast of the Greek island of Crete (Fig. 1-2).

North of, and parallel to, the Cyprean Arc are three features that mimic the curvature observed at the Cyprean Arc. These features are i) the Misis-Kyrenia Lineament and its onland continuations, the Misis Mountains of southeastern Turkey and the Kyrenia Range in northern Cyprus, ii) the Cilicia-Adana Basin, in particular the present-day basinal portion, the Cilicia Basin, the focus for this study, and iii) the Taurus Mountains of southern Turkey. These three arcuate features constitute the study area for this thesis (Fig. 1-3).

The Misis-Kyrenia Lineament is a positive bathymetric anomaly on the seafloor of the Eastern Mediterranean that extends from the Kyrenia Range at the northern tip of Cyprus towards the Misis Mountains in southeastern Turkey (Fig. 1-4). This lineament defines the limits of the Misis-Kyrenia Fault Zone, a transtensional fault zone observed along the Misis-Kyrenia Lineament. This lineament effectively separates the Cilicia Basin in the north from the Latakia and Iskenderun Basins to the south (Fig. 1-4).

The Cilicia-Adana Basin lies immediately north of the Kyrenia Range, Misis-Kyrenia Lineament and the Misis Mountains. Detrital sediments transported by the

Ceyhan, Seyhan and Tarsus rivers flowed into the northeastern end of the Cilicia-Adana basin filling it with sediment. The filled part of the basin is referred to as the Adana Basin; the unfilled portion is known as the Cilicia Basin (Fig. 1-4). The Cilicia Basin has been divided into two distinctive sections based on a marked contrast in physiographic characteristics and structural styles The northeast-southwest trending, eastern portion of the Cilicia Basin is referred to as the inner Cilicia Basin; the west portion of the Cilicia Basin, having an east-west trend is referred to as the outer Cilicia Basin. The outer Cilicia Basin is deeper than the inner basin as indicated on bathymetric charts of the region (Fig. 1-4). It was originally thought that the evaporites were restricted to the deeper part of the Cilicia Basin (outer Cilicia Basin) and were absent from the inner, shallower part of the basin (Mulder, 1973). Later work showed that the evaporite unit was present in the inner basin as well as the outer basin (Aksu et al., 1992 a).

The Cilicia Basin presently occupies a fore-arc setting with respect to the Cyprean Arc. This basin developed during the Oligocene to early Miocene as part of a larger foreland basin. This foreland basin was composed of the present-day Cilicia and Adana Basins and extended south over the then buried Kyrenia Terrane of Cyprus. The eventual exhumation of the Kyrenia Terrane and the Misis-Kyrenia Lineament divided the ancestral basin into a north Cilicia-Adana Basin and a southern Mesaoria Basin.

The Taurus Mountains in southern Turkey rim the northern edge of the Cilicia Basin (Fig. 1-4). These mountains largely formed during the Oligocene (Rögl et al., 1978) as an initial consequence of the north-south shortening phase that later resulted in the collision of the Eurasian and Syrian-Arabian Microplates. The uplift and subsequent

erosion of the Taurus Mountains was the source for large quantities of detrital sediment that fed the Seyhan, Ceyhan and Tarsus rivers (Aksu et al., 1992a) and contributed to the progradational infilling of the Adana Basin.

Few published works describe the salt tectonics of the Cilicia Basin in any detail. The early publications in the Cilicia Basin deal with the initial seismic imaging of the salt structures in the basin and the definition of any preferred orientations of these structures (eg. Mulder, 1973; Mulder et al., 1975; Woodside 1976, 1977; Smith, 1977 and Evans et al., 1978). Two more recent papers (Aksu et al., 1992 a and b) concentrate on the Quaternary sedimentary history and the architecture of the inner Cilicia Basin. The most in-depth description of the structural and sedimentological features of the Cilicia Basin is covered in two papers by Calon et al. (in prep.) and Aksu et al. (in prep.). The completed work is purely descriptive and outlines some of the major structural and sedimentary characteristics and trends observed in the Cilicia Basin. To date, no work has been completed on the salt tectonic activity of the Cilicia Basin and its association with the regional tectonic framework of the Eastern Mediterranean.

1.2 Evaporite Deposition in the Mediterranean Region

The Messinian was a time of great change in the Mediterranean. The collision and suturing of the of the African Plate (Syrian-Arabian Microplate) and the Eurasian Plate at the Bitlis-Zagros Suture closed the gateway between the Mediterranean Sea (the Neo-Tethys Ocean) and the and the Indo-Pacific Ocean (Panthalassa) (Fig. 1-5). The closure of this gateway resulted in a much drier Mediterranean climate and the eventual

evaporation of the Mediterranean Sea known as the Messinian Salinity Crisis (Hsü et al., 1973, Clauzon et al., 1996). A ~2000 m thick evaporite unit that is found beneath the seafloor in the deepest portions of the Mediterranean Basin suggests that an amount of seawater ~ 40 - 150 times the volume of the present-day Mediterranean Sea was required to create the thickness of evaporites found in the region. The western outlet to the Atlantic Ocean, the Strait of Gibraltar (Fig. 1-5), facilitated the deposition of the thick evaporite unit as it periodically opened, allowing for the intermittent refilling of the Mediterranean Basin (Hsü et al., 1973).

The evaporites in the Mediterranean were first discovered during Leg 13 of the Deep Sea Drilling Project (DSDP; Ryan et al., 1973). The shipboard scientific crew had a difficult time comprehending and explaining how a thick evaporite unit could be deposited over such a great area of the Mediterranean. Many theories were proposed to explain the presence of these evaporites; however, the prevailing and most readily accepted theory involves many complete evaporations of the entire Mediterranean Basin.

It is still quite difficult to believe that the entire Mediterranean could evaporate completely and the Mediterranean sea level could drop ~3000 m below its present level. Considering the fact that the Mediterranean Sea has a present area of 2.5 million km^2 and a water volume of 3.7 million km^3 (Hsü et al., 1973), it is no surprise that there was much resistance to this theory.

The large-scale desiccation theory proposed by the DSDP shipboard scientific crew inspired and initiated numerous studies in the Mediterranean Sea. Much of this work provided new evidence to further support the desiccation theory. The detection of

deep-sea canyons along the marginal areas of the present-day Mediterranean Sea shows that ancient river channels fed a very shallow Mediterranean Sea during the Messinian Salinity Crisis (Chumakov, 1973; Clauzon, 1978, 1982; Barber, 1981). The discovery of the true magnitude of the evaporite unit (greater than two kilometers thick) in central portions of the Mediterranean Sea provided more support for the theory of desiccation. The large volumes of seawater calculated as a requirement for the deposition of such great thicknesses of salt in the Mediterranean necessitated many episodes of desiccation of the Mediterranean Basin, strongly supporting the desiccation theory.

Despite the vast amount of research into the origin of the evaporites, great debate still exists about exactly how the evaporites were deposited. In fact, endless models have been proposed to explain the origin and process of evaporite deposition in the Mediterranean.

1.2.1 Models of Evaporite Deposition

Numerous models have been proposed for the setting of evaporite deposition in the Mediterranean: the shallow basin - shallow water model (Nesteroff, 1973), the deep basin - deep water model (Schmalz, 1969), the deep basin - shallow water model (also known as the desiccated deep basin model) (Hsü et al., 1973), and various models which attempt to combine various aspects of these models into one.

Hsü, Cita and Ryan proposed the original "Salinity Crisis" theory of evaporite deposition after Leg 13 drilling of the Deep Sea Drilling Program (DSDP) in 1972. According to Hsü et al. (1973), deep marine sediments below, above and within the

evaporite sequence proves that the Mediterranean Basin was a deep basin during the Middle and Late Miocene. Minerological, petrographical, sedimentological and geochemical data suggested that the evaporites, deposited during the latest Miocene (Messinian), were deposited in shallow waters or subaerially in a sabkha-like environment (Ryan et al., 1973). The depositional sequences within evaporite cores from Leg 13, Site 124 of the DSDP showed a cycling pattern of inundation or flooding followed by desiccation. Oxygen isotope data of Fontes et al. (1972) and Hsü et al. (1973) shows that the wide range of oxygen isotope values for Mediterranean evaporites is similar to the range observed in known playa lake (sabkha) deposits and quite unlike the narrow range of oxygen isotopic values characteristic of marine evaporites (Fig. 1-6). These combined findings show that there were periods of both deep-water sedimentation and shallow subaerial sedimentation during the deposition of the Messinian evaporite sequence.

The pattern of evaporite distribution within a basin depends on the geometry of the basin. Isolated basins tend to form a 'bulls-eye' pattern of evaporites with the least soluble salts (eg. carbonate) precipitating first to form an outer ring with salts of increasing solubility being deposited inwards toward the center of the basin (ie. anhydrite and halite) (Fig. 1-7). In basins that are not isolated a tear-drop pattern of evaporite distribution is observed with carbonates depositing near the opening to the basin while anhydrite and halite are deposited at the distal end of the basin, away from the opening (Fig. 1-8). Studies of the pattern of evaporite deposition within individual Mediterranean basins showed that most evaporites displayed a bulls-eye evaporite distribution pattern

(Hsü et al., 1973) typical of isolated basins rather than tear-drop shaped patterns common in partially restricted basins.

Geomorphological studies of Mediterranean basins also supported the shallow subaerial deposition of evaporites. If a very shallow pool of water covered the Mediterranean Basin, river systems would have to cut down through the present-day continental shelves and slopes to reach the flat-bottomed playas at Messinian sea level 2000 to 3000 meters below present-day sea level. Channels and canyons from these river systems have been documented in southern France, Italy, Corsica, Sardina and North Africa by Chumakov (1973), Clauzon (1978, 1982), and Barber (1981) (Fig.1-9).

In the deep basin - shallow water model, Hsü et al. (1973) suggested that a deep Mediterranean Basin existed in the middle to late Miocene. This basin became isolated from Indo-Pacific seawater following the collision and suturing of Eurasia and Africa (Syrian-Arabian Microplate). Atlantic Ocean seawater input was periodically closed off at the Strait of Gibraltar. The Mediterranean began to shallow, eventually desiccating and depositing evaporites in salt lakes (playas) and sabkhas during the Messinian. The Strait of Gibraltar repeatedly opened during the Messinian to allow the Mediterranean Basin to refill, then closed to facilitate evaporation of seawater and desiccation. This continued evaporation of seawater permitted the formation of an evaporite unit which reached a maximum thickness of ~2 km.

As with any theory, the passage of time provides evidence that does not fit the original theory. For example, data from foraminifera and coral reefs in marginal Mediterranean basins suggests evaporites were deposited under open-marine conditions

(Rouchy and Saint-Martin, 1992). These evaporites deposited at entirely different elevations than the majority of the Mediterranean basins and at an earlier time than that in other areas of the Mediterranean (Clauzon et al., 1996). When evidence that contradicts components of the original theory is presented, modifications are made to the original theory and new models are proposed. One such model, put forward by Clauzon et al. (1996) attempts to satisfy much of the conflicting data related to the "Messinian Salinity Crisis" by proposing a multi-stage model. This model suggests that two distinct and successive phases of evaporite deposition occurred in two different types of basins (Fig. 1-10). The first phase of evaporite deposition occurred ~ 5.75 to 5.60 ma and consisted of a cooling period followed by a minor fall in sea level. Only marginal basins of the Mediterranean underwent evaporite deposition at this time (satisfying those who believe in a shallow basin-shallow water deposition of evaporites). A second phase of evaporite deposition occurs from 5.60 to 5.32 ma following a period of warming. The global sea level was high at the time; however the Mediterranean was isolated and underwent a major drop of ~ 1500 - 3000 m. During this time, the main part of the Mediterranean Basin experienced evaporite deposition while large channels (present-day deep sea canyons) were cut into the continental shelves and slopes as rivers incised their valleys to accommodate the lowering base level. The water from these channels and intermittent seawater influxes from Strait of Gibraltar replenished the desiccating Mediterranean Sea (as described by the deep basin - shallow water model). Continuing evaporation of the seawater resulted in the build-up of the thick Messinian evaporite unit that is observed in DSDP and ODP drill holes throughout the Mediterranean Sea.

The bathymetry of the Eastern Mediterranean is such that the seafloor of the Cilicia Basin is at a higher elevation than that of the main part of the Eastern Mediterranean seafloor (Fig. 1-4 and Fig. 1-5). Small variations in the Messinian sea level would affect the central portion of the Mediterranean Basin, but would have no influence on the 'elevated' Cilicia Basin. The > 2 km thick evaporite sequence observed in central portions of the Mediterranean basin would not be expected in the Cilicia Basin as it would not benefit from any partial refilling the Mediterranean might undergo.

The Cilicia Basin presently has an eastward tilted seafloor with the inner portion of the basin being at a higher elevation than the outer part of the basin (Fig. 1-4). If this were also the case during the Messinian then a small rise in sea level may only affect the outer Cilicia Basin and not the inner basinal region. A comparison between evaporite characteristics (composition, thickness etc.) in the inner and outer Cilicia Basin would be able to confirm or disprove this hypothesis. Unfortunately, well data in the Cilicia Basin is available only in the innermost basinal area.

Rivers such as the Göksu, Tarsus, Ceyhan and Seyhan that flow into the present-day Cilicia Basin (Fig. 1-4) may have provided freshwater input to the basin at times when the sea level was above the level of the seafloor of the Messinian Cilicia Basin. If the sea level were to fall below the Messinian seafloor these rivers would flow out of this basin and into the deeper Mediterranean Basin. It is conceivable that channels exist along the ancient margins of the Cilicia Basin, having been carved out as rivers flowed into the lower basinal areas during the Messinian. These channels may have cut into the evaporite unit or its enveloping sedimentary cover or sedimentary basement in the past. Present day

bathymetry maps of the Cilicia Basin show the presence of what appears to be incised channels in the inner basin that may have formed in response to subsea currents that originally flowed down pre-existing canyons in the basin.

Studies by Biju-Duval et al. (1978) showed that the Misis-Kyrenia Lineament had been elevated since at least the latest Miocene, shutting off access to seawater at the eastern end of the Cilicia Basin (except in cases where sea level rise was sufficient to inundate the Misis-Kyrenia Lineament and reach the Cilicia Basin). Small seawater-filled depressions would become isolated mini-basins should the sea level fall below the level of the seafloor of the Cilicia Basin. The presence of a lip or ridge at the western end of the basin would increase the maximum size the basin could reach and still become isolated from the main part of the Mediterranean (Fig. 1-11). Evaporites in the basin would display the bulls-eye pattern of evaporite distribution, which is typical of an isolated basin. Some uncertainty arises when hypothesizing the distribution of evaporites in the outermost regions of the Cilicia Basin because it is unclear whether the basin was open to the west during the Messinian or if it was partially closed (or entirely closed during low sea-level) by the Aksu-Kyrenia Lineament and the Anamur-Kormakiti High. The absence of well data from these parts of the Cilicia Basin only increases this uncertainty.

A tear-drop pattern of evaporite distribution may also be possible in the Cilicia Basin. If sea level was slightly above the Cilicia Basin seafloor, portions of the inner basin would have been aerially exposed and seawater would flow into the Cilicia Basin at its western end. The basin would no longer be isolated and therefore would not reflect the

bulls-eye pattern of evaporites observed in an isolated basin. Instead, the basin may display a tear-drop pattern of evaporite distribution characteristic of a basin that is only partially restricted, having an opening at one end (Fig. 1-12).

1.2.2 Evaporite Composition and Character

Well data from the Adana Basin and the easternmost (inner) Cilicia Basin show that the evaporite deposits in this area consist of a lower gypsum and anhydrite unit overlain by a thicker halite unit (Yalçın and Görür, 1984). These evaporites are similar to those found throughout the entire Mediterranean during various legs of the Deep Sea Drilling Project (DSDP) and Ocean Drilling Project (ODP).

Initial reports of Leg 42A of the DSDP suggest that several environments could account for the deposition styles of Mediterranean evaporites (Garrison et al., 1978). The composition and depositional environment of evaporites in the Cilicia Basin are expected to be similar to those observed elsewhere in the Mediterranean. The Cilicia Basin should exhibit some or all of the evaporite characteristics observed during Leg 42A of the DSDP. A brief summary of the evaporites at the Mediterranean DSDP sites of Leg 42A (Fig. 1-13) and the interpreted depositional environments are outlined below.

Site 371 is located on the southern edge of the Balearic Abyssal Plain (Fig. 1-13). Coring in this location found 2 m of nodular to laminated anhydrite above 2 m of dolomitic mudstone. The anhydrite in the cores displayed 3 dominant forms; laminated and bedded anhydrite, bedded mosaic to nodular mosaic anhydrite and "chicken wire" mosaic anhydrite (Garrison et al., 1978). The nodular style anhydrite found at this site is

quite similar to that in the Persian Gulf sabkha environments. The dolomitic mudstone is typical of shallow subaqueous deposition. The resulting interpretation of the depositional environment of these sediments is that of a prograding Sabkha (Garrison et al., 1978).

At Site 372 (Fig. 1-13; East Menorca Rise) the evaporites are predominantly composed of laminated gypsum, with some nodular gypsum, bounded at top and bottom by dolomitic marls. Sedimentary structures within the laminated gypsum, such as repeating cycles of cross bedding, ripple marks, and rip-up breccias, form the basis of the interpretation of the depositional environment. Garrison et al. (1978) interpreted these deposits as very shallow water evaporites in flat or lagoonal environments with intermittent subaerial exposure. The repetition of the sedimentary structures in the core led them to believe that the area was periodically exposed to storm-like events.

In the Ionian Sea (Site 374; Fig. 1-13) sediments are composed of dolomitic mud and mudstone, cyclically bedded mudstone and laminated gypsum as well as layered to nodular anhydrite and halite. The dolomitic mud and mudstone were interpreted to have formed in a subaqueous environment; gypsum and mudstone cycles were interpreted as a shallow subaqueous to subaerial evaporite flat; the nodular anhydrite and halite was interpreted as a sabkha environment (Garrison et al., 1978).

In the Florence Rise (Site 376; Fig. 1-13) the evaporites consist of two main groups, i) gypsum with interbeds of clastics and marlstones and ii) coarse recrystallized halite, nodular to laminated white anhydrite with enterolitihic folds and chicken wire textures, and banded halite. These evaporites have been interpreted as shallow subaqueous (gypsum and marlstone) to sabkha (halite and nodular anhydrite) deposits.

The evaporites are overlain by marlstones with turbiditic interbeds that have been interpreted as an alternation of hemipelagic sediment and turbidites (Garrison et al., 1978).

In the North Cretan Basin (Site 378; Fig. 1-13) coarse selenitic gypsum was the main evaporite lithology suggesting a shallow subaqueous depositional setting. Dolomitic caliche was also retrieved at Site 378, formed by partial diagenesis in a subaerial environment (Garrison et al., 1978).

The wells drilled in the easternmost end of the Cilicia Basin (Karataş and Seyhan; Fig. 1-13) show that the composition of the evaporites was a combination of gypsum and anhydrite with halite. The evaporites in the Cilicia Basin could therefore have the same depositional characteristics or depositional environments interpreted for the DSDP evaporites.

1.3 Scientific Objectives

The main scientific objectives of this thesis are:

1. to analyze the distribution of evaporites in the present-day Cilicia Basin and determine what this distribution means in terms of the morphology (size and shape) and bathymetry of the pre-Messinian basin,
2. to provide a cursory evaluation of the maturity of salt structures in the Cilicia Basin,
3. to map fault assemblages and salt bodies in the Cilicia Basin
4. to study the placement and orientation of tectonic elements in the Cilicia Basin

and identify various tectonic systems which may be able to explain this arrangement

5. to suggest a process by which the tectonic systems identified in the Cilicia Basin could have developed and evolved within the tectonic framework of the Eastern Mediterranean region.

Figure 1-1: Location of the Cilicia Basin, Eastern Mediterranean

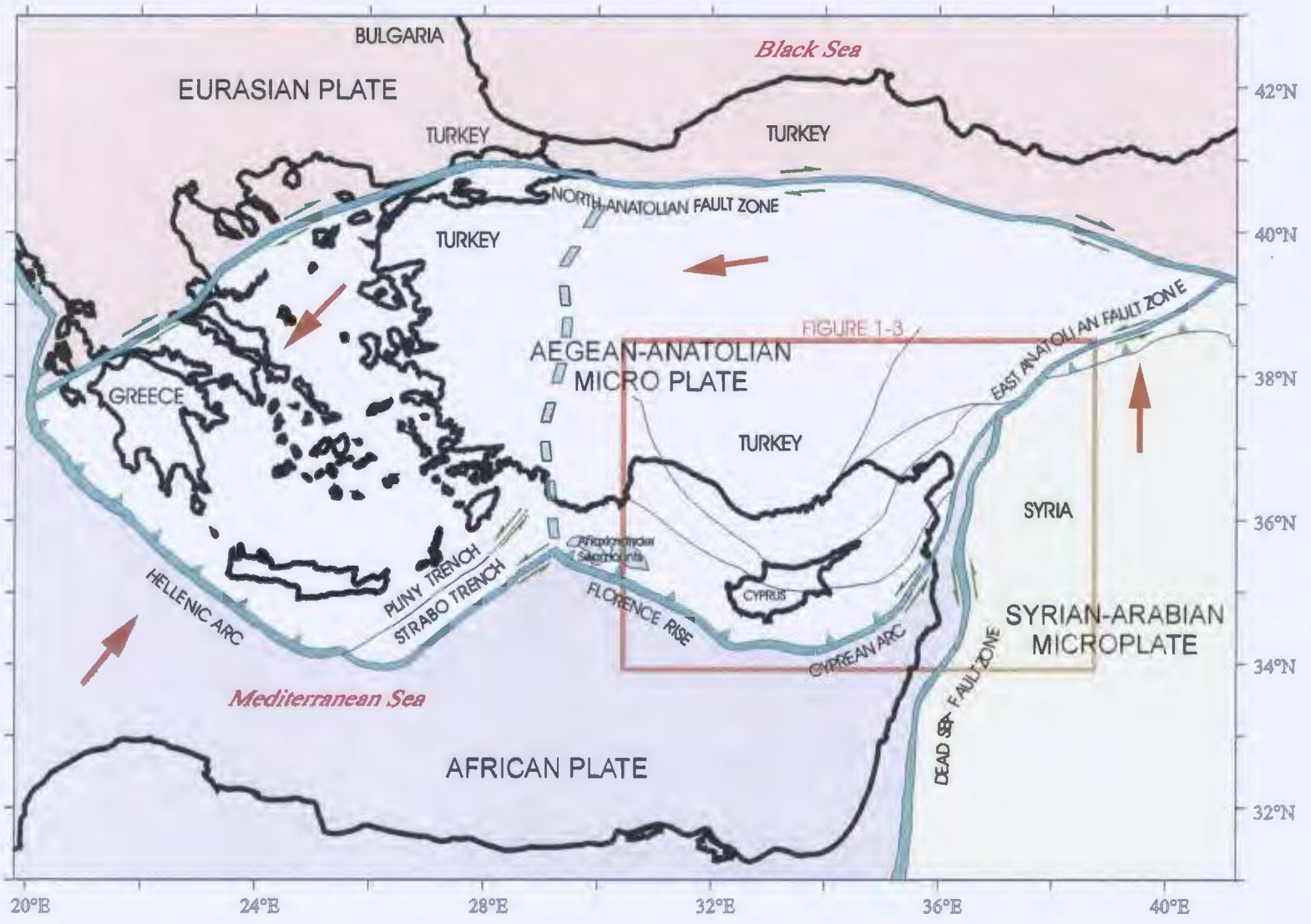

Figure 1-2:Plate tectonic map of the Eastern Mediterranean region showing plates, major fault zones and plate movement directions (Modified from Aksu et al., 1992a).

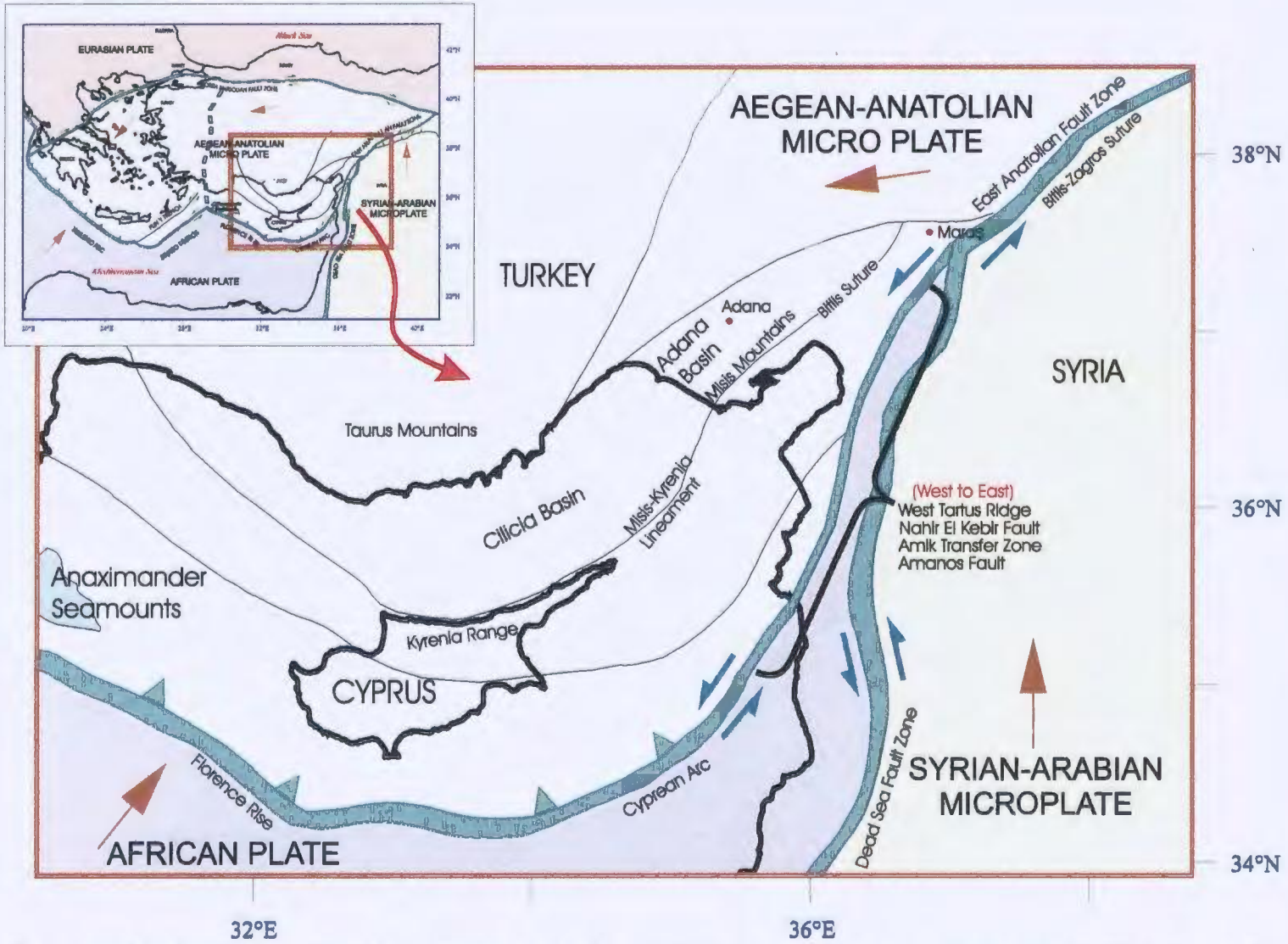

Figure 1-3: Plate tectonic map of the Cilicia Basin study area showing plates, major fault zones and plate movement directions (Modified from Aksu et al., 1992a).

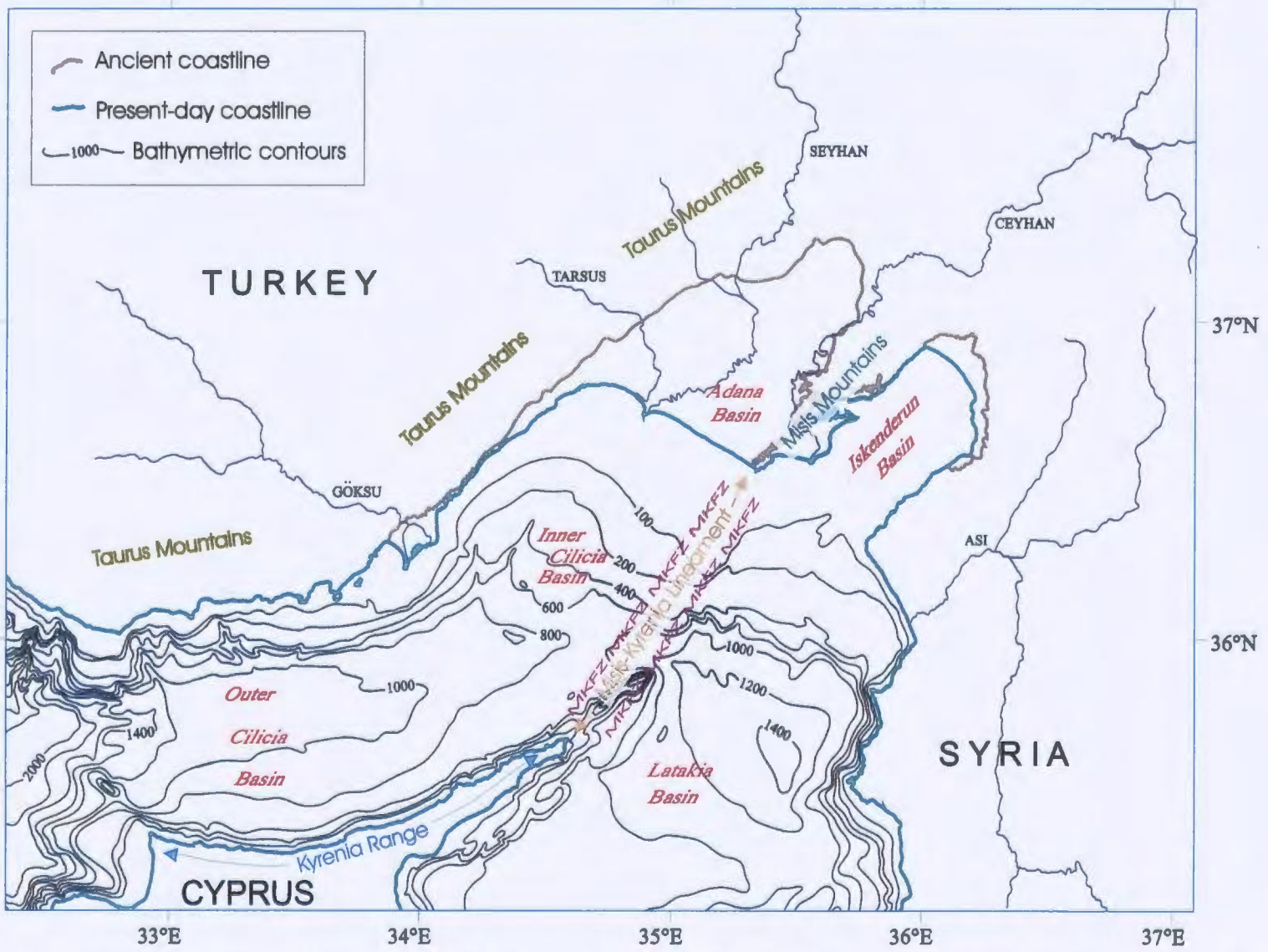

Figure 1-4: Bathymetry map of the Cilicia Basin (MKFZ=Misis-Kyrenia Fault Zone) showing major tectonic features (modified from Aksu et al., 1992a).

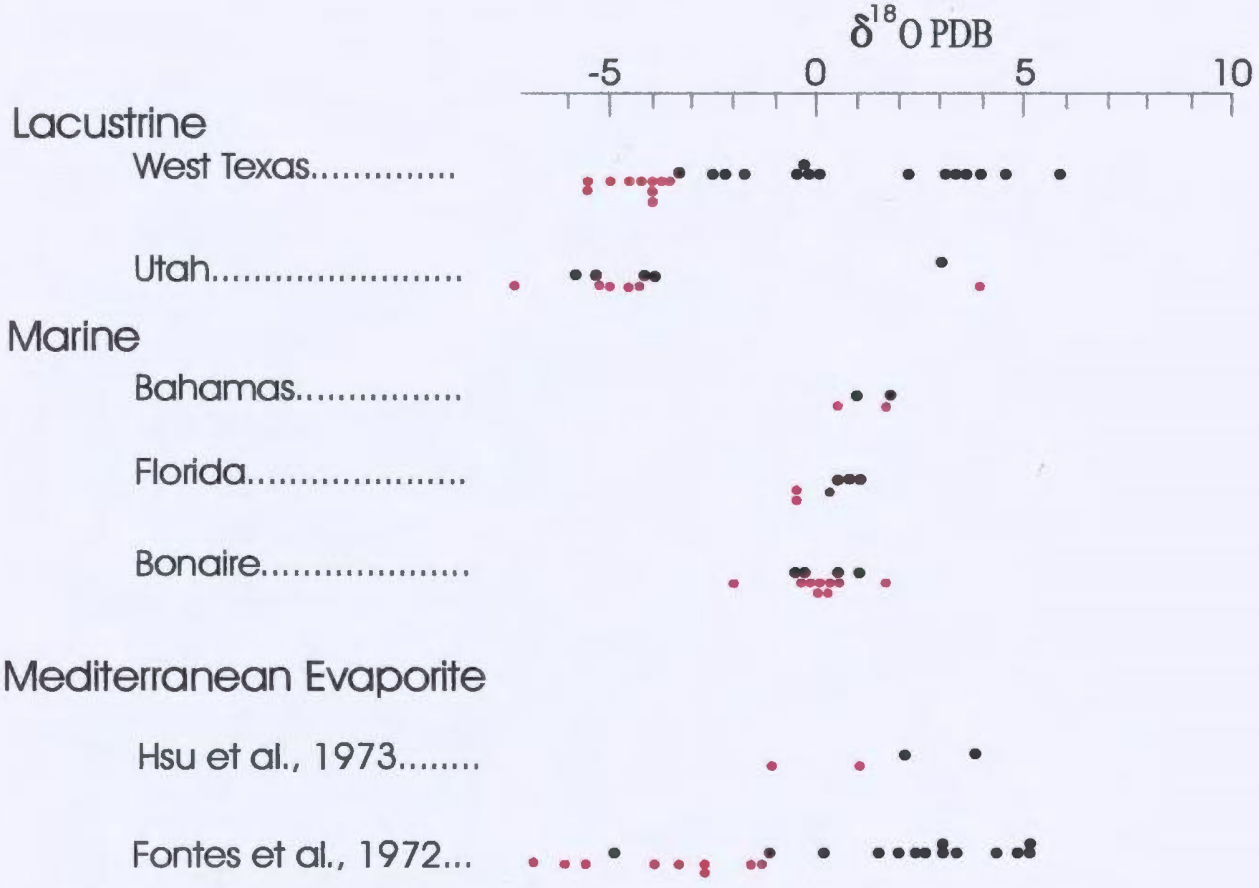

Figure 1-6: Oxygen isotope range of the Mediterranean evaporites compared to marine and playa (lacustrine) evaporites. • =dolomite; • =calcite (Hsu et al., 1973).

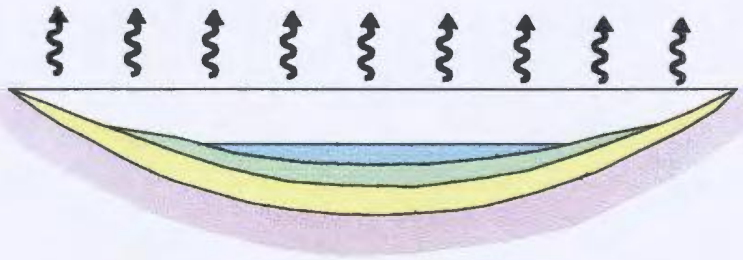

a) cross section

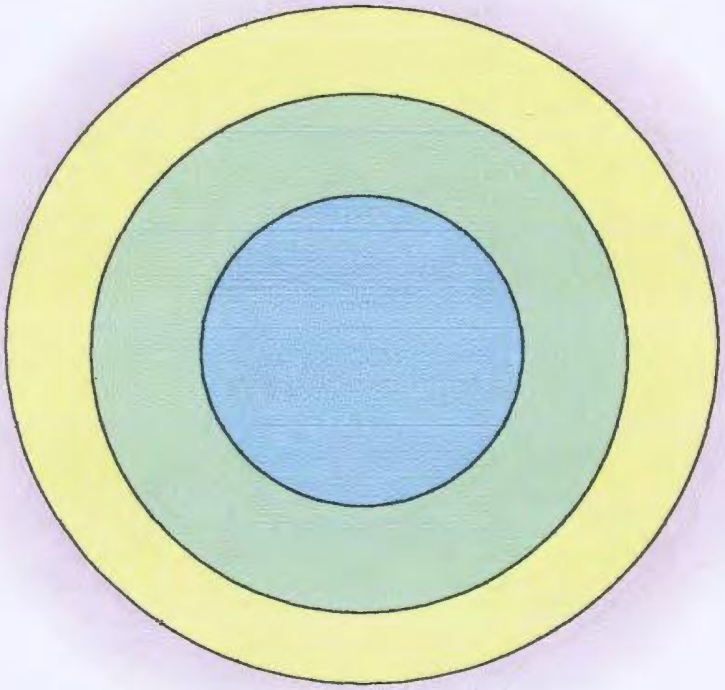

b) map view

Figure 1-7: Idealized bull's eye pattern of evaporite distribution typical of isolated basins. Yellow = carbonates; green = gypsum; blue = halite. (After Hsu et al., 1973)

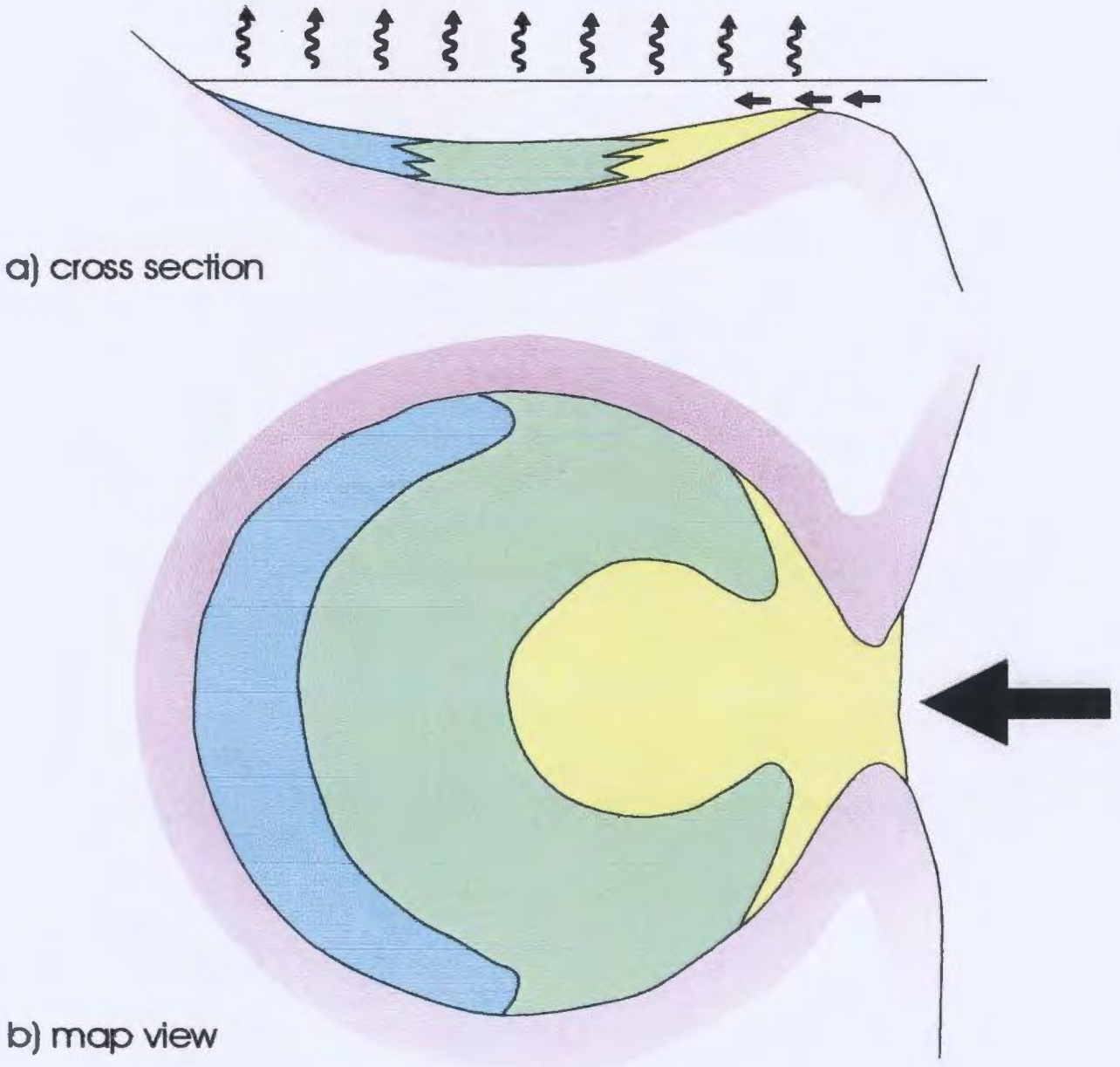

Figure 1-8: Idealized tear drop pattern of evaporite distribution typical of partially restricted basins. Yellow = carbonates; green = gypsum; blue = halite. (After Hsu et al., 1973)

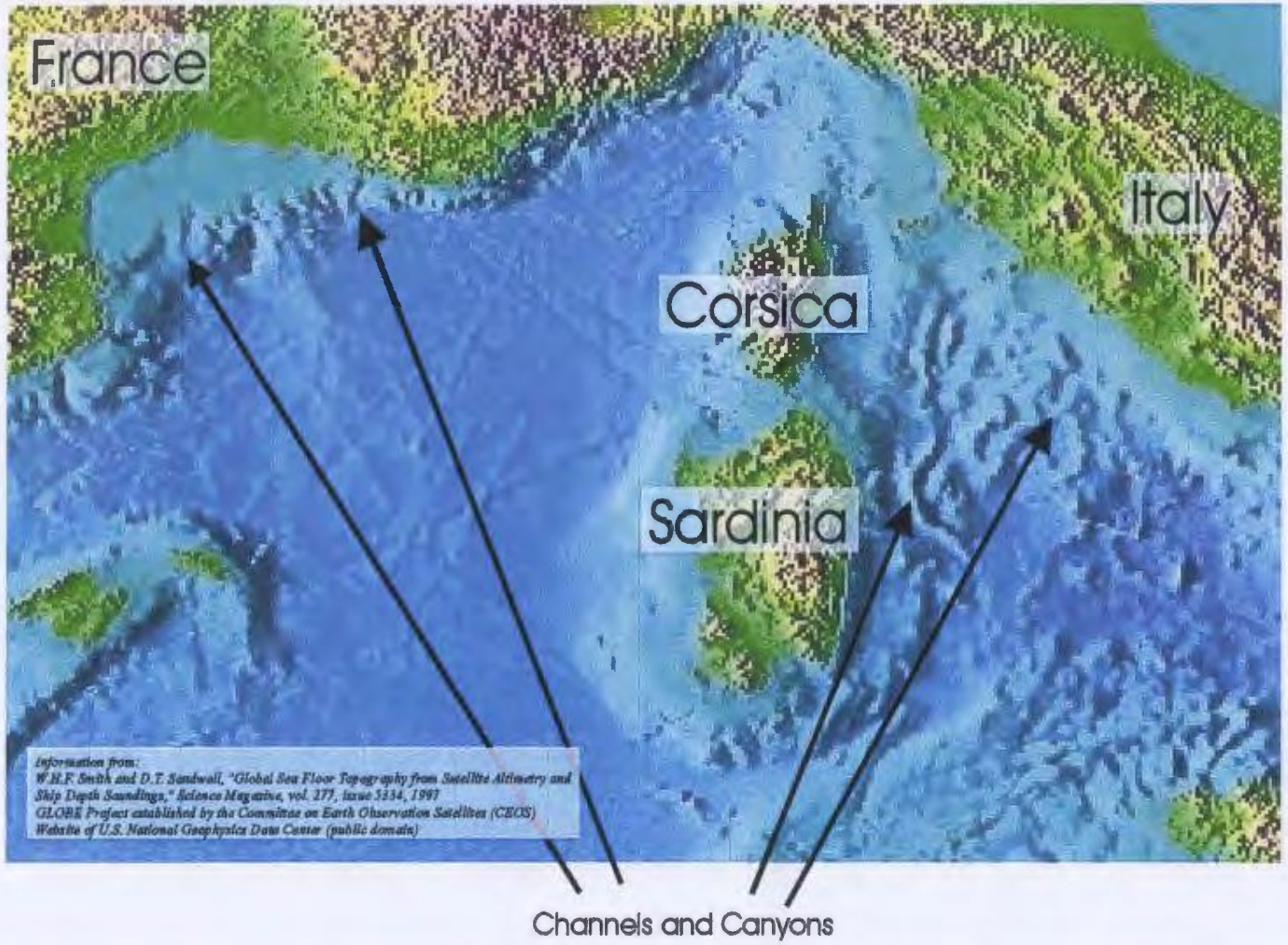

Figure 1-9: Bathymetry map of the Mediterranean Basin showing that, in the past, the Mediterranean was likely covered by a very shallow pool of water. River systems would have to cut down through what are the present-day continental shelves and slopes to reach the flat-bottomed playas at Messinian sea level 2000 to 3000 meters below present-day sea level. The erosional nature of these rivers and channels would result in the formation of large channels and canyons such as those which have been documented in southern France, Italy, Corsica and Sardinia.

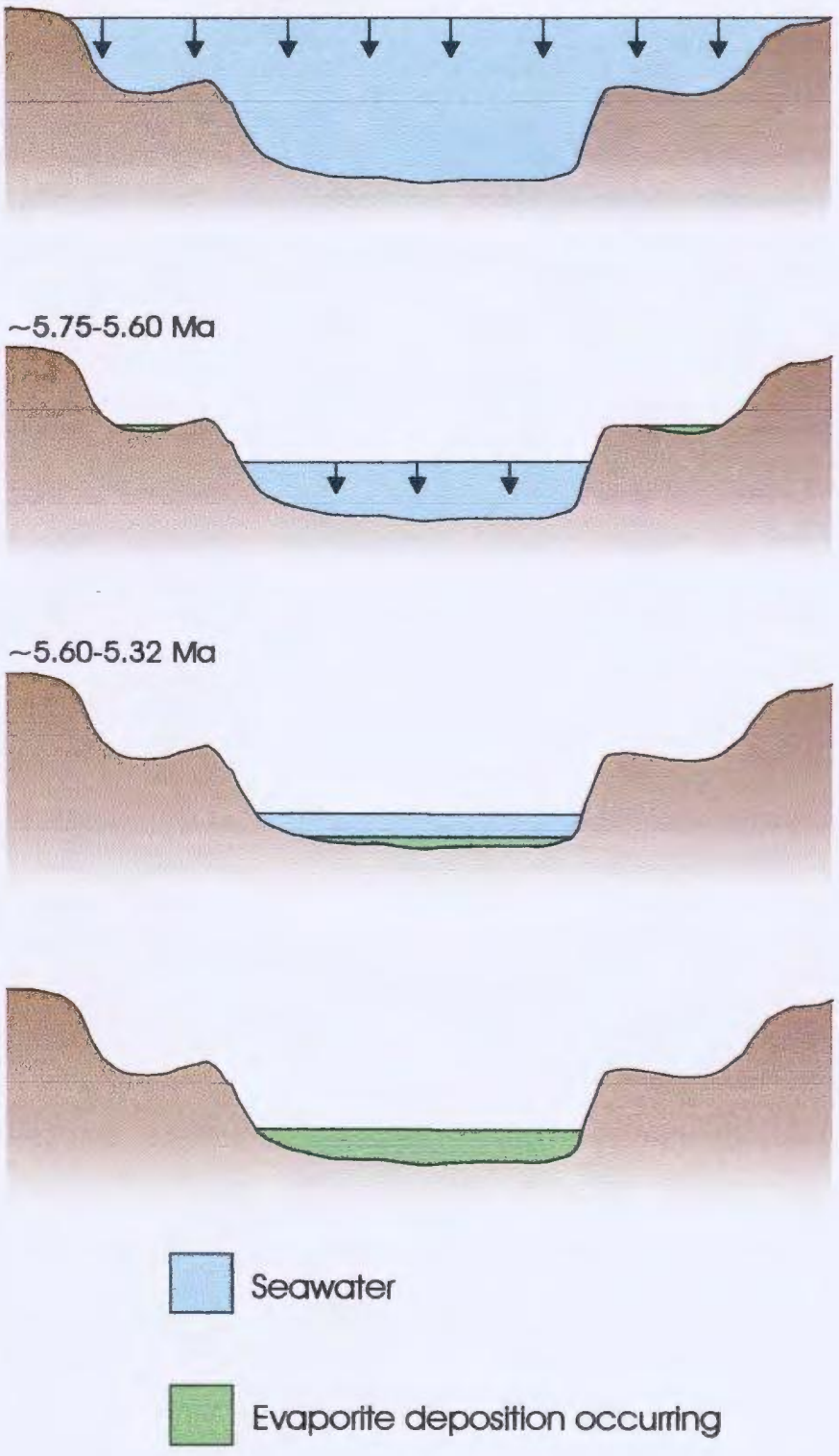

Figure 1-10: Diagrammatic representation of model of evaporite deposition proposed by Clauzon et al. (1996).

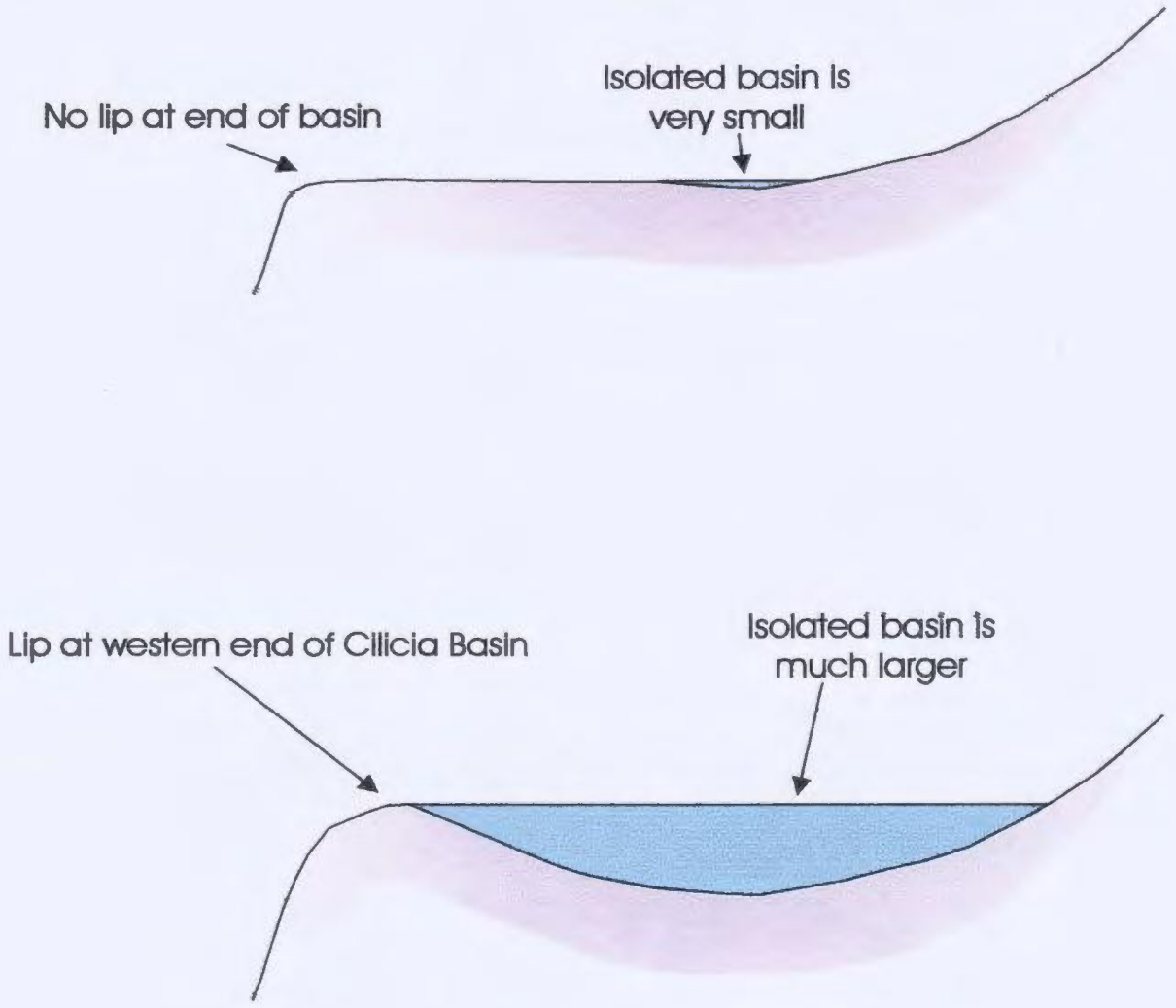

Figure 1-11: If the Cilicia Basin has a lip at it's western end then it can fill up more than the same basin could without that lip thereby increasing the maximum size the basin can reach and still become isolated from the main part of the Mediterranean.

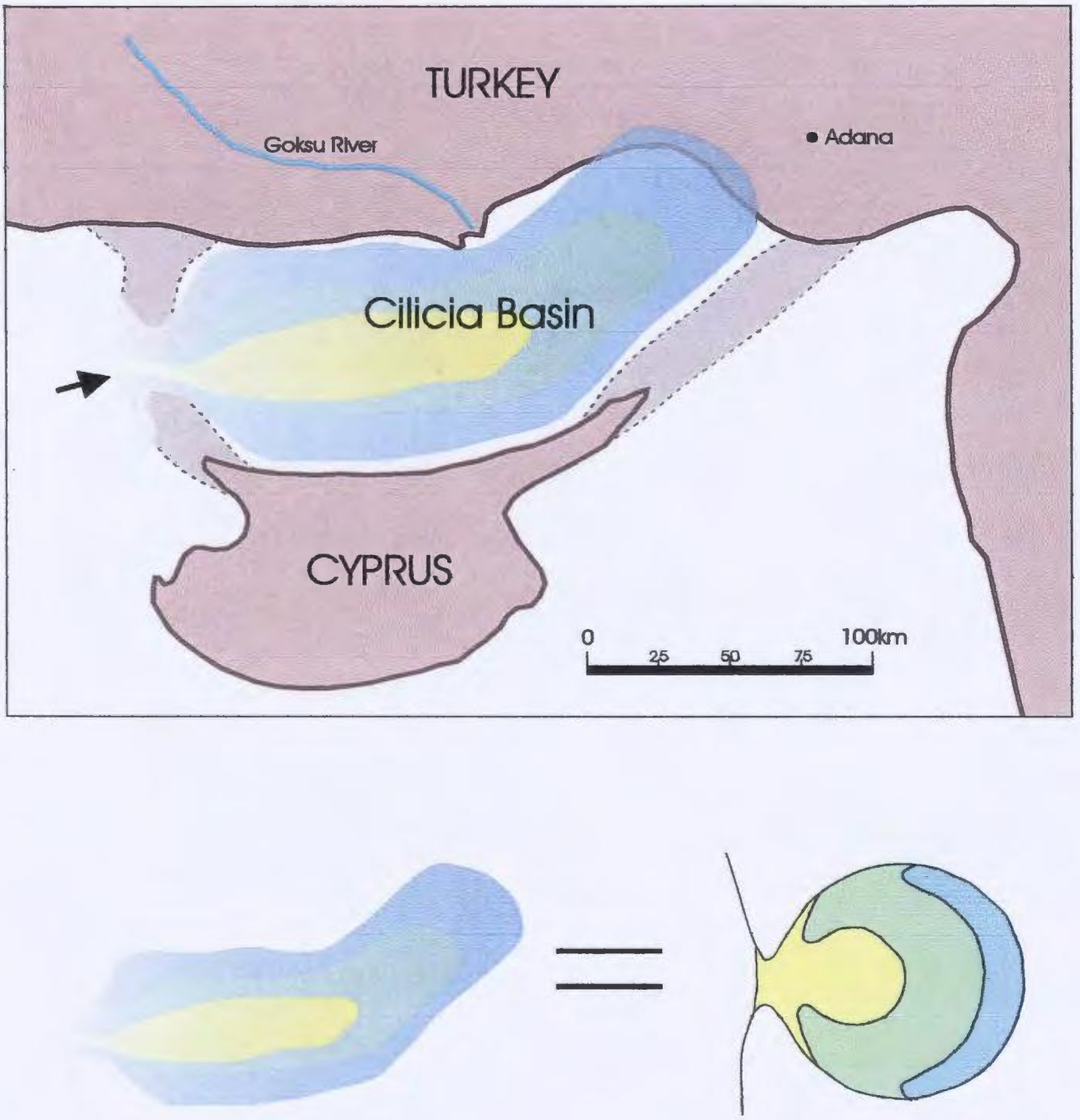

Figure 1-12: The Cilicia Basin likely displays a tear drop pattern of evaporite distribution which is characteristic of a partially restricted basin.

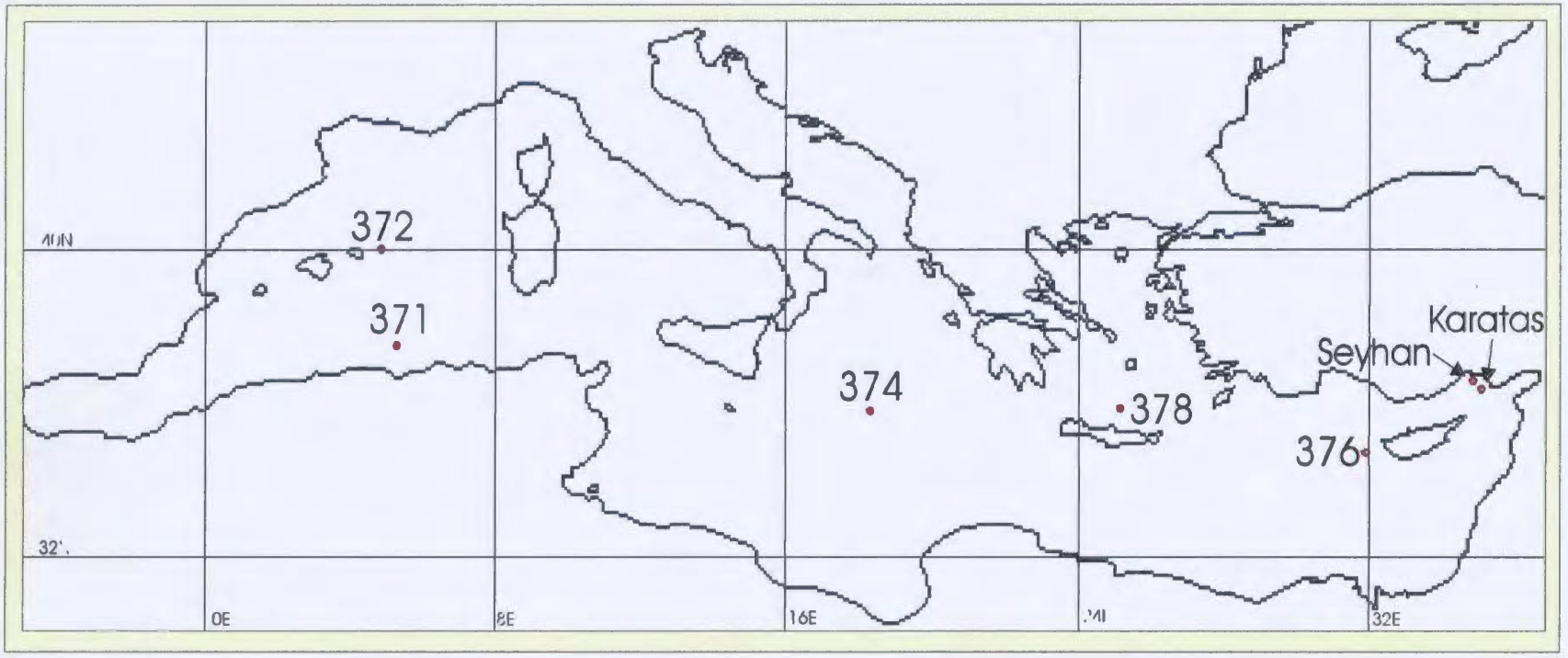

Well	latitude	longitude
371	37.5980	5.2592
372	40.0800	4.7965
374	35.8478	18.1963
376	34.8720	31.8075
378	35.9278	25.1162

Figure 1-13: Locations of selected wells which penetrate evaporites in the Mediterranean(Garrison et al., 1978).

2. EVAPORITE DIAPIRISM

Because evaporites have a low viscosity and density and are more ductile at low temperatures than most buried sediments, they respond to variations in the stress field in a unique and unconventional way. The deformation of evaporites is quite complex and may seem unpredictable; however, extensive studies of natural evaporite structures, as well as modeling, have shown that the movement of evaporites follows some general rules and conforms to basic models. These models have been developed, and continue to be developed, by well-known and well-respected scientists such as Balk (1936, 1949), Chapple (1978), Davis and Engelder, (1985) Vendeville and Jackson (1992 a, b), Duval, Cramez and Jackson (1992) Jackson and Vendeville (1994), Jackson, Vendeville and Schultz-Ela (1994) Remmelts, (1995), Ge, Jackson and Vendeville (1997).

Overburden sediments lying above the evaporite unit undergo brittle deformation rather than experiencing the ductile deformation that is observed in the evaporites. This contrast in viscosity commonly results in the decoupling of the evaporite unit and its overburden.

In some instances, evaporites become mobilized so much that they form a salt canopy or salt sheet that is above the original salt source-layer. This salt canopy can undergo further diapirism creating numerous levels of salt and diapirs. Such an occurrence is commonly observed in the Gulf of Mexico where there are multiple layers of salt arising from one source layer. This secondary salt is known as allochthonous salt. The original salt layer is referred to as autochthonous salt or 'in-situ' salt. The evaporites in the Cilicia Basin and the Mediterranean are believed to be autochthonous (in-situ) salt.

This chapter concentrates on the characteristics and features of autochthonous salt ignoring the characteristics of transported allochthonous salt bodies.

For ease of communication, the generic term 'salt' is given to a wide range of evaporite lithologies. Pure halite, gypsum and anhydrite or any combinations thereof are collectively referred to as 'salt' or 'evaporites'. On a local scale these evaporites may react differently to applied stresses however, on the regional scale resolved in seismic sections, these differences are minimal.

There are a number of different components and considerations when studying the deformation of salt bodies. Among the most important components of a salt tectonic system are the trigger for diapirism, the stages of diapir growth, the coupling and or decoupling of sedimentary overburden and evaporites, and the nature of the deformational stresses (compression or extension). Also important to the deformation of an evaporite unit is the relative timing of the deformational event in relation to the evolution of the diapir. These relationships can be identified through various indicators of salt and sediment movement that can be observed in the region of the salt body.

2.1 Trigger for Diapirism

Originally it was accepted that the density contrast between the salt and its overburden was the trigger for diapirism. Simply stated: less dense salt will flow up through sediments of greater density driven by buoyancy (eg. Jenyon, 1986). In fact, this mechanism, although feasible, is not the most plausible mechanism of triggering salt diapirism. While density contrasts aid in the growth of diapirs, it is more likely that

extension (or less frequently contraction) initiates the growth of diapirs (Vendeville and Jackson 1992a, Jackson and Vendeville 1994). This is most obvious in an example from the Persian Gulf where evaporites are Precambrian to Cambrian in age. These evaporites sat dormant throughout the Ordovician to Permian while up to 5 km of greater density overburden was piled on top of them. It was in the Triassic to Jurassic that these evaporites began to form diapirs, a time that marks the commencement of regional extension (Rowan, 1999) that eventually lead to the opening of the Tethyan Ocean.

2.2 Stages of Diapir Formation in a Basin

Experimental modeling undertaken by Vendeville and Jackson (1992 a, b) and Jackson and Vendeville (1994) showed that the process of diapir formation is closely related to extensional tectonics. In a salt-bearing succession undergoing extension, there are three progressive stages in the evolution of a salt diapir. These stages are known as reactive diapirism, active diapirism and passive diapirism (Fig. 2-1).

Salt diapirs do not form as a direct result of contraction. When present in contractional settings, salt diapirs have either i) formed in an extensional setting and experienced further growth in a contractional setting or ii) formed as a consequence of thinning and extension at the outer arc of a contractional feature (Jackson and Talbot, 1991).

2.2.1 Reactive Diapirism

Reactive diapirism is the initial stage in the growth of a diapir (Fig. 2-1).

Extension thins the sedimentary overburden and produces a graben at the surface. The sedimentary load is locally decreased above this part of the evaporite unit allowing the formation of an upward indentation at the salt-sediment interface as the sediments isostatically adjust. This upwards indentation is referred to as an 'inverse graben'. Diapirism is initiated as the evaporites respond to this extension by filling in the indentation from the inverse graben. The outcome of this salt movement is the creation of a small conical diapir that will gradually grow with continued extension.

2.2.2 Active Diapirism

Once the overburden is thinned sufficiently, differential fluid pressure between the salt and its overburden will cause the reactive diapir to punch through the overburden to reach the surface. This process is known as active diapirism (Fig. 2-1) and is equivalent to the piercement diapirism that was originally thought to be the dominant cause of salt diapirism (Bishop, 1978). The previously accepted rule of seismic interpretation was that faults at salt diapirs formed during the initial piercement of a diapir into the overburden and radiated outward from that diapir in plan view; these faults were termed 'radial faults'. It is now accepted that the faults around a salt diapir develop after diapir formation as a result of the lateral withdrawal of salt to feed the growing diapir during the next stage of diapir growth (passive diapirism; see below, section 2.2.3) (Kolarsky, 1997).

2.2.3 Passive Diapirism

Once the diapir reaches the surface it will continue to feed off the salt source-layer in a passive manner (Fig. 2-1). This process, known as passive diapirism, is analogous to the concept of downbuilding put forth by Barton (1933). This is a process by which the diapir crest strives to keep up with new sedimentation, remaining at the level of the seafloor, while the overburden sinks into the depleting salt source-layer. Faulting is commonly initiated as a result of the salt withdrawal from the source layer. These withdrawal-related faults have been classified by Fails (1990) as being either transverse (cutting across the diapir) or tangential (curving alongside the diapir). In the case of faults that curve tangential to the diapir, cusping of the salt at the diapir margins may occur. This cusping is gentle along the upper, shallow parts of the fault with more pronounced cusping at greater depths where faults are stronger (Rowan, 1999). Once the source layer has been depleted, the diapir stops growing despite any density contrast existing between the salt and its overburden. This termination of diapir growth is a consequence of the absence of differential fluid pressure that was originally provided by the source layer.

2.3 Types of Deformation in Evaporite Basins

There are two main types of deformation in evaporite basins: thick-skinned deformation and thin-skinned deformation. These types of deformation can be observed in both the contractional and extensional regimes. Sometimes both thick-skinned and thin-skinned deformation can be observed along a single cross section within a basin; at other times only one of these types of deformation will affect a basin.

2.3.1 Thick Skinned Deformation

Thick-skinned deformation involves the deformation of the salt layer as well as the sediments above and below the salt unit (Fig. 2-2). In this type of deformation the overburden or 'suprasalt' and the basement sediments or 'sub-salt' react to regional deformation as a single unit or, more commonly, they are deformed separately, detaching along the evaporite unit. This type of deformation is commonly referred to as 'basement-involved'.

2.3.2 Thin Skinned Deformation

Thin-skinned deformation only affects the salt and the overburden sediments ('suprasalt'), but not the basement sediments ('sub-salt') (Fig. 2-3). In examples of thin-skinned deformation the salt acts as a detachment horizon above which the overburden deforms. The faults in the overburden generally sole within this salt detachment horizon.

2.4 Evaporites in the Extensional Domain

Extension is the most common form of deformation observed in autochthonous (in-situ) salt layers (Rowan, 1999). Jackson and Vendeville (1994) show that there is a close association between salt diapirism and regional extension, in both time and space. Diapirism is generally preceded by extensional events thereby creating a temporal correlation between regional extension and salt diapirism. Spatially, diapirs are often located alongside the extensional faults in a region (Fig. 2-4).

2.4.1 Thick-Skinned Extension

Thick-skinned (basement-involved) extension is observed when the evaporite layer is present before major extensional events occur in the basin. Upon the initiation of extension offset is created in the basement sediments (sub-salt strata). These extensional faults do not continue to propagate upwards through the salt. The salt migrates to accommodate the offset observed along the extensional basement faults. The overburden sediments are then draped across the offset portion of the basement (a drape fold). The most common result of this process is the formation of a large evaporite bulge above the footwall portion of the basement fault (Fig. 2-5; Remmelts, 1995). It is important to note that during thick-skinned deformation the growth of diapirs is not restricted to the areas above extensional faults; both diapirs and extensional faults can be found independent of each other. The Horn Graben and the Dutch Graben in the North Sea are good examples of situations in which there are numerous extensional faults that are independent of the salt diapirs and vice versa (Fig. 2-6; Nalpas and Brun, 1993).

2.4.2 Thin-Skinned Extension

Thin-skinned extension is exhibited in an area where evaporite deposition is concurrent with or prior to the formation of faults in the evolving basin. Thin-skinned extension is restricted to only the suprasalt strata and is accommodated by gravitational spreading and/or gravitational gliding. This type of extension can produce symmetrical or asymmetrical salt features and associated symmetrical or asymmetrical grabens. Studies of asymmetric graben and diapir formation in sandbox models completed by Jackson and

Vendeville (1992c) demonstrated that the formation of grabens during thin-skinned extension is a step-by-step process of reactive, active and passive stages. Later, Vendeville and Jackson (1994) were able to produce symmetrical grabens and salt diapirs in sandbox models undergoing thin-skinned extension. These studies helped identify basin characteristics that control the symmetry or asymmetry of structural and salt tectonic features in a region.

Whether a symmetrical or asymmetrical graben or diapir is observed is dependant on two major factors as demonstrated in the sandbox model experiments of Jackson and Vendeville (1992 a, b, c, 1994).

i) *Detachment slope*: The slope of a salt detachment will often determine whether or not grabens and diapirs are symmetrical. A horizontal detachment slope such as that found in the central portion of a basin will favour symmetrical reactive diapirs, whereas even a slightly dipping detachment results in the formation of asymmetrical features because the presence of sloping detachments favours asymmetrical faults which dip in the downslope direction (Fig. 2-7).

ii) *Ratio of the rate of aggradation (sedimentation) to the rate of extension*: the rates of sedimentation and extension and their relationship to each other can also play an important part in determining whether a graben or diapir is symmetrical or asymmetrical (Fig. 2-8; Jackson et al., 1994). For example, a high rate of sedimentation in a basin undergoing a low rate of extension will result in listric growth faults and rotated half grabens. An intermediate ratio of sedimentation to extension will result in the formation of symmetrical grabens with reactive diapirs. A low sedimentation rate compared to the

rate of basin extension would favour the formation of passive diapirs with negligible faulting. It is also notable that a rapid sedimentation rate during extension may restrict or suppress the growth of diapirs whereas at the same rate of extension, a slow sedimentation rate would favour reactive diapirism.

2.4.3 Raft Tectonics: Extreme Thin-Skinned Extension

During thin-skinned extension overburden sediments deform by brittle means and are effectively broken into fault blocks by the various extensional faults that accommodate regional extension. Generally the listric normal faults separating various fault blocks have a moderate amount of offset which permits the fault blocks to remain in contact with each other (hanging wall overlies footwall) in what is referred to as a 'pre-raft' stage (Fig. 2-9). In extreme cases of thin-skinned extension, the offset between adjoining fault blocks is so great that these fault blocks uncouple and separate from each other (hanging wall does not rest on footwall), these isolated fault blocks are known as rafts (Fig. 2-9; Duval et al., 1992). It is common for younger (symmetrical or asymmetrical) secondary basins to fill the space created between the rafts during extension. The evaporites in this type of setting generally well up underneath these basins in areas of the overburden which thinned as a result of the listric normal faulting (Fig. 2-9).

2.5 Evaporites in the Contractional Domain

Evaporites can be found in one of three main contractional settings (regions

undergoing shortening) (Rowan, 1999). These contractional settings are i) in the frontal portions of collisional fold-and-thrust belts, ii) at the toe of progradational systems and, iii) in basins that are inverted during regional contraction, following initial extension.

2.5.1 Deformation in Frontal Portions of Fold and Thrust Belts

Chapple (1978) noted that all fold and thrust belts had numerous common features including a characteristic wedge shape, a basal zone of décollement below which there is no deformation (generally a low viscosity horizon, but not necessarily a salt décollement) and a large amount of horizontal contraction above the décollement which is focused at the back of the wedge. This mechanical model is analogous to the deformation that a wedge of snow would undergo if pushed by a bulldozer (Fig. 2-10).

When an active fold belt is underlain by salt it behaves quite differently than the same fold belt would behave if it were not underlain by salt. A fold belt underlain by salt will generally have no consistent fault vergence (a characteristic that is related to the weakness of the salt) whereas a fold belt that is not underlain by salt has a regular vergence towards the foreland (Fig. 2-11; Davis and Engelder, 1985). Other characteristics of fold belts underlain by salt are the presence of narrow, generally symmetrical polyclinal (box-fold) anticlines which are separated by comparatively broad and flat bottomed synclines, the typical appearance of simple salt-cored detachment folds and an infrequent occurrence of low-angle thrust faults and the common observation of steep, high-angle reverse faults which may cut one or both limbs of these anticlines (Davis and Engelder, 1985). Fault bend folds above fundamental thrusts are rare in the

frontal portion of salt-involved fold-and-thrust belts, except in cases where shortening is so great that it can no longer be accommodated for in detachment folds. Harrison and Bally (1988) suggested that multiple levels of faulting might occur in a single anticline within a fold and thrust belt. The inner parts of the anticline experience early faulting which is short lived, outer portions of the anticline experience faulting at a later time but it is generally longer lived. It is this diachronous faulting that causes problems when attempting to restore salt detached folds (eg. Parry Islands Fold Belt, Melville Island, Canadian Arctic Islands).

The external geometry and internal deformation of a fold and thrust belt is dependant on four factors as determined by the 'Critical Wedge Taper Theory' of Davis et al. (1983) (Fig. 2-12):

i) the topographic slope at the front of the fold belt

ii) the dip of the basal detachment surface

iii) the coefficient of internal friction (or internal strength of the rock)

iv) the coefficient of sliding friction (or resistance to shear)

One of the more significant characteristics of salt is that it has a very low resistance to shear which results in fold belts with a more tapered cross-section; with a wider belt of deformation (ie. the thrusts will propagate a farther distance outward); and, with more symmetrical structures than observed in fold belts not underlain by salt (Fig. 2-13; Davis and Engelder, 1985). Jaumé and Lillie (1988) further modified these factors, noting that the dip and structure of the basal detachment surface controls the geometry observed in a fold and thrust belt, and that the distribution of salt (ie. the location of salt, thickness of

salt, relation of salt to other structures) can have some control on the geometrical outcome.

2.5.2 Thick-Skinned Deformation in Inverted Basins

Graben inversion is common in intracratonic basins undergoing regional compression as well as in rift basins that experience a change from extension to compression. Inversion of the original extensional structures squeezes hanging wall blocks upwards reversing the original sense of fault movement from normal (extensional) faulting to reverse faulting. The basement ('subsalt'), evaporites and the overburden ('suprasalt') all undergo regional compression and shortening. The orientation of older salt structures, original basement faults, and any extension-related structures relative to the direction of compression is an important factor in determining the location and geometry of the features that will be formed in both the salt and overburden during the compressional stage. The deformation observed in these inverted basins becomes quite complex, frequently resulting in a decoupling of the overburden ('suprasalt') from the basement ('subsalt') along the salt detachment (Rowan, 1999). Weak salt layers result in the formation of pop-up structures and fish-tail structures during graben inversion (Fig. 2-14). Differences in the strength of individual overburden layers can also have profound effects on the deformation observed in these inverted basins (Letouzey et al., 1995).

2.6 Evaporites in Progradational Systems

Prograding sedimentary systems often display an up-slope region of extension,

where extension was initiated through gravity gliding (movement of a rock body in response to gravitational instability). Further downslope of the extensional region is a zone of shortening which balances the effects of extension. This zone of shortening is located at the toe of the progradational system and is generally associated with either under-compacted shales or salt. McClay et al. (1998) created analogue models to simulate the differential loading of a ductile substrate by a prograding delta wedge. Their models demonstrated that younger delta-top extensional growth fault grabens generally form over older, buried, delta-toe fold and thrust belts. McClay et al. (1998) further noted that extension on the top of the delta wedge caused thinning of the polymer (evaporite) layer followed by the development of a series of seaward facing extensional faults, and ensuing landward facing extensional faults. At the toe of progradational systems, reverse faults commonly have an arcuate trace in map view, especially when these faults are confined by basin edges (eg. modeling of Koyi, 1996). The dominant thrust direction is away from the toe of the progradational system; however, back thrusting is occasionally observed (Cobbold et al., 1989; Koyi, 1996, McClay et al., 1998). The shortening (contraction) observed at the toe of progradational systems is driven by a combination of the gravity gliding of up-slope sediments and the gravity spreading of the salt layer which is created as both prograding sediments and the salt react to gravitational forces.

Progradational loading is the process by which a delta, shoreline or alluvial fan outbuilds a sedimentary deposit during its seaward advance. This process may independently create a mechanism by which autochthonous (in situ) salt underlying the outbuilding sedimentary pile can be mobilized. Differential loading progressively drives

salt basinward causing it to eventually well up into diapirs (Fig. 2-15; Ge et al., 1997). This process is quite infrequent in nature, however, some spectacular examples of the mobilization of salt by progradational loading can be observed in the Gulf of Mexico, Gulf of Yemen and the Campos Basin. The reason for this uncommon occurrence is because in order for displaced salt to result in the formation of a diapir, the overburden must be very thin. This means that differential loading must begin almost immediately after deposition of evaporites. If there is significant overburden prior to the commencement of differential loading, diapirs will not form without extension (Jackson and Vendeville, 1994). Modeling by Ge et al. (1997) and McClay et al. (1998) displays the various stages of the process of differential loading over a thin overburden for an open-ended basin (Fig. 2-16), while Letouzey et al. (1995) display how this system acts in a basin in which the salt extends across the entire basin (Fig. 2-17).

In both the gravitational gliding and progradational loading scenarios there is a deformational sequence that is frequently observed in modeling experiments and can also be inferred for field examples. The initial stages of shortening produce broad, low relief, symmetrical detachment folds (buckle folds) (eg. North Sea; Fig. 2-18A). Continued shortening will result in an increase in the fold amplitude which is followed by the formation of steep reverse faults that eventually break through the anticlines as shortening progresses (eg. Perdido foldbelt, Gulf of Mexico; Fig. 2-18B). The evaporites under these anticlines wells up into the space created by the fold amplification process and related faulting to produce salt-cored anticlines.

2.7 Kinematic Analysis of Salt Structures

There are features in seismic sections that prove the salt in a basin has experienced deformation (faulting, folding, migration, diapirism etc.). These features are best referred to as kinematic indicators but are not to be confused with the term 'kinematic indicators' as used in the analysis and interpretation of ductile shear zones (eg. rotating garnets etc.). In this study, kinematic indicators simply refers to any structural or sedimentary feature observed in seismic sections which allows the seismic interpreter to determine that there has been movement of some feature relative to another (eg. the rise of a salt diapir relative to its surrounding sedimentary overburden). Kinematic indicators of this type may be found within the evaporite unit or in the sediments immediately surrounding the evaporites. When present, these kinematic indicators provide information about what may have caused evaporites to move, how the evaporites responded to that initial action, and what might have occurred in the time since the application of that initiatory force.

2.7.1 Kinematic Indicators Within the Evaporite Unit

The evaporites themselves often provide information about their kinematic history. This is especially true for evaporites interbedded with fine muds or other sediments that show up as marker horizons on seismic sections. Everything from the geometry of the evaporites to the presence of salt welds and fault welds (Jackson and Cramez, 1989) and faults in the evaporite unit potentially provide information about the movements that the salt body has undergone since its deposition.

Geometry of Evaporites

The geometry of evaporites is a fundamental indicator of evaporite movement within a basin. When evaporites are deposited, their upper boundary is a relatively flat or gently curved and continuous surface regardless of the basement topography. Upon deformation, salt will commonly well up to form bulbous or linear salt structures such as salt diapirs, salt walls, salt stocks, salt pillows, etc. The mere presence of these structures is enough to prove that salt has moved since its deposition. The geometry of these structures can tell the maturity of the salt structure, that is, whether salt has just began to move or if it has been moving for some time. A summary diagram from Jackson and Talbot (1991) displays the wide variety of evaporite geometries with an indication of relative maturities for these structures (Fig. 2-19). Using such a model, it is possible to get an idea of the extent of growth or diapirism that the evaporites have undergone.

Salt Welds or Fault Welds

Salt welds and fault welds are features that show the absence of salt at a location where salt was initially present, thereby indicating salt withdrawal from that area (Jackson and Cramez, 1989). A salt weld, as defined by Jackson and Talbot (1991), is a "surface or zone joining strata originally separated by autochthonous (in situ) or allochthonous (mobilized) salt. The weld is a negative salt structure resulting from the complete or nearly complete removal of intervening salt" (Fig. 2-20 (salt weld)). A fault weld is simply a salt weld along which there was significant fault slip or shear (Fig. 2-21; Jackson and Talbot, 1991). Salt welds are a critical element of salt system geometry. Not

only do salt welds and fault welds record the previous location of salt, they also indicate the pathway and the geometry of salt evacuations. This is extremely important in constructing palinspastic restorations, particularly in allochthonous salt systems (eg. Gulf of Mexico) where salt may have migrated to a different stratigraphic position along what is presently a salt or fault weld (Fig. 2-22). In seismic sections, salt welds and fault welds are often difficult to interpret. Both types of welds are characterized by discontinuous, high amplitude reflectors demonstrating discordance on either side of the weld (Jackson and Cramez, 1989). The high amplitude character of a weld is due to small pods of relict salt which line the weld surface resulting in high velocity contrasts between salt and sediments. These welds can have any orientation because although they form by the evacuation of salt from a horizontal source layer, they can also form by evacuation of salt from upright or leaning salt feeders such as the stem of a salt stock or salt tongue (Jackson and Talbot, 1991; Fig. 2-23).

Evidence of Faulting

It is common for salt to be interbedded with thin sediment layers as a result of their formation in a desiccating environment. Intermittent influxes of water will carry suspended sediment that settles onto, and becomes incorporated in, the evaporite layer. These sediment layers may record faulting or folding within the evaporite unit or may simply show flow patterns within the salt. When combined with information about tectonic activity in a region, these features can provide a wealth of information about how salt reacts to the stresses in a region.

Flow patterns in evaporites are commonly observed in natural examples but are often below the resolution of seismic sections or are poorly imaged due to problems with the acquisition or processing of the data.

2.7.2 Kinematic Indicators in Sediments Surrounding Evaporites

The kinematic indicators found in sediments surrounding evaporites are among the most informative, because they record not only the final configuration of salt, faults and sediment around a salt structure, but quite often these sediments, through their stratigraphic and structural architecture, provide a record of the intermediate steps occurring during the evolution of the salt structure.

Onlaps and Truncations

The presence of onlaps and truncations in seismic sections is a definite indicator of a period of movement in a basin. In basins undergoing both regional tectonics and salt tectonics, the onlaps and truncations observed above or at the sides of a salt structure are not necessarily the result of salt tectonic activity and may, in fact, be caused by regional tectonic forces (faulting, subsidence, sea level changes, etc.).

An onlap, as defined by Jackson and Talbot (1991) is the "termination of sub-horizontal strata (or seismic reflections) against a dipping surface (typically a sequence boundary or salt contact) such that each stratum extends farther across the dipping surface than does the underlying stratum." The presence of an onlap indicates that the dipping surface (sequence boundary or salt contact) was elevated above the horizontal

level of regional deposition for a given time (Fig. 2-24).

A truncation is the "removal and termination of dipping strata by subaerial or subaqueous erosion to form a sequence boundary. Truncations cutting across anticlines or fault blocks indicate that these structures had surface relief at the time of erosion." This relief could also be due to growth of a salt structure that might push sediments upwards, in an anticlinal shape, causing them to be eroded (Fig. 2-25). Truncations can also occur when the top of a sequence is downcut by erosion and infilled with younger sediments (Fig. 2-25). This type of a truncation is referred to as a down-cutting truncation.

Interpreting onlaps and truncations in seismic sections can become extremely complicated in areas of salt withdrawal. Jackson and Cramez (1989) show how an onlap succession can resemble a downlap truncation after salt withdrawal (and diapir growth) at the periphery of a salt pillow (Fig. 2-26).

Thinning and Thickening of Strata

The thinning and thickening of strata at the margins or the crest of a salt structure can tell a great deal about the salt movements in a basin. Thinning of strata (convergence of seismic reflectors) above salt indicates the addition of salt to an area, generally by salt withdrawal from nearby regions. Thickening strata (diverging seismic reflectors) above salt generally indicate the removal of salt from an area either by dissolution or salt migration.

Thinning strata above a salt structure indicate that the salt structure is undergoing growth. The thinning of numerous sediment layers above a salt structure results in the

formation of a 'condensed section' above the diapir. A condensed section contains the same complete sediment sequence that is observed at the borders of the salt structure but in a thinner package of sediment (Fig. 2-27). The growth represented by the thinning sediments above the salt structure is the result of salt withdrawal from neighbouring regions (therefore thickening of strata is observed at the sides of the salt structure) in order to feed the growing salt structure.

Thickening of strata above a salt structure indicates the removal of salt from the salt structure itself; this is referred to as sagging. The removal of salt from the salt structure is generally accompanied by thinning of sediments at its margins. The continual sagging of a salt structure commonly results in extension and graben formation at the crest of the salt structure (Vendeville and Jackson, 1992b).

A reversal in vertical motion above a diapir, such as a switch from diapir growth to diapir sag or vice versa, is referred to as structural inversion (Jackson and Talbot, 1991). In seismic sections, such a reversal would be observed directly above the salt structure. Thinning strata (converging reflectors) overlain by thickening strata (diverging reflectors) in a seismic section are indicative of a period of growth at the salt structure followed by sagging. Thickening strata (diverging reflectors) overlain by thinning strata (converging reflectors) indicate a period of diapir sag followed by diapir growth (Fig. 2-28). The principles of structural inversion were developed in the context of regional tectonics; however, used on a very localized scale, the identification of salt-related structural inversion in a seismic section is an effective tool in salt tectonic analysis.

When sediment 'thicks' occupy a syncline at the margins of a circular or sub-

circular salt structure the syncline is referred to as a rim syncline. If the sediment-filled synclines are located at the margins of a linear salt structure they are referred to as marginal synclines. The sediment accumulation in a rim or marginal syncline is referred to as a peripheral sink. A primary peripheral sink is located at the sides of a growing salt pillow and consists of sediments that thin toward the pillow (Fig. 2-29; Jackson and Talbot, 1991). A secondary peripheral sink accumulates at the margins of a growing salt diapir as it withdraws salt from its precursor pillow. The sediments of a secondary peripheral sink thicken towards the salt diapir (Fig. 2-30; Jackson and Talbot, 1991). The presence of rim synclines and marginal synclines and their associated peripheral sinks, indicates that salt withdrawal from the source layer has taken place at the margins of a salt structure in order to accommodate the growth of that structure.

2.8 Temporal Kinematic Divisions of Sedimentary Overburden

There are three divisions of the sedimentary sequence that allow one to make an interpretation of the relative timing of kinematic events (rise of diapirs, diapir sag etc.) observed in seismic sections. These divisions are made on the basis of the timing of sedimentation relative to the timing of deformation. The three temporal divisions of the sedimentary overburden are pre-kinematic, syn-kinematic and post-kinematic (Fig. 2-31).

2.8.1 Pre-kinematic Sediments

Pre-kinematic sediments are those sediments that existed before the salt movement or deformation began. It is common to see pre-kinematic strata that have been

folded, faulted or truncated as a result of subsequent salt migration or tectonic deformation. Pre-kinematic sediments are of more or less constant thickness and generally lie directly above the evaporite unit and below any syn-kinematic sediments (Jackson and Talbot, 1991).

2.8.2 Syn-kinematic Sediments

Syn-kinematic sediments are those which were deposited during the process of salt flow or other deformation events. These syn-kinematic sediments overlie the pre-kinematic sediments and commonly display many of the kinematic indicators mentioned in section 2.7.2. They provide a majority of the information available about salt migration as they display the thinning and thickening strata, as well as the onlaps and the truncations, which indicate that salt has moved (Fig. 2-32). The deformations observed in this layer may represent large-scale tectonic deformations or very localized salt tectonic deformation such as that observed at a single salt diapir. It is important to note that a syn-kinematic unit can be quite variable over a small area. For example, a large salt diapir may display sagging of its southern flank in three different seismic lines but the episodes of sagging may not have been concurrent. Sagging may have begun in the east and continued westward creating a single syn-kinematic unit that is varied in space and time along that salt wall. Alternatively, sagging may have been occurring in the eastern end of the salt structure while growth occurred in the west. In both instances, the temporal kinematic divisions cannot be treated as sequence stratigraphic units but must be looked at as a record of salt tectonic events that lacks the ability to correlate the timing of the

event across seismic sections.

2.8.3 Post-kinematic Sediments

Post-kinematic sediments are deposited after all salt flow or deformation has ceased. The sediments in this layer overlie the syn-kinematic sediments and fill indentations in the top of the syn-kinematic layer. These indentations reflect the paleotopography on the syndepositional surface at the time of cessation of salt movement. The post-kinematic sediment layer often displays onlaps or truncations at its base as a result of the in-filling style of their deposition (Fig. 2-33). Any thickness changes observed in the postkinematic sediments are not attributable to salt flow or regional deformation but rather reflect the indentations at the top of the syn-kinematic layer, or occur as the result of the uneven subsidence of sediments, facies related thickness changes or other non-tectonic process.

Syn-kinematic sediments and post-kinematic sediments may overlap in space and time because of the variable growth and salt flow histories at every point along a salt wall. Commonly the kinematic divisions of syn-kinematic and post-kinematic sediments are not linked to the lithologies of the sediments nor are they temporally or spatially correlative. This overlap is due to the variability in local salt flow histories that is commonly observed between two neighbouring diapirs or even along strike at a single diapir.

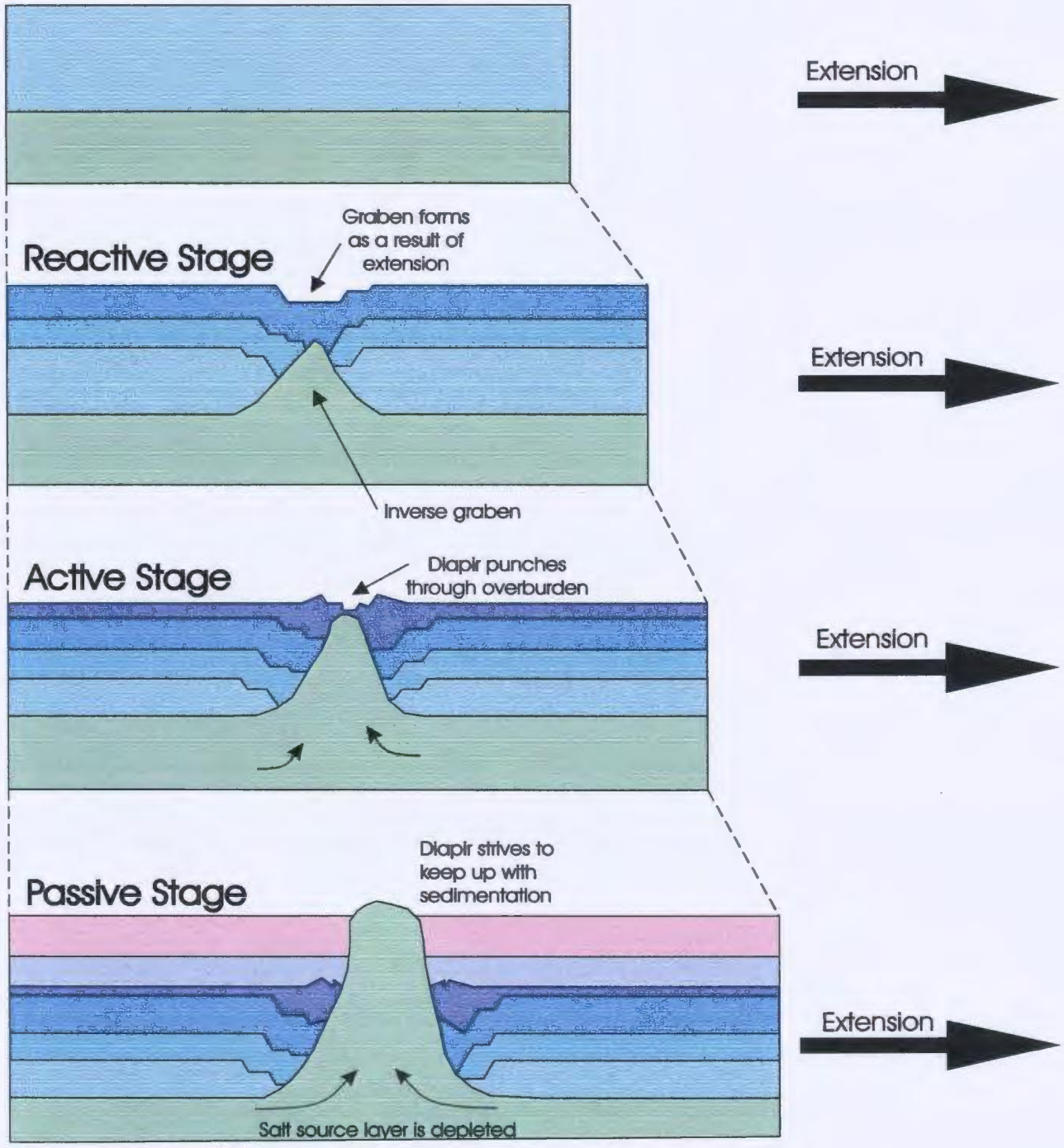

Figure 2-1:The three stages in the evolution of a salt diapir in the extensional domain as identified by Vendeville and Jackson (1992a) are Reactive, Active and Passive.

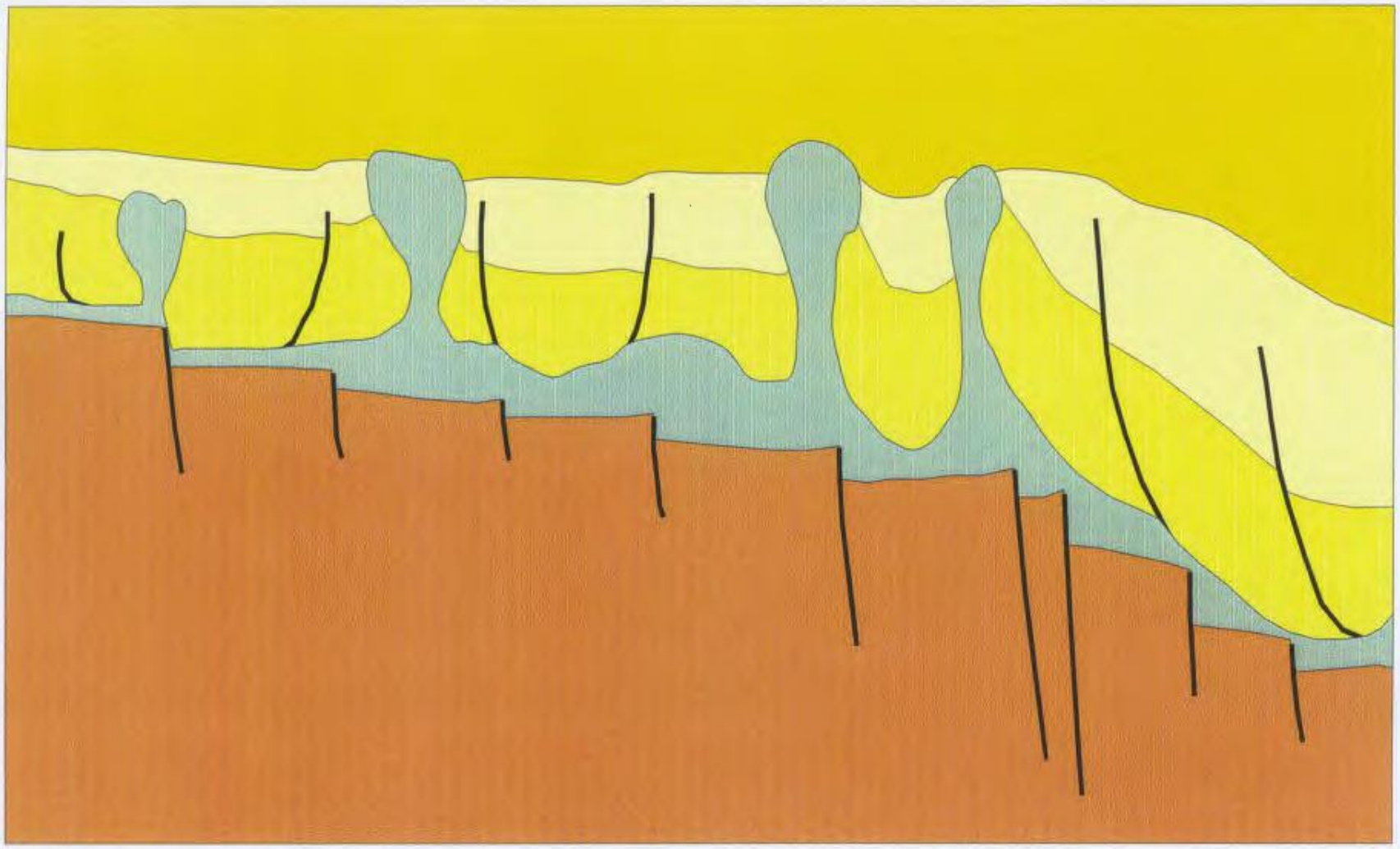

Figure 2-2: Thick-skined or 'basement-involved' deformation. The sediments above and below the evaporite unit are deformed (after Nalpas and Brun, 1993).

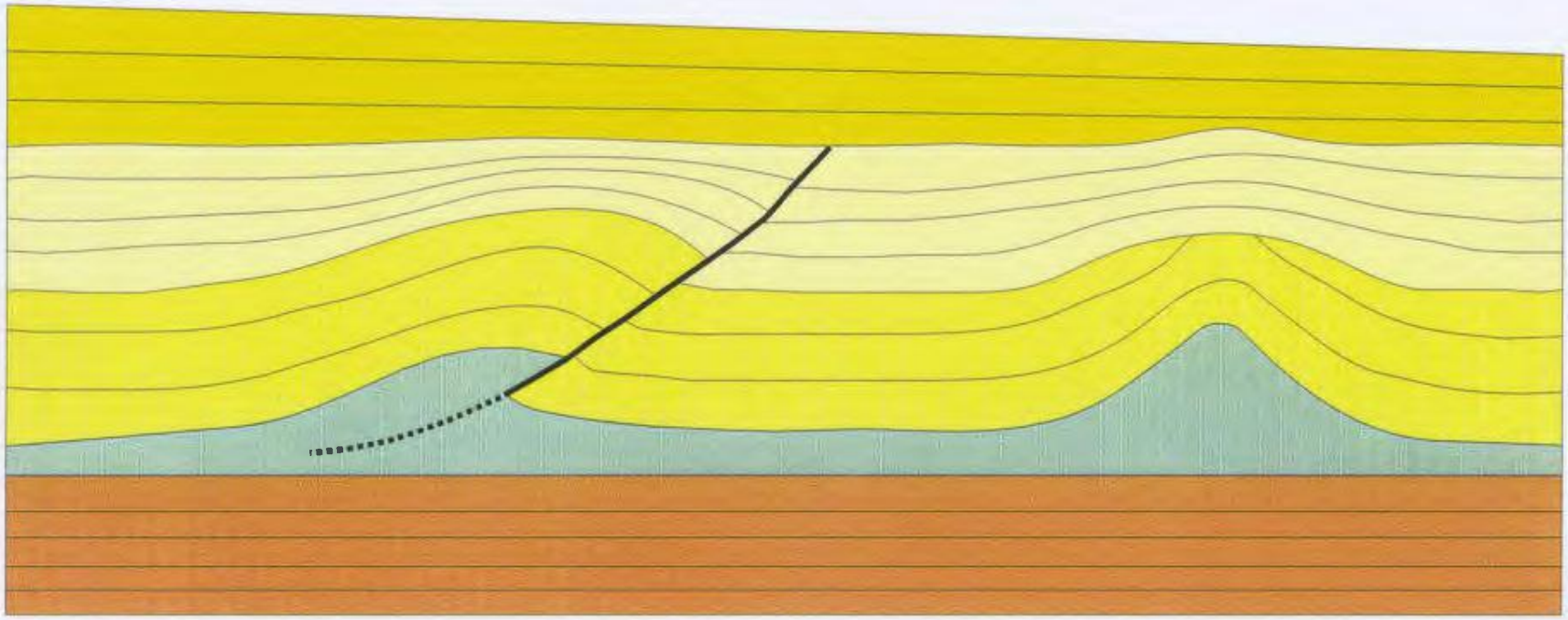

Figure 2-3: Thin skinned deformation. The sediments above the evaporite unit are deformed, sediments below the evaporite unit are not deformed.

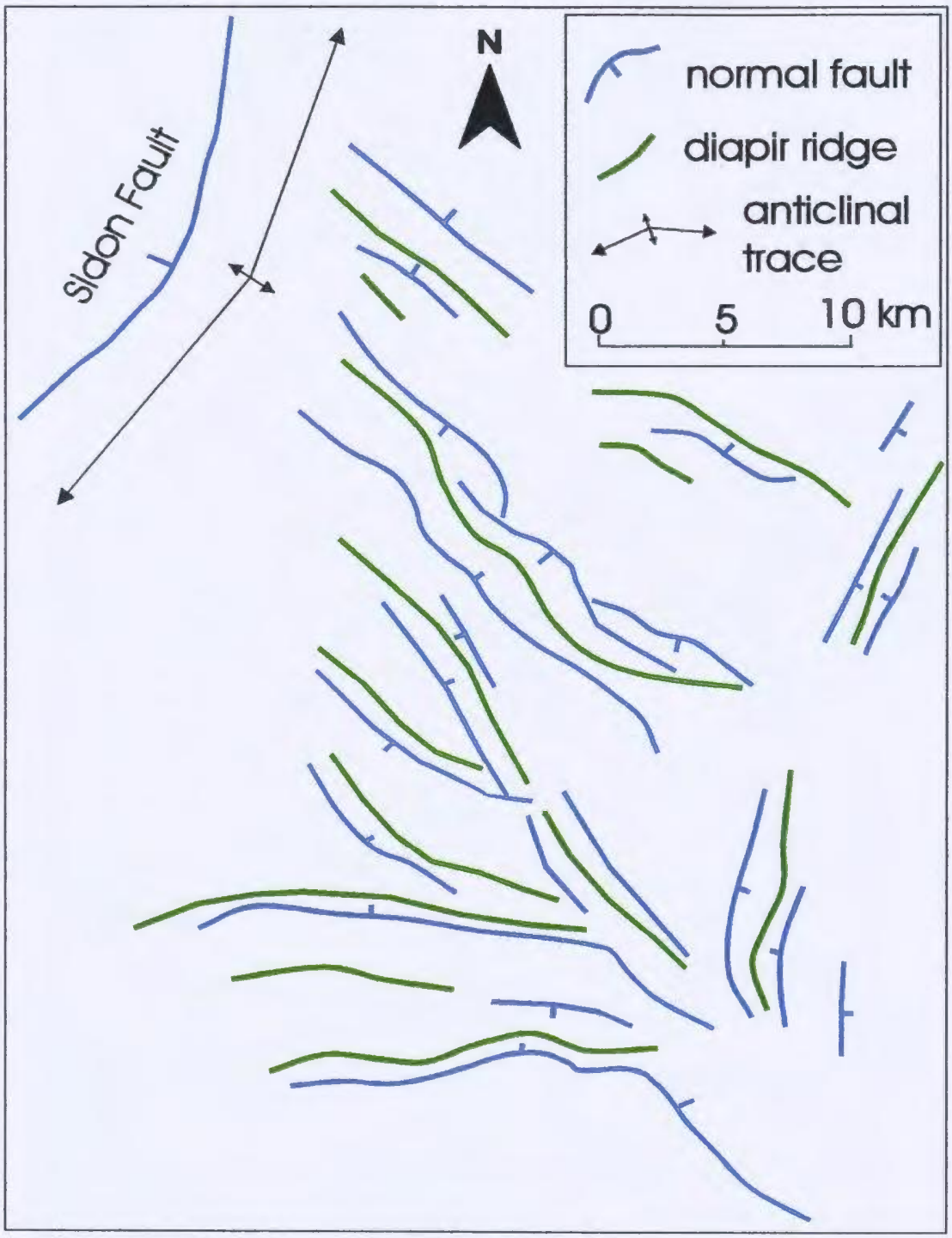

Figure 2-4: Spatial association between salt diapirism and extensional faults in the Levant Basin, southeast of Cyprus.
(After Jackson and Vendeville, 1994)

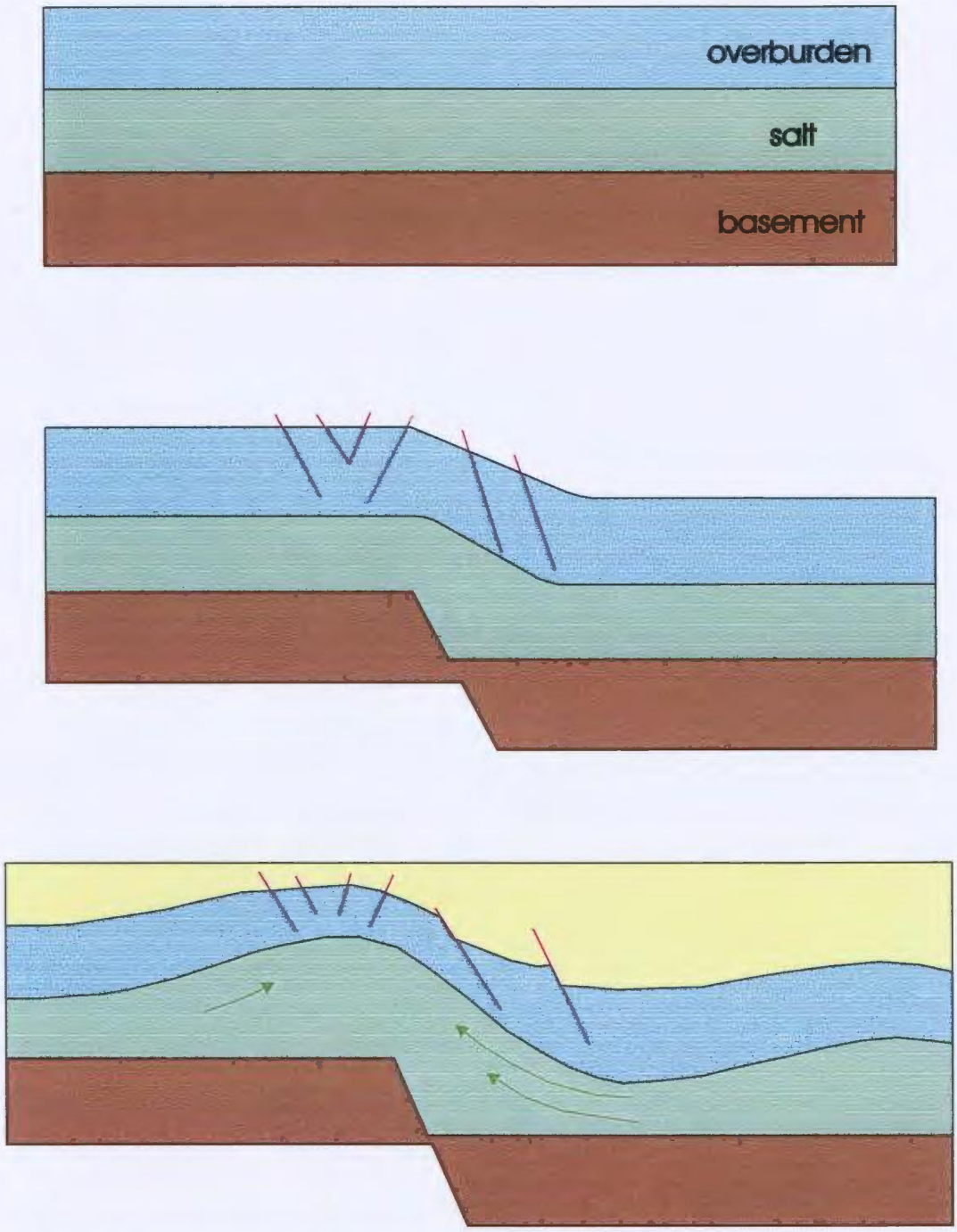

Figure 2-5: Thick-skinned or 'basement involved' extension. Extensional fault does not propagate through the salt, but is instead accommodated by movement of the salt. Overburden becomes draped over salt in a 'drape fold'. Evaporites flow to the higher location after normal (extensional) faults cause overburden to sink into salt layer (from Remmelts, 1995).

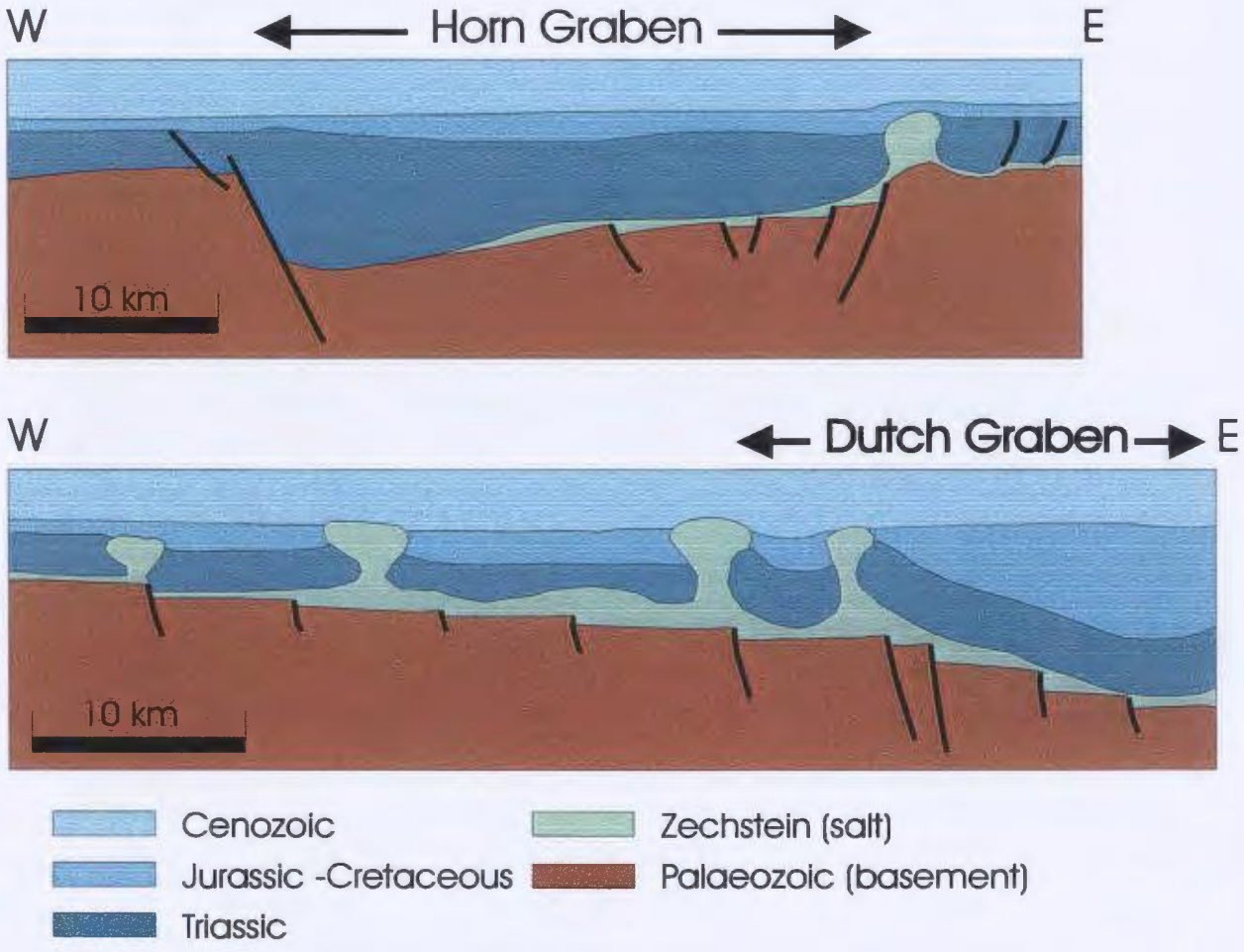

Figure 2-6: Examples of thick-skinned deformation in which the locaton of salt diapirs is independant of the location of underlying basement faults (from Nalpas and Brun, 1993).

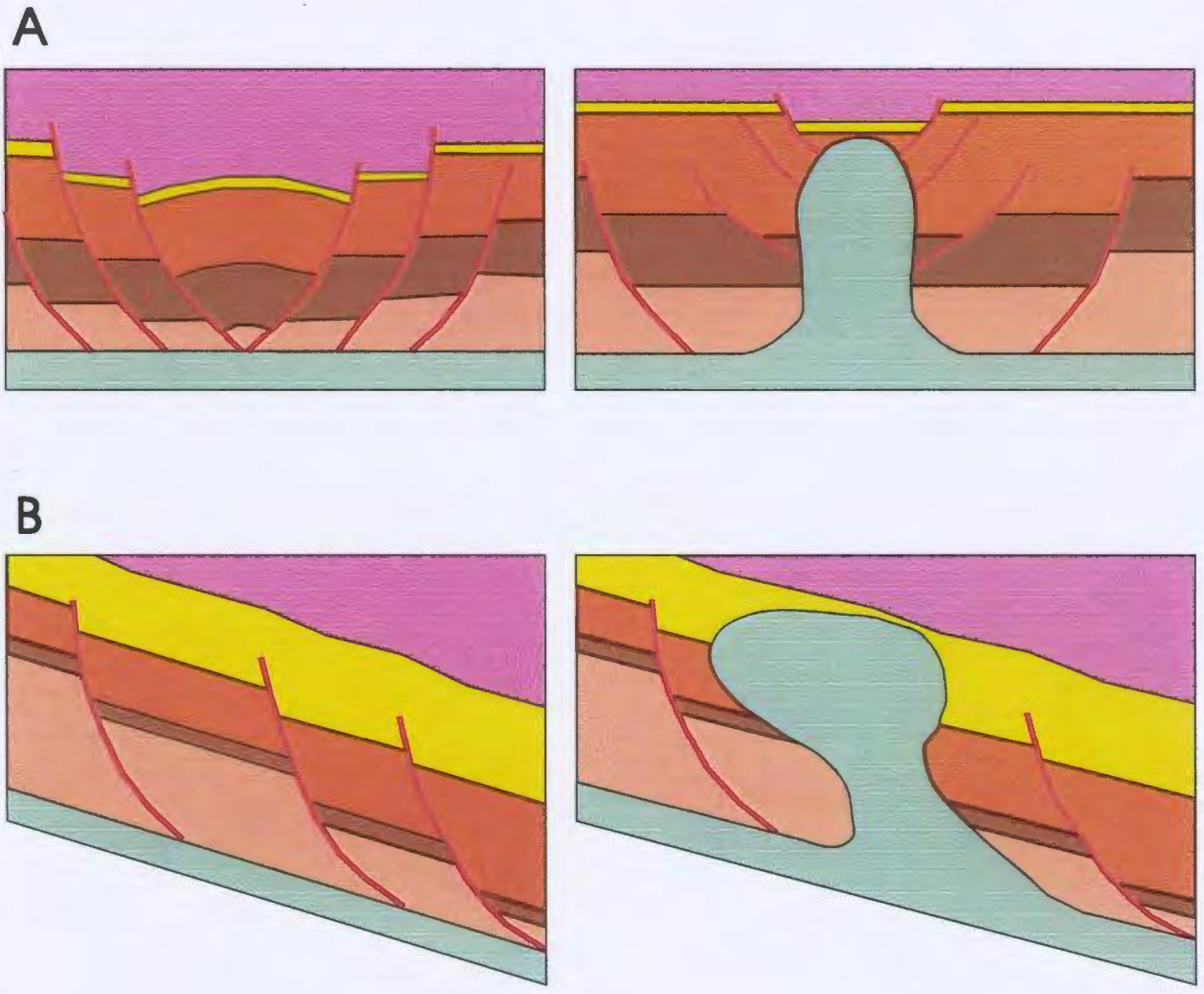

Figure 2-7: The angle of the detachment surface can control whether or not a graben and/or diapir is symmetrical or not. A) a horizontal detachment favours symmetrical grabens and diapirs; B) a sloping detachment produces asymmetrical grabens and diapirs because in such a system asymmetric faults with a downslope vergence are favoured.

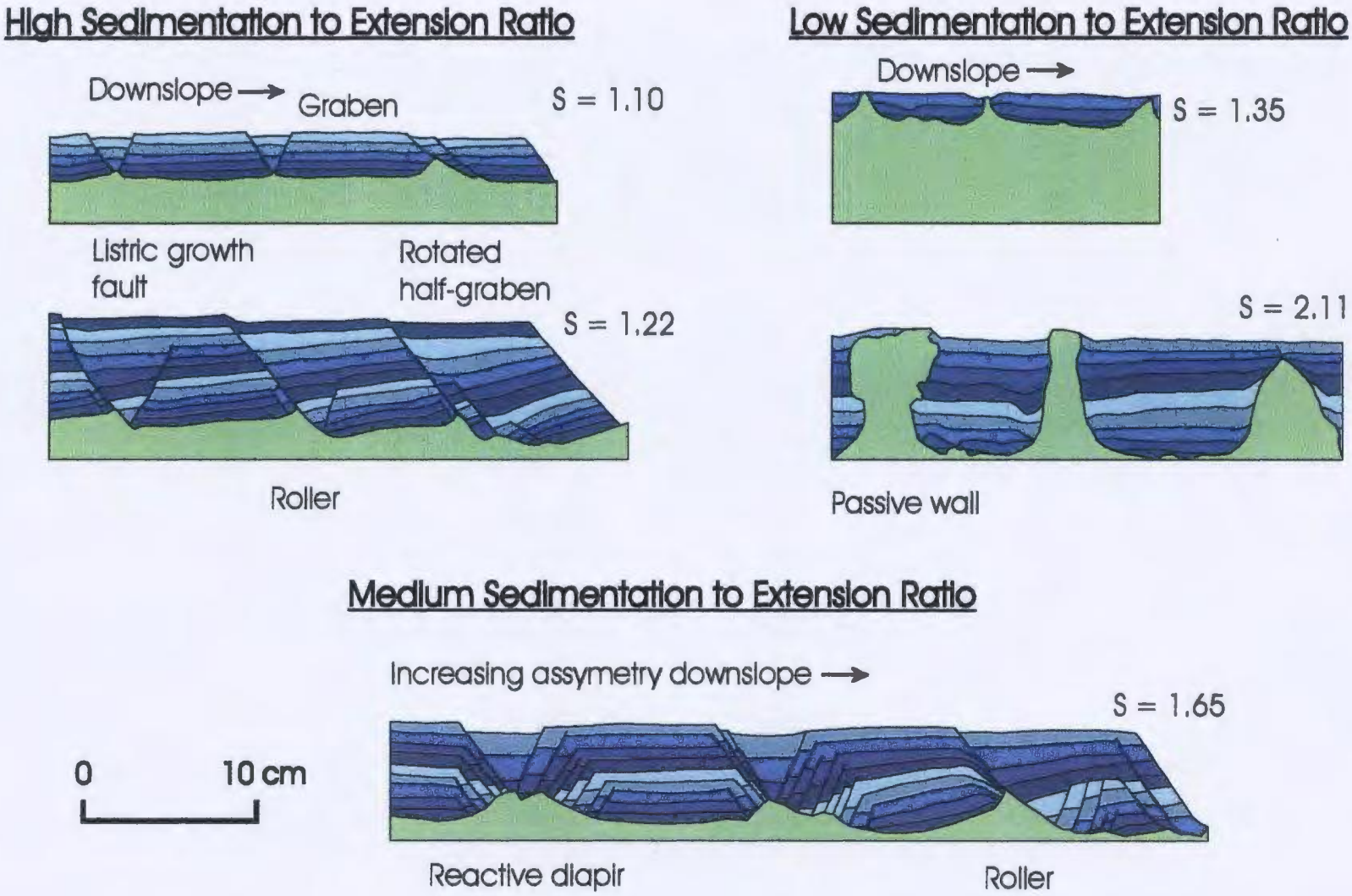

Figure 2-8: Models of diapir growth in relation to sedimentation to extension ratio (S is a measure of finite stretch). (Jackson et al., 1994).

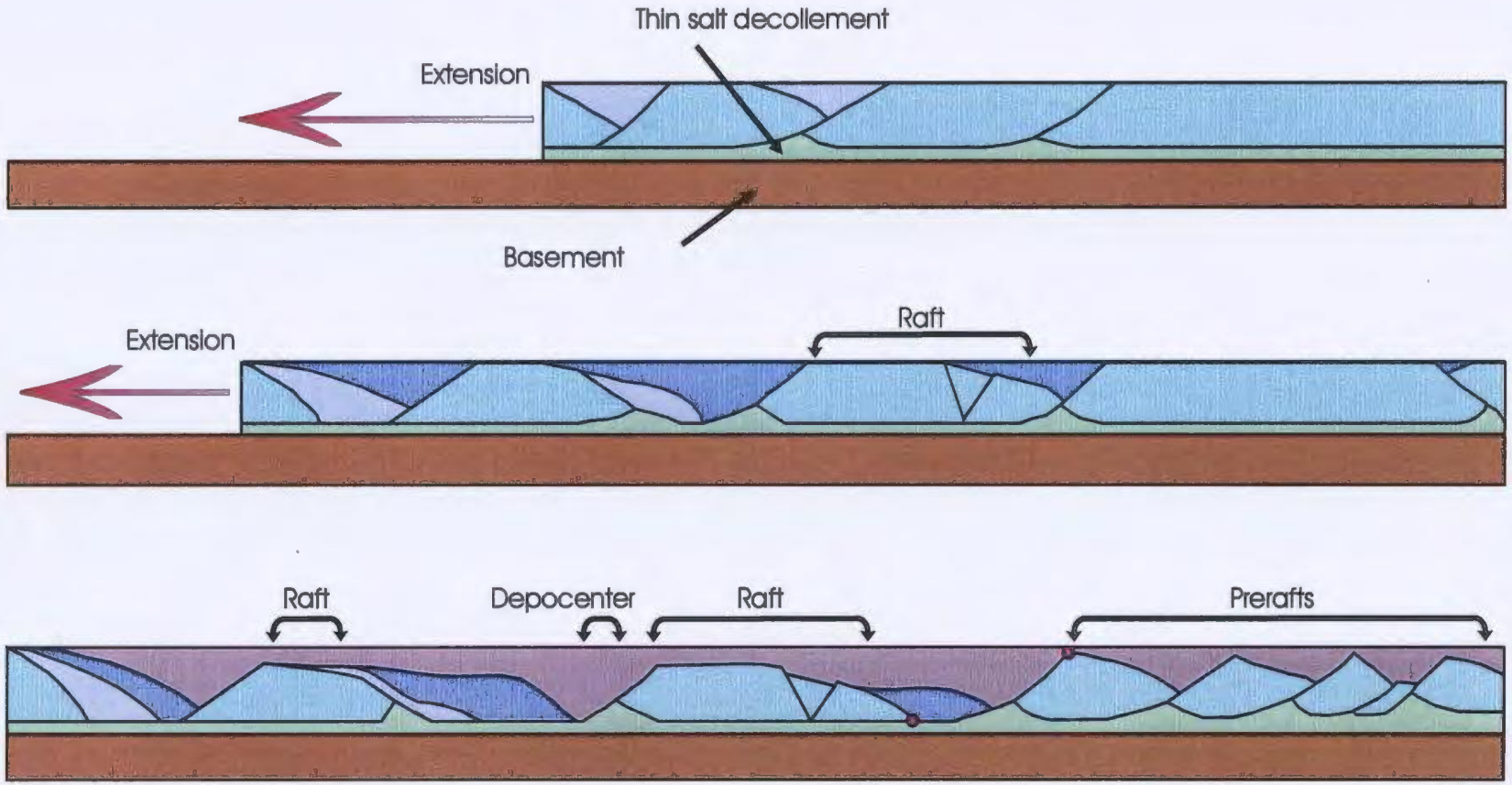

Figure 2-9: Process of raft tectonics during thin-skinned extension (adapted from Jackson and Talbot, 1991) Prerafts remain in mutual contact and hanging walls rest on their original fotwalls after faulting. Rafts separate so far that they are no longer in mutual contact and their hanging walls no longer rest on their original footwalls. The basement , not having undergone extension, remains the same length throughout. Weak rocks such as shale can also act as a decollement in the place of salt (Duval et al., 1992).

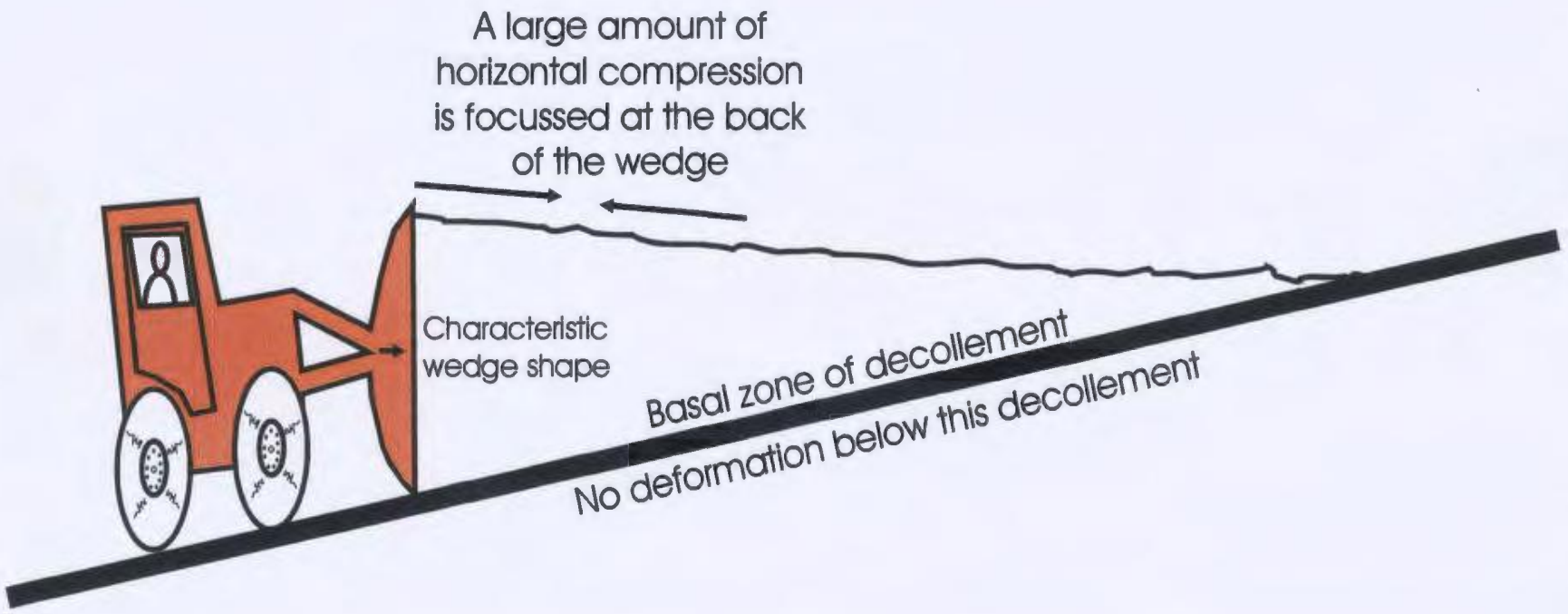

Figure 2-10: Chapple (1978) noted that fold-and-thrust belts had numerous characteristics in common even though they may occur in different areas. These belts of deformation undergo stresses analogous to the deformation that a wedge of snow undergoes when pushed by a bulldozer.

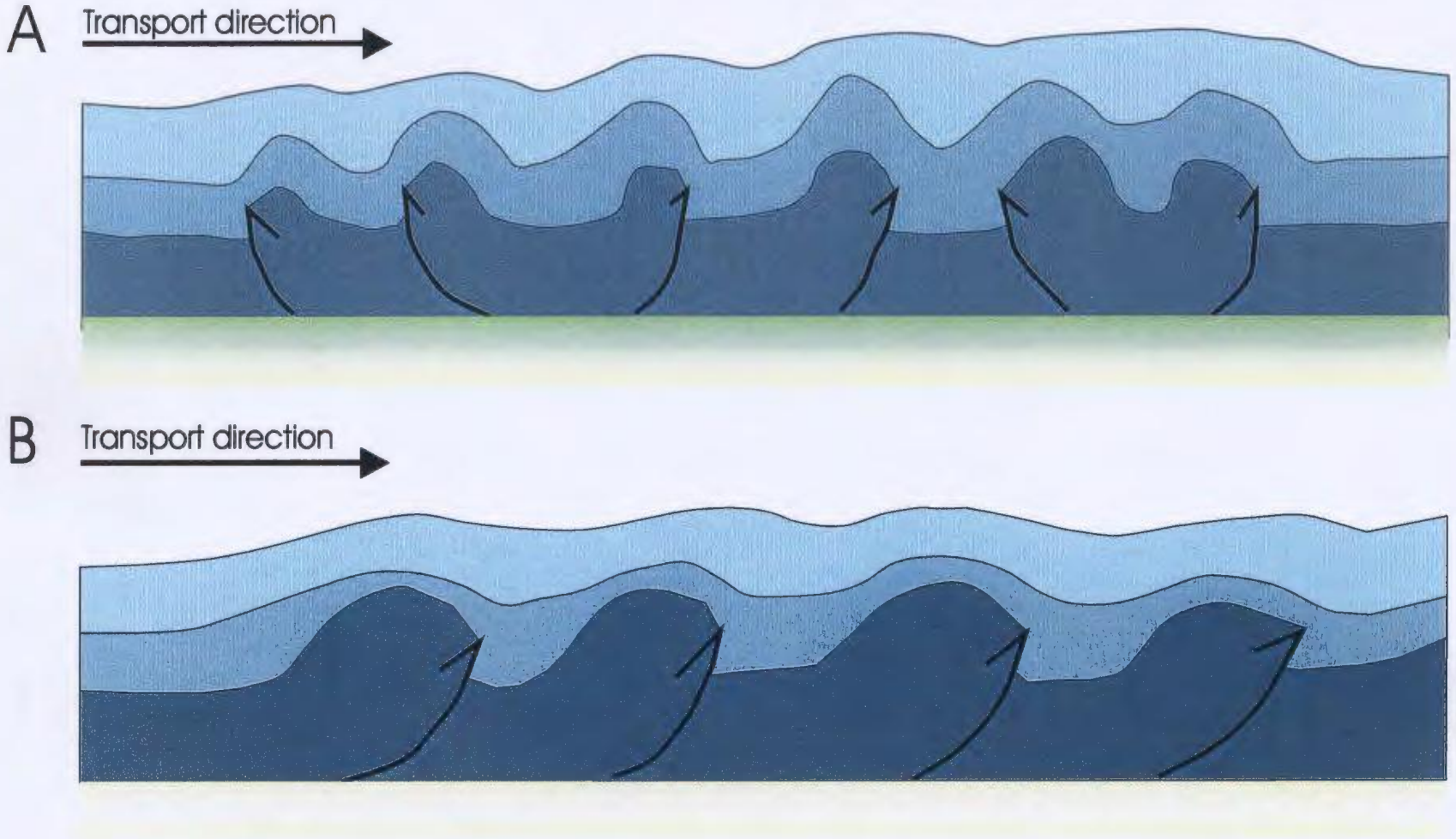

Figure 2-11: Cartoons illustrating fold-and-thrust belts underlain by salt versus nonsalt substrate. A) The thrust belt underlain by salt (green) has no preferred fault vergence B) a thrust belt not underlain by salt has a preferred vergence towards the foreland (Davis and Engelder, 1985).

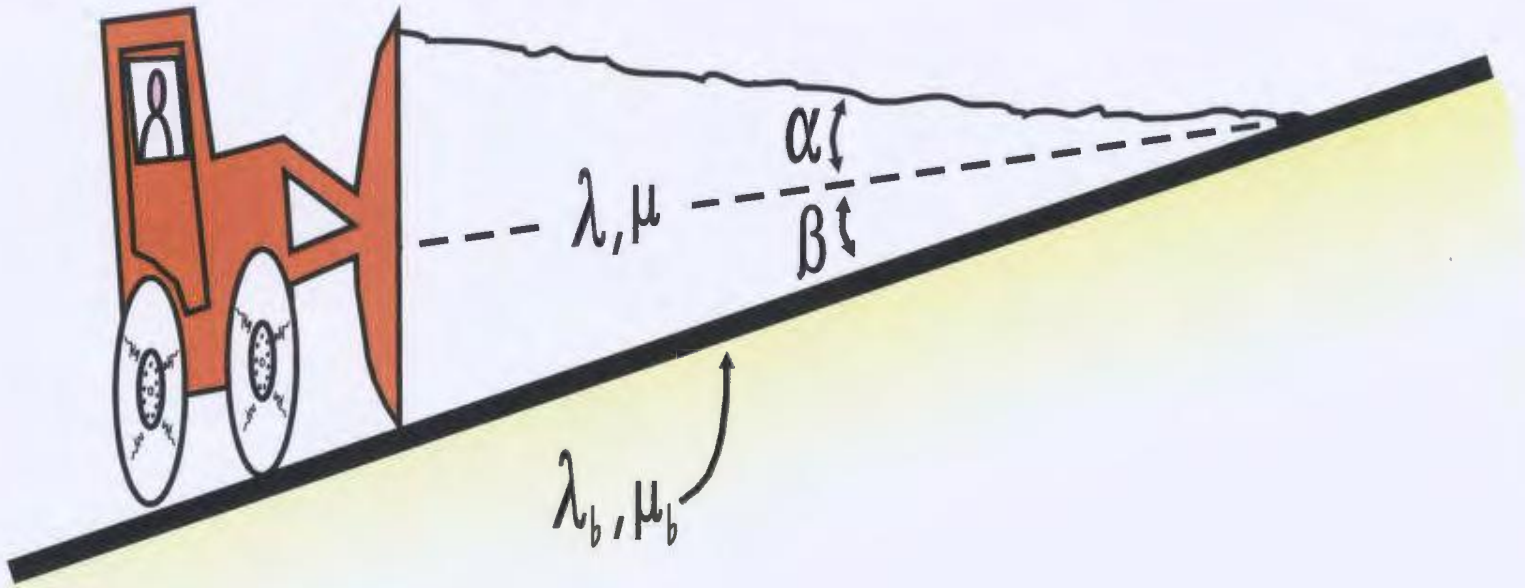

Figure 2-12: Factors influencing the mechanical deformation of fold-and-thrust belts are the same as those influencing a wedge of snow pushed in front of a snowplow.

α = topographic slope at front of fld belt

β = dip of basal detachment surface

μ = coefficient of internal friction (or internal strength of rock)

μ_b = coefficient of sliding friction (or resistance to shear)

λ, λ_b = pore fluid pressure factors (After Davis et al., 1983)

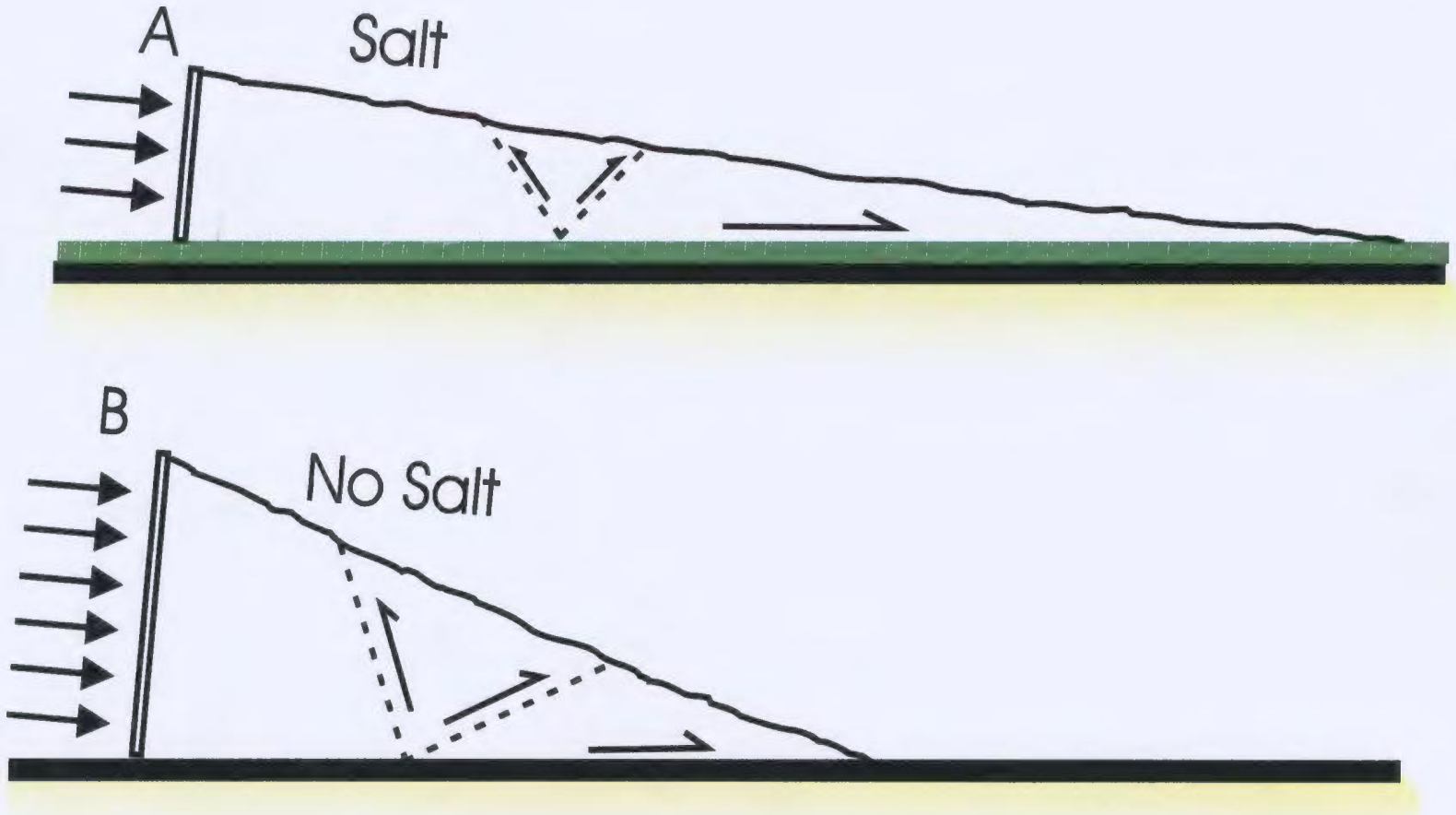

Figure 2-13: Cartoons illustrating fold-and-thrust belts underlain by salt versus nonsalt substrate. A) The thrust belt underlain by salt (green) has a narrower cross sectional taper, a wider deformational belt and nearly symmetrical structures, compared to B) a thrust belt not underlain by salt (After Davis and Engelder, 1985).

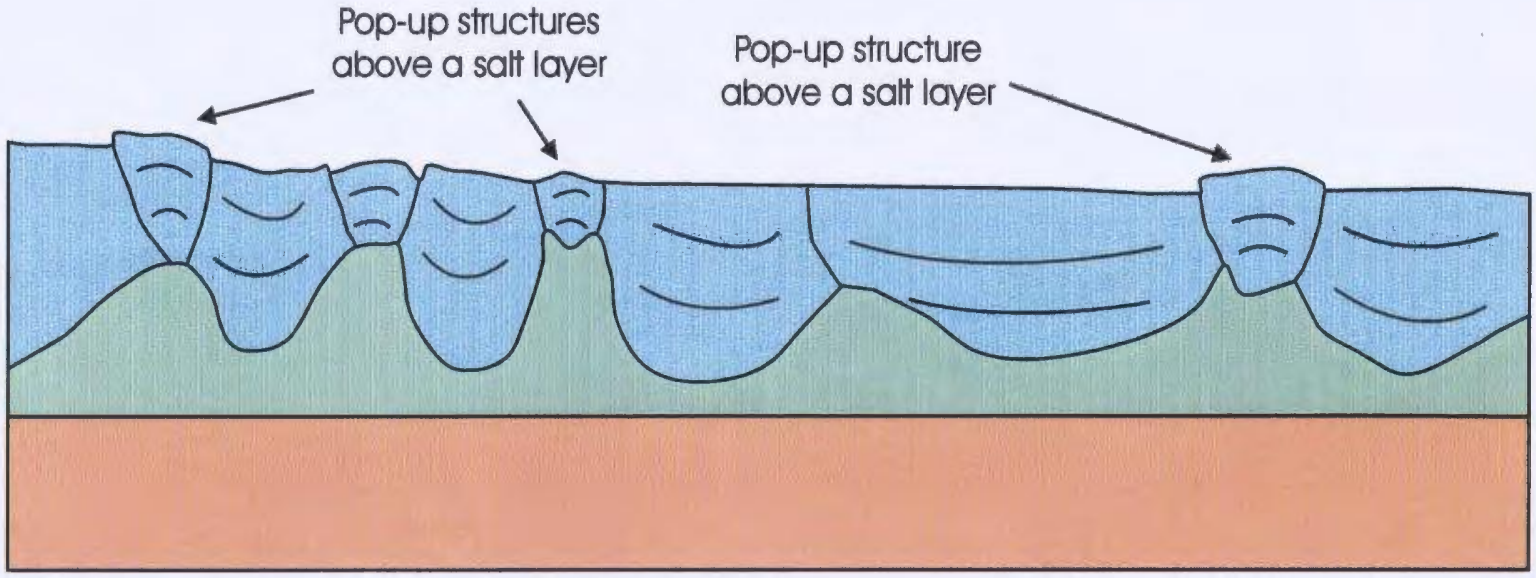

Figure 2-14: Pop-up structures may develop during folding due to growth of underlying salt structures (Modified from Letouzey et al., 1995).

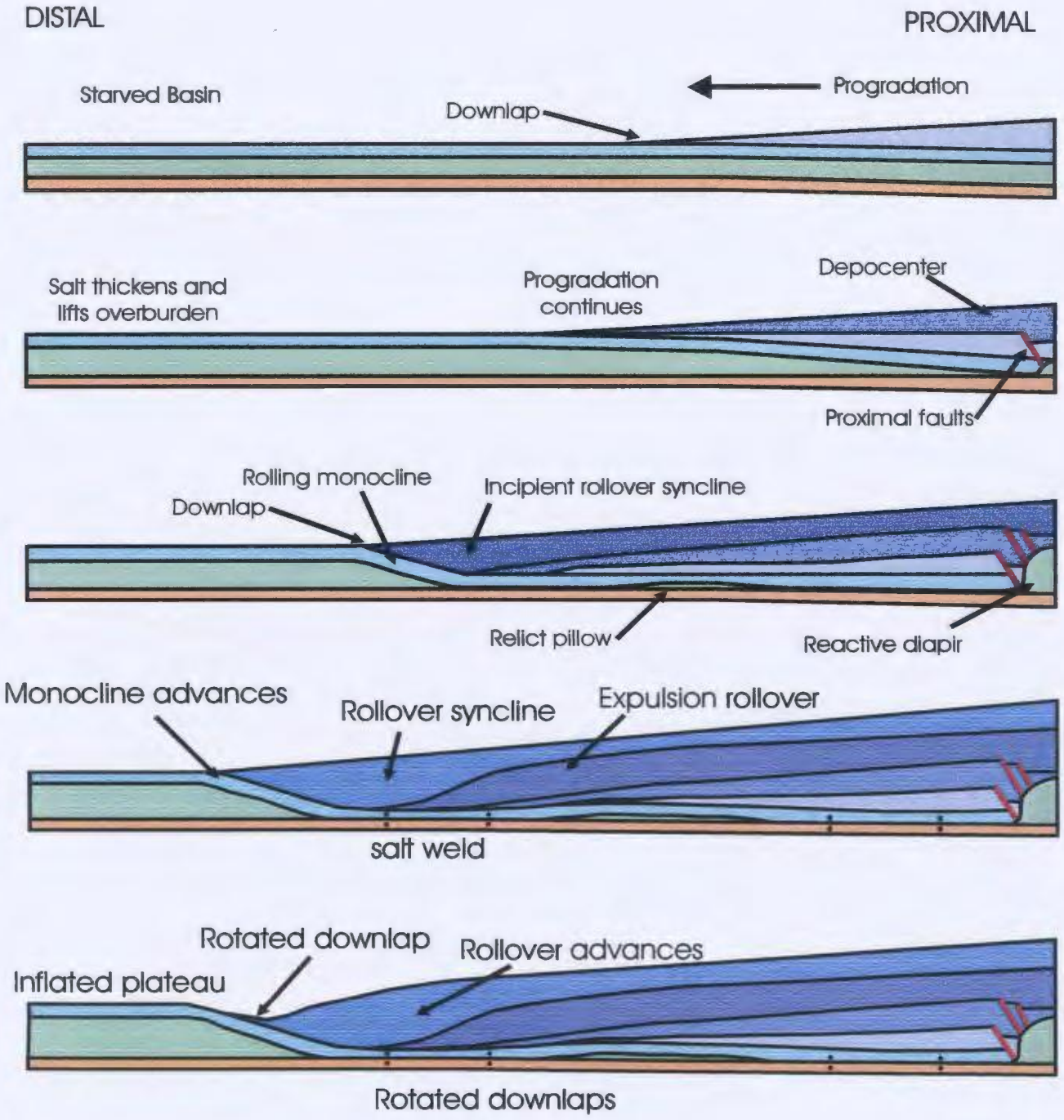

Figure 2-15: Mobilization of evaporite unit by delta progradation (from Ge et al., 1997).

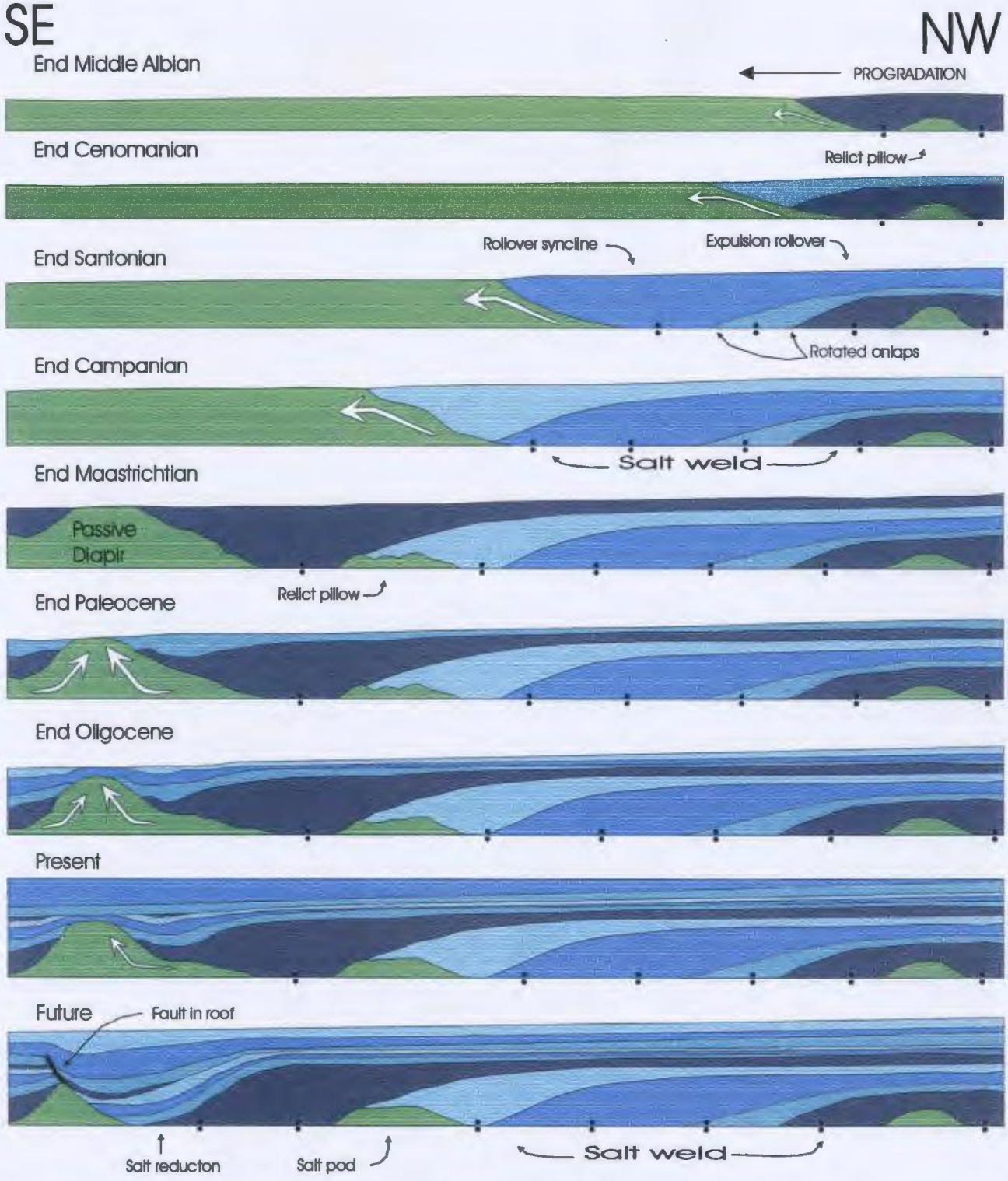

Figure 2-16: Modeling by Ge et al. (1997)and McClay et al. (1998) displaying a multistage representation of the process of differential loading over a thin overburden in an open-ended basin (from Ge et al, 1997).

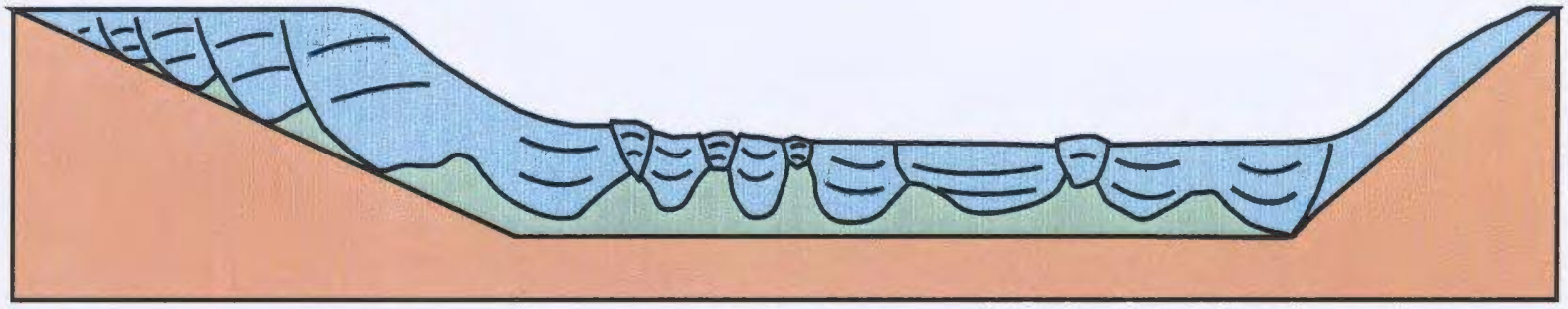

Figure 2-17: Modeling by Letouzey et al.. (1995) displayins the end result of the process of differential loading in a confined basin.

A

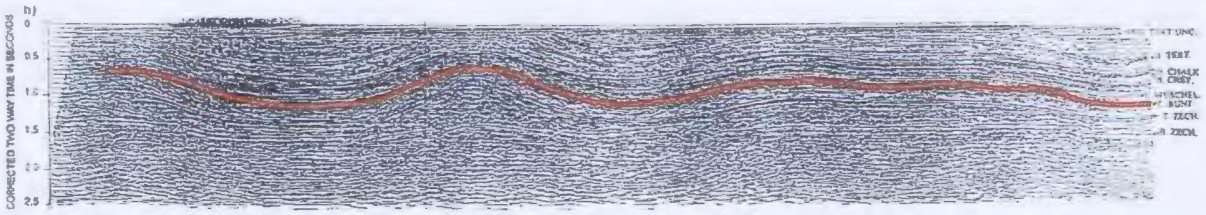

B

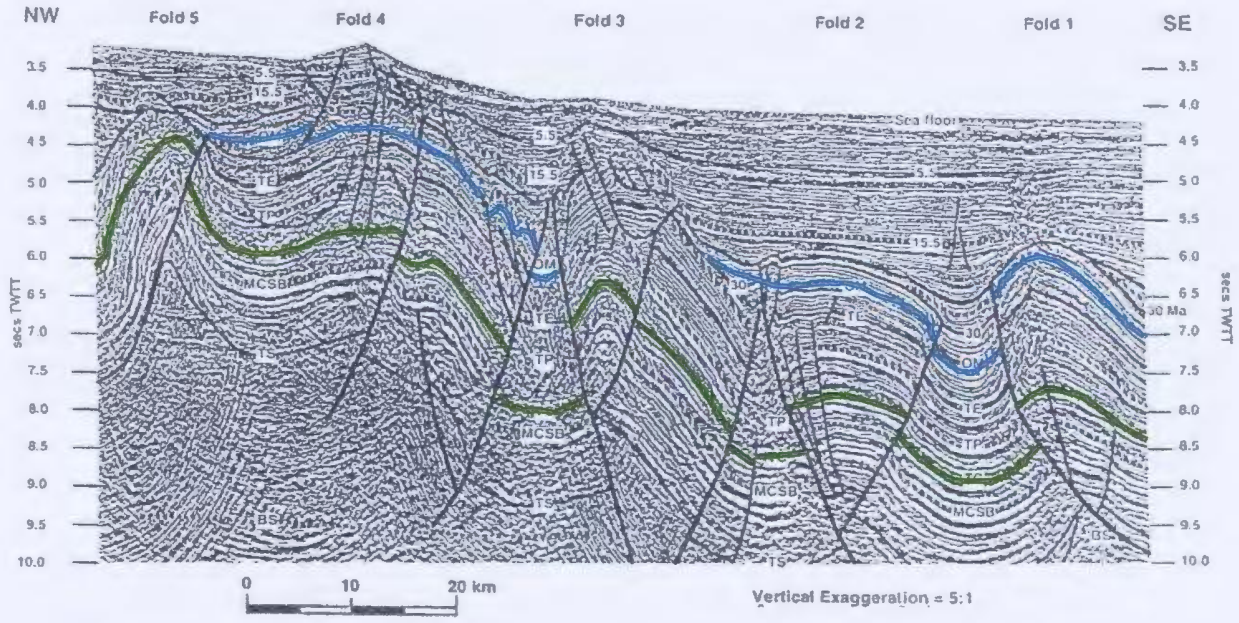

Figure 2-18: A) Seismic section showing broad, low relief buckle folds from the North Sea (Hughes and Davidson, 1993). B) Seismic section of faults breaking through crests of anticlines in the Peridido fold belt, Gulf of Mexico (Trudgill et al., 1995).

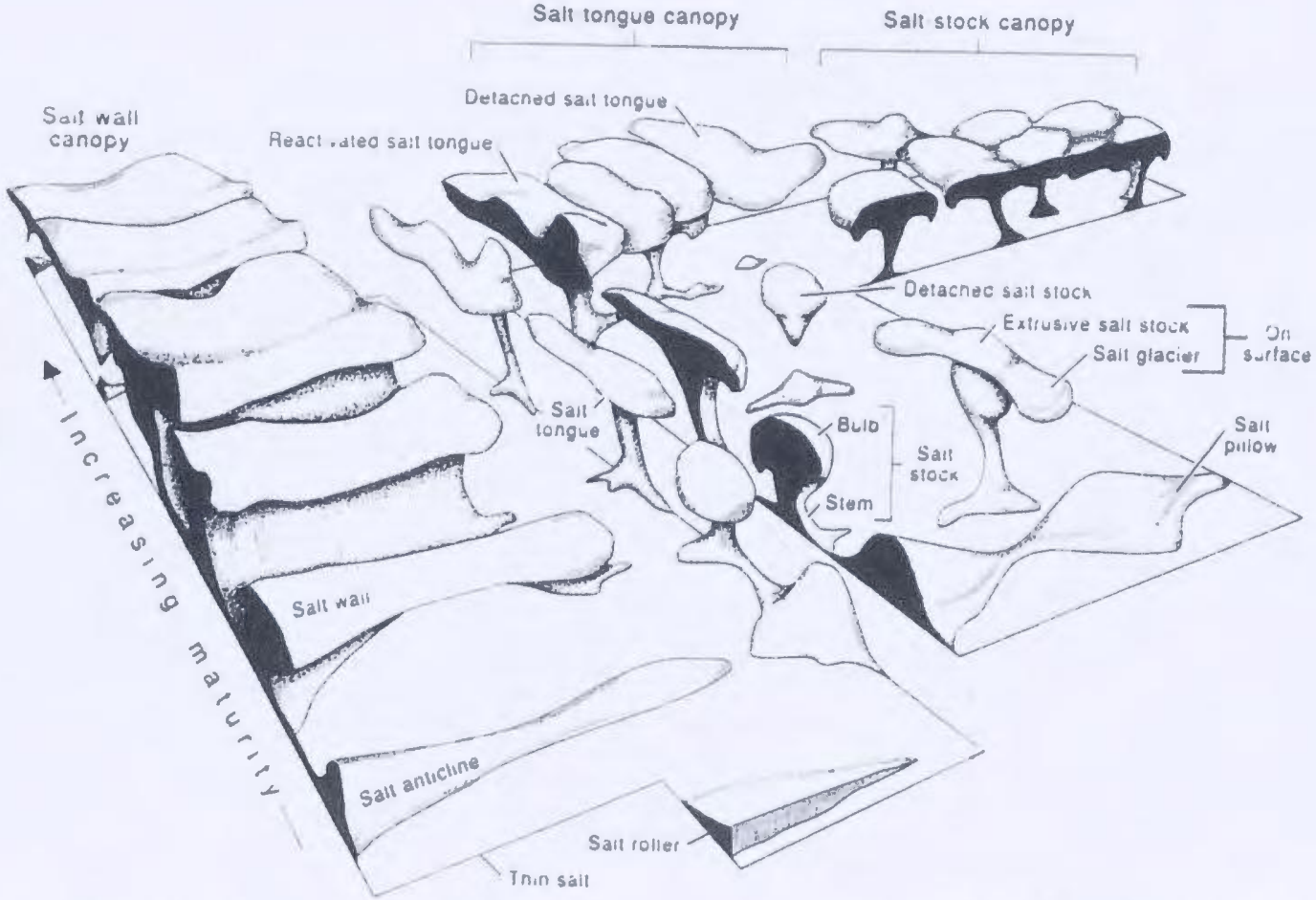

Figure 2-19: Block diagram showing schematic shapes of known classes of salt structures. Structural maturity and size increase towards the composite, coalesced structures in the background. Structures on the left are those arising from a line source; those on the right arise from a point source (Jackson and Talbot, 1991).

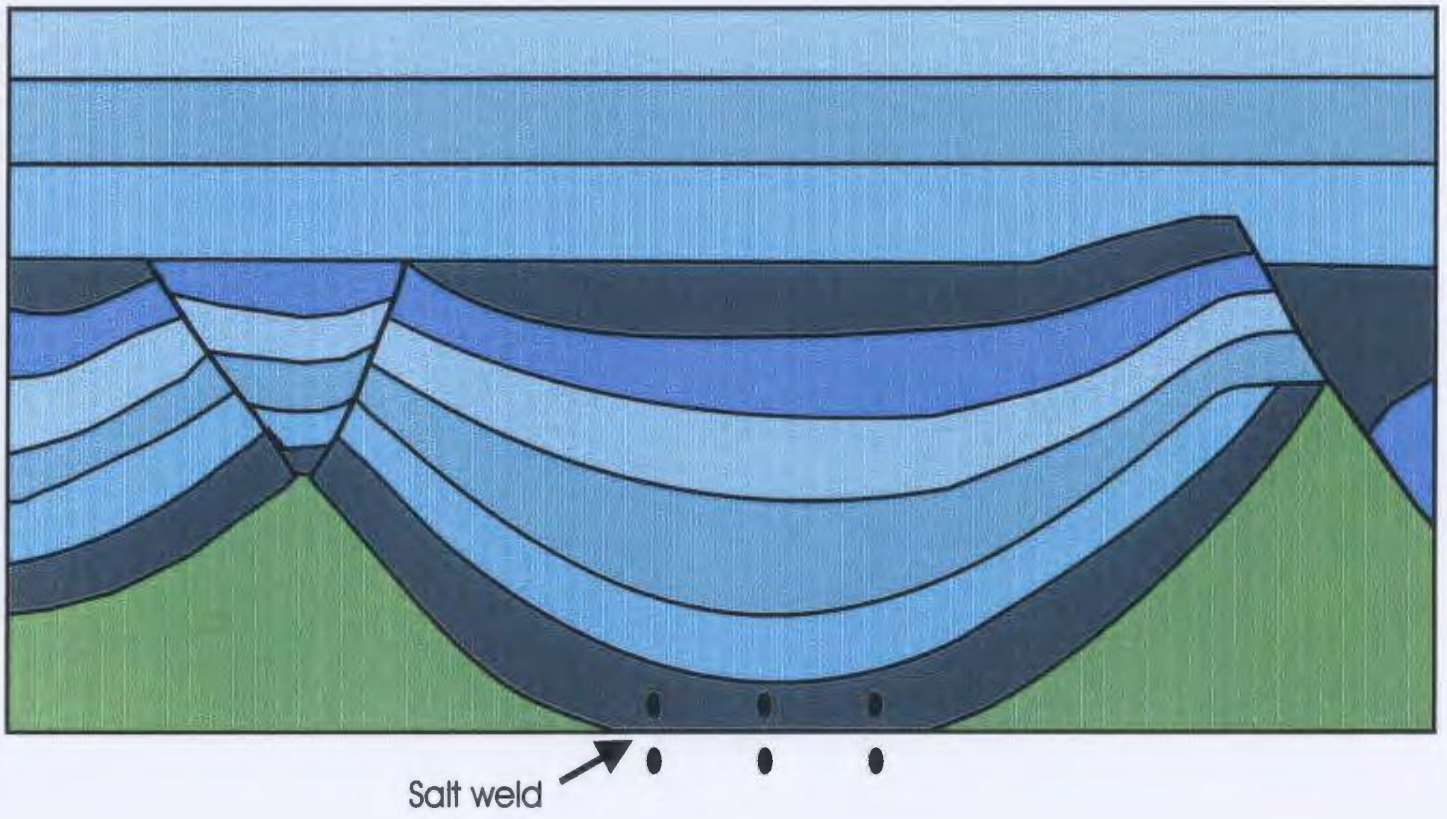

Figure 2-20: A salt weld forms in an area where the salt has been completely evacuated and strata above the original evaporite unit rest on the strata which were originally below the evaporite unit.

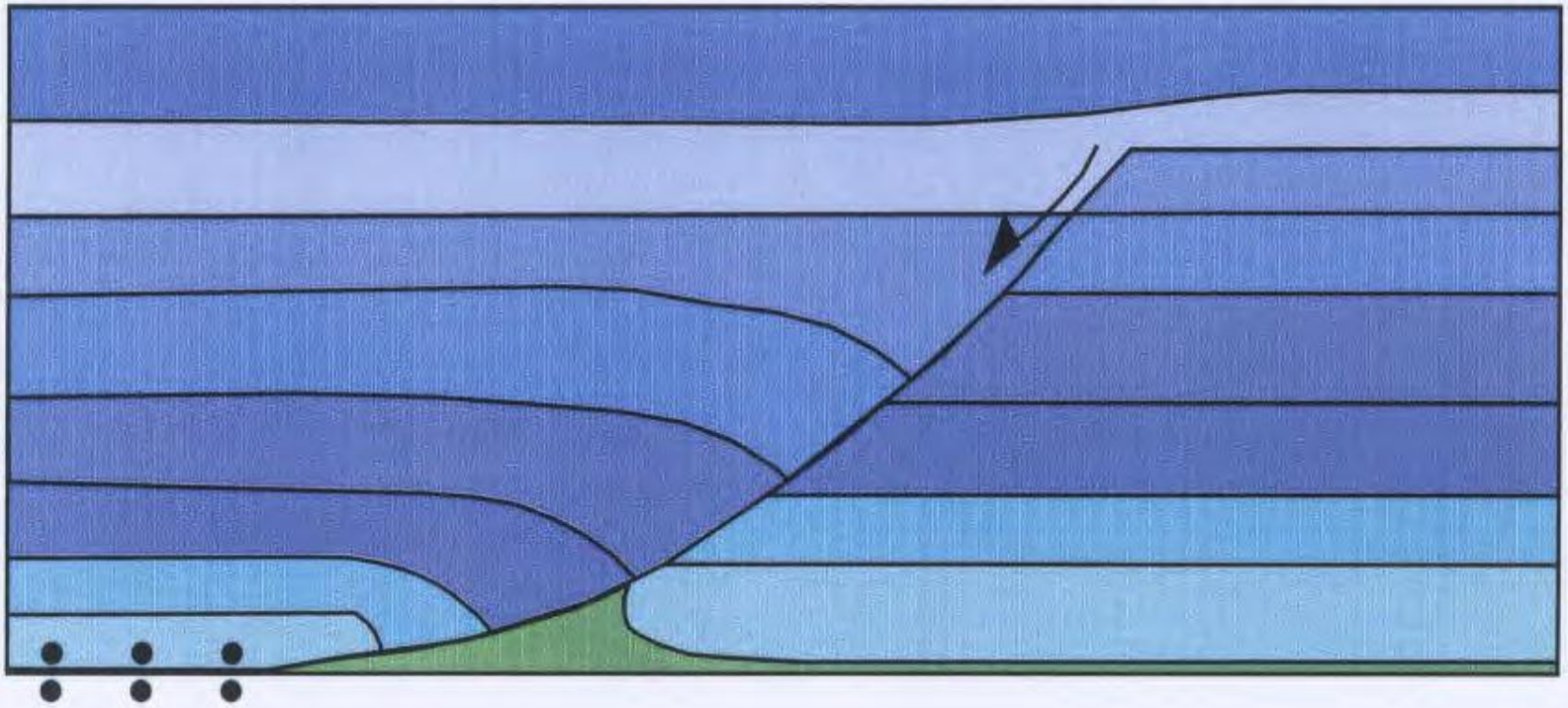

Figure 2-21: A fault weld along a listric extensional fault.

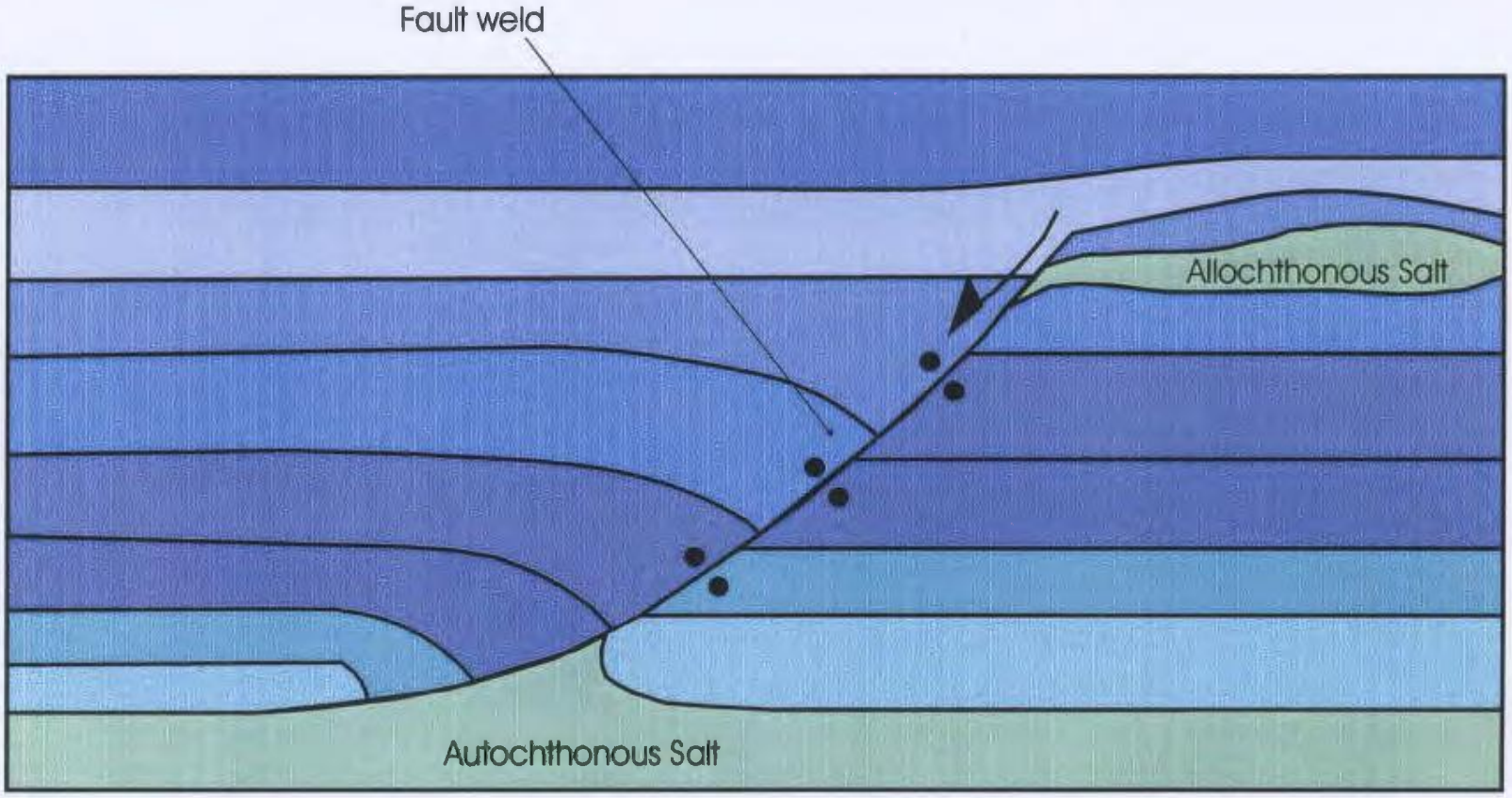

Figure 2-22: A fault weld dividing allochthonous salt from autochthonous salt.

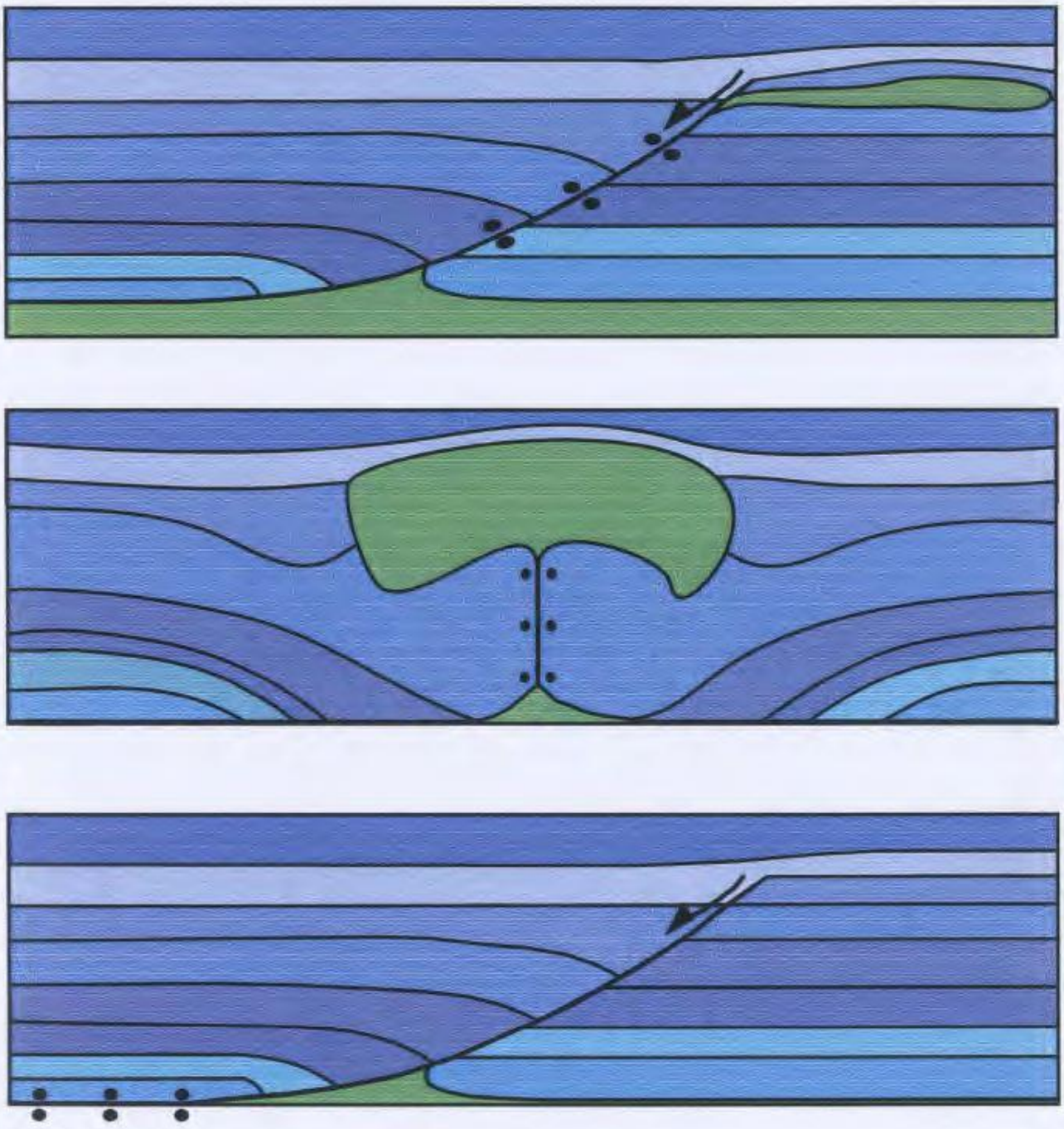

Figure 2-23: Examples of fault welds or salt welds showing various orientations (leaning, upright and horizontal).

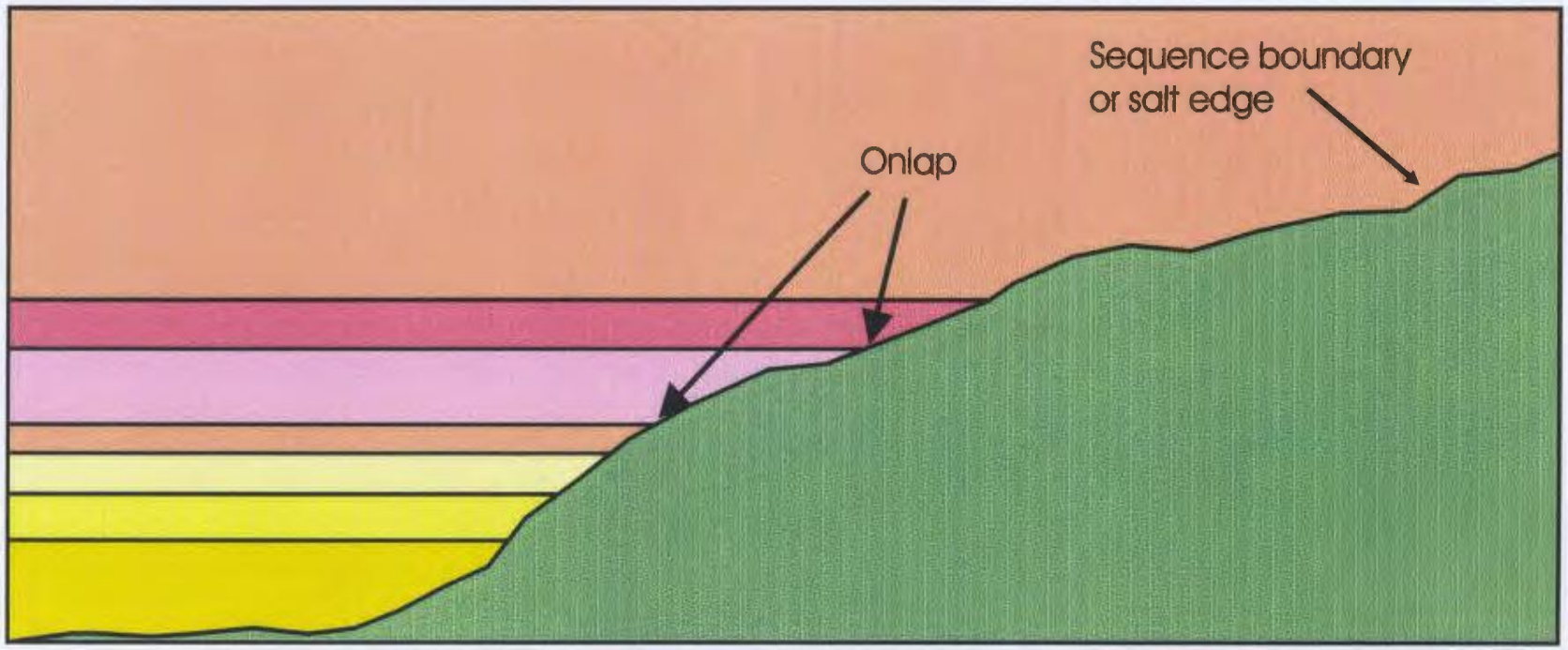

Figure 2-24: Onlap of sediments against a salt structure or a sequence boundary

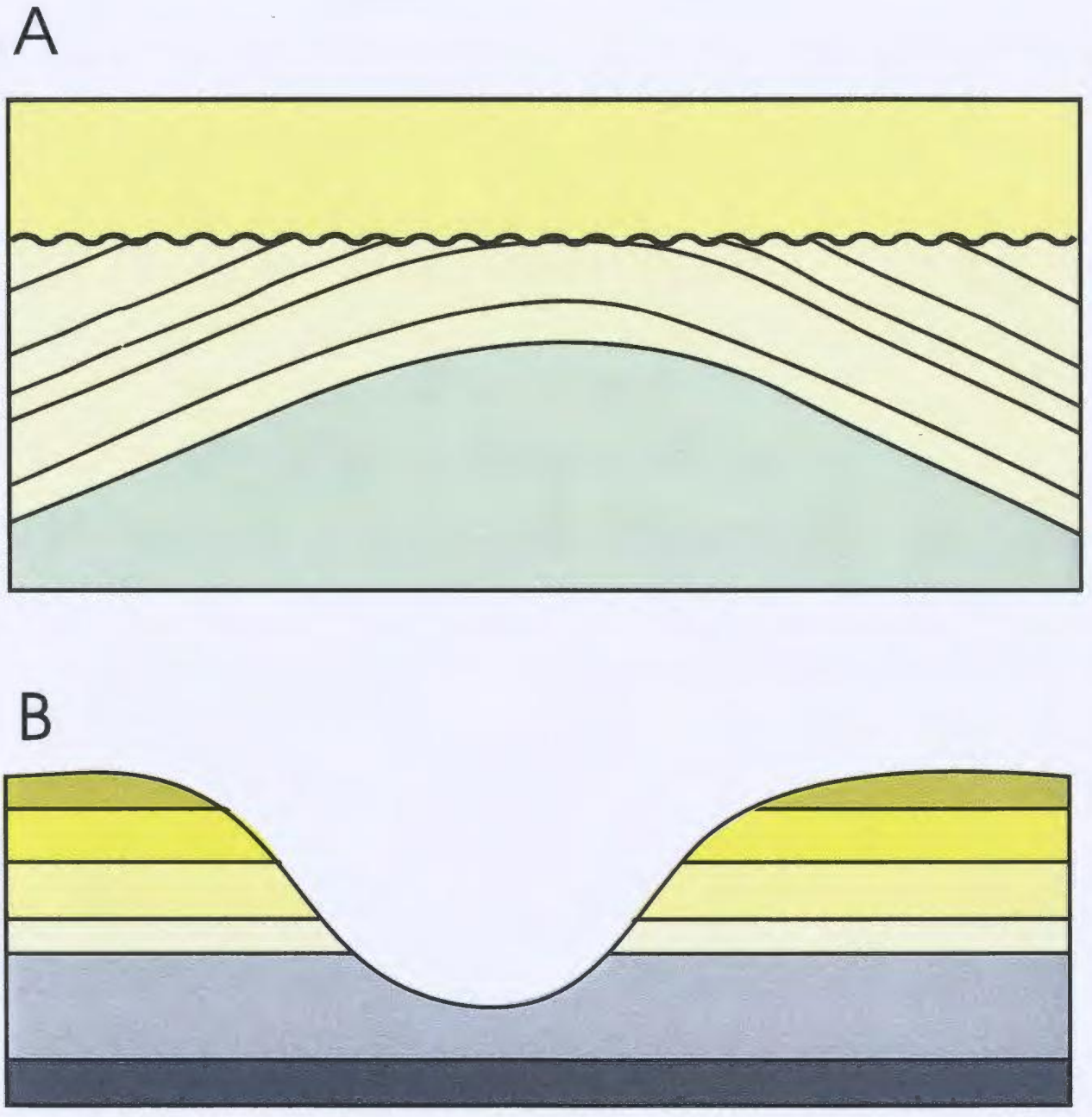

Figure 2-25: Truncation of sediments due to A) erosion (referred to as an erosional truncation) and B) downcutting by fluvial systems or their equivalent (referred to as downcutting truncation).

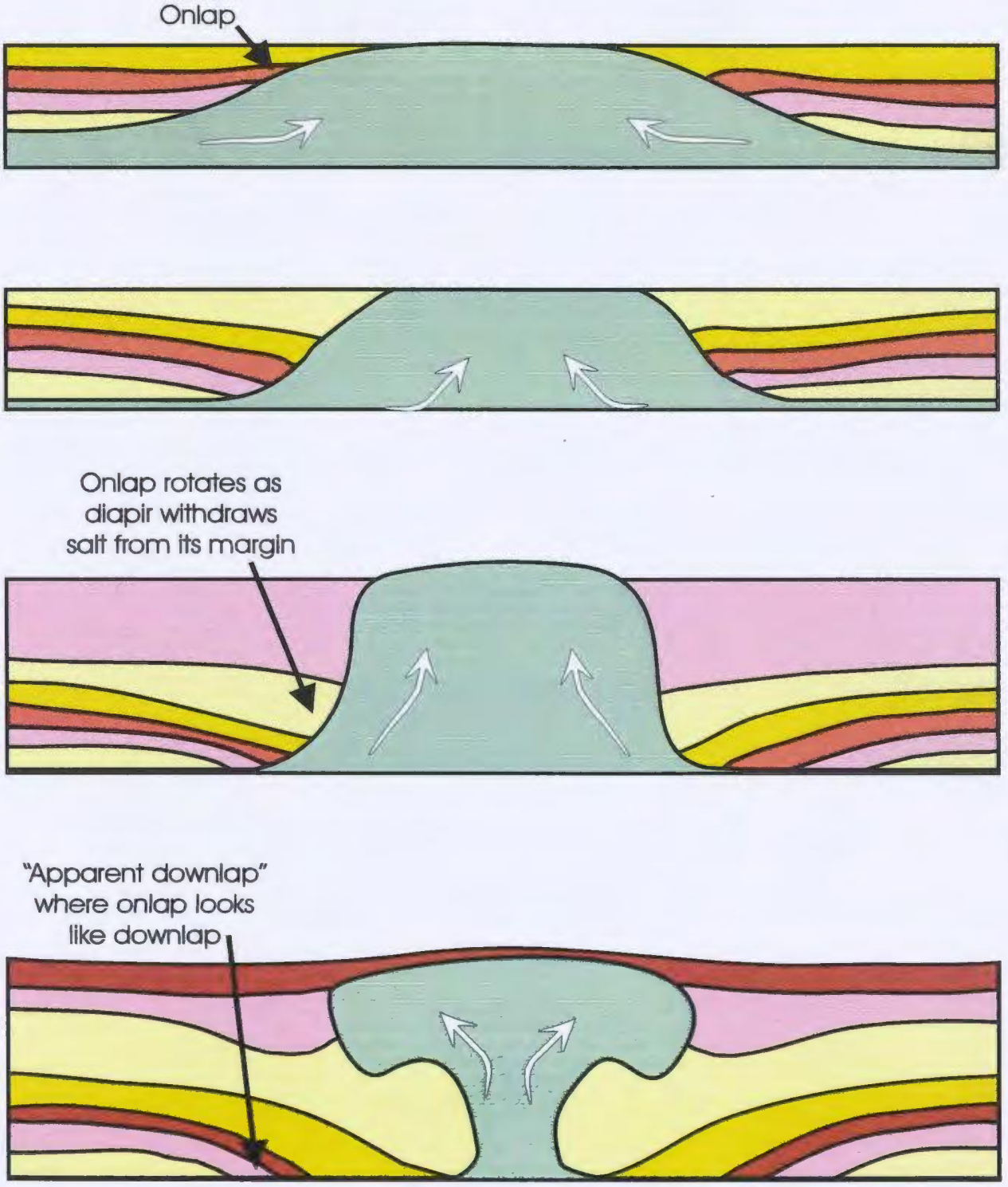

Figure 2-26: Creation of 'apparent downlap' where onlapping strata rotate as salt is withdrawn from the margin of a diapir.

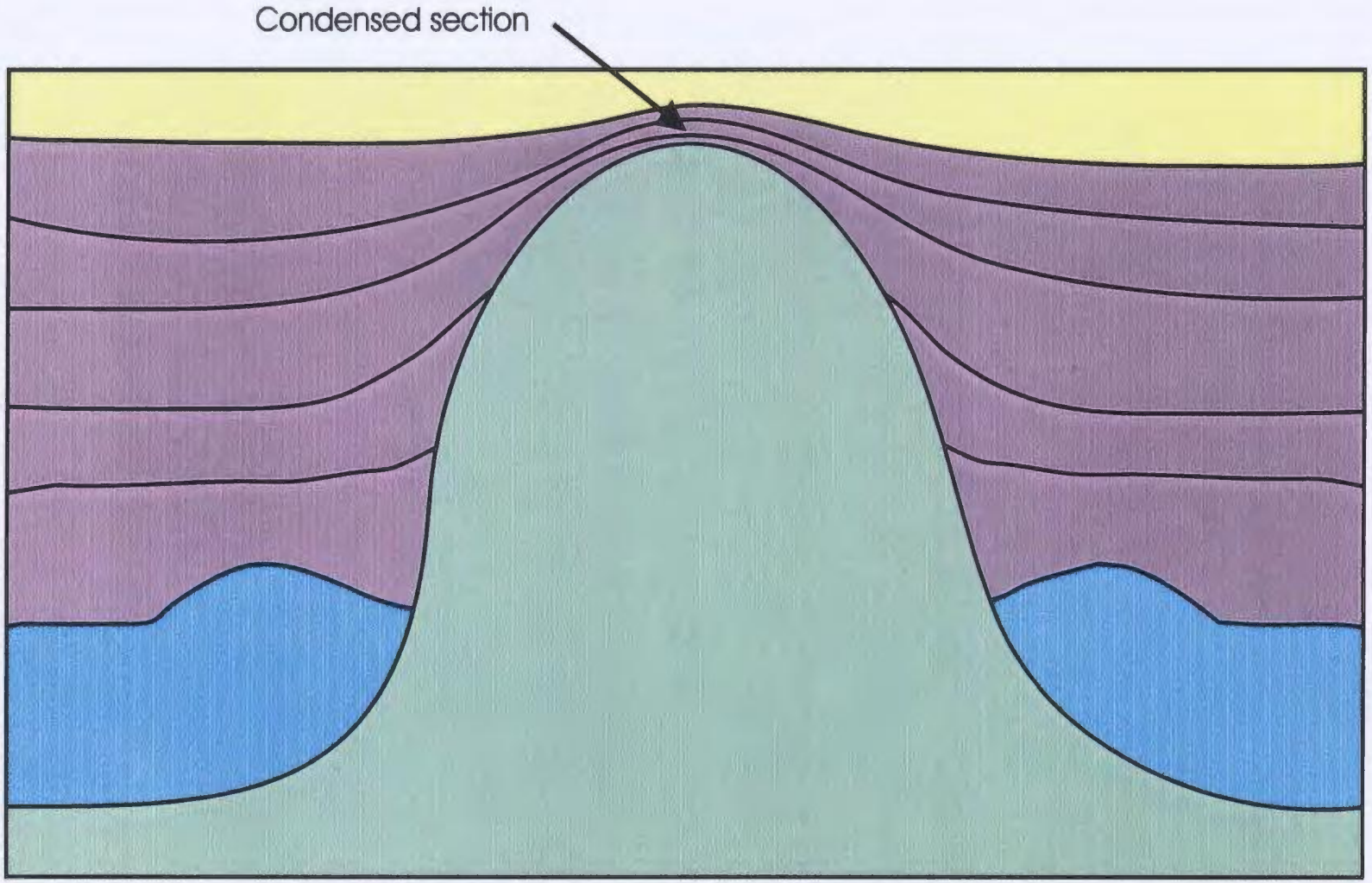

Figure 2-27: A condensed secton of strata is commonly observed at the crest of a diapir that is undergoing growth. A condensed section is a group of thinned strata that are the same as the strata to the sides of a structure, only much thinner.

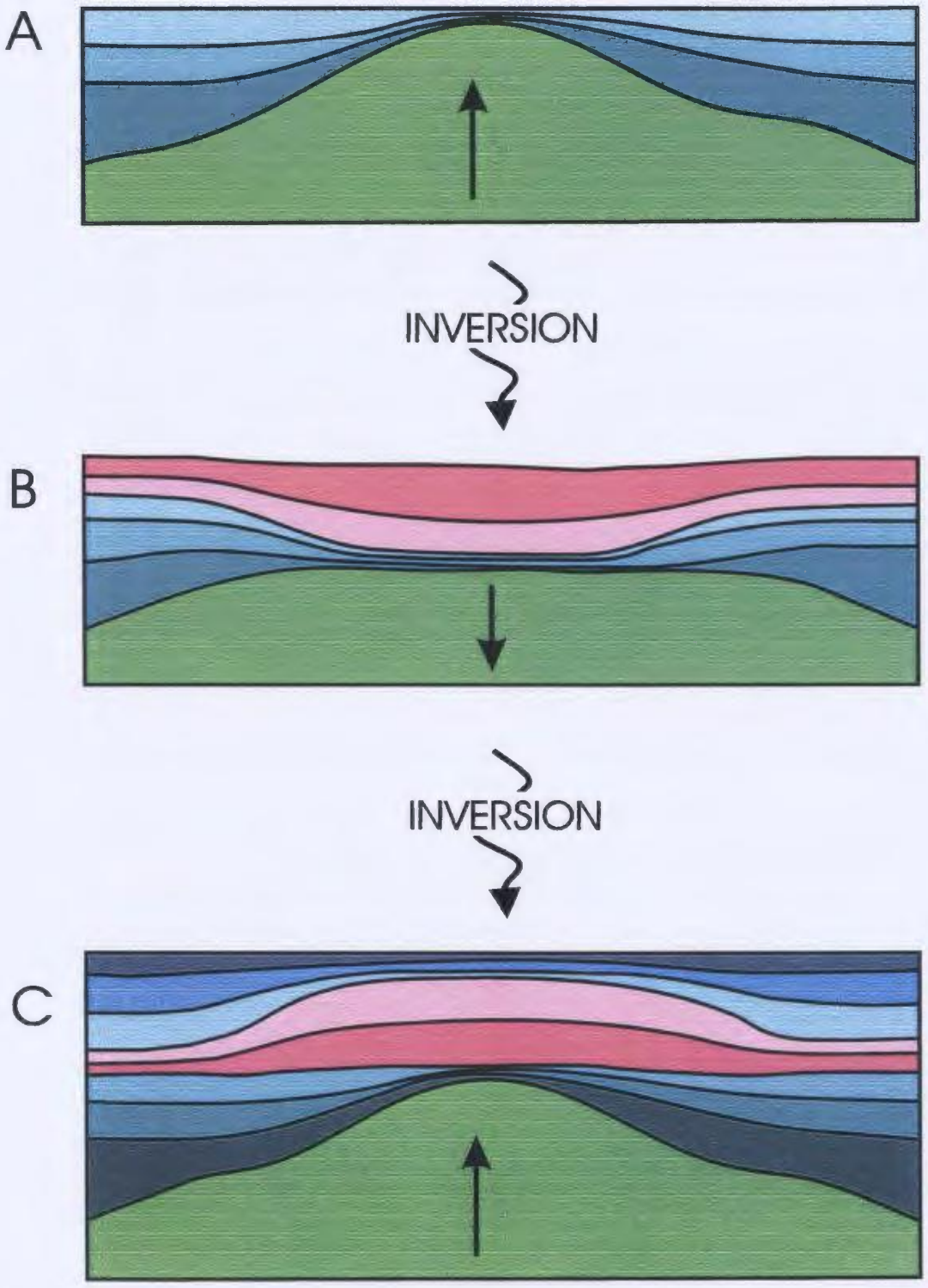

Figure 2-28: Structural inversion above a salt diapir. A) Diapir rise - thinning above diapir, truncation above diapir, inward onlap B) Diapir sag - thickening above diapir, truncation elsewhere, outward onlap; C) Renewed diapir rise - thinning above diapir, truncation above diapir, inward onlap (Jackson and Talbot, 1991).

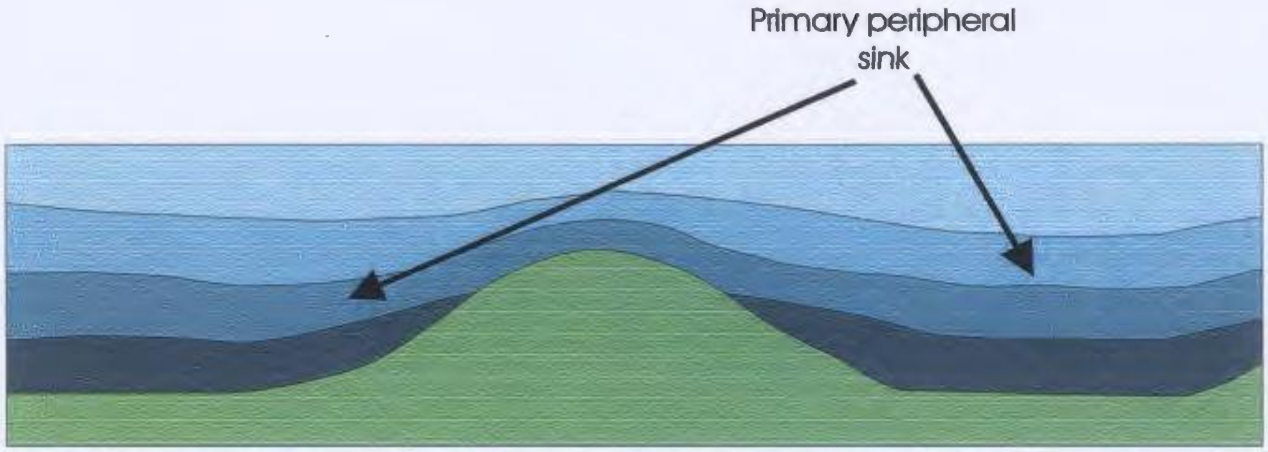

Figure 2-29: A primary peripheral sink forms when a salt pillow begins to grow and sediments thicken away from the pillow..

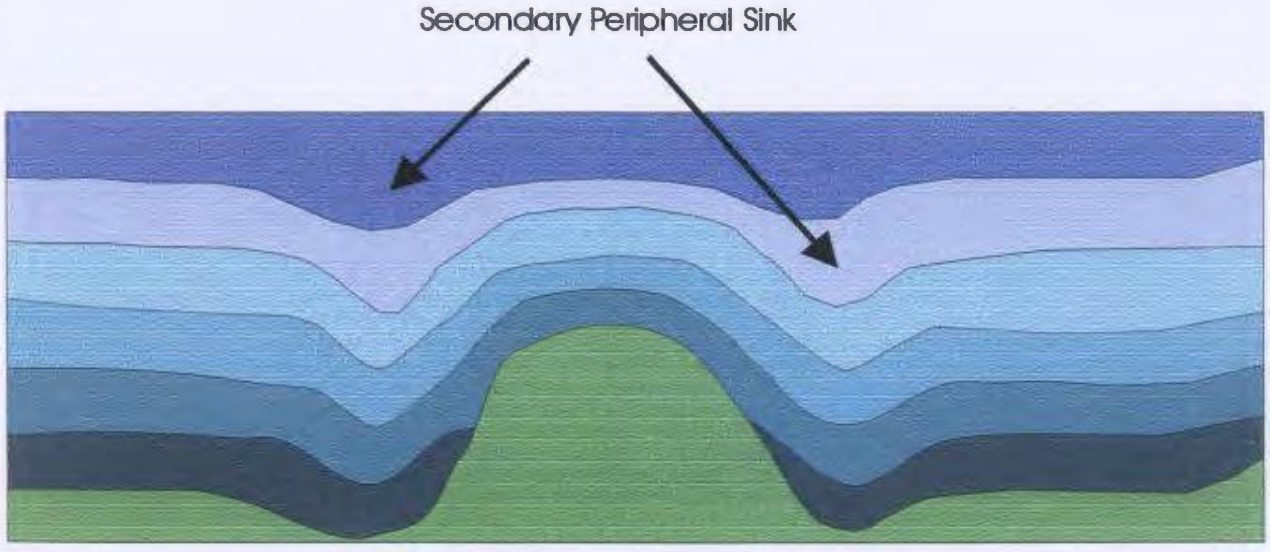

Figure 2-30: A secondary peripheral sink forms when a diapir withdraws salt from its precursor pillow and source layer causing sediments at the margins of the diapir to thicken in a sediment sink.

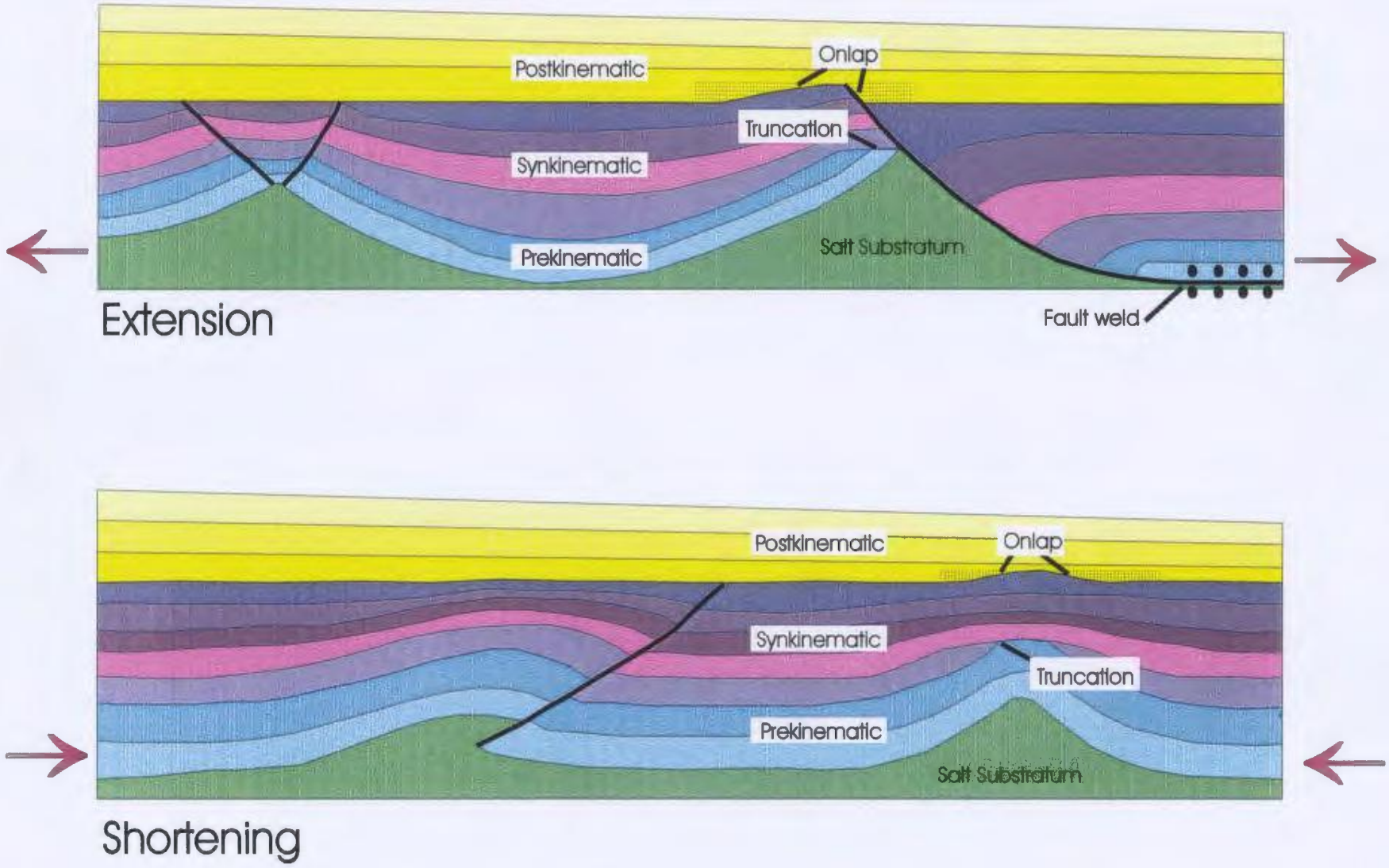

Figure 2-31: Prekinematic, synkinematic and postkinematic strata above an evaporite unit undergoing extension or shortening (Jackson and Talbot, 1991).

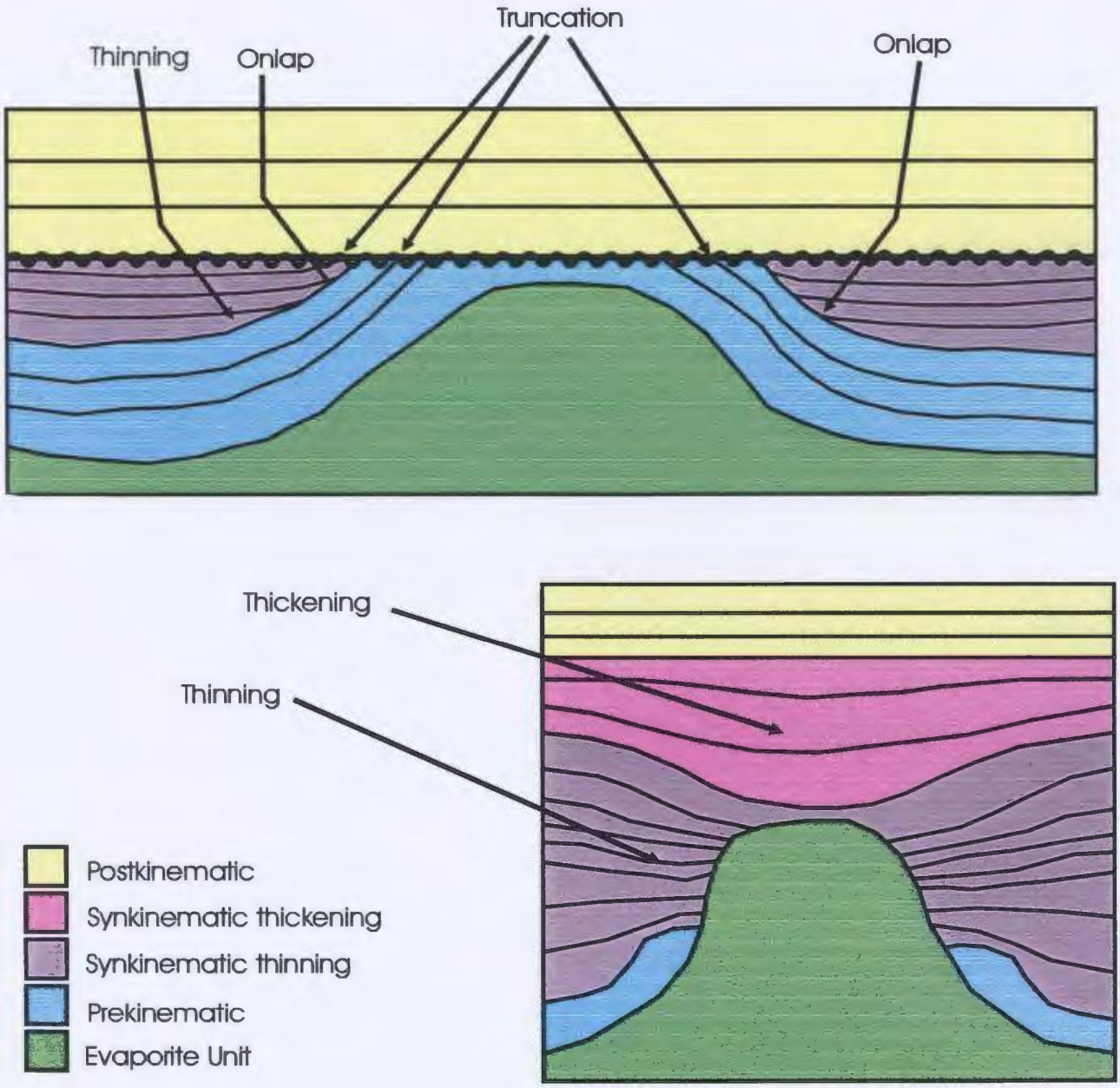

Figure 2-32: Thinning, thickening, onlap and truncation relationships in synkinematic sediments.

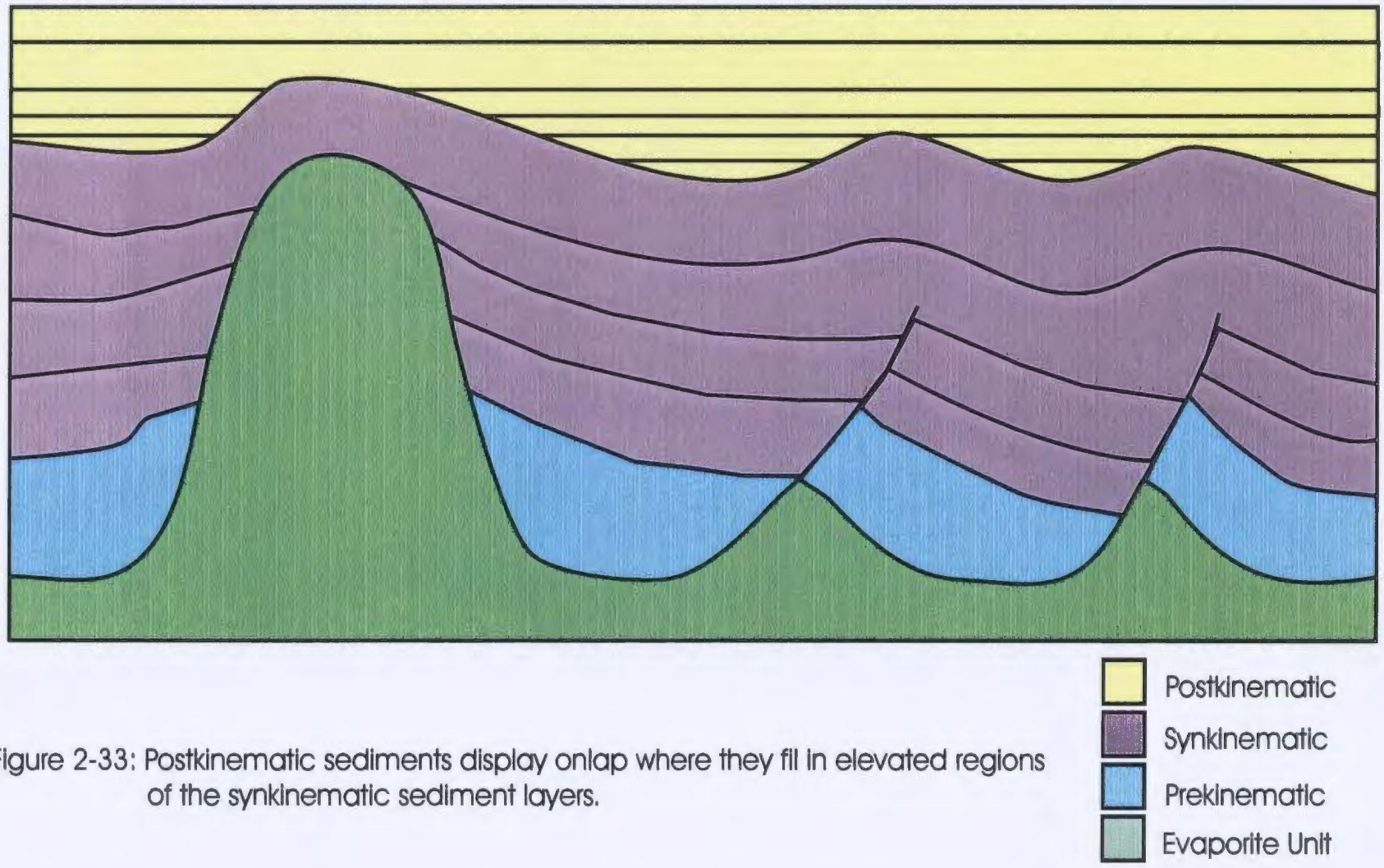

Figure 2-33: Postkinematic sediments display onlap where they fil in elevated regions of the synkinematic sediment layers.

3. DATA ACQUISITION AND TECHNIQUES

The data used in this thesis consists of i) ~1000 km of multi-channel seismic reflection profiles collected in 1991 and 1992 by Ali Aksu and Jeremy Hall (of Memorial University of Newfoundland, MUN) using the MUN seismic systems on the RV Koca Piri Reis of the Institute of Marine Sciences and Technology (IMST), ii) ~1500 km of multi-channel seismic profiles provided by the Turkish Petroleum Corporation, iii) lithostratigraphic data from 5 onshore and offshore exploration wells, provided by Turkish Petroleum Corporation.

The source for the MUN multichannel data consisted of a Halliburton sleeve gun array, operating guns of 40, 20 and 10 inches^3 (656, 328 and 164 cm^3) with a total volume of approximately 120-200 inch^3 (1966-3277 cm^3). Shots were fired at 25 m intervals with an average vessel velocity of 5.5 knots. Reflections were received on a 48 x 12.5 m multi-channel streamer; fixes were taken every 10 minutes (approximately 1.7 km between fixes). The full 48 channels of the streamer recorded the 1991 data whereas the 1992 data was collected on the nearest 12 channels of the streamer. This resulted in 12-fold (1991) and 3-fold (1992) data that was recorded digitally for three seconds (with delay dependant on water depth) at a 1-millisecond sample rate using a DFS V instrument. The multichannel data were processed at MUN, with automatic gain control, short-gap deconvolution, velocity analysis, normal move-out correction, stack, filter (typically 50-200 Hz bandpass), f-k time migration and adjacent trace sum. Despite modest source volume and fold of stack, reflections are imaged to 2-3 seconds two-way

time below seabed, even in 1500 m water depth (Aksu et al., in prep).

In this thesis, thickness variations in seismic profiles are given in two-way travel time. The following interval velocities can be used for approximate depth conversions: 1500 m/s in water, 1700 m/s in Plio-Quaternary, 4000 m/s in Messinian evaporites and 3000 m/s in pre-Messinian siliciclastic succession.

A seismic grid, with a grid spacing ranging between 4 and 22 km between seismic sections, was used to study the regional salt tectonics and the structures linked to salt features in the Cilicia Basin. Seismic sections used in this study were interpreted and analyzed using the techniques and examples of Mitchum et al. (1977), Bally (1987), and Myers and Milton (1996). Guidelines for the interpretation of salt structures and their surrounding sediments were obtained from salt tectonics and structural models established in works by Jenyon (1986), Jackson and Cramez (1989), Vendeville and Jackson (1992a, 1992b), Jackson and Vendeville (1994), Letouzey et al. (1995), Ge et al. (1997), and others.

Simple correlations were made in the study area between large-scale features such as synclines and anticlines. These features were mapped on a mylar-covered basemap in order to delineate any major basinal trends. Faults were correlated in the Cilicia Basin by following these anticline-syncline trends. Mapping of the faults was achieved by transferring the position of correlative faults onto a basemap and then connecting these fault positions with a best-fit fault trace for all of the data points along a particular fault. The resultant fault map is the simplest possible interpretation that satisfies all structures in the data set. It is not an absolute, definitive map of structures in the Cilicia Basin.

Salt structures and faults in the Cilicia Basin were mapped from seismic data based on the premise that salt and faults are often spatially associated (Jackson and Vendeville, 1994). The salt bodies were analyzed on an individual basis to determine their developmental maturity and to determine the past movement of the evaporite unit based on large-scale salt kinematic indicators in the sediments at the margins of these salt structures. The faults were broken down into a series of tectonic groupings or families based on fault classification, geometry and orientation within the basin, characteristics which are a reflection of the formation mechanism for the faults.

Salt bodies and fault families were grouped as tectonic systems in cases where there were obvious salt-fault associations or were kept as individual units in cases where such associations were not clear. These associations consisted of salt-fault interactions evident in the placement, orientation, timing of development and/or timing of reactivation of various structures in the Cilicia Basin.

The tectonic systems that were identified were initially analyzed as individual units then were linked together in a wholistic structural system that was further studied in the regional tectonic framework of the Eastern Mediterranean.

4. SEISMIC STRATIGRAPHY

Numerous works have suggested that the most appropriate unit for stratigraphic analysis of a seismic section is the depositional sequence (Mitchum et al., 1977; Myers et al., 1996). "A depositional sequence is a stratigraphic unit composed of a relatively conformable succession of genetically related strata and bounded at its top and base by unconformities or their correlative conformities"(Mitchum et al., 1977).

The boundaries of the depositional sequence, the sequence boundaries, are the surfaces marked by reflector terminations picked on the seismic lines. These entities are generally strong reflectors that are laterally continuous over large areasAccurate definition and correlation of depositional sequences requires that the sequence boundaries are delineated and traced throughout the data set using crossovers to tie intersecting seismic sections together.

The sequence boundaries are a combination of unconformities and their associated conformities within the seismic data set. An unconformity, as defined by Mitchum et al. (1977) is a surface with observable discordances showing evidence of erosion or non-deposition that separates younger strata from older strata and represents a significant hiatus.

Three such unconformable surfaces were identified within the suprasalt (above salt) strata and were correlated on the seismic grid in the study area. These sequence boundaries are referred to as SB1, SB2 and SB3 in order of age from oldest to youngest (Figs. 4-1 thru 4-3; colored peach, blue and purple, respectively). Other sequence boundaries which are easily discernable in the study area are the 'S-Reflector' (yellow)

which distinctly marks the top of the pre-Messinian (basement) successions, when it can be imaged on seismic sections (ie. when the seismic signal is not attenuated by the evaporite unit before reaching the S-Reflector), the 'N-Reflector' (cyan) which marks the base of the evaporite unit and the "M-Reflector" (green) which marks the uppermost Messinian and lies at the top of the evaporite unit where present (Figs. 4-1 thru 4-3). In localized regions, such as at basin margins or paleotopographic highs, the S-Reflector, the N-Reflector and the M-Reflector converge to form a single boundary. Such boundaries are likely the result of salt withdrawal in the basin forming a salt weld.

4.1 The S-Reflector

The S-Reflector is a fairly continuous marker that defines the top of the Messinian acoustic basement in the seismic data used in this study. In the Cilicia Basin, this reflector is clearly observed in seismic lines crossing the Misis-Kyrenia Lineament (Fig. 4-3). In parts of the Cilicia Basin away from the Misis-Kyrenia Lineament, the S-Reflector is generally not evident because it is either below the evaporite unit, and therefore poorly imaged (eg. Fig. 4-2), or because it is below approximately 3 seconds (two-way time) and is therefore masked by multiples in the seismic data.

4.2 The N-Reflector

The N-Reflector, when present, is a single strong reflector or a series of strong, parallel reflectors that mark the base of the evaporite succession in the Cilicia Basin (Figs. 4-1 and 4-3). Generally, this reflector is a poorly imaged feature in seismic

sections (Fig. 4-2), because it is located directly below the evaporite unit. The high velocity and locally great thickness of the evaporite unit result in the creation of velocity pull-ups in the N-Reflector in time sections. For interpretation purposes, a 'pseudo-depth' surface can be constructed from the imaged N-Reflector to remove the effects of velocity pull-ups (Fig. 4-4). The construction of a 'pseudo-depth base salt' enables a more accurate idea of the thickness of salt below a diapir. A pseudo-depth surface for the N-Reflector (base salt) is constructed by multiplying the thickness of the evaporite unit by a basin-wide constant and adding that value to the base salt (Rowan, 1999; Fig. 4-4). This constant is based on the velocity contrast between salt and surrounding sediments as well as the depth of burial of salt and sediments. In the Cilicia Basin a constant of approximately 1.2 seems to work well throughout the basin. The N-Reflector marks the beginning of the Messinian Salinity Crisis in the Mediterranean Sea and is probably early Messinian in age. The presence of multiples makes it difficult to determine whether this horizon is the same as the S-Reflector or if it has an onlap relationship with the S-Reflector in this region (Fig. 4-3).

4.3 The Evaporite Unit

The evaporite unit of the Cilicia Basin is a combination of gypsum, anhydrite and halite (Yalçin and Görür, 1984). In coastal portions of the Cilicia Basin these evaporites may be in the form of carbonates rather than the gypsum, anhydrite or halite that was found in central regions of the basin. The evaporite unit generally images as a series of discontinuous, varying amplitude seismic reflectors (Figs. 4-1 thru 4-4). These reflectors

are parallel and horizontal over much of the data set; however, in various salt structures throughout the Cilicia Basin these reflectors are tilted or dipping mimicking the surface topography of the evaporite unit (Fig. 4-4). Locally there are strong, high-amplitude reflectors within the evaporite unit (Figs. 4-1 thru 4-5). These strong reflectors may represent muddy intervals where marls and shales may have been intermittently deposited during episodes of basin refilling and desiccation. Alternatively, these high amplitude reflectors may mark the presence of a distinct marker interval composed of chalky massive limestone containing *Discospirina* foraminifera. This marker interval has widespread occourence in the upper Miocene strata in Cyprus (Orszag-Sperber et al., 1989), and lies in the upper part of the Miocene Pakhna Formation of the Dhali Group. If this is the case, the evaporite unit identified on seismic sections in this study actually represents not only the Messinian evaporites but may also include shaly, sandy and/or shelly limestones, chalk-marl beds, calcarenites, coarse conglomerates or reef facies of the upper Dhali Group. The *Discospirina* marker is approximately 15 to 30 m thick in areas of northwest Cyprus and may be interlayered with marly shales for a total thickness of greater than 50 m (Bagnall, 1960). This marker horizon may be resolved in seismic if it is predominantly composed of massive limestone. A 50 m interval of such a composition would create a substantial velocity contrast between the marker and surrounding evaporites that would be easily identified in high-resolution reflection seismic.

Regardless of its composition, this marker bed locally exhibits a somewhat disorderly expression within the evaporite sequence. Closer analysis reveals that this is in fact due to a system of northward-directed, low-angle thrust faults and related folds that

occurs within the evaporite sequence (Fig. 4-5). It is referred to as the "Intra-Salt Fold/Thrust family" and is discussed in detail in Section 5.2.

The evaporite unit displays three external forms as described by Rowan (1999). These are: sheeting, wedging and mounding. The sheet geometry is that of undisturbed or weakly disturbed evaporites whereas wedges and mounds reflect the disturbed character of evaporites as salt rollers, salt pillows and salt walls.

The evaporite sequence exhibits an onlap relationship with pre-Messinian strata at the edges of the Cilicia Basin (Fig. 4-3). The basinal onlaps indicate that the basin edges were elevated with respect to deposition during the Messinian. This conclusion is in agreement with the findings of Mulder et.al. (1975) and Biju-Duval et al. (1979).

Downcutting truncations are observed in the northern part of the Cilicia Basin where channels cut into the top of the Messinian evaporite sequence (Fig. 4-6). These channels, located immediately south of Turkey, are filled with younger, early Pliocene sediments. Similar Pliocene-filled channels are described from Corsica, Crete, Algeria and Cyprus in studies by Aleria (1980), Delrieu et al. (1993), Rouchy et al. (1980; Figure 1-9). These channels likely cut into Messinian evaporites in the process of feeding lower, more central regions of the Mediterranean Basins.

The extent of evaporite distribution in the Cilicia Basin has been mapped from seismic sections (Fig. 4-7). This limit is mapped at the merging point of the base salt and top salt reflectors (N-Reflector and M-Reflector, respectively) at the basin edges. This distribution map represents the *minimum* basin area during the Messinian and does not consider the potential for salt withdrawal (and the subsequent formation of salt welds) at

the basin margins (Fig. 4-8). This evaporite distribution map can be used to estimate the approximate shape of the Cilicia Basin during the deposition of evaporites. Once again, extreme caution must be taken when making these estimations because evaporites may have originally extended much further into the present-day onland regions than is indicated by the Messinian minimum basin area map.

4.4 The M-Reflector

A distinct seismic reflector can be observed on all seismic lines utilized in this study. This easily discernable sequence boundary has been referred to as the 'M-Reflector' by Ryan (1969). The M-Reflector is present not only in the Cilicia Basin, but throughout the entire Mediterranean area. This marker has been identified during deep sea drilling (DSDP) as the top of a Messinian evaporite sequence (Hsü et al., 1978). The M-Reflector is a prominent, well-defined and continuous reflector or series of reflectors that mark an erosional unconformity between the Miocene and Pliocene epochs in the eastern Mediterranean (Figs. 4-1 thru 4-5). It is important to note that this marker does not necessarily provide a latest Messinian time equivalent horizon throughout the study area, because erosion was not of equal magnitude throughout the basin. The M-Reflector locally displays angular unconformity with the Messinian evaporite succession (Fig. 4-5). This sequence boundary may actually be a salt weld in some regions, especially in areas where evaporites have been removed from the basin margins or the margins of large salt structures by salt withdrawal in order to feed the growing salt structures. In such cases the S-Reflector, the N-Reflector and the M-Reflector all collapse to form a single seismic

reflector that represents areas where salt is absent (a salt weld).

4.5 Depositional Sequence A

Depositional Sequence A is a diverse sedimentary package with moderate to low seismic reflectivity that is located directly above the evaporite sequence. This depositional sequence has parallel, converging and diverging reflectors, as well as transparent regions with no discernable internal reflections at all (Fig. 4-1). Locally this depositional sequence displays onlap, toplap (offlap), downlap and truncations.

Most reflectors in Depositional Sequence A terminate against the margins of the basin in an onlap relationship (Figs. 4-3 and 4-9). These reflectors generally overstep the basin edges of salt (collapsed S, N and M-Reflectors) indicating that the basin deepened between evaporite deposition and the onset of sediment deposition. A prominent onlap geometry is observed at the basin edges indicating the presence of a paleoslope that exists at the basinal terminus. Away from the basin margins, Depositional Sequence A displays onlapping in a basin-fill reflector sequence. This depositional sequence fills depressions and channels in the top of the evaporite unit, producing onlap with the underlying evaporites as topographic lows are filled with sediment (Figs. 4-3 and 4-9).

Depositional Sequence A displays progradational sedimentation in a northwest to southeast oriented seismic section (Fig. 4-1) located at the northern boundary of the Cilicia Basin. The nearshore progradational sediments have a sigmoidal profile in seismic sections; distal sediments have oblique profiles in the seismic sections. This progradational sequence exhibits offlap (toplap) and downlap relationships with the

upper and lower sequence boundaries respectively (Fig. 4-1).

In general, Depositional Sequence A maintains a relatively constant thickness over the study area. In areas where Depositional Sequence A does not maintain constant thickness, it is thinned by onlap at basin edges, or onlap or truncation against salt features within the basin (Figs. 4-3 and 4-10). Also, Depositional Sequence A locally thickens due to growth at extensional faults (Fig. 4-11).

4.6 Sequence Boundary 1

Sequence Boundary 1 is an erosional unconformity that is marked by the first high amplitude reflector immediately above the low amplitude reflectors of Depositional Sequence A (Figs. 4-1 and 4-2). This continuous reflector locally terminates reflectors of Depositional Sequence A and is commonly onlapped by Depositional Sequence B. Sequence Boundary 1 falls within the Pliocene sequence. In the north, this sequence boundary terminates along the northernmost shelf edge of the Cilicia Basin near the southern coast of Turkey. To the south, this sequence boundary terminates against the Misis-Kyrenia Lineament in the eastern, inner Cilicia Basin or, in the western Cilicia Basin, this sequence boundary terminates against an apparent basement high near the central portion of the outer Cilicia Basin (Fig. 4-12).

4.7 Depositional Sequence B

Depositional Sequence B is Pliocene in age, consisting of a series of high amplitude, continuous, parallel reflectors that locally display diverging and converging

reflections (thickening and thinning of the sedimentary package) above salt features. This depositional sequence appears to maintain constant thickness over large areas within the contractional domain (Figs. 4-4 and 4-5), but locally may display onlap and/or thinning relationships with Sequence Boundary 1 at thrust-cored or fold-cored culminations within Depositional Sequence A (Fig. 4-13). Depositional Sequence B locally displays growth (thickening) in the extensional domain at the sides of salt structures and in the hanging walls of many listric faults (Fig. 4-14).

In the outermost Cilicia Basin, Depositional Sequence B terminates against east - west trending transtensional faults at the N and S margins of the basin. Just east of this area, still in the outer basin, this depositional sequence terminates against dominantly extensional faults (with possible minor strike-slip components) over the remainder of the outer basin. To the south, Depositional Sequence B appears to continue over the top of the Aksu-Kyrenia Lineament at the outermost Cilicia Basin. In the remainder of the outer Cilicia Basin (i.e. the innermost portion of the outer basin), this depositional sequence pinches out towards, and is terminated at, a transtensional fault zone at the northern edge of the Kyrenia Range in Cyprus.

In the inner Cilicia Basin, Depositional Sequence B commonly exhibits internal downlapping reflectors that indicate progradation off the shelf and slope areas near southern Turkey. In the south, this depositional sequence also thins toward the Misis-Kyrenia Lineament where it terminates against the same transtensional fault zone that bounds the outer basin.

4.8 Sequence Boundary 2

Data from exploration wells drilled by the Turkish Petroleum Corporation (Türkiye Perolleri Anonim Ortaklığı, TPAO) in the innermost Cilicia Basin (Fig. 1-13) indicates that Sequence Boundary 2 approximately defines the boundary between the Pliocene and Pleistocene intervals. As there is no well control in the outer portion of the Cilicia Basin, it can only be assumed that Sequence Boundary 2 will continue to define the Pliocene-Pleistocene boundary in the Outer Cilicia Basin. Sequence Boundary 2 is a continuous, high amplitude reflector that is present over the entire Cilicia Basin. This reflector is the uppermost, high amplitude reflector in Depositional Sequence B (Figs. 4-1 and 4-2). It terminates at the edges of the basin and also terminates against the Misis-Kyrenia Lineament. Sequence Boundary 2 is also located in small basinal regions located between peaks at the crest of the Misis-Kyrenia Lineament and at the top of the Aksu-Kyrenia Lineament (Fig. 4-15). Unfortunately, no drilling has been completed in these areas so the presence of Sequence Boundary 2 is unconfirmed.

4.9 Depositional Sequence C

Depositional Sequence C is a low amplitude depositional sequence that is almost acoustically transparent on MUN seismic data (Figs. 4-3 thru 4-5). This depositional sequence consists of sediments from the Quaternary Period (Pleistocene?) as indicated by its position directly above Sequence Boundary 2 which is the boundary between the Tertiary and Quaternary (Pliocene-Pleistocene). This depositional sequence is composed of parallel and uniformly dipping reflectors which share the same basin-edge

relationships as Depositional Sequence B, terminating against east - west trending transtensional faults in the northern part of the outermost Cilicia Basin and against dominantly extensional faults in the remainder of the north edge of the outer basin. At the southern part of the outer basin Depositional Sequence C continues over the Aksu-Kyrenia Lineament but pinches out towards, and is terminated at, a transtensional fault zone at the northern edge of the Kyrenia Range in Cyprus. Depositional Sequence C pinches out to the north at the shelf edge near southern Turkey in the inner Cilicia Basin. This depositional sequence thins toward the Misis-Kyrenia Lineament and terminates against the transtensional fault zone at the south of the inner basin.

Sections of patchy, contorted or chaotic reflectors are observed in Depositional Sequence C (Fig. 4-16a), and have been interpreted as either gas charged sediments or gravity flow phenomena (mud flows, debris flows, turbidites, etc.). These features are found in seismic lines at the northern edge of the outer Cilicia Basin. The largest of these patchy reflector packages is ~1 ms thick and 125 m wide in cross section. These phenomena may be the result of shelf instability related to tectonic subsidence of this part of the basin as indicated by low angle fault systems in Plio-Quaternary sediments which can be interpreted as gravity-driven slides (Fig. 4-16b).

Depositional Sequence C commonly displays local thickening at the sides and above salt structures in the Cilicia Basin. These thickness variations are due to salt movement and will be discussed in the chapter on kinematic interpretations (Chapter 6). Thickness variations also occur in areas where no evaporites are present. In these locations, Depositional Sequence C has a convex downward external form showing that

localised areas of high accommodation for sedimentation existed, probably because of salt withdrawal or large offset on extensional faults (Fig. 4-17).

4.10 Sequence Boundary 3

Sequence Boundary 3 is the first in a series of higher amplitude reflectors located above the low amplitude reflectors of Depositional Sequence C (Figs. 4-1 thru 4-5). This sequence boundary is almost flat lying throughout the data set except in areas of young or active faulting. This continuous reflector is onlapped by Depositional Sequence D in areas where this young contraction has produced fold and thrust structures that were elevated above the seafloor before deposition of Depositional Sequence D. This reflector may lie near the Pleistocene-Holocene boundary; however, the limited well data in the area cannot confirm this. In the north part of the Cilicia Basin, this sequence boundary converges with both Sequence Boundary 2 and the seafloor towards the Southern Turkish coast, possibly terminating at transtensional faults in the outer basin. To the south, this sequence boundary terminates high on the sides of the crests of the Misis-Kyrenia Lineament to the east, but continues above the Aksu-Kyrenia Lineament to the west.

4.11 Depositional Sequence D

Depositional Sequence D is a series of very high amplitude parallel reflectors located just below the present-day seafloor in the Cilicia Basin (Figs. 4-1 thru 4-5). At the northern edge of the outer Cilicia Basin, patches of contorted or chaotic reflectors within Depositional Sequence D have been interpreted as gravity flows. These chaotic

reflector intervals can be up to 1 ms thick and may have a cross sectional width of >250 m in some areas (Fig. 4-16a). These gravity flows are in the same area as those in Depositional Sequence C and may also have resulted from shelf instability or from tectonic subsidence in this part of the basin (see section 4.9, Fig.4-16a and b).

A 50 m wide and ~2 ms deep channel cuts into the top of Depositional Sequence D in the outer Cilicia Basin near the Anamur and Bozyazi Rivers (Fig. 4-18). An erosional truncation of the reflectors in Depositional Sequence D occurs at the boundary of this channel. There is no sedimentary infilling of this channel suggesting that it is a path for the present-day currents coming from the rivers of southern Turkey.

Depositional Sequence D often drapes fold-thrust culminations within Depositional Sequence C that were elevated when Depositional Sequence D deposition began. Several onlap unconformities may be stacked against the flanks of the culminations. These relationships suggest that tectonic growth in this depositional sequence is very recent. In some locations, tip points of the thrust faults actually break through Depositional Sequence D to the seafloor showing that these faults are presently active.

Depositional Sequence D also extends across the top of the Aksu-Kyrenia Lineament where it displays erosion and angular unconformities just below the present-day seafloor (Fig. 4-19). At this location, growth strata observed in Depositional Sequence D show that the Aksu-Kyrenia Lineament continued to grow in the Quaternary and is still growing today.

Thickening above and at the margins of salt structures is common within this

depositional sequence. As these characteristics are linked to the movement of evaporites in the Cilicia Basin, they will be discussed in the chapter on kinematic indicators (Chapter 6).

4.12 Seafloor Horizon

The uppermost reflector in all seismic sections used in this study is the seafloor horizon. This horizon is a high amplitude reflector which has bathymetric relief related to faulting (thrust, extensional and transtensional faults), salt diapirism, channel cutting and other erosional or tectonic processes (Fig. 4-1). The depth to this horizon is indicated on a map of the bathymetry of the Cilicia Basin (Fig. 1-4).

4.13 Large Scale – Basin Wide Distribution and Thickness Patterns

The creation of an isopach map of the evaporite unit is not possible in the Cilicia Basin because of the previously mentioned difficulties encountered when attempting to pick the base salt (N-Reflector) in seismic sections. Because the Pliocene-Quaternary sediment package oversteps the evaporite unit everywhere in the Cilicia Basin, these problems are not encountered and it is possible to create a Pliocene-Quaternary sediment isopach map (Fig. 4-20).

The Plio-Quaternary isopach map shows a marked thickening of the Plio-Quaternary succession in the northeast portion of the inner basinal area that is believed to be a prograding delta succession. Thicknesses in this region can be as great as 3.00 sec TWT. The outer Cilicia Basin appears underfilled in comparison to the inner basin (Fig

4-20 and 4-21a) and displays a marked thickness variation between the northern and southern portions of the outer basin with the northern part of the basin having a much thicker Plio-Qaternary succession (1.0 sec TWT) than the southern part (0.4 sec TWT) (Fig 4-20 and 4-21b).

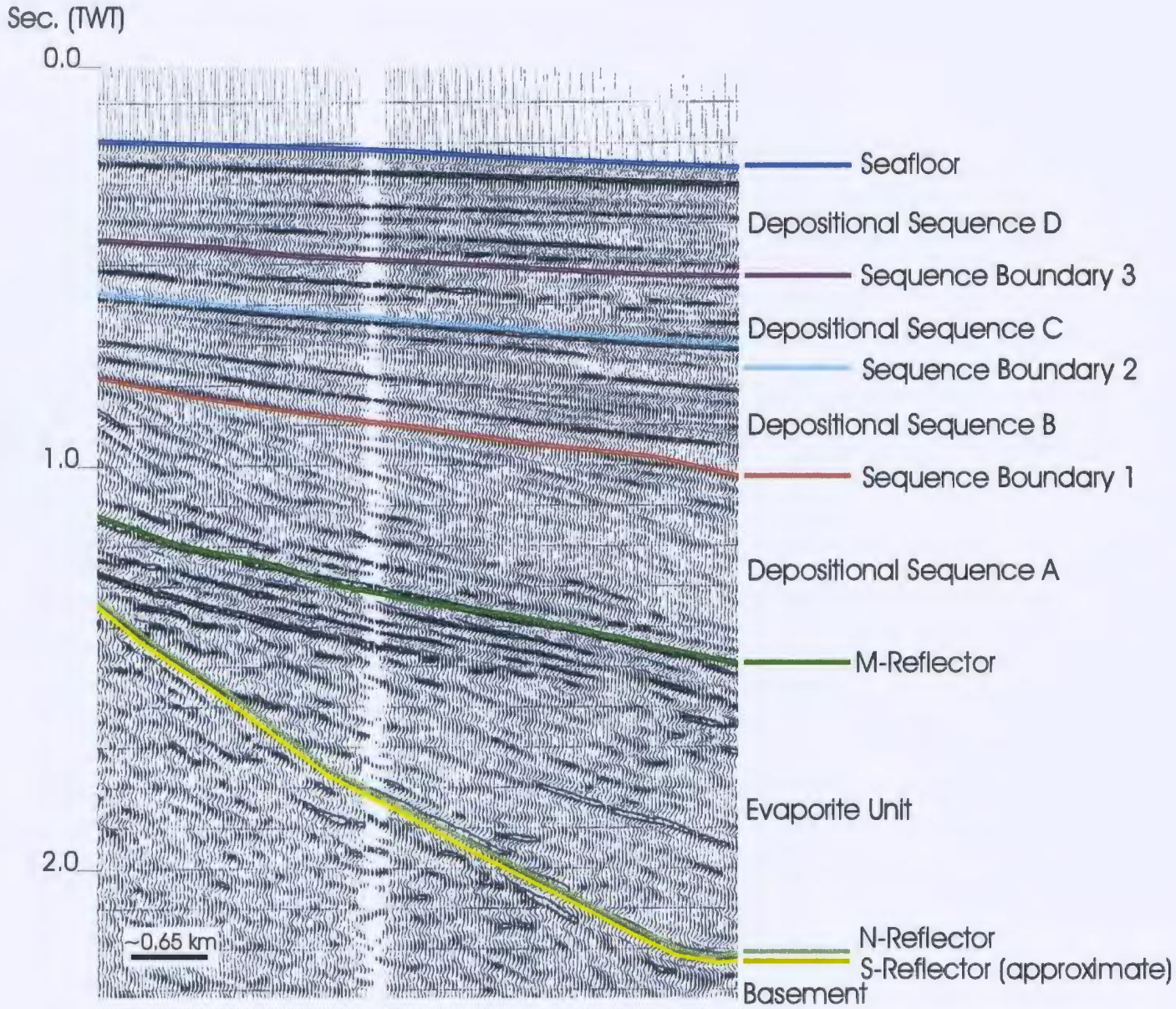

Figure 4-1: Seismic Stratigraphy near the northern margin of the Cilicia Basin.

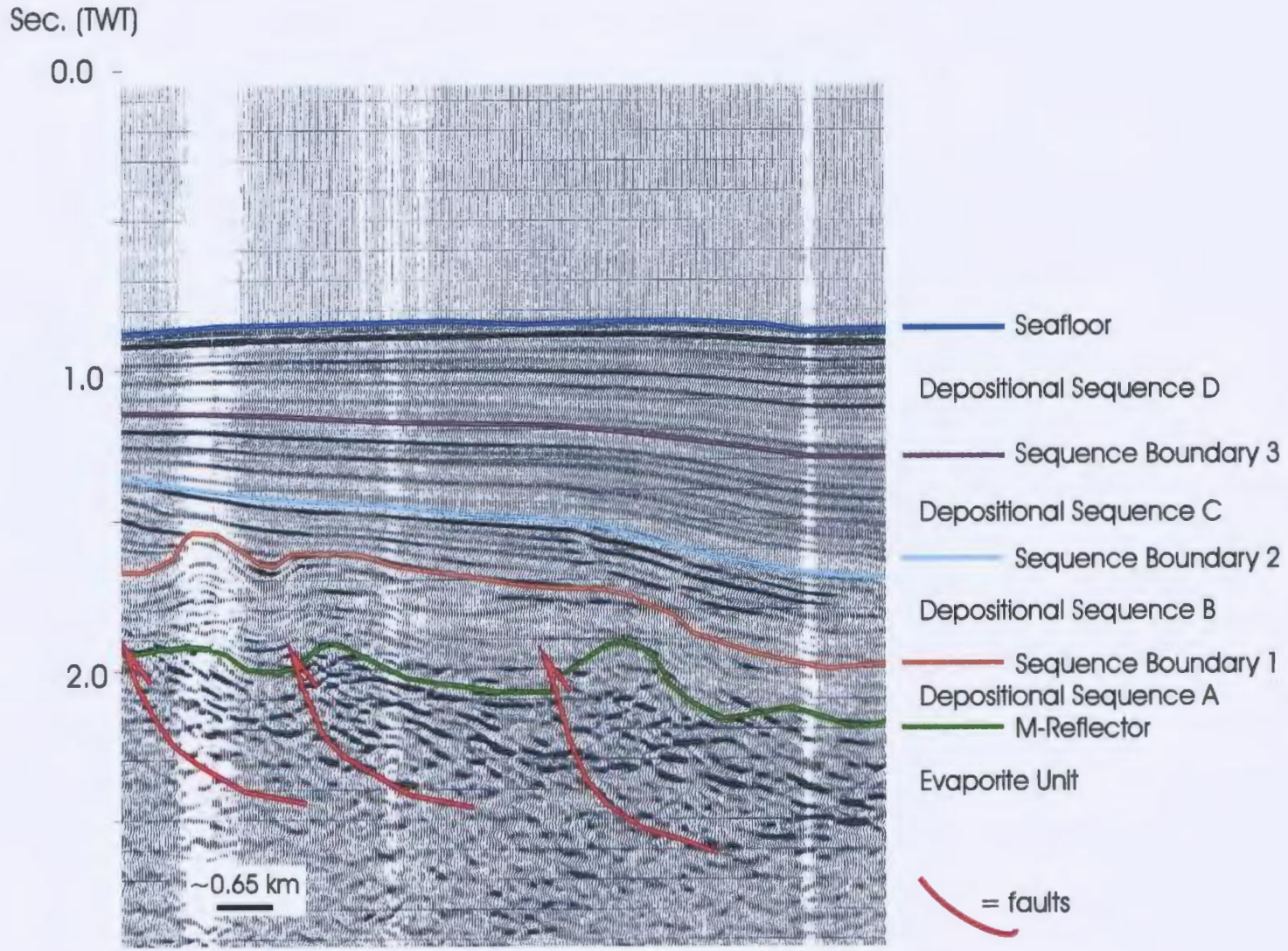

Figure 4-2: Seismic Stratigraphy above thrusted evaporites in the Cilicia Basin

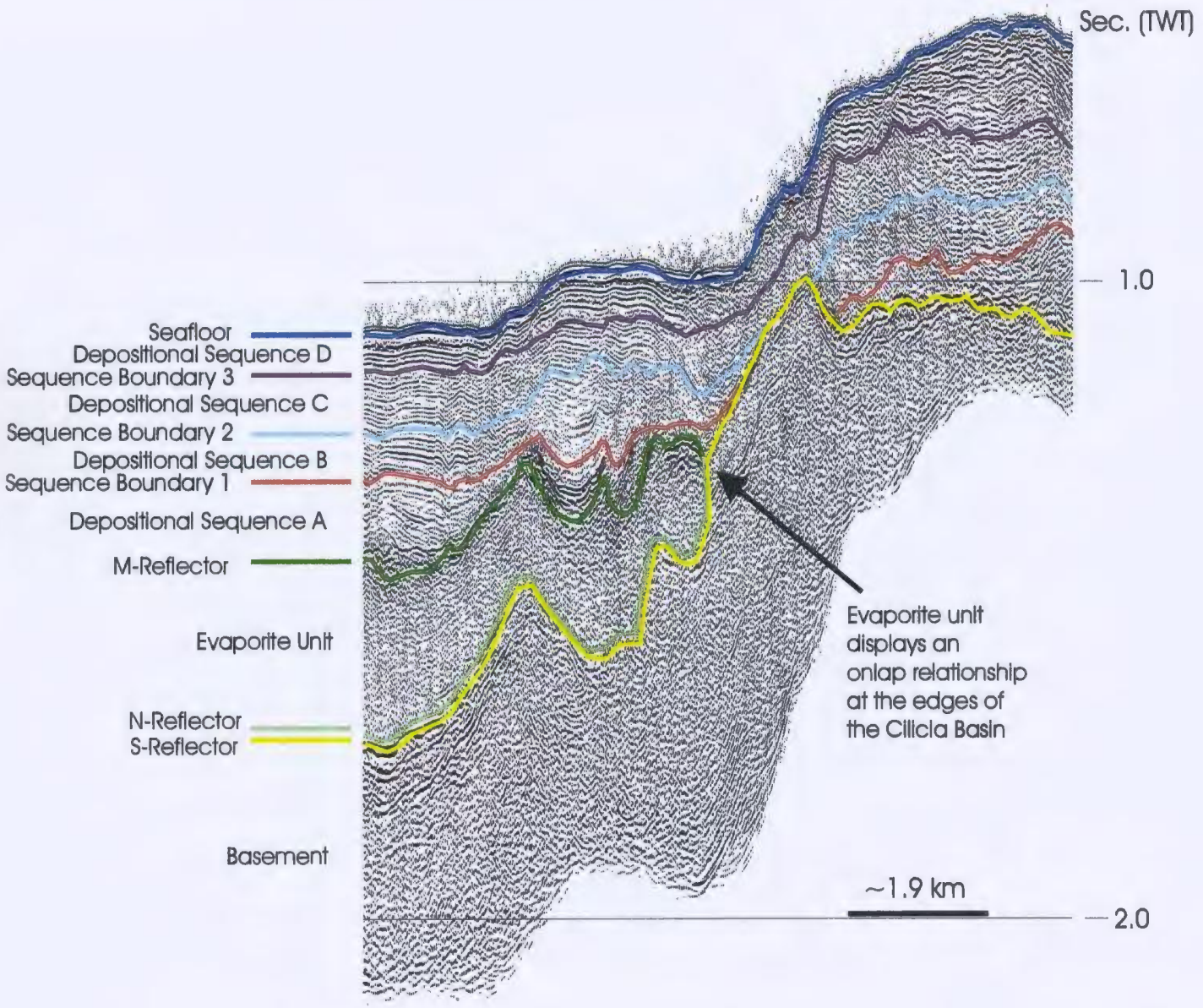

Figure 4-3: Seismic Stratigraphy near the Misis-Kyrenia Lineament in the Cilicia Basin.

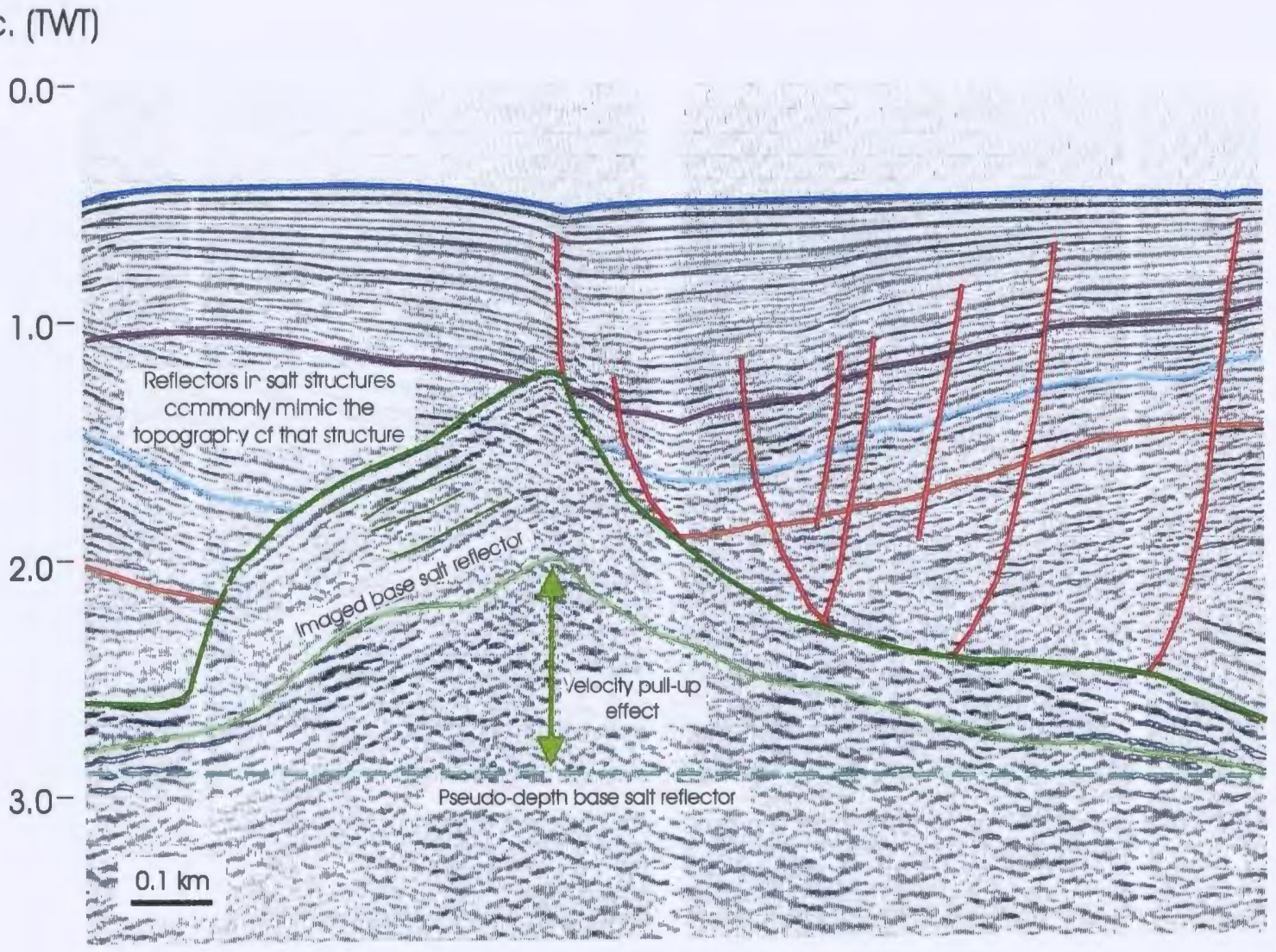

Figure 4-4: Seismic Stratigraphy of the Cilicia Basin showing the creation of pseudo-depth base salt reflector to artificially remove the effect of velocity pull-ups below salt structures.

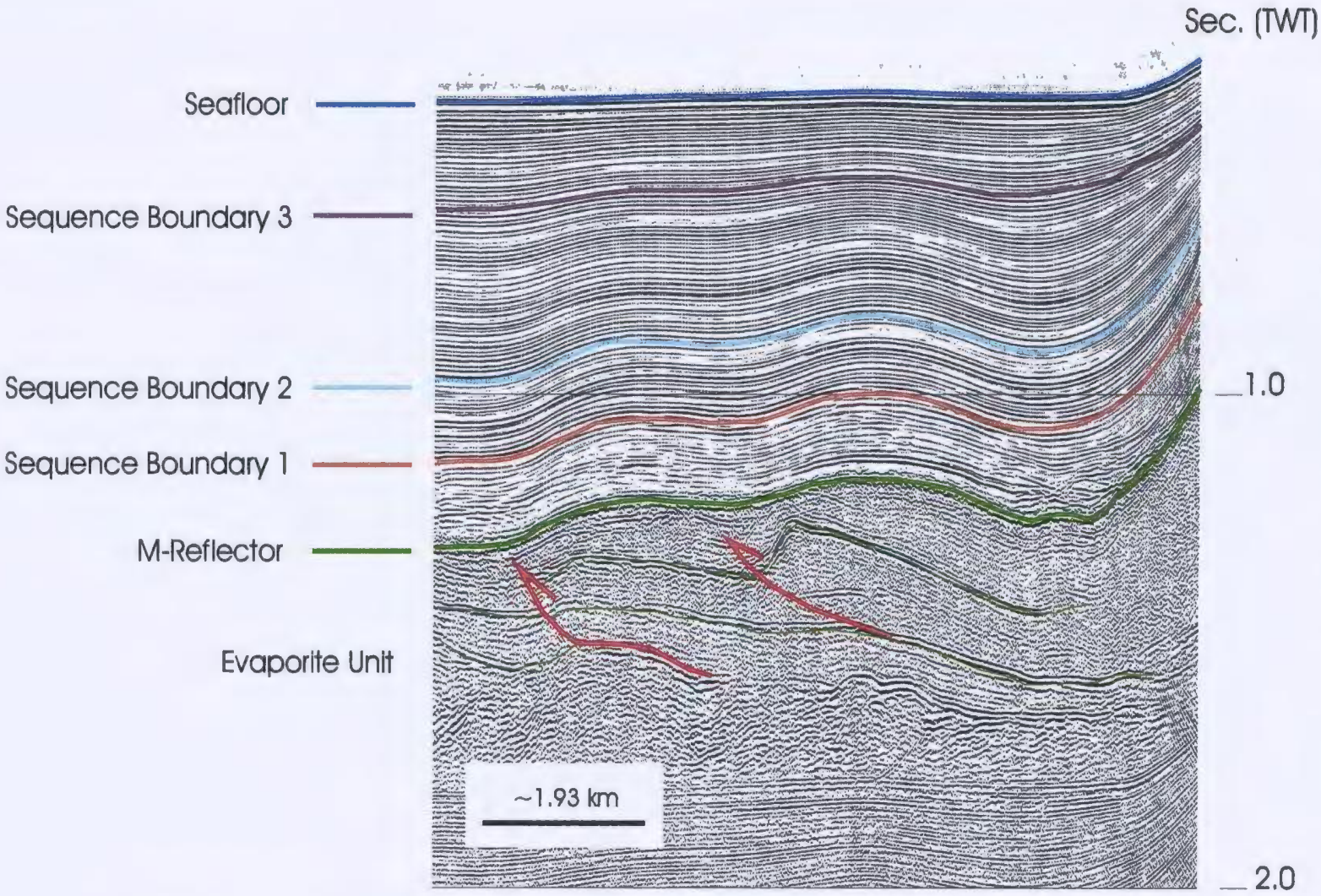

Figure 4-5: High amplitude reflectors within the evaporite unit display a series of northward-directed, low-angle thrust faults.

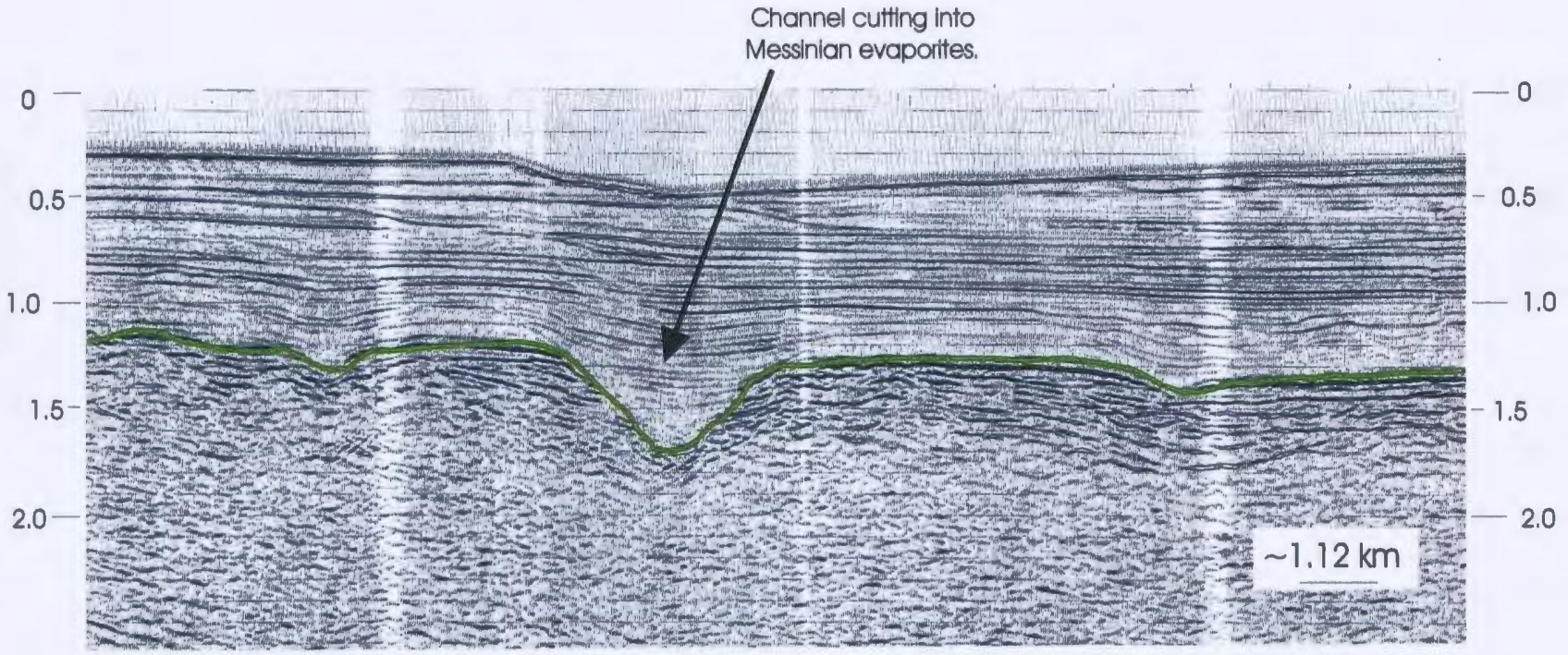

Figure 4-6: During the Messinian, channels cut into the top of the evaporite succession near the northern edge of the Cilicia Basin. These channels likely formed at times of lower sea level when rivers fed lower, more central portions of the Mediterranean Basins.

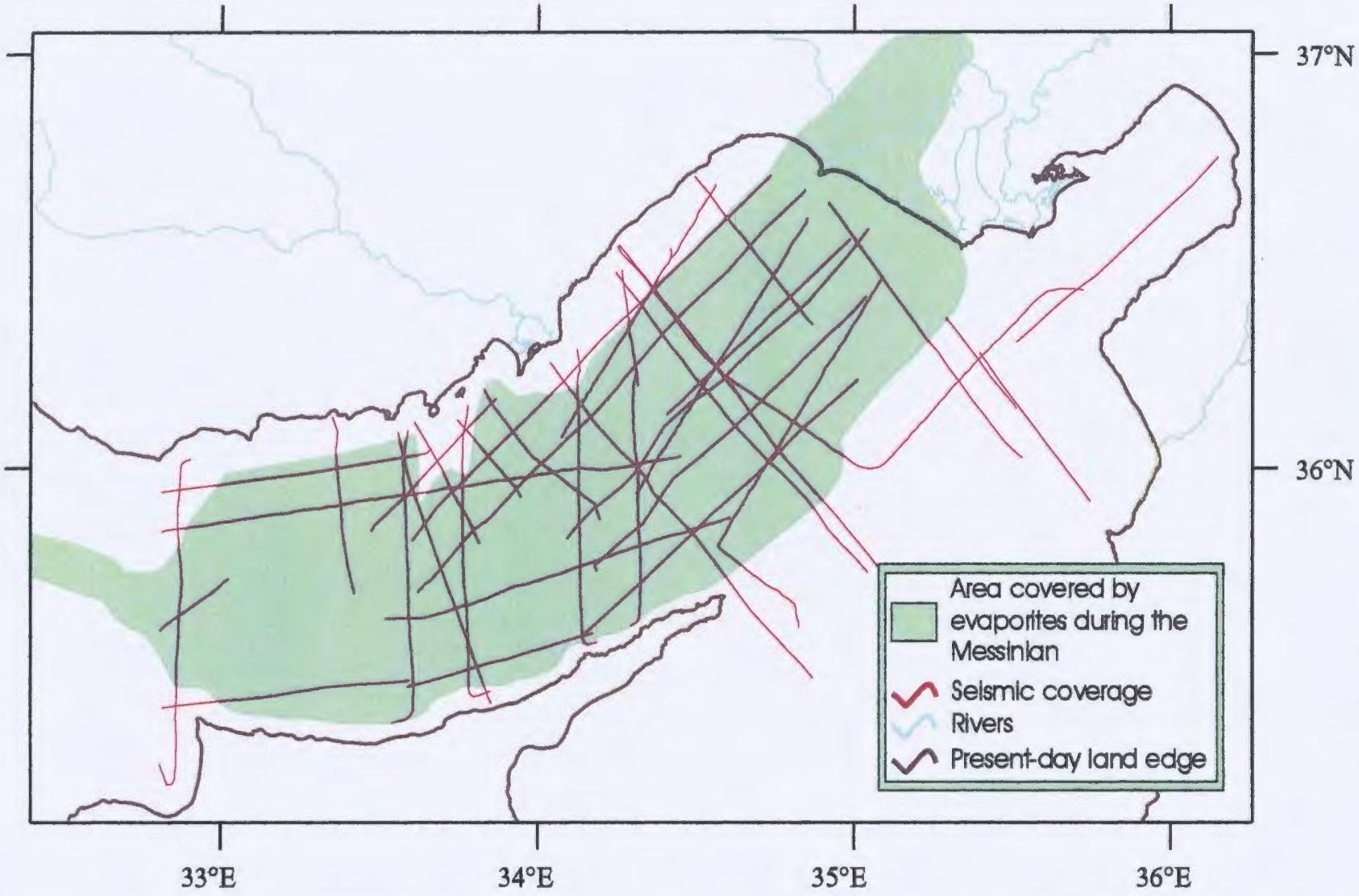

Figure 4-7: Mapped extent of evaporite distribution in the Cilicia Basin. This distribution represents the *minimum* basin area during the Messinian and does not consider the potential for salt withdrawal from the basin margins.

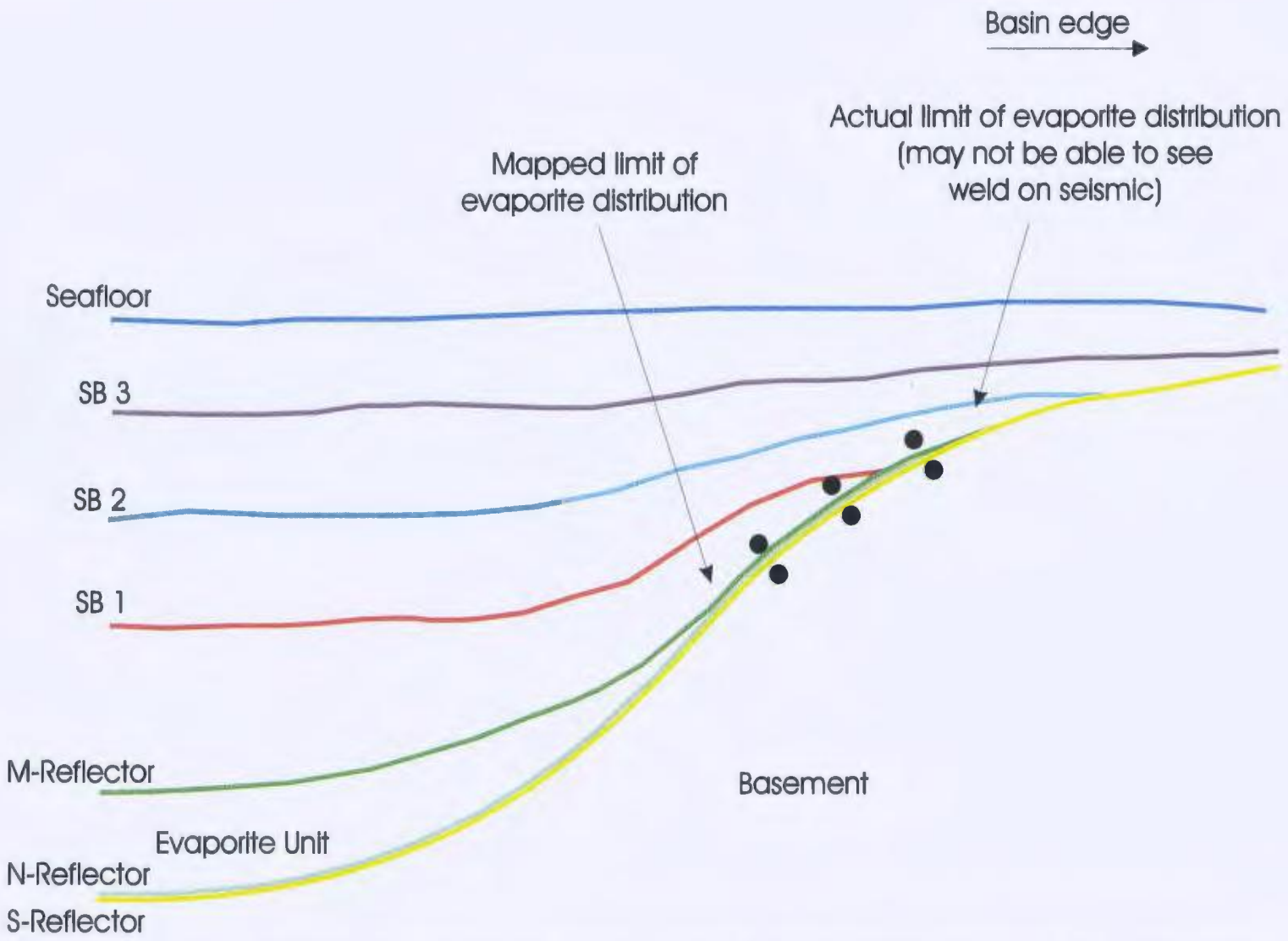

Figure 4-8: Mapping of limit of evaporite distribution represents the minimum basin area during the Messinian because it does not take salt withdrawal at the basin margins (and the subsequent formation of salt welds) into account.

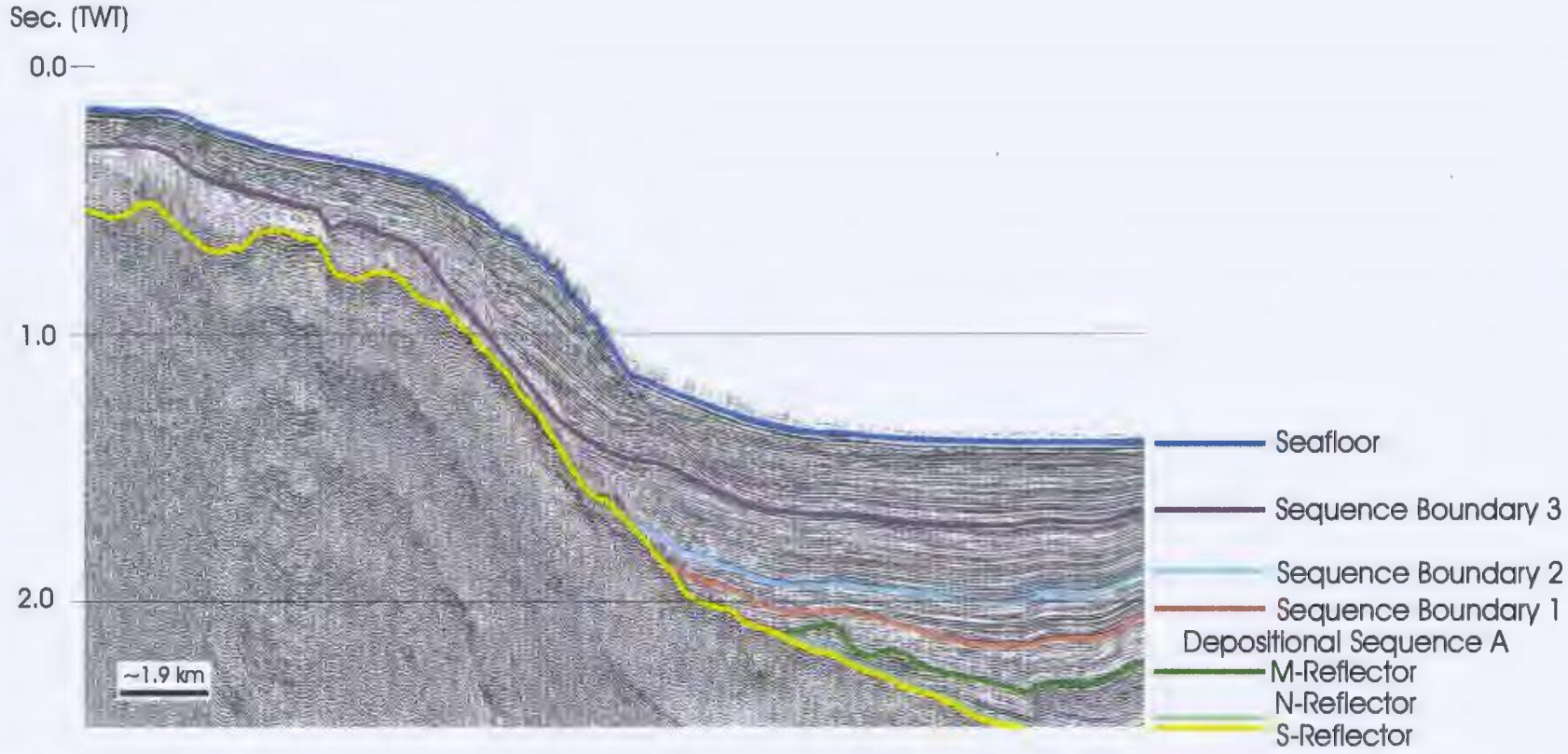

Figure 4-9: Reflectors in Depositional Sequence A terminate against the basin margins in an onlap relationship, overstepping the basin edges of evaporite distribution. This sequence fills depressions in the top salt horizon.

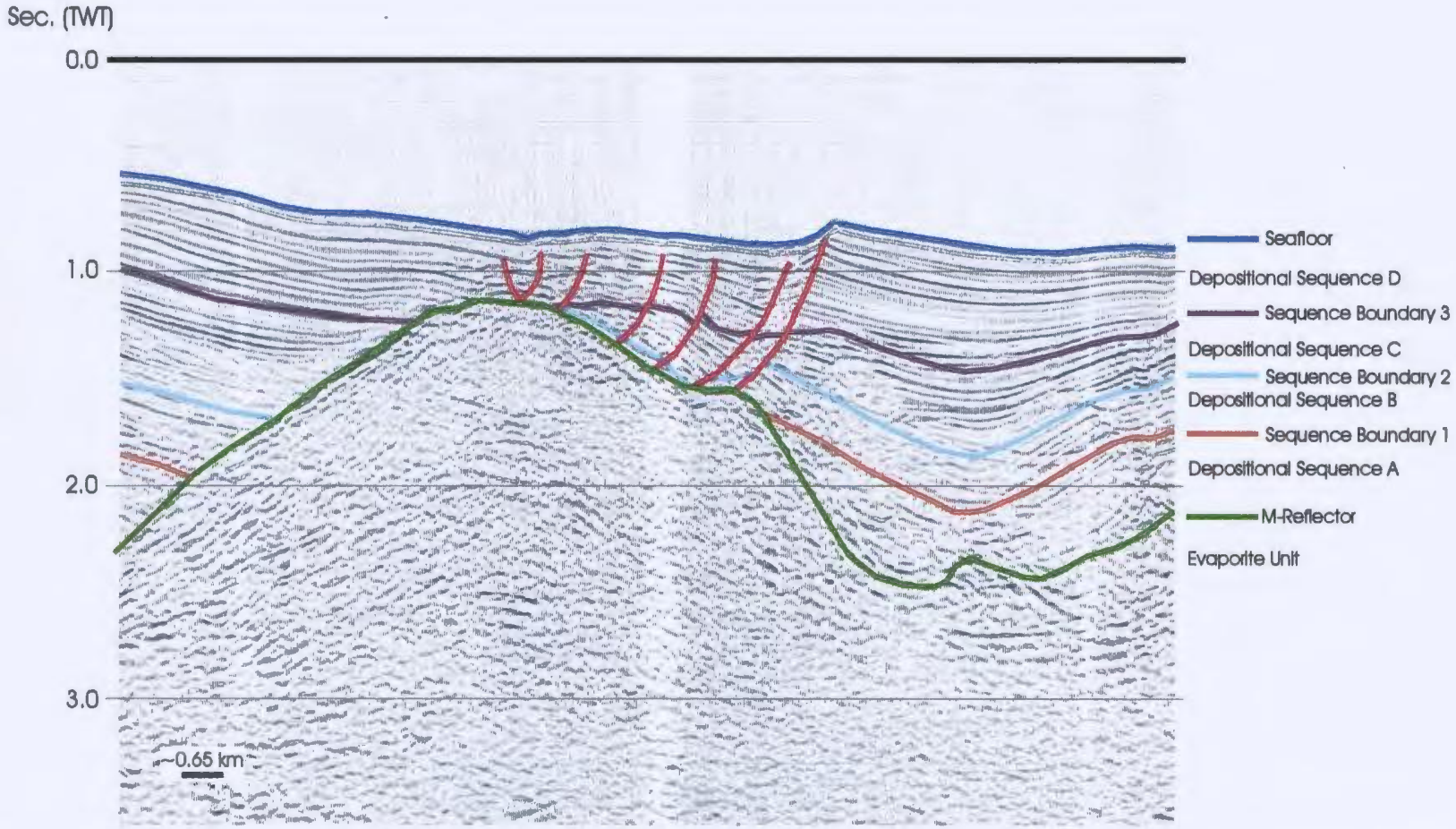

Figure 4-10: Generally, Depositional Sequence A maintains a constant thickness over the basin; however, onlap at basin edges, or onlap and truncation at salt features within the basin, can cause the sequence to thin.

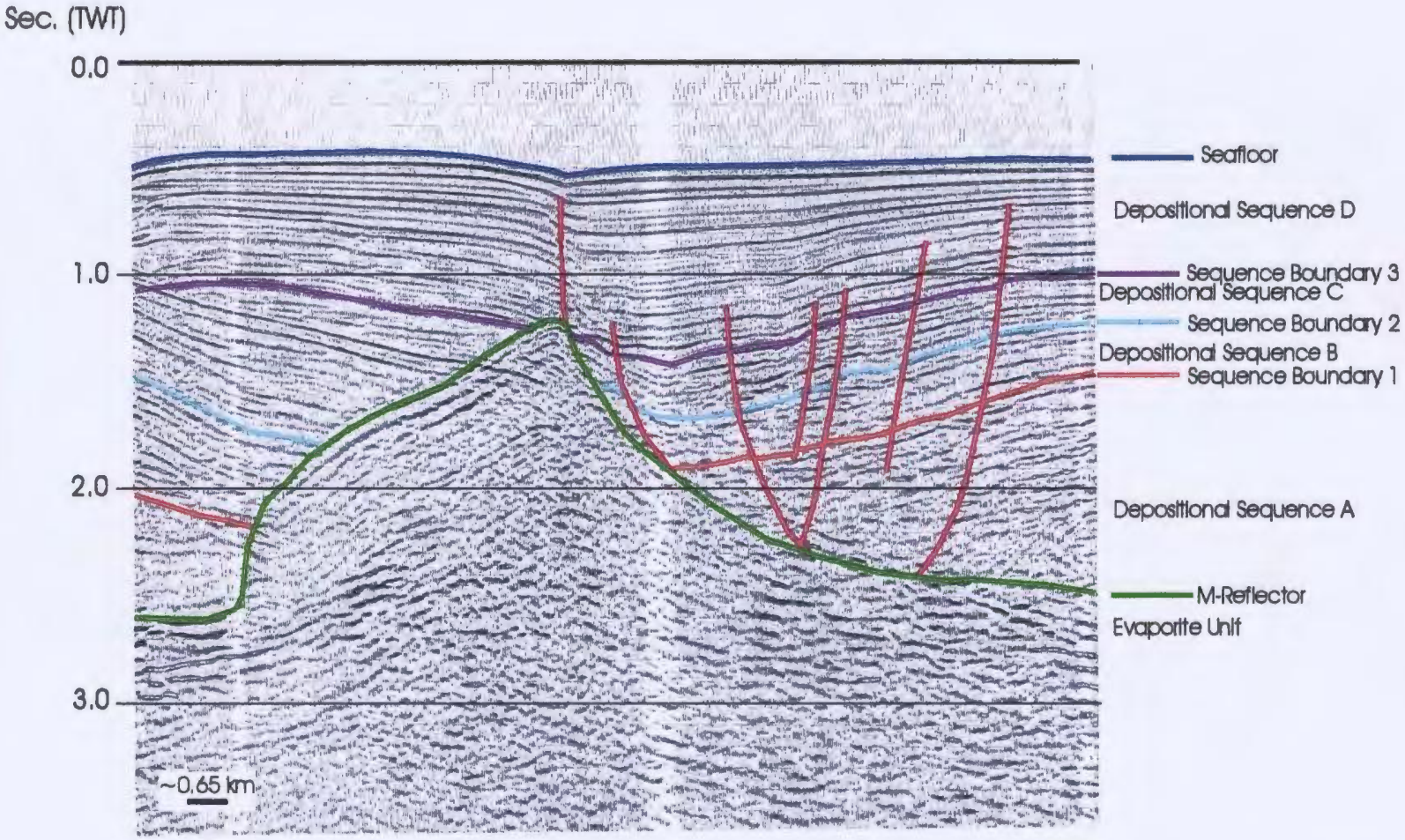

Figure 4-11: Generally, Depositional Sequence A maintains a constant thickness over the basin; however, sediment thickening is observed above many extensional faults due to growth during faulting.

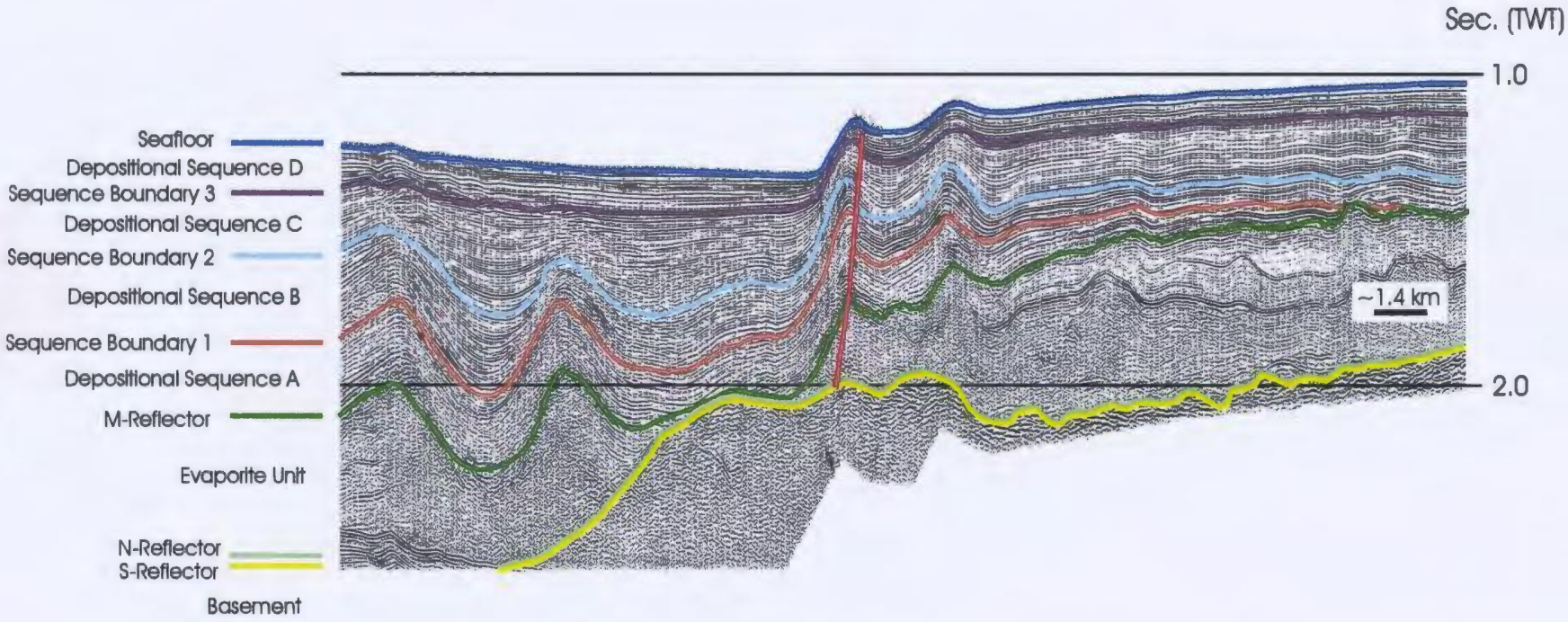

Figure 4-12: Sequence Boundary 1 terminates against an apparent sub-salt high near the central portion of the Outer Cilicia Basin.

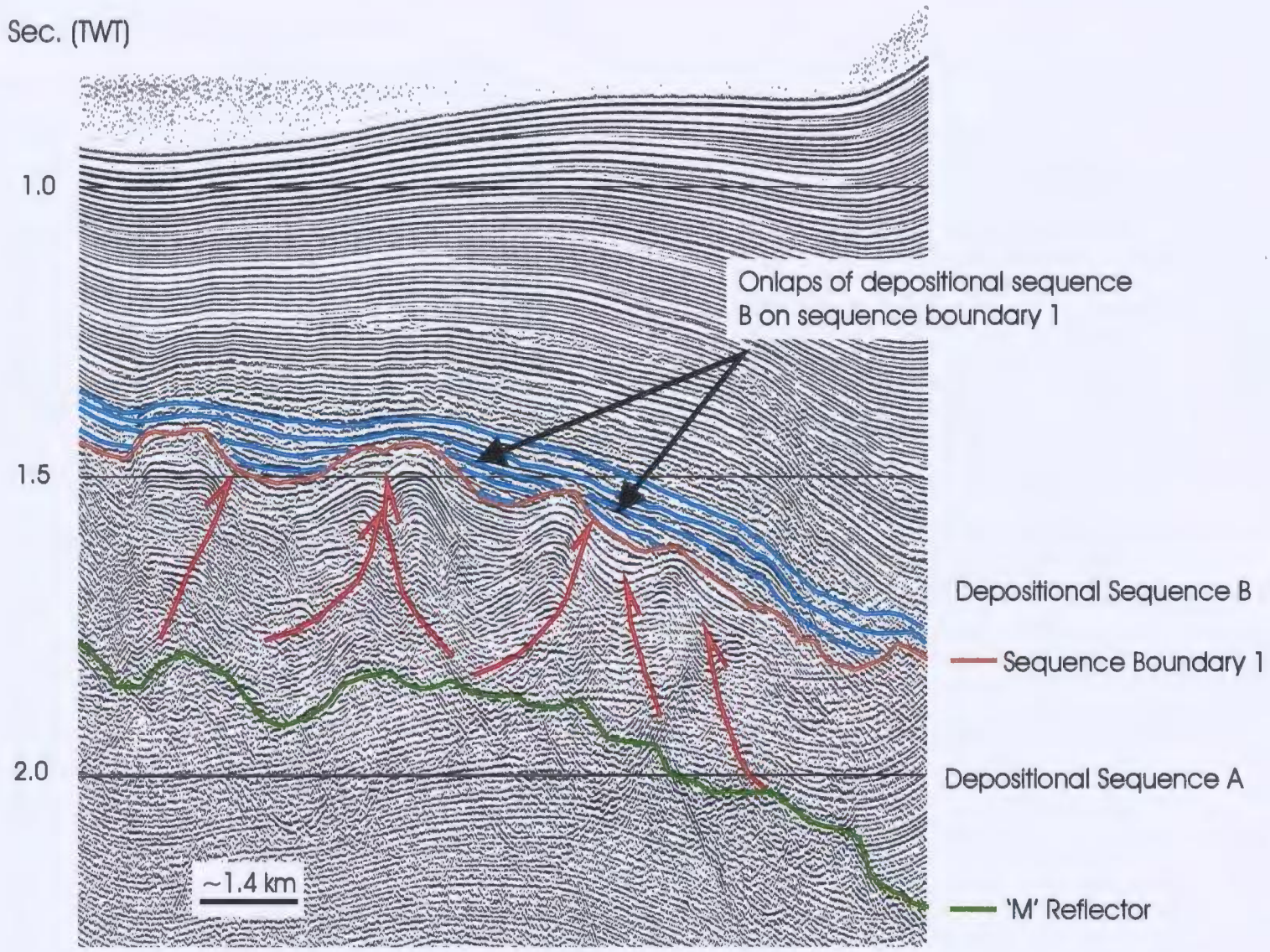

Figure 4-13: Depositional sequence B locally displays onlap with sequence boundary 1 at thrust culminations within depositional sequence A.

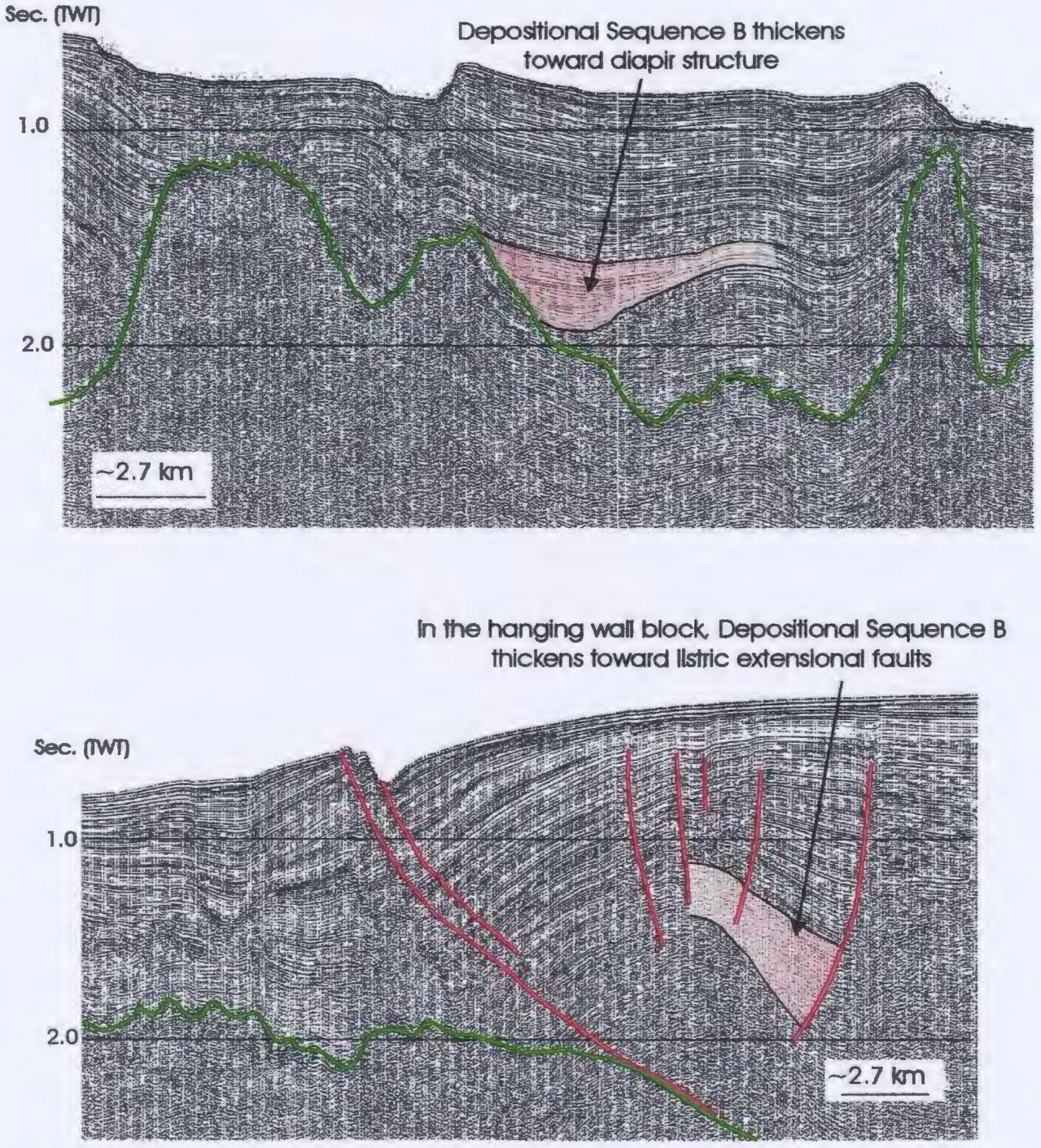

Figure 4-14: Depositional Sequence B locally displays thickening at the sides of salt structures and in the hanging wall of listric faults in the extensional domain.

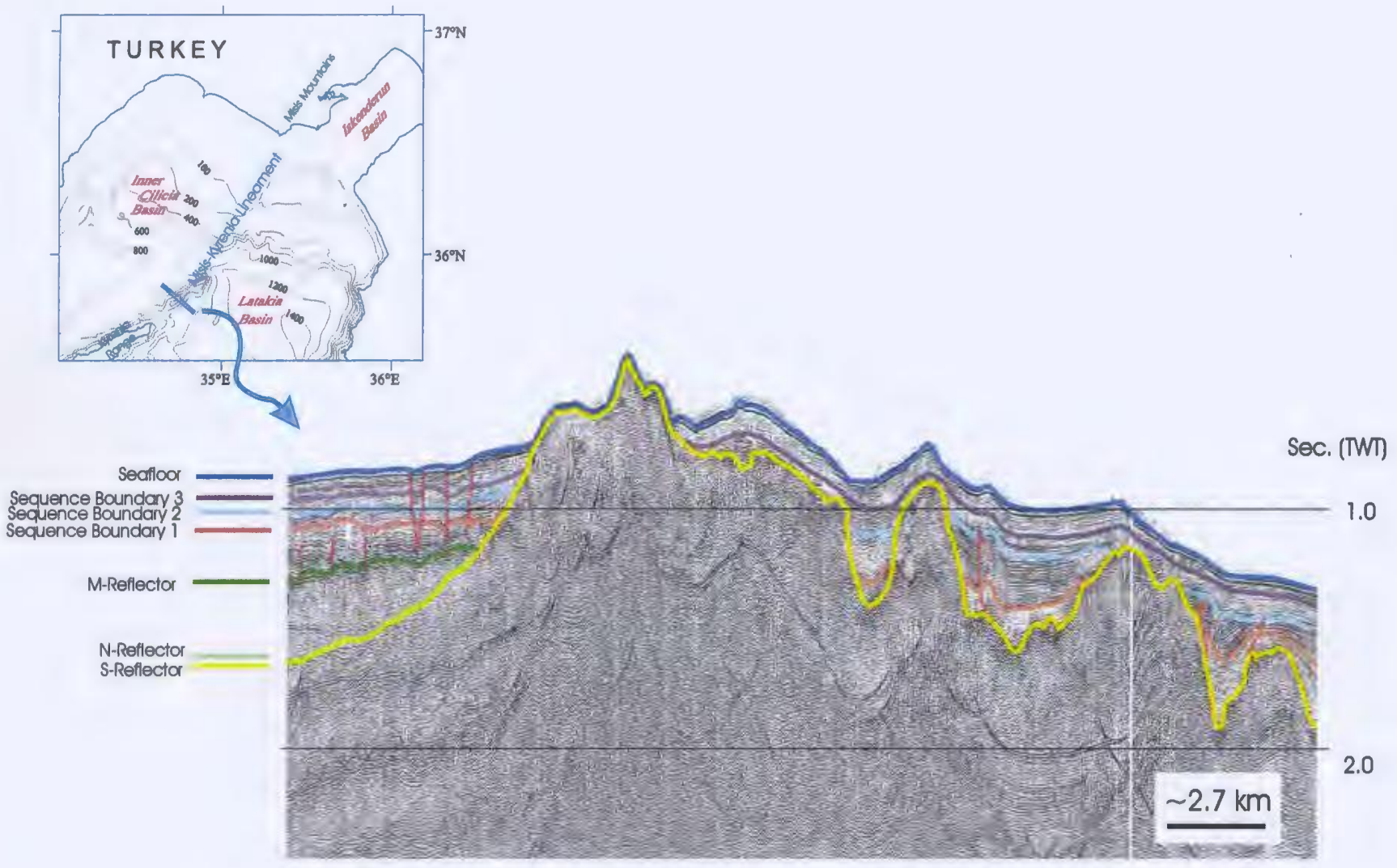

Figure 4-15: Depositional Sequences A through D, and therefore sequence boundaries 1 through 3, potentially fill small sub-basins located between the peaks at the crest of the Misis-Kyrenia Lineament. No drilling has been completed in these regions to confirm this.

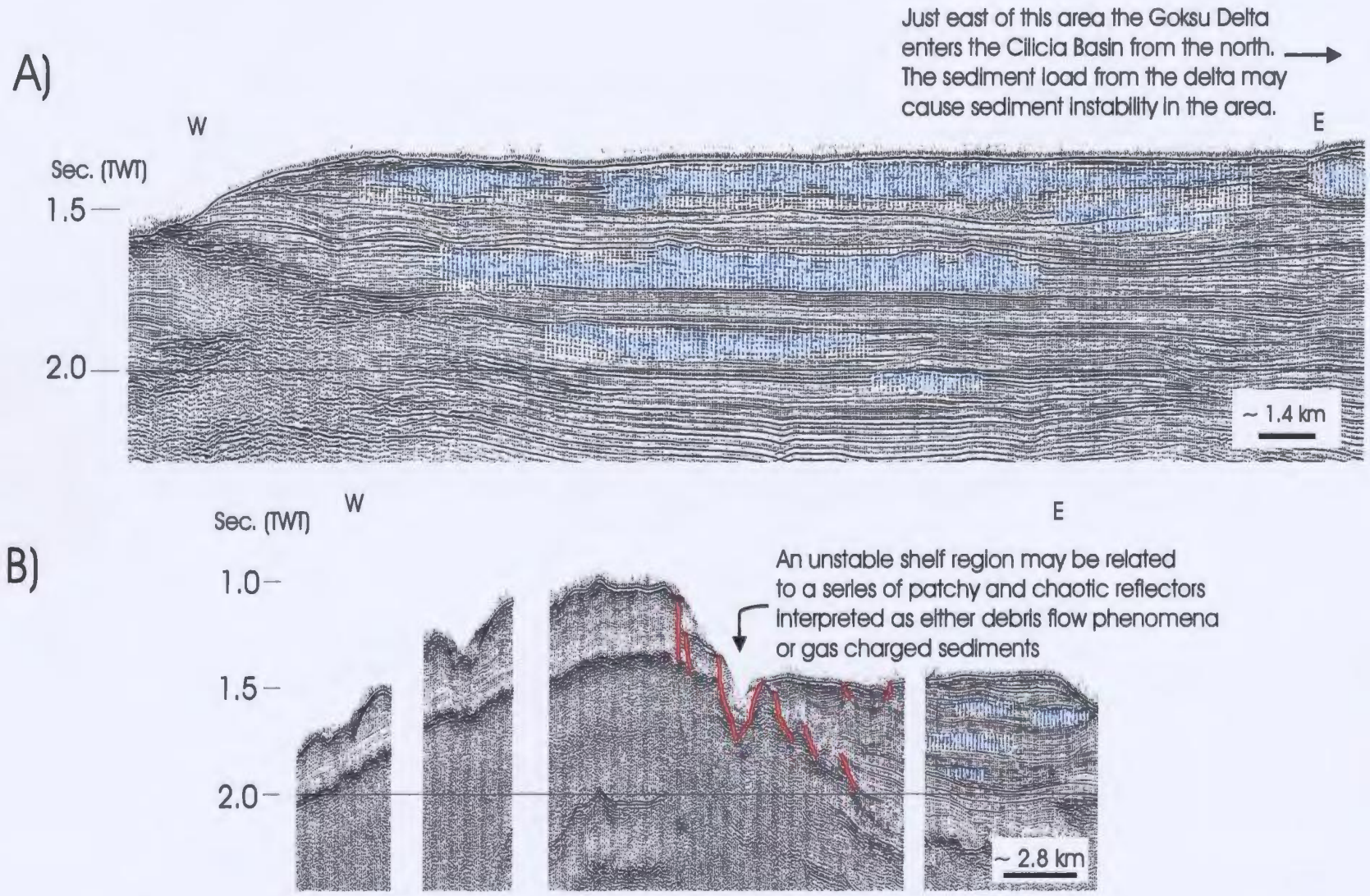

Figure 4-16: A) Patchy, contorted and chaotic reflectors in depositional sequences C and D have been interpreted as gravity flow phenomena (related to shelf instability to the west, at the Anamur Kormakiti High, or to the east, where the Goksu Delta feeds into the Cilicia Basin) alternatiely the chaotic reflectors may be gas charged sediments. B) Shelf instability to the west of the region shown in 4-16 (A) may have caused a disurbance which fed gravity flows in the area.

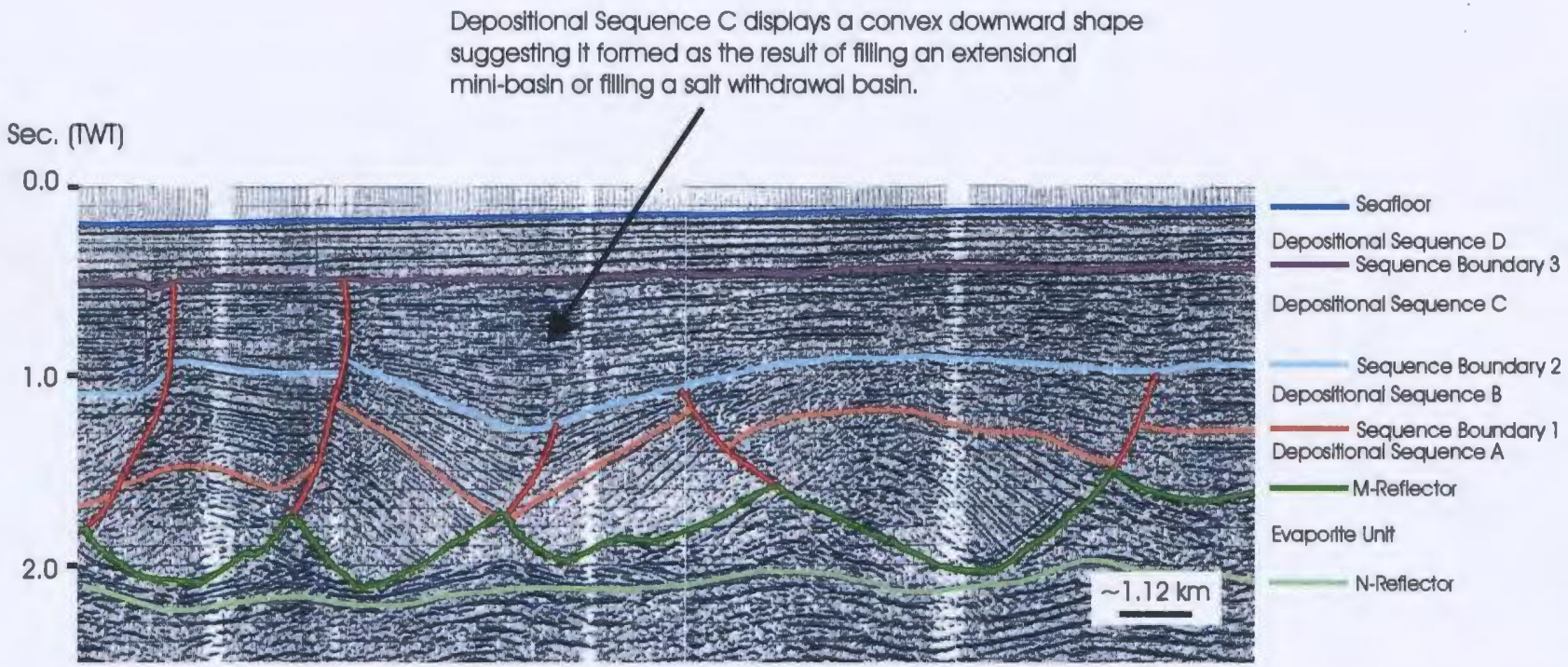

Figure 4-17: Depositional Sequence C displays convex downward strata which likely filled a small extension related basin or a salt withdrawal basin.

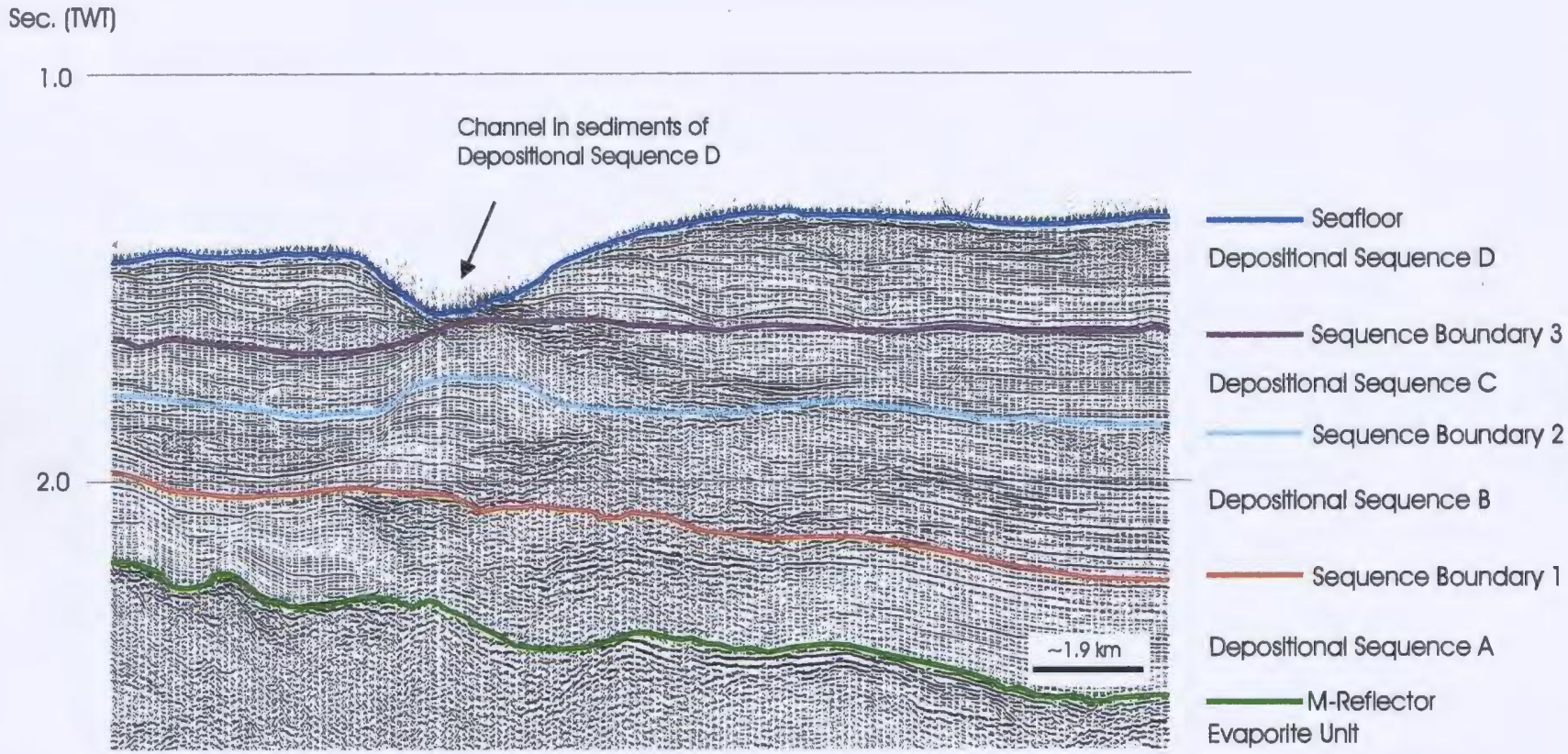

Figure 4-18: A channel approximately 5 km wide and 200ms deep is cut into the top of depositional sequence D in the outer Cilicia Basin near the Anamur and Bozyazi Rivers.

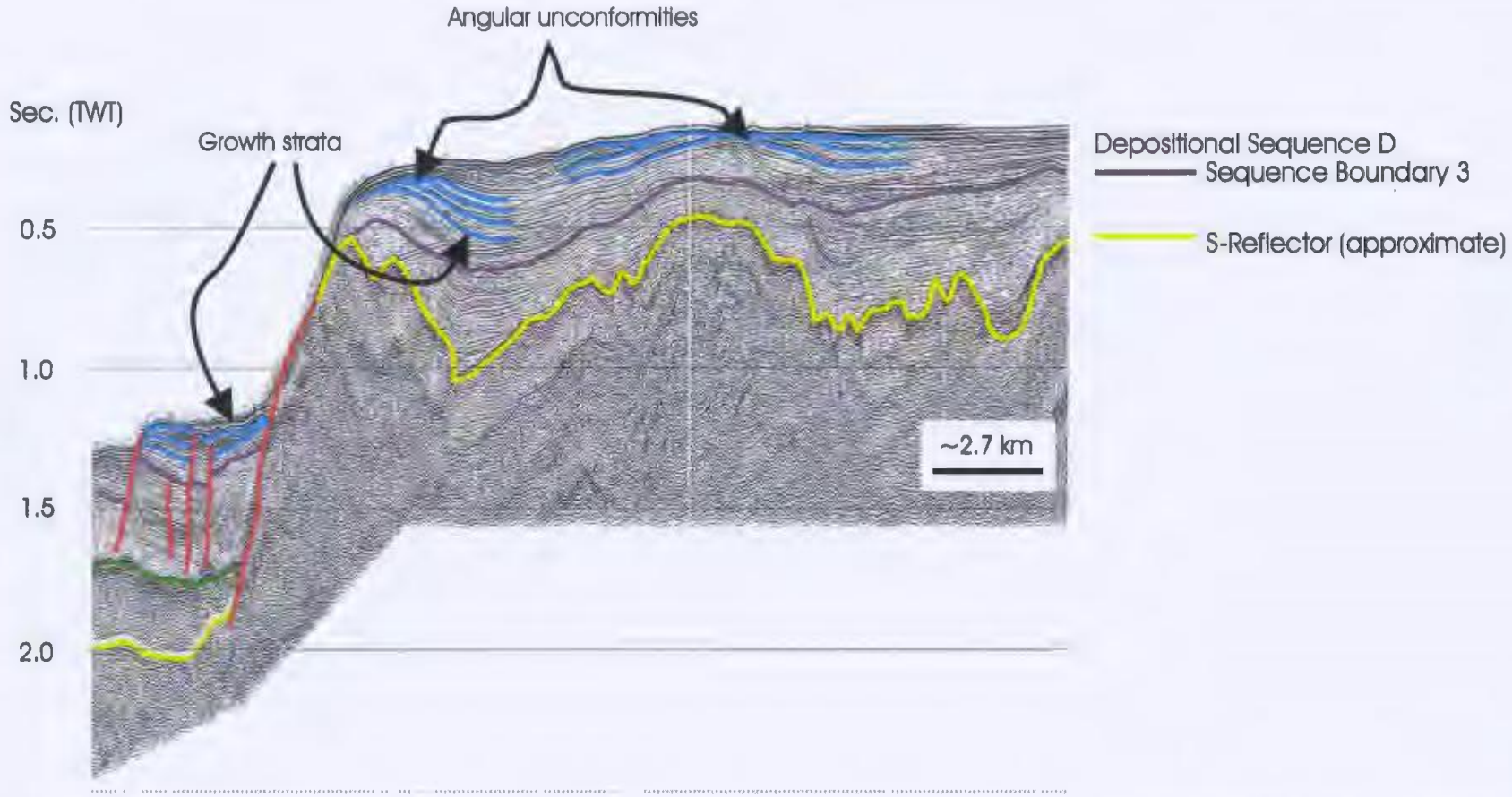

Figure 4-19: Depositional Sequence D displays erosion and angular unconformity just below the present-day seafloor. Growth strata in depositional sequence D suggest that the Aksu Kyrenia Lineament continues to grow today.

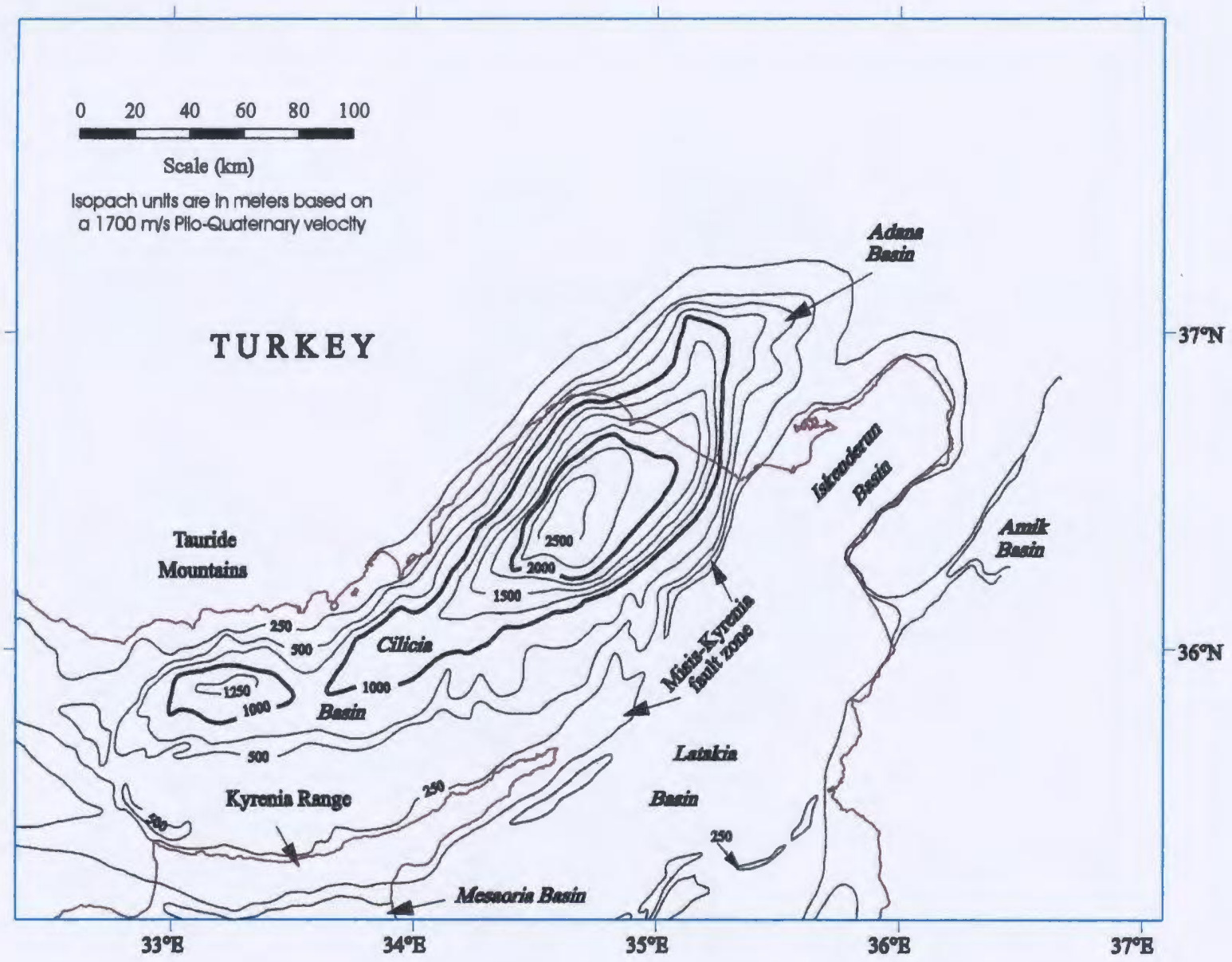

Figure 4-20: Pliocene-Quaternary sediment isopach map (fromAksu et al., 2003).

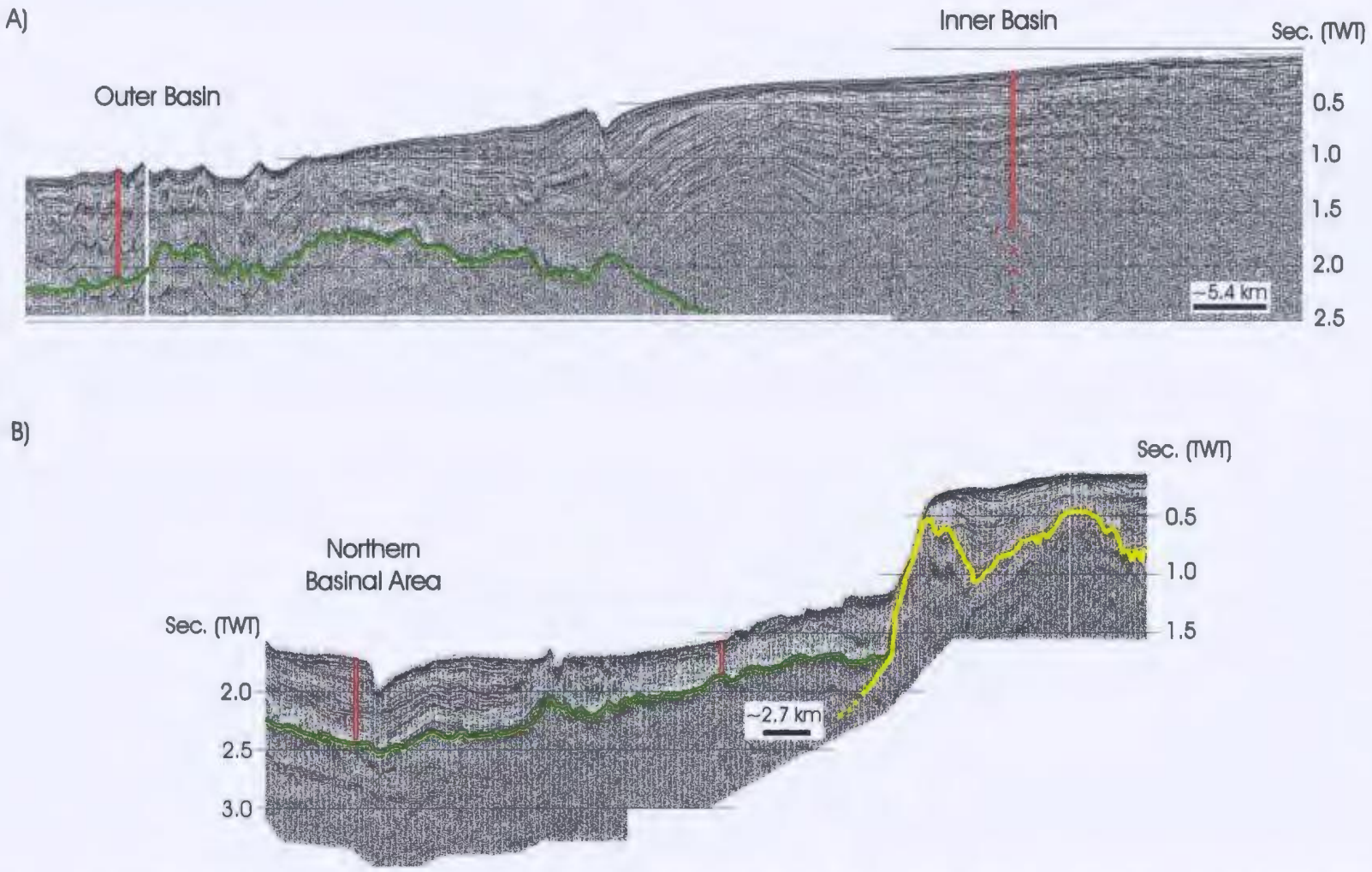

Figure 4-21: Thickness variations in Plio-Quaternary strata in the Cilicia Basin. A) The Plio-Quaternary cover is thicker in the inner Cilicia Basin than it is in the outer Cilicia Basin. B) The Plio-Quaternary cover is thicker in the northern portion of the outer Cilicia Basin than it is in the southern part of the outer Cilicia Basin.

5. FAULT ASSEMBLAGES IN THE CILICIA BASIN

Seven major regional fault systems have been identified in previous work completed in the region surrounding the Cilicia Basin. These fault systems are the Misis-Kyrenia Fault Zone, the Kyrenia Fault Zone, the Misis Fault Zone, the Kozan Fault Zone, the Northern Outer Cilicia Fault Zone, the Central Outer Cilicia Fault Zone, and the Ecemiş Fault Zone (Fig. 5-1). Drs. Aksu, Calon and Hall of Memorial University completed preliminary mapping of faults in the Cilicia Basin (Aksu et al., 1992; Aksu et al., in prep.). Their map presents a compilation of their own findings as well as the findings laid out in previous studies of the Eastern Mediterranean region and is an excellent source for information on the pre-defined fault zones in the Cilicia Basin.

Of the major regional fault systems in the Cilicia Basin, five are important when studying the salt tectonics of the region: the Misis-Kyrenia and Misis Fault Zones, the Kyrenia Fault Zone, the Kozan Fault Zone and the Central Outer Cilicia Fault Zone. These fault systems are responsible for the formation of the Cilicia Basin. The Northern Outer Cilicia Fault Zone is not related to the salt tectonics of the region, as it is located beyond the depositional edge of salt. The remaining fault system, the Ecemiş Fault Zone is not related to the formation of the Cilicia Basin. It is a sinistral strike slip fault zone that runs in an approximately north northeast-south southwest orientation directly west of the northwestern edge of the Cilicia Basin (Fig. 5-1). The main activity along this fault zone is pre-Miocene in age; it was de-activated by the Plio-Quaternary, and did not act as a fundamental basin-forming fault.

This study delineates five major fault assemblages, or fault families, that occur

within the Cilicia Basin (Fig. 5-2). The first of these fault families is the "Basin-Forming Fault Family." These faults are those that resulted in the formation of the upper Miocene-Present Cilicia Basin. The second fault family, the "Intra-Salt Fold/Thrust Fault Family" includes thrust faults that are entirely contained within the evaporite unit in the central portion of the outer Cilicia Basin. The third family of faults in the Cilicia Basin is the "Listric Extensional Fault Family." These faults are found above the evaporite unit in the northeastern portion of the Cilicia Basin. The fourth fault family in the Cilicia Basin is the "Toe-Thrust Fault Family." These faults are situated to the southwest of the Listric Extensional Fault Family in the Cilicia Basin. The fifth and final fault family is linked to extensional/transtensional faults of the Central Outer Cilicia Fault Zone and is referred to as the "Central Fold/Thrust Fault Family".

The various fault zones identified in this study and in work by Aksu et al. (1992 a, in prep.) effectively divide the Cilicia Basin into three distinct domains: an inner extensional domain, an outer contractional domain (that includes the Intra-Salt Fold/Thrust Family and the Central Fold/Thrust Fault Family) and a central boundary zone (separating the inner and outer basins).

It is conceivable that some of the fault families identified in this study may actually be the marine extensions of fault zones already delineated onland. In addition, these fault families experience some overlap with those marine faults and fault zones identified in works by Mulder (1973), Mulder et al. (1975), Evans et al. (1978) Aksu et al. (1992 a, in prep).

5.1 Basin-Forming Fault Family

The Basin-Forming Fault Family is a series of extensional and transtensional faults located at the north and south margins of the Cilicia Basin (Fig. 5-2 and Fig. 5-3 [insert 1]). These faults are easily identified on seismic lines from the outer Cilicia Basin; however, they are quite difficult to identify on seismic lines from the inner basin because of poor seismic coverage and poor imaging due to a shallow water depth (lots of multiples) at the basin margins.

The faults of the Basin-Forming Fault Family were responsible for the initial development and the continued deepening of the Cilicia Basin during the late Miocene to Present. Many of these faults can be detected at levels below the base of the evaporite unit and some have fault tip points as shallow as the uppermost millisecond of the Quaternary sequence suggesting that the faults of the Basin-Forming Fault Family are still active in certain areas of the basin.

The faults of the Basin-Forming Fault Family curve with the coastlines of southern Turkey and northern Cyprus reflecting the dissimilar alignment of the inner and outer regions of the Cilicia Basin (Fig. 5-3 [insert 1]). Poor seismic coverage in the inner basin prevents proper mapping of the faults of the Basin-Forming Fault Family. Earlier work by Aksu et al. (1992, and in prep.) shows that the faults of the Basin-Forming Fault Family appear to have normal separation with downthrow into the basin. Based on regional kinematics, these workers inferred the presence of a sinistral strike-slip component along the Basin-Forming Faults in the inner basin.

The Basin-Forming Fault Family is the only fault family identified in this study

that does not have large-scale salt features, such as rollers or salt walls, associated with the faulting. This fault family was responsible for the deepening of the Messinian depocenter (during the latest Messinian) and is primarily located outside the edge of the evaporite basin. These faults helped to define the size and shape of the Cilicia Basin.

The faults of the Basin-Forming Fault Family that are located at the eastern and southern margins of the Cilicia Basin are a part of the Misis-Kyrenia Fault Zone (inner Cilicia Basin) and the Kyrenia Fault Zone (outer Cilicia Basin), respectively. Near the centerline of the outer Cilicia Basin the Central Outer Cilicia Fault Zone, also part of the Basin-Forming Fault Family, consists of a series of faults that straddle the evaporite basin but did not influence the deposition of evaporites. Along the northern and western margins of the Cilicia Basin the faults of the Basin Forming Fault Family are the Northern Outer Cilicia Fault Zone (outer Cilicia Basin) and the Kozan Fault Zone (inner Cilicia Basin), respectively.

5.1.1 Misis-Kyrenia Fault Zone and Misis Fault Zone

The Misis-Kyrenia Fault Zone and the Misis Fault Zone (Figs. 5-1 and 5-3 [insert 1]) are two zones of northeast-southwest trending transtensional faults. These fault zones are located at the margin of the Misis-Kyrenia Lineament in the marine area between the Cilicia and Latakia Basins and at the margins of the Misis Mountains in southeastern Turkey. These sub-vertical faults are located at the sides of a submarine horst block. The horst block was originally a pre-Messinian basement high that developed in response to late Miocene (Tortonian) thrusting (Mulder et al., 1975; Kelling et al., 1987; Aksu et al.,

in prep). Deeper sub-salt sedimentary successions (Miocene and older) in the Cilicia Basin are known to record the presence of this thrusting event in a series of southeast and south directed thrust structures which are observed both north and south of the Misis-Kyrenia Lineament (Aksu et al., in prep.). These faults overprinted the earlier fold-thrust structures and were predominantly transtensional along the Misis-Kyrenia Lineament (Aksu et al., 1992), and strike-slip at the Misis Fault Zone (Kelling et al, 1987). This transtensional and strike-slip faulting along the pre-Messinian basement high formed the large horst structure that runs from the Misis Mountains in Turkey to the northeastern tip of the Kyrenia Range in Cyprus. The margins of this horst structure are abruptly truncated against steep faults bounding the west wall of the horst, no typical structures normally associated with dip slip faults (e.g. drag, roll-over etc.) are observed therefore suggesting a strike-slip movement. Seaward of the truncated margin of the horst structure, a zone of Plio-Quaternary sediments locally display surficial gravity slide structures presumably generated by movements on the fault zone. Only a thin veneer of Plio-Quaternary sediments covers the crest of the horst.

In seismic sections from the inner Cilicia Basin, the Misis-Kyrenia lineament is observed as a bathymetric high on the seafloor that is approximately 200 ms above the regional seafloor (Fig. 5-4). The transtensional faults in this part of the basin (Misis-Kyrenia Fault Zone) have an average of 100 to 200 ms vertical offset at the seafloor with an undetermined amount of lateral offset. Vertical offsets measured at the M-Reflector in the inner basin are generally small as well (<200 ms).

The Misis Fault Zone and the Misis-Kyrenia Fault Zone meet in the southeastern

corner of the inner Cilicia Basin. To the west, in the outer Cilicia Basin, the Misis-Kyrenia Fault Zone is linked to another large extensional fault system, the Kyrenia Fault Zone.

5.1.2 Kyrenia Fault Zone

The Kyrenia Fault Zone (Figs. 5-1 and 5-3 [insert 1]) consists of a series of moderate to steeply north dipping faults that are located along the northern coast of Cyprus (southern margin of the outer Cilicia Basin). To the east, this fault zone extends seaward from the northeastern tip of Cyprus to link with the Misis-Kyrenia Fault Zone; to the west, the Kyrenia Fault Zone extends seaward to link with the Aksu-Kyrenia Lineament. The Kyrenia Fault Zone is located at the north and south boundaries of the Kyrenia Terrane of Cyprus (Robertson, 1990).

The Kyrenia Terrane in northern Cyprus was part of an unstable shelf of late Paleozoic to Mesozoic age which experienced south-directed thrusting during the Eocene before being buried by Early Eocene fluvial conglomerates. During the Oligocene to Miocene the Kyrenia Terrane underwent drastic subsidence followed by south directed thrusting in the late Miocene to Pliocene. The subsidence was recorded in a 2 km thick package of deep-water calcareous turbidites (i.e. the Kythrea Flysch) that overlies the fluvial conglomerates (Robertson and Woodcock, 1986). The late Miocene fold/thrust belt consists of a series of E-W trending culminations separated by small piggy-back basins filled with Torotonian calcarenites and Messinian evaporates (Calon et al., 2003 a and b; in prep) In the Plio-Pleistocene, the Kyrenia Terrane experienced a period of drastic uplift to form the present-day Kyrenia Range (Robertson, 1990). The Kyrenia

Fault Zone is located along the northern flank of the Kyrenia Range in the hinterland portion of the fold/thrust belt. It straddles the backlimb of the dominant thrust sheet in the belt comprising the Paleozoic-Mesozoic slivers that define the spine of the range on land.

In the outer Cilicia Basin, along the northern side of the Kyrenia Range in Cyprus, north-dipping faults of the Kyrenia Fault Zone define bathymetric highs (terraces) at the present-day seafloor, and are associated with comparable normal sense offsets on the M-Reflector (Fig. 5-5). Dip separations on these faults increases from east to west (~340-425 m in the east and >935 m in the west). This variation in dip separation cannot be explained by extensional faulting alone. It is likely that they are transtensional faults associated with significant scissor motion. A component of strike-slip could account for the somewhat erratic offsets observed in the Plio-Quaternary marker horizons along these fault traces.

The faults of the Kyrenia Fault Zone began to form at the hinterland portion of the late Miocene Misis-Kyrenia thrust culminations as it divided the Oligocene-Miocene ancestor basin into two smaller basins (the Cilicia Basin and the Mesaoria Basin in Cyprus). The faults of the Kyrenia Fault Zone are still active today as indicated by growth strata in the uppermost sediments at the southern part of the outer basin and by fault scarps at the seafloor (Fig. 5-6). Thick packages of Pliocene-Recent sediments terminate at large fault scarps near the basin edge. The growth strata at the faults in the southern part of the outer Cilicia Basin suggest two distinct times for the development of the faults of the Basin-Forming Fault Family. An earlier episode of faulting displays growth strata low in the Plio-Quaternary succession (Fig. 5-7), whereas a later episode of

faulting, landward of the first faults, produces growth in the uppermost part of the Plio-Quaternary sequence (Fig. 5-7). The earlier episode of transtensional faulting may have overprinted extensional faults that were present in the evaporite unit at the southern part of the basin before the initiation of movement along the faults of the Basin-Forming Fault Family. This overprinted intra-salt extension is a part of the Intra-Salt Fold/Thrust Fault Family that is described in section 5.2.

5.1.3 Central Outer Cilicia Fault Zone

Interpretive cross-sectional line drawings from Eastern Mediterranean seismic lines (Fig. 5-8; Biju-Duval et al., 1978; Kempler and Garfunkel, 1991) show a large, deep-rooted high angle fault near the centerline of the outer Cilicia Basin. The seismic data used in this study do not resolve the details of the architecture of this fault zone in this area. However, the seismic lines display a 12 km zone across which the evaporite unit and its Plio-Quaternary cover are offset (Fig. 5-9). Dip separations on the M-Reflector range from 340-510 m with downthrow towards the northern basement compartment. In addition, the thickness of the Plio-Quaternary succession increases from ~255 m in the southern outer Cilicia Basin to ~765 m in the northern basin compartment. Thus, the presence of a large east-west trending extensional fault family is inferred in the central portion of the outer Cilicia Basin. This is understood to be a system of basement rooted, steeply north dipping faults downthrowing Messinian to Recent successions to the north, and effectively dividing the Plio-Quaternary depocenter into two, largely underfilled sub-basins. This extensional fault family is coincident with a series of

overlying salt structures (section 5.5) suggesting activity on these faults is primarily post-evaporite. The axis of the evaporite basin lies in the center of the southen portion of the outer basin confirming that the evaporites were deposited before the faulting took place. This is further supported by the presence of fold and thrust structures within the evaporite unit (the 'Intra-Salt Fold/Thrust Family' section 5.2) which are truncated by the M-Reflector and postdated by the faults of the Basin Central Fault Zone.

5.1.4 Northern Outer Cilicia Fault Zone

Located at the northern margin of the outer Cilicia Basin, the Northern Outer Cilicia Fault Zone is approximately 15 km wide. This fault zone is located about 1-10 km offshore of the southern coast of Turkey underlying the narrow shelf region (Fig. 5-1 and 5-3 [insert 1]). It is an east-west trending and south-dipping array of extensional faults that transect the pre-Messinian basement (Aksu et al., in prep.) but lie outside the edge of evaporite deposition in the northern outer Cilicia Basin. In the area south of the Göksu Delta, the Northern Outer Cilicia Fault Zone passes into a complicated transfer zone linking with the northeast-southwest trending Kozan Fault Zone that bounds the northern margin of the inner Cilicia Basin (Aksu et al., 1992, and in prep.).

This fault zone is characterized by two styles of faults (Figure 5-10); A) a series of high-angle faults in pre-Messinian basement, mainly having a southern dip but locally defining horst-graben structures associated with early Pliocene growth strata and, B) low angle south dipping extensional faults defining gravity slide structures throughout the thick Plio-Quaternary succession that onlaps the basin slope and associated with

numerous stacked debris flows. Fault activity along the high angle faults (Type A) is considered cause for the oversteepening of the slope at the basinward margin which gives rise to the formation of low angle extensional faults (Type B) and gravity slide structures.

5.1.5 Kozan Fault Zone

The Kozan Fault Zone is located along the northwestern edge of the Cilicia Basin (Fig. 5-1 and Fig. 5-3 [insert 1]). On land, in the region of the Adana Basin, the Kozan Fault Zone is an approximately 15 km wide, northeast striking, oblique slip fault system with inferred sinistral strike-slip and down-to-basin normal separation (Calon et al., in prep). The Kozan Fault Zone extends eastward to merge with the East Anatolian Fault Zone.

In the north part of the inner Cilicia Basin, the marine portion of the Kozan Fault Zone lies approximately 15 km offshore and is 12 km wide. Gravity slide structures have been identified in a region to the immediate southeast of this fault zone (Aksu et al., 1992b). In this study, the faults of the Kozan Fault Zone lie at the end of the seismic data set and, therefore, are not well represented on the fault map of the Cilicia Basin (Fig. 5-3 [insert 1]). Four small extensional or transtensional fault segments, likely belonging to the Kozan Fault Zone, can be delineated on seismic sections from the northern part of the inner basin, near the large salt structures of the boundary domain.

5.2 Intra-Salt Fold and Thrust Family

The Intra-Salt Fold/Thrust Family, located in the outer Cilica Basin, consists of a

series of gently south dipping stacked thrust surfaces defining a shallow imbricate stack with associated thrust-related folds resembling ramp anticlines with long, gently south dipping backlimbs and short, more steeply north dipping forelimbs (Figs. 5-2 and 5-11). The orientation of these faults is roughly east-west and extends across the width of the evaporite unit in the outer Cilicia Basin. In the central portion of the outer Cilicia Basin these faults are overprinted by the upright fold/thrust structures of the Basin Central Fault Family (see section 5.5). In the north, the leading thrust faults of the Intra-Salt Fold/Thrust Fault Family cause the upwards arching of overburden sediments and the local thickening of the evaporite unit (Fig. 5-11 and 5-12). This fault family is well developed in the central and western portions of the outer Cilicia Basin but its extent in the eastern part of the basin is more difficult to delineate in part due to interference with the Toe-Thrust Fault Family (section 5.5). The intricacies of the geometry and kinematics of this fault family are interpreted in the section 7.4.

The erosional event marked by the M-Reflector caused a reduction in the elevation of most thrust structures within the evaporite unit. The erosion created local angular unconformities across the crests of thrust-related folds in the evaporites and also created disconformities at the base of the lower Pliocene unit in the backlimb regions of the thrusts (Fig. 5-12).

Because the faults of the Intra-Salt Fold/Thrust Fault Family are located within the evaporite unit, they can only be identified on those sections where evaporites display internal reflectors. The MUN seismic data provides good images of these internal reflector patterns, especially in the outer Cilicia Basin. In Turkish Petroleum data and

MUN data from the inner Cilicia Basin both the internal evaporite reflectors, and the Intra-Salt Fold/Thrust family of faults, are absent.

5.3 Listric Extensional Fault Family

The Listric Extensional Fault Family displays a close association between faulting and the formation and eventual growth of salt structures in the inner Cilicia Basin. This relationship is a typical situation and has been noted in numerous other basins exhibiting extension and mobile salt (see section 2.4).

5.3.1 Faults of the Listric Extensional Fault Family

The faults of the Listric Extensional Fault Family (Figs. 5-2 and 5-3 [insert 1]) are steep, curvilinear, concave-upwards fault surfaces that gently curve and sole onto the top of, or within, the evaporite unit in the inner Cilicia Basin (Fig. 5-13). These faults occur primarily in the thick Plio-Quaternary delta succession and, although they sometimes penetrate the evaporite horizon, they do not affect the base of salt that appears as a smooth, very gently south dipping surface. The faults of this fault family display a normal, extensional fault separation that divides the sedimentary overburden into numerous inverted, horn-shaped fault blocks (Fig. 5-13). These faults are arranged in a fault fan that occupies the entire inner Cilicia Basin, terminating at the northwestern and southeastern margins of the basin but continuing onland to the northeast into the Adana Basin. The faults in this fault fan have curved traces in plan view with a north northwest-south southeast strike in the southern end of the inner basin and an east northeast-west

southwest strike in the north end of the basin; the two orientations of fault sets appear to merge near the centerline of the inner basin but connectivity of the fault sets remains undetermined due to poor seismic coverage.

The irregular spacing of the seismic grid utilized in this study (Fig. 5-3 [insert 1]) means that many interpretations of the seismic data set are possible. Previous works by Aksu et al. (1990) and Aksu et al. (in prep) have mapped this area as containing a series of north-south trending extensional faults that are linear in plan view and which abut the Kozan Fault Zone, a northeast-southwest trending fault zone, near the northern margin of the basin (Fig. 5-14). The interpretation made in this study is slightly different and is based on curving the extensional faults of the fault fan alongside the eastern flanks of the three large salt structures in the boundary domain of the Cilicia Basin. This interpretation is not a unique nor definitive solution, however, I feel that the interpretation presented in this study is valid based on salt tectonic and structural principles and is therefore worthy of consideration.

Sediments in the hanging walls of the faults of this fault family commonly exhibit thickening due to growth on the extensional faults. The extension, which is concurrent with sediment deposition, rotates hanging wall domains causing growth of sedimentary sequences in the hanging wall, with thickening towards the extensional fault (Fig. 5-13).

The dips of the fault surfaces of these extensional faults remain relatively consistent with few major changes in vergence observed across the fault fan (Fig. 5-3 [insert 1]). The most obvious change in fault vergence occurs just east of the central of three large salt structures in the boundary domain of the Cilicia Basin. Faults closest to

this salt structure dip to the east and are separated from west-dipping faults by an extensive anticline structure (Fig. 5-2 and 5-15a). Comparable reversals in the dip of listric faults are observed in the northern part of the basin where they produce similar, but smaller, anticlinal structures (Fig. 5-15 b). Much further east of these anticlines, another change in fault dip occurs where the west dipping faults meet with a group of east dipping faults. The differing dip directions of the faults in this area create a synclinal structure due to the thickening of sediments in the hanging walls that formed a downward curving series of growth strata (Fig. 5-3 [insert 1] and 5-13).

An intimate association is observed between the faults of the Listric Extensional Fault Family and the salt structures in the Cilica Basin. The most notable of these salt-fault associations occurs in the region of the salt rollers and the salt walls (section 5.3.2).

In the western portion of the inner basin, the faults of the Listric Extensional Fault Family terminate near the three salt structures in the boundary domain of the Cilicia Basin. The irregular seismic grid spacing in this area between the salt features (Fig. 5-3 [insert 1]) does not allow the detailed tracing of the listric faults in areas between or alongside the salt structures. The listric faults in the fault fan do not cut through the boundary domain into the outer portion of the Cilicia Basin therefore must terminate in the boundary domain. These faults are mapped on the assumption that they sole against the steep sides of the three large salt features in the boundary domain. This approach is consistent with the common occurrence of faults that are tangential to salt bodies previously described in sections 2.2.2 and 2.2.3.

5.3.2 Salt Structures Associated With the Listric Extensional Fault Family

Small triangular prismatic salt structures are observed beneath most of the extensional faults in the listric fault fan (Fig. 5-13). Correlations between various seismic lines indicate that these salt structures are continuous features that extend over lengths of 20 km or more. The crests of these salt bodies are between 2 km and 4 km apart with average dimensions of 0.5 to 0.7 km in height and 2 to 3 km width. Large fault blocks of grounded Plio-Quaternary overburden sediments commonly occupy the space between individual salt structures. Approximately 1.9 to 2.1 sec (TWT) of the same overburden sediments overlay the prismatic salt bodies in seismic sections.

In plan view (Fig 5-3 [insert 1]) the salt structures in the inner Cilicia Basin are oriented along the strike of extensional faults within the listric fault fan. This association between faults and salt rollers suggests that the salt features in the inner Cilicia Basin formed and grew as a linked system with the faults of the fault fan. It appears that the location of the salt structures was controlled by the location of the listric faults.

In the southwest, the faults of the Listric Extensional Fault Family terminate alongside three large salt structures in the boundary domain of the Cilicia Basin (Fig 5-3 [insert 1]). These salt structures effectively mark the division between the inner extensional domain of the basin and the outer contractional domain. These three large salt structures have a roughly linear trend and generally form inverted cone shapes without any overhanging peripheries (Fig. 5-16).

The more northerly of the three salt structures in the boundary domain is roughly 28 km long, 7 km wide and 3.4 km high and has an approximately east-west orientation.

This salt body has a pointed crest with a steep, flat to concave southern flank which is in normal fault contact with the overburden in the inner basin but is concordant with the overburden in the boundary domain (Fig. 5-17), and a northern, convex flank which is has a gentler slope than the southern flank and is concordant with the overburden in both the boundary domain and at the edge of the inner extensional domain. This salt structure is overlain by 1.5 sec (TWT) of overburden sediments at its shallowest depth in seismic sections.

In between the northern and central salt walls there is a broad antiform within the Plio-Quaternary sediment cover that is disected by faults of the Listric Extensional Fault Family in the inner basinal region (Fig 5-18).

The central salt structure is aligned northwest-southeast and is approximately 21 km long by 10 km wide, and 3.4 km high. The crest of the salt structure is overlain by 2.3 sec. (TWT) of overburden sediments at its shallowest recorded depth (Fig. 5-19). This salt body has a rounded crest topped by a series of small extensional faults forming a synformal graben structure in the Plio-Quaternary succession. This graben appears to ground out and terminate at the western margin of the salt body in the region of two broad, low-amplitude salt diapir crests. The flanks of the central salt structure are convex and have similar slope angles.

In the region between the central and southern salt bodies there is a small salt pillow that appears to be related to thrust faults within the evaporite unit (Fig. 5-20). The pillow structure is overlain by 1.3 s. (TWT) of unfaulted Plio-Quaternary sediments.

The southernmost of the three salt structures is approximately 9.5 km long, 3.7

km wide and is oriented north-south (Fig. 5-20). This salt structure is narrower than the northern and central salt structures, but is equally high at 3.4 km from the base of salt to the crest. The crest of this salt structure is overlain by approximately 300 ms of overburden at its highest elevation in seismic lines. The flanks of this structure are convex and have approximately equivalent slope angles.

5.4 Basin Central Fault Family

The Basin Central Fault Family, located in the Plio-Quaternary succession in the central portion of the outer Cilicia Basin, consists of a series of near vertical, east-west trending reverse faults displaying small to moderate stratigraphic offset. These faults occupy a 14 km wide zone in the central portion of the outer Cilicia Basin (Fig. 5-2 and Fig. 5-3 [insert 1]) where they form anticlinal structures which are commonly cored by evaporates.

5.4.1 Faults of the Basin Central Fault Family

Some of the reverse faults of the Basin Central Fault Family have a notable south-directed vergence, while northward vergent faults are less common and, when present, are very limited in their lateral extent (Fig. 5-3 [insert 1]). These faults root within the evaporite unit (Fig. 5-21) and display a great deal of cross-sectional and along strike variability in fault vergence as well as in shape, amplitude, and symmetry/asymmetry of associated folding in the Plio-Quaternary succession.

5.4.2 Salt Structures Associated With the BasementCentral Fault Family

The salt structures of the Basin Central Fault Family are divided into two subdomains (Fig. 5-22). In the north subdomain, there are 1-3 large salt anticlines with high structural relief (~0.5 sec TWT), separated by large peripheral sinks (rim synclines). These anticlines are bounded to the north by a thick Plio-Quaternary succession that thickens up to 1.2 sec (TWT) into the northern outer basin area. In the south subdomain, there is a series of low relief (0.1 - 0.2 sec TWT), narrowly spaced anticlines developed on the platform of the southern outer basin. These anticlines are covered by a thin Plio-Quaternary blanket approximately 0.4 sec (TWT) thick.

5.5 Toe-Thrust Fault Family

The faults of the Toe-Thrust Fault Family occupy an approximately 16 km wide belt in the eastern end of the outer Cilicia Basin (Fig. 5-2 and 5-3 [insert 1]). These faults are closely associated with salt cored anticlinal structures in the portion of the Cilicia Basin that is immediately west of the three large salt structures in the boundary domain. In plan view, these faults have arcuate traces that follow the trend of the most central of the three large salt structures of the boundary domain. The orientation of this fault family is northwest-southeast.

5.5.1 Faults of the Toe-Thrust Fault Family

The faults belonging to the Toe-Thrust Fault Family are relatively shallow-dipping thrust faults that appear to sole within the evaporite unit (Fig. 5-23). The lateral

tiplines of these faults terminate near the north and south edges of the Cilicia Basin. These thrust faults have no apparent preferred vergence. The lack of a preferred thrust direction is indicative of a fault belt that detaches on a weak décollement horizon (see Chapter 2, section 2.5.1).

The faults at the outer edge of the Toe-Thrust Fault Family are curved toward the outer basin when studied in plan view (Fig. 5-3 [insert 1]). Those fault traces furthest away from the three salt structures display greater curvature than those that are closest to the salt structures. This increased curvature must be the result of some additional tectonic force within the basin. A node feature is delineated in the area where the Toe-Thrust Fault Family and the Basement-Linked Fault Family meet (Fig. 5-3 [insert 1]).

5.5.2 Salt Structures Associated With the Toe-Thrust Fault Family

Salt structures related to the Toe-Thrust Fault Family consist predominantly of salt pillows and/or salt anticlines in the cores of anticlines, many of which are broken by thrust faults (Fig. 5-21 and 5-23). The salt pillows are generally low-amplitude salt structures that are concordant with the overburden sediments whereas the salt anticlines display a marked discordance with overburden sediments, often forming angular unconformity at anticline crests. Faulted salt anticlines are commonly thrust over the lowermost overburden sediments as the folds tightened and faulted creating disconformities.

Salt-cored anticlines closest to the salt walls of the boundary domain are much more attenuated (higher amplitude, tighter folding, thrusted, etc.) than those anticlines

and pillows that lie further from the salt walls. Those salt cored anticlines closest to the boundary domain are generally tightly folded and often faulted, displaying approximately 300 ms offset on the M-Reflector whereas anticlines further from the boundary domain are much broader and more loosely folded commonly showing less than 150 ms offset on the M-Reflector. Faulted anticlines are generally more asymmetric than the unfaulted anticlines, however, this may be due to the greater distance of unfaulted anticlines from the salt walls at the boundary domain (most likely the focus of deformation) as compared to the faulted anticlines which are adjacent to the boundary domain.

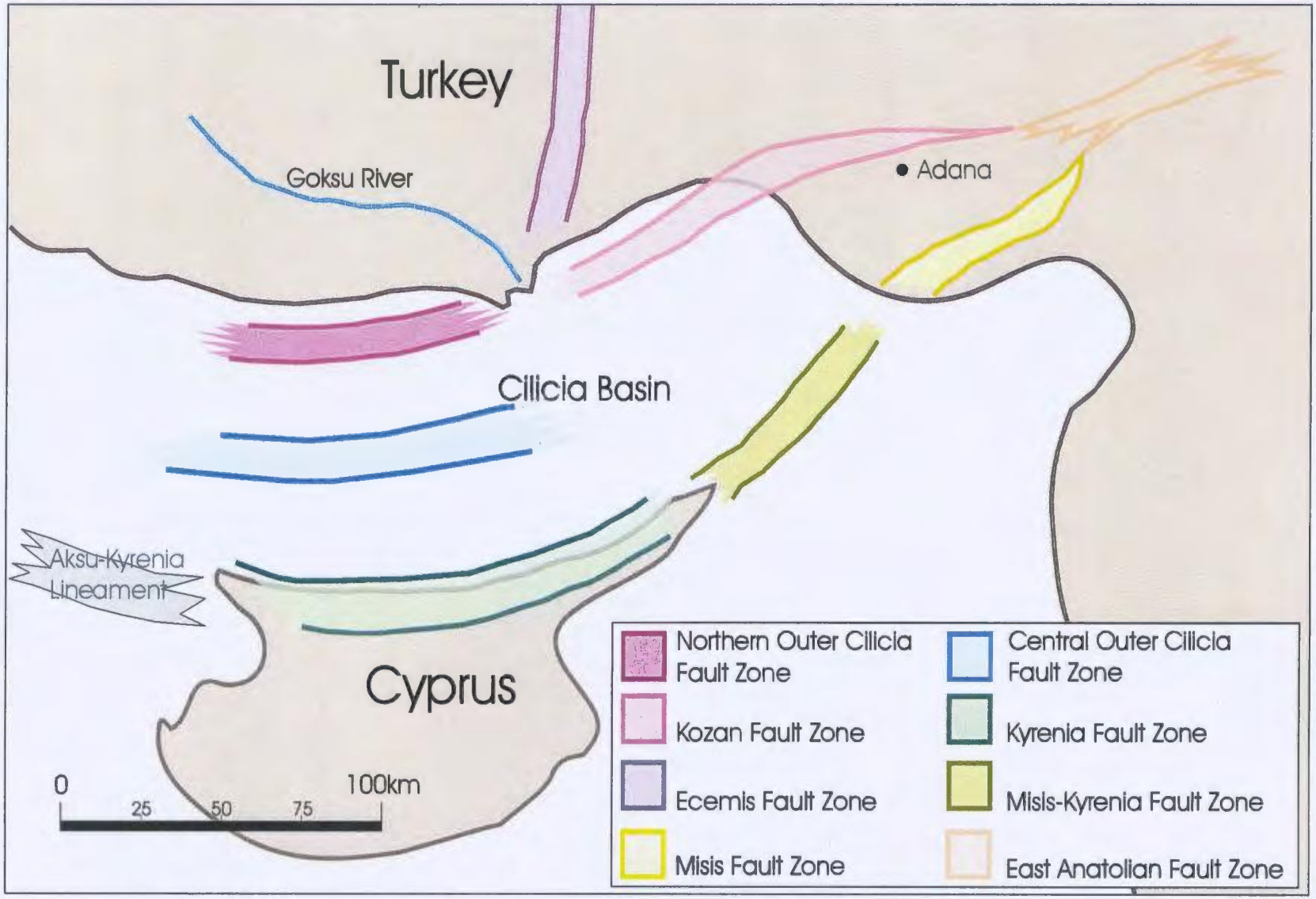

Figure 5-1: Approximate locations of the major fault assemblages previously identified in the Cilicia Basin, Eastern Mediterranean

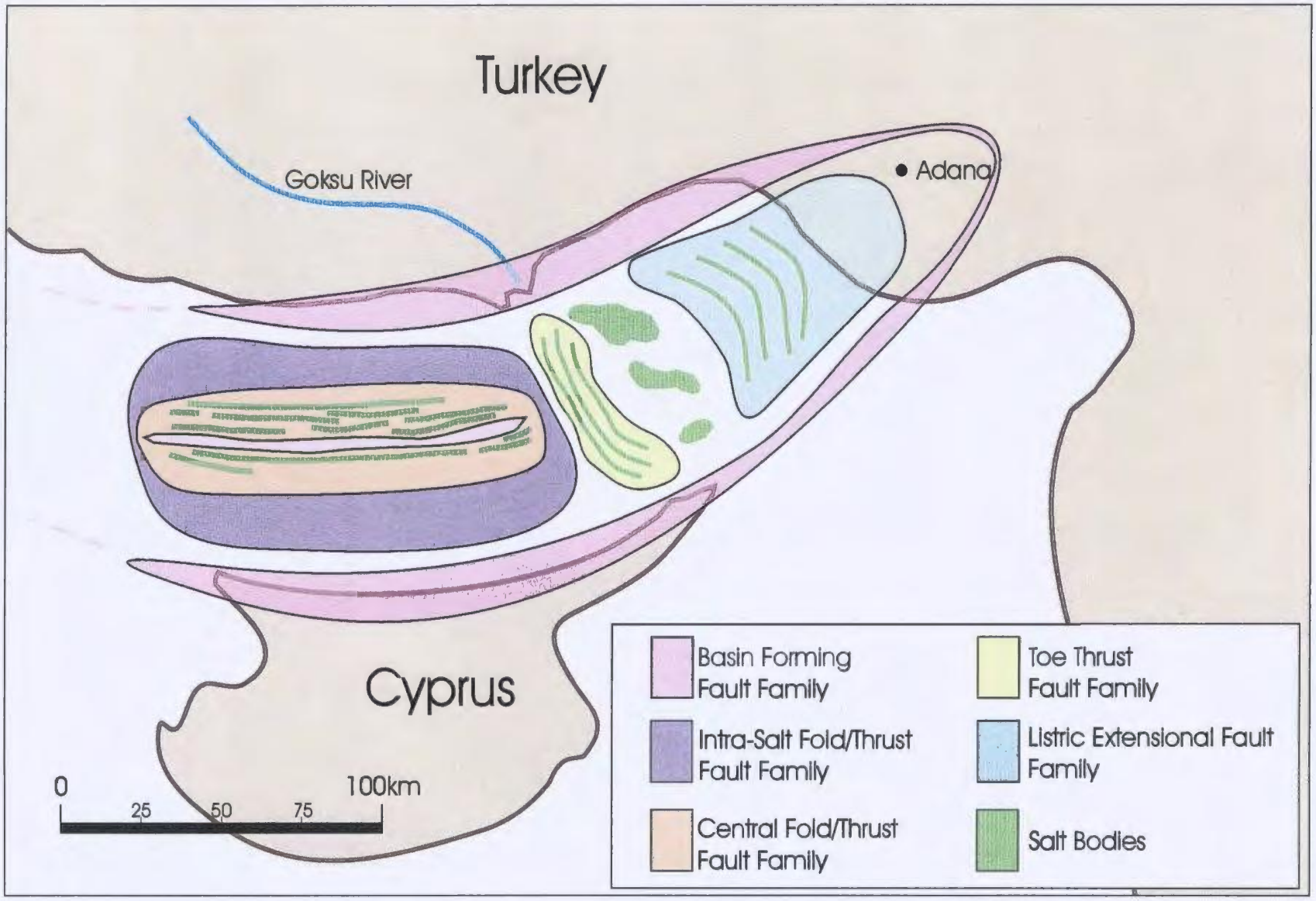

Figure 5-2: Approximate locations of the five major fault families outlined in this study of the Cilicia Basin, Eastern Mediterranean.

Figure located in back pocket.
INSERT 1

Figure 5-3: Fault map of the Cilicia Basin with seismic grid spacing, location of salt structures and position of seismic lines with respect to salt walls.

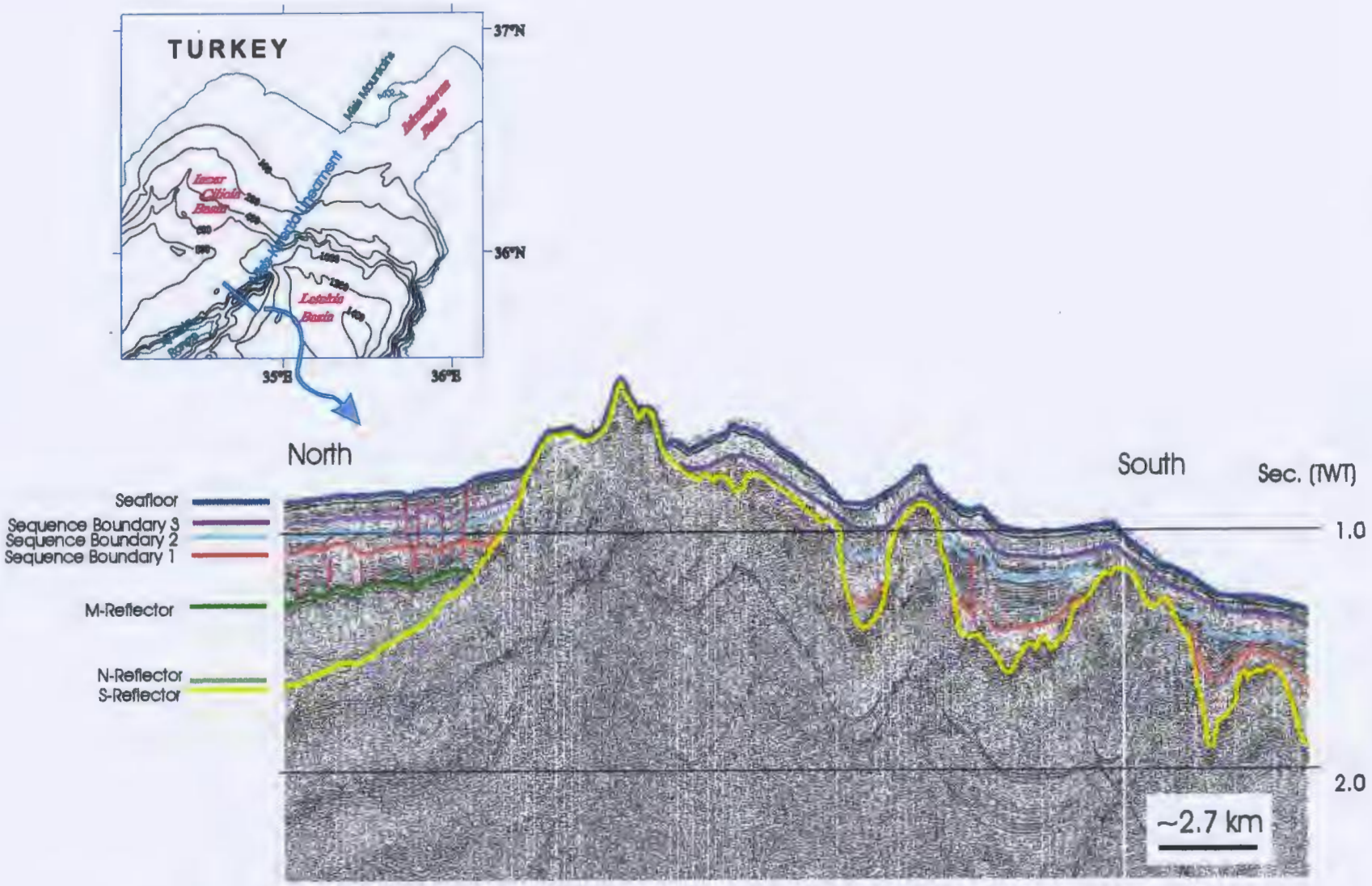

Figure 5-4: Seismic sections from the Inner Cilicia Basin show the Misis-Kyrenia Lineament is a bathymetric high, approximately 200 m above the regional seafloor.

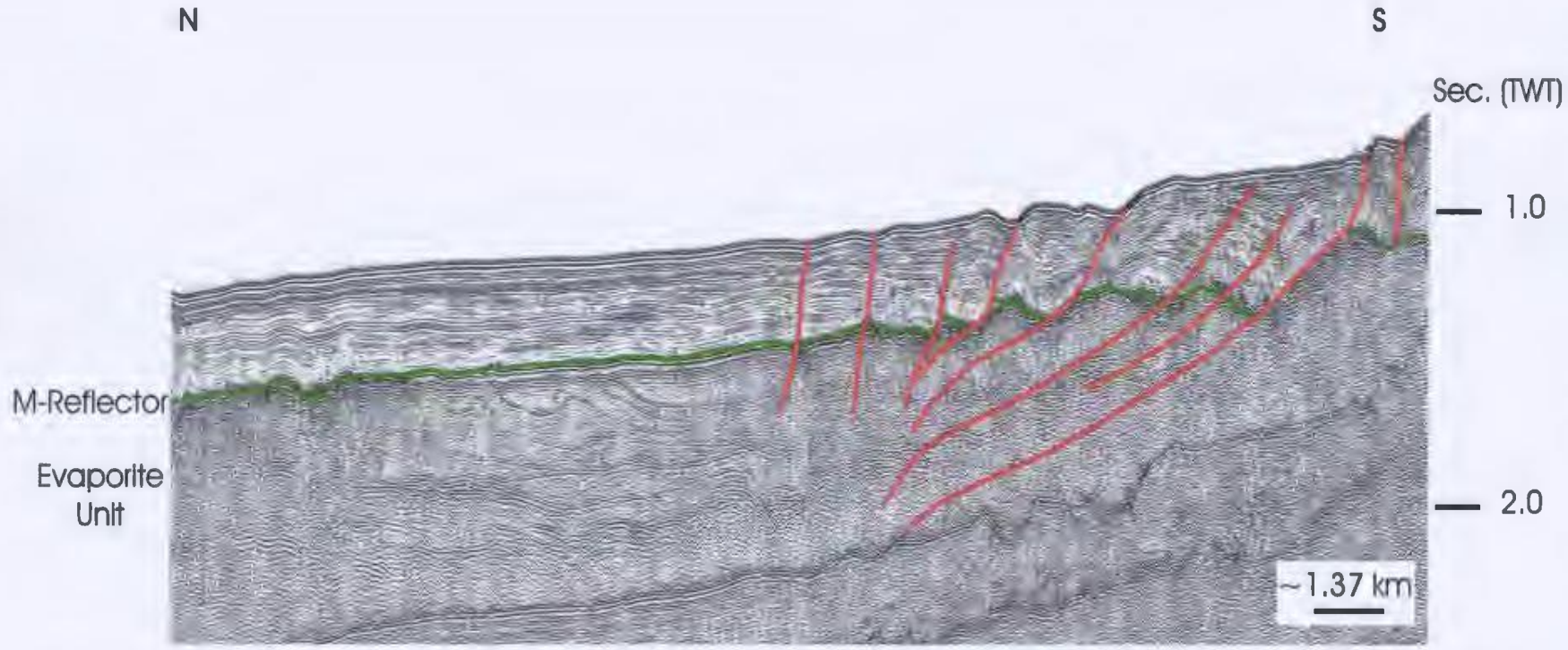

Figure 5-5: Along the northern side of the Kyrenia Range (in the southern part of the Cilicia Basin), north-dipping faults of the Kyrenia Fault Zone define bathymetric highs (terraces) at the present-day seafloor, and are associated with comparable normal sense offsets on the M-reflector.

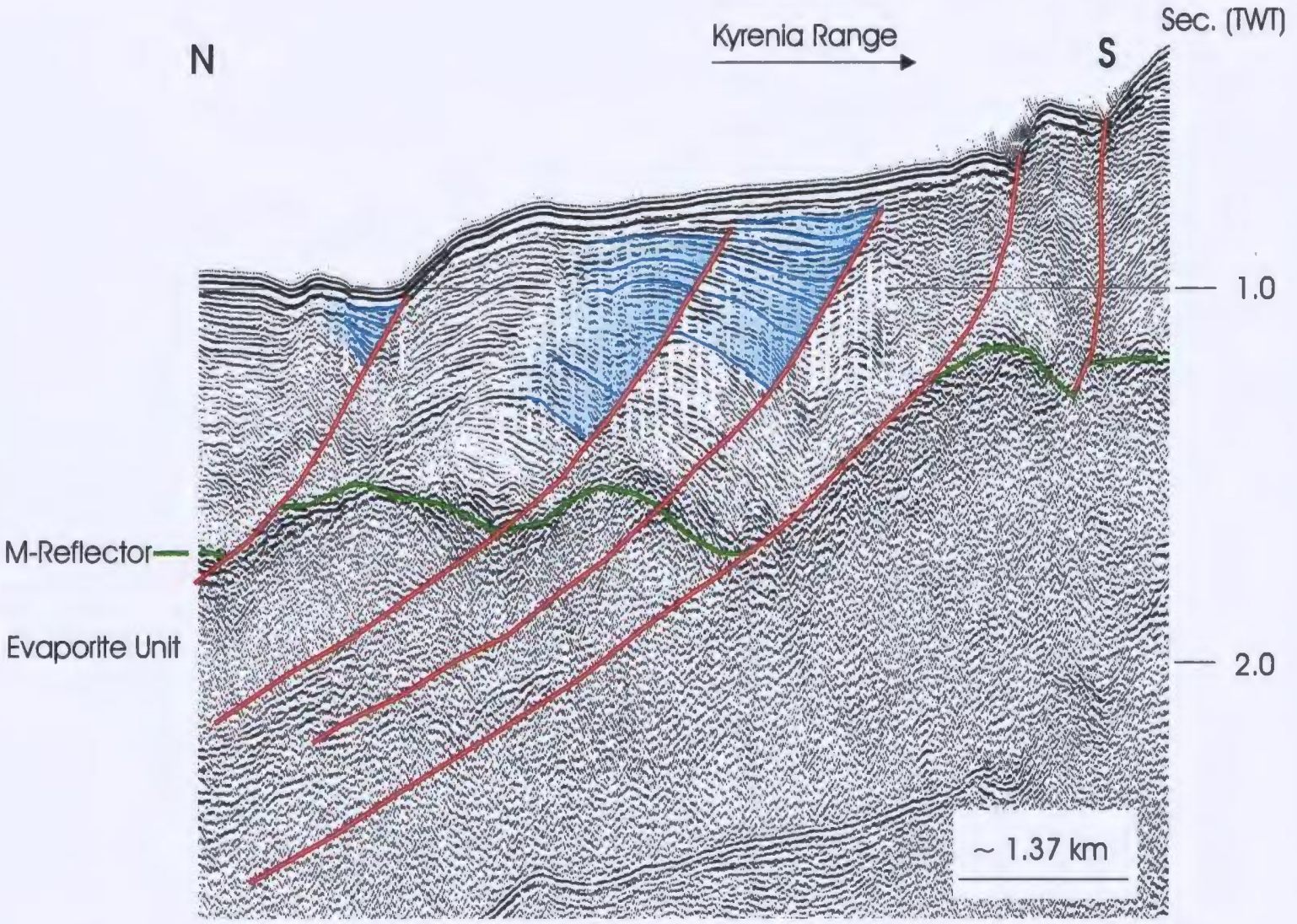

Figure 5-6: The faults at th Kyrenia Fault Zone are still active today as indicated by growth strata in the uppermost sediments at the southern part of the outer Cilicia Basin.

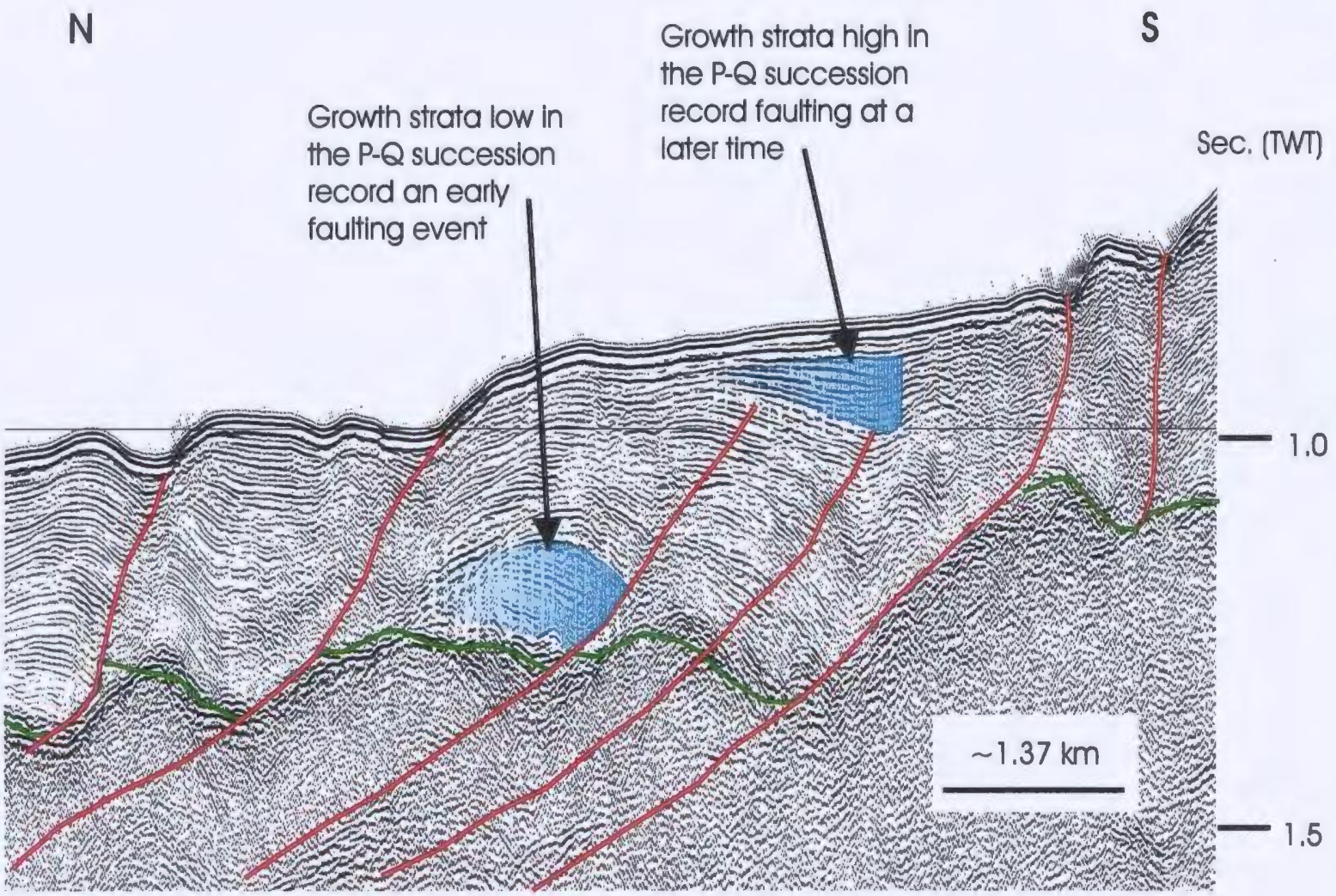

Figure 5-7: An early episode of faulting displays growth strata low in the Plio-Quaternary succession, whereas a later episode of faulting, landward of the first faults, produces growth in the uppermost part of the Plio-Quaternary sequence.

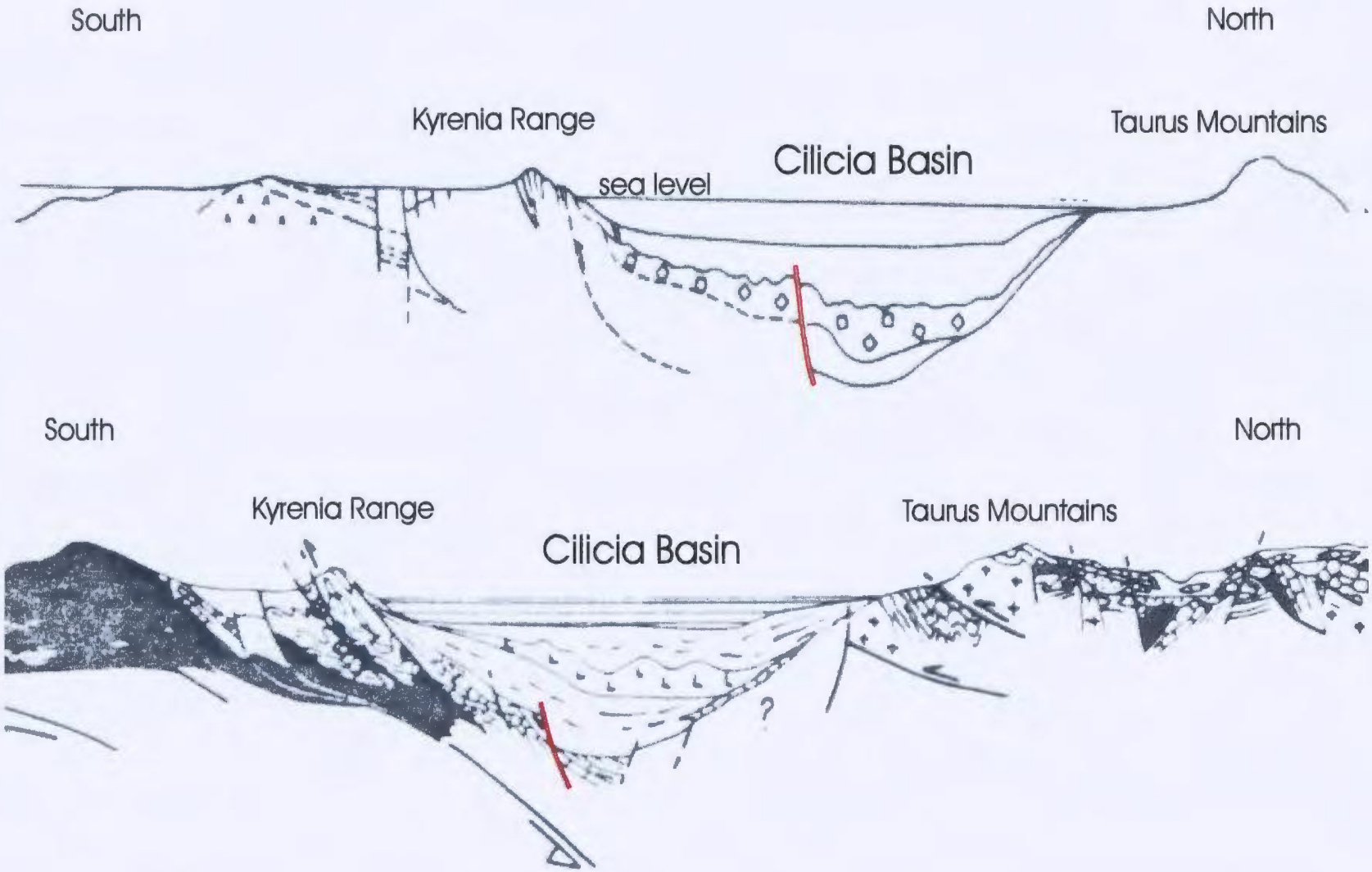

Figure 5-8: Line Drawings from Kempler and Garfunkel (1991) and Biju-Duval et al. (1978) show a large extensional fault at the centre of the Cilicia Basin which appears to influence salt deposition.

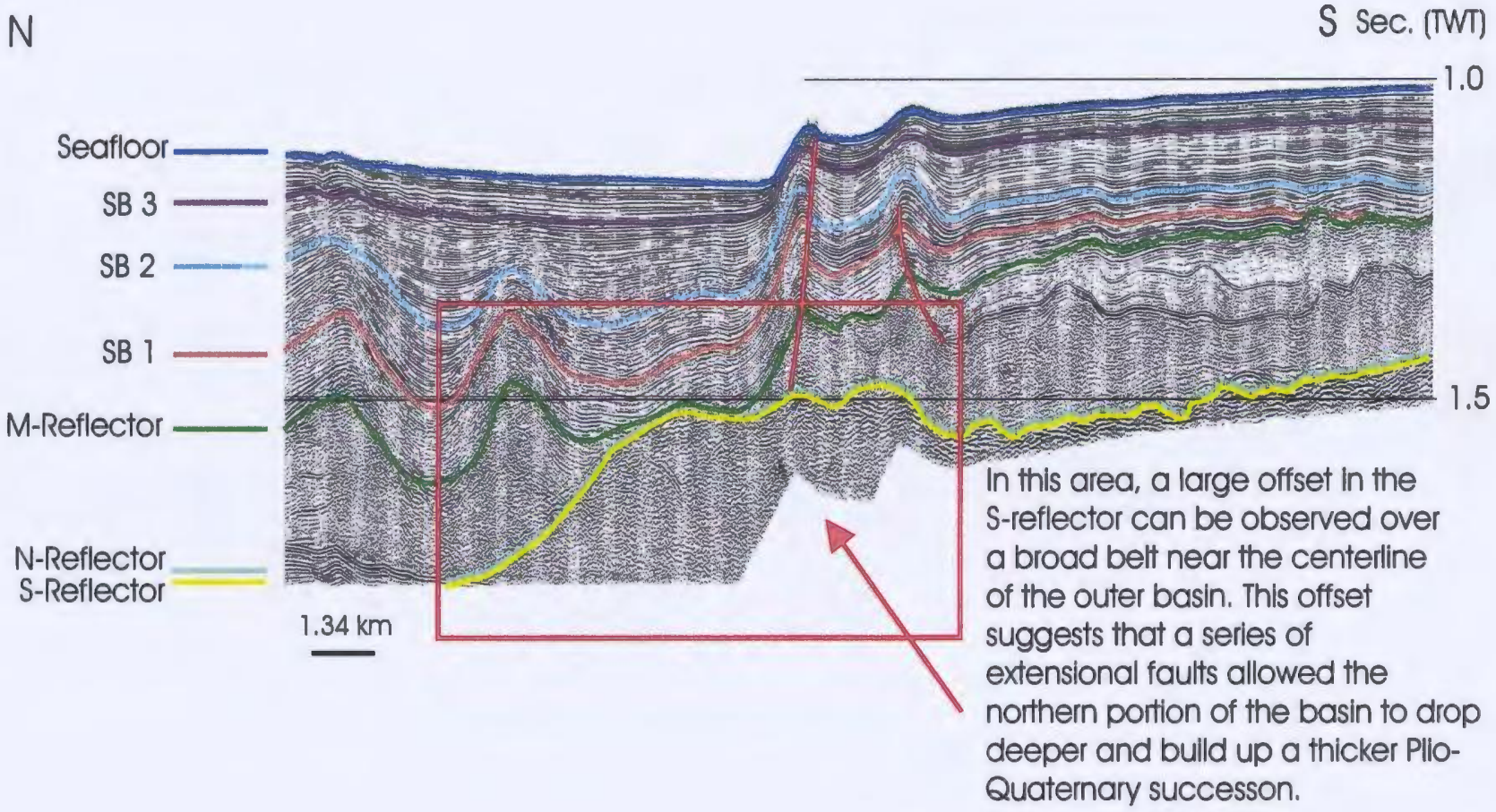

Figure 5-9: The presence of a large east-west trending, extensional fault system has been inferred in the central portion of the outer Cilicia Basin. This inference is based on a large offset observed at the S-reflector which is continuous over an approximately 12 km belt in north-south oriented seismic lines.

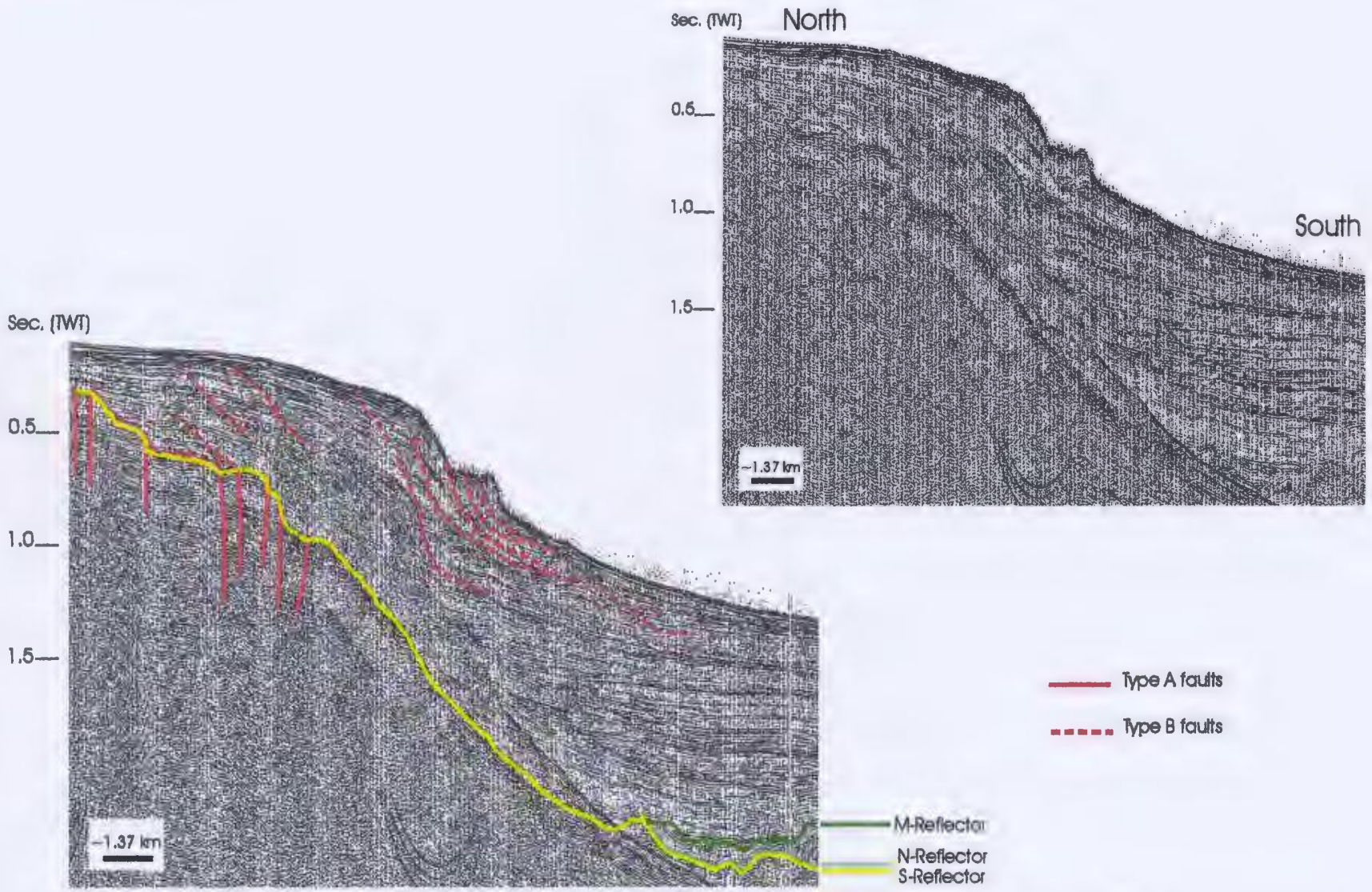

Figure 5-10: The Northern Outer Cilicia Fault Zone is characterized by two distinct fault types. The first of these types, the Type A faults, are high angle extensional faults that resulted in the formation of horst and graben type structures. These faults likely caused the oversteepening of the basinward slope sediments, resulting in the formation of the low-angle Type B faults which form gravity slide structures.

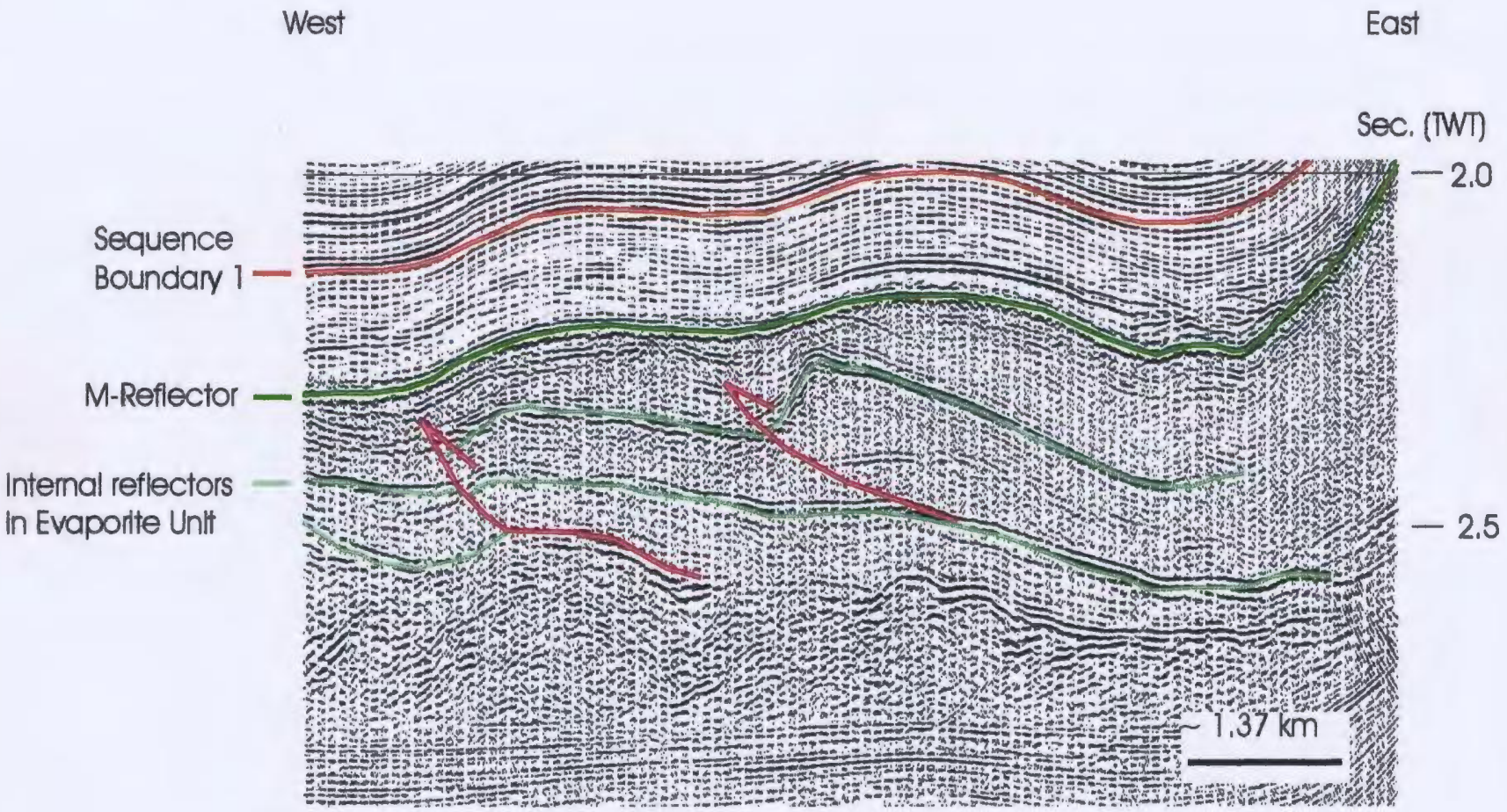

Figure 5-11: The Intra-Salt Fold/Thrust Family consists of a series of gently south dipping stacked thrust surfaces defining a shallow imbricate stack with associated thrust related folds resembling ramp anticlines with long, gently south dipping backlimbs and short, more steeply dipping forelimbs.

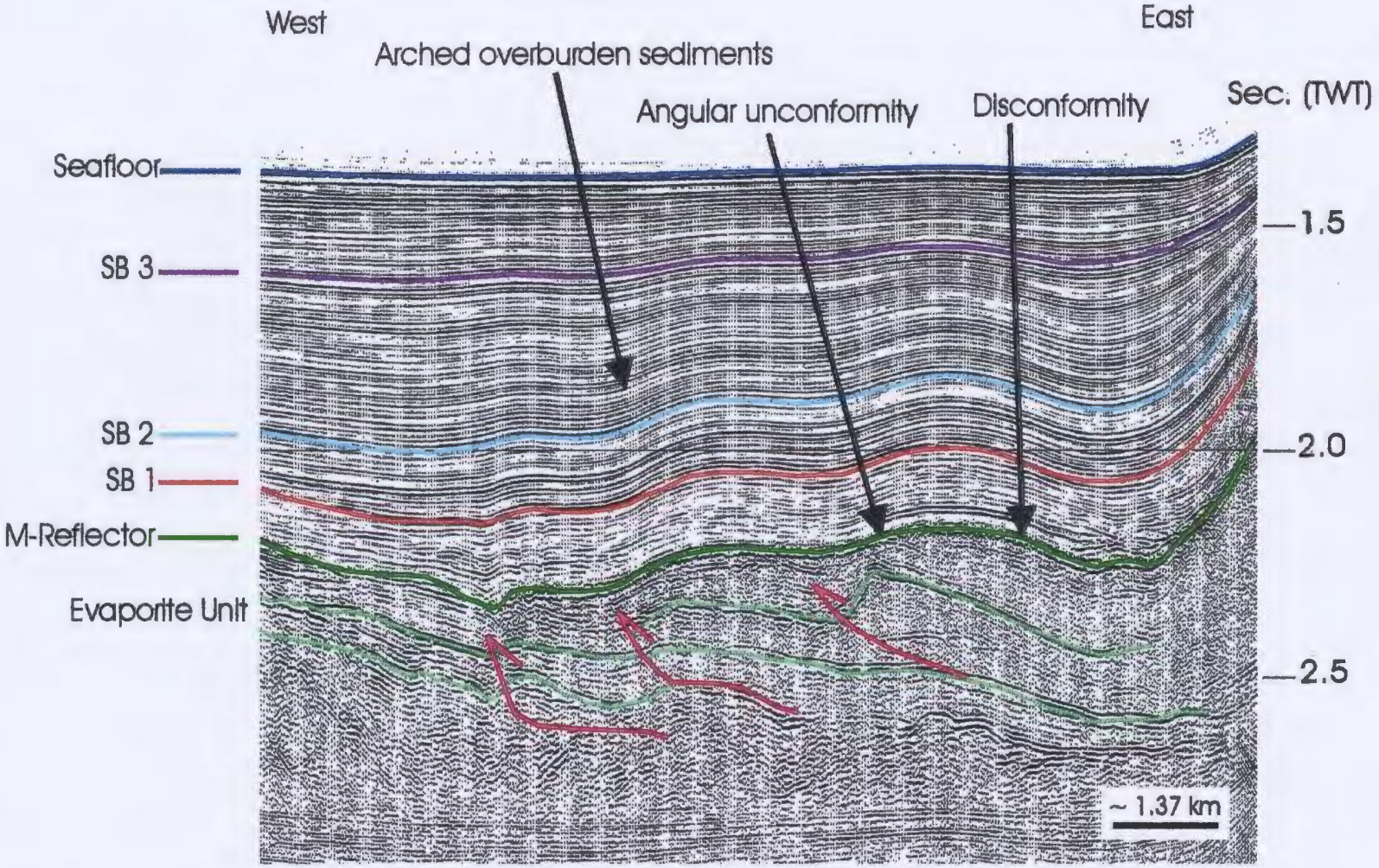

Figure 5-12: The leading faults of the Intra-Salt Fold/Thrust Family cause the upwards arching of overburden sediments and the local thickening of the evaporite unit. Erosion at the crests of the thrusted evaporites (represented by the M-reflector) created local angular unconformities at the crests of folds/thrusts and also created disconformities in the backlimb regions of these folds.

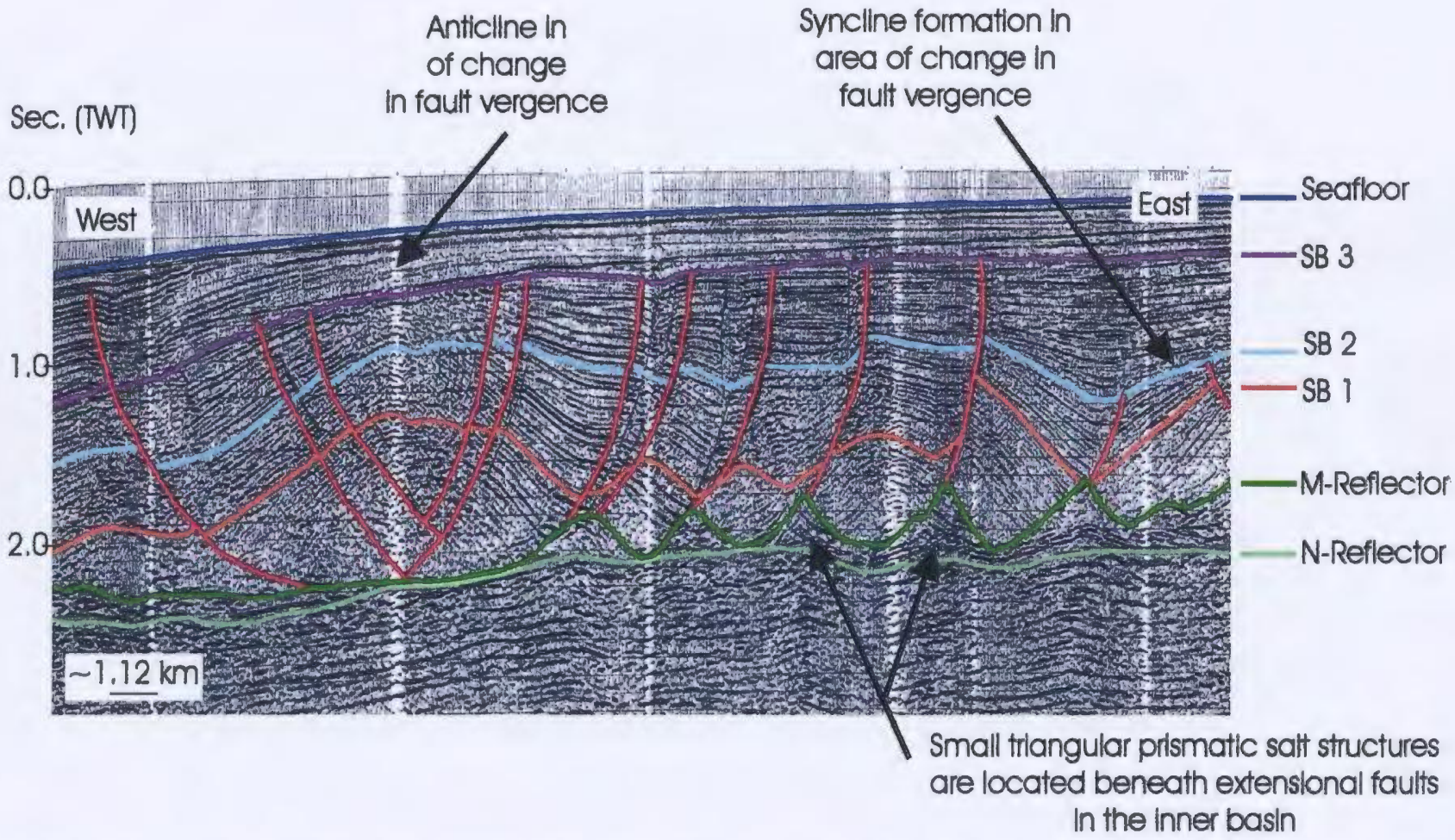

Figure 5-13: The faults of the listric extensional fault family are steep, curvilinear, concave upwards fault surfaces that gently curve and sole on the top of, or within, the evaporite unit in the Inner Cilicia Basin without penetrating through to the base salt horizon. Small triangular prismatic salt structures are located beneath most of the extensional faults. Changes in the vergence direction of the faults in this fault family (often related to movement of the evaporites) result in the formation of overburden synclines and anticlines related to the extensional nature of the faulting.

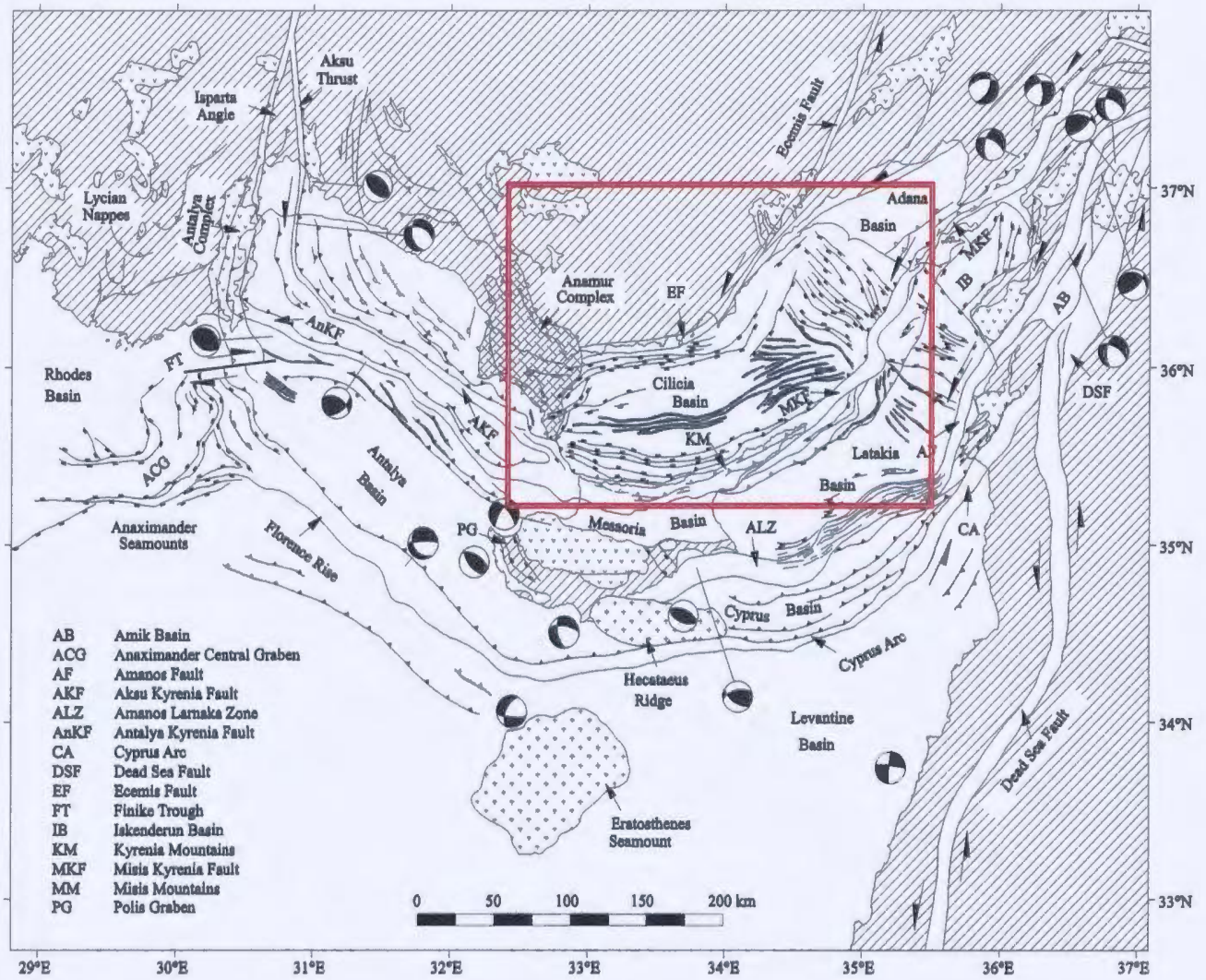

Figure 5-14: Fault mapping in the inner portion of the Cilicia Basin, completed by Aksu et al. (1992a) shows a fault interpretation in which the NW-SE trending faults intersect the NE-SW extensional faults. This is slightly different than the interpretation presented in this thesis.

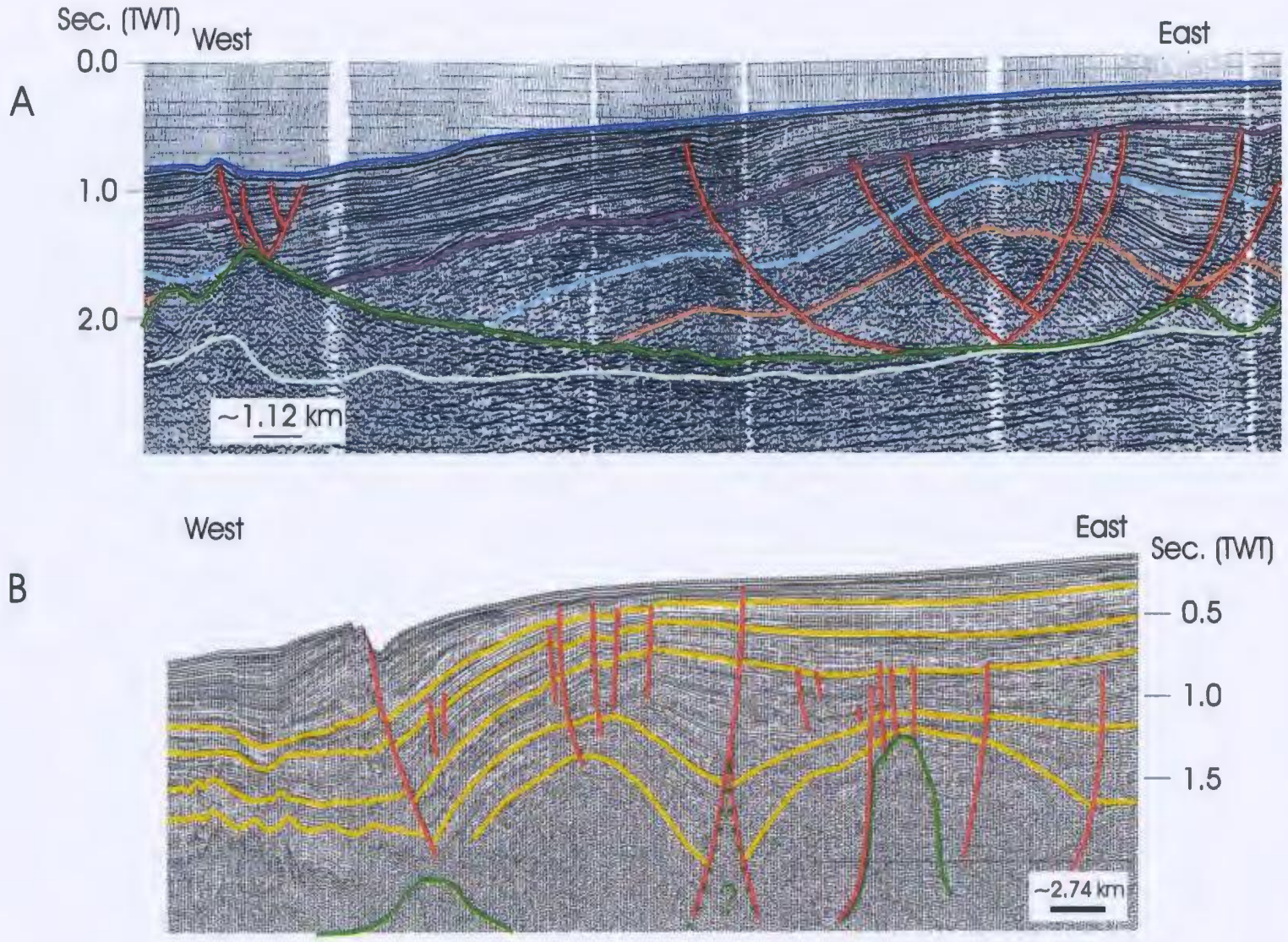

Figure 5-15: A) Faults closest to the central salt wall in the Cilicia Basin display a change in vergence seperated by an anticlinal structure. B) Further east of the large salt walls, more anticlines can be observed where there are changes in fault vergence.

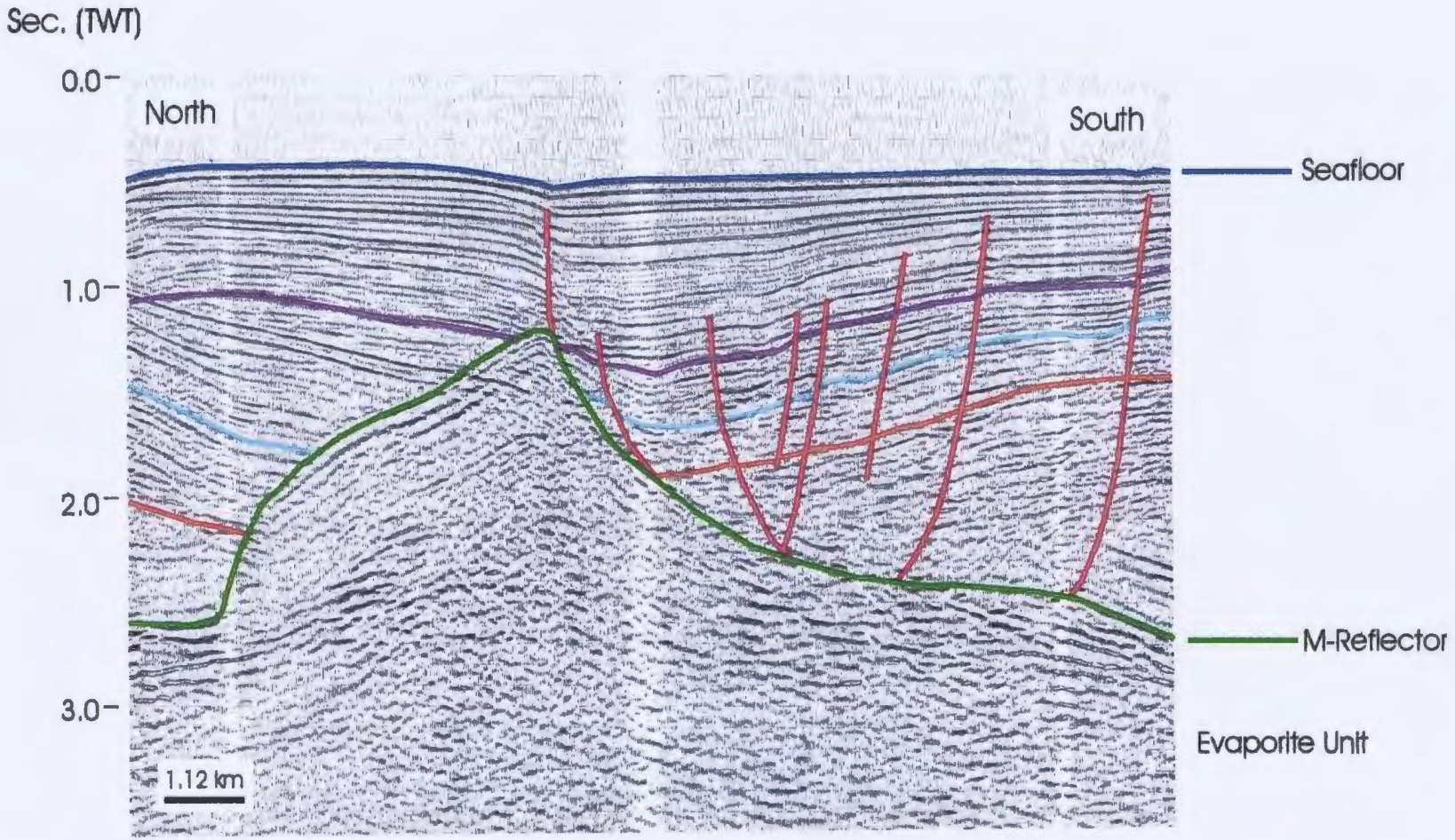

Figure 5-16: Typical morphology of large salt structures in the boundary domain of the Cilicia Basin. Notice there are no overhanging peripheries and the external form is roughly that of a inverted cone.

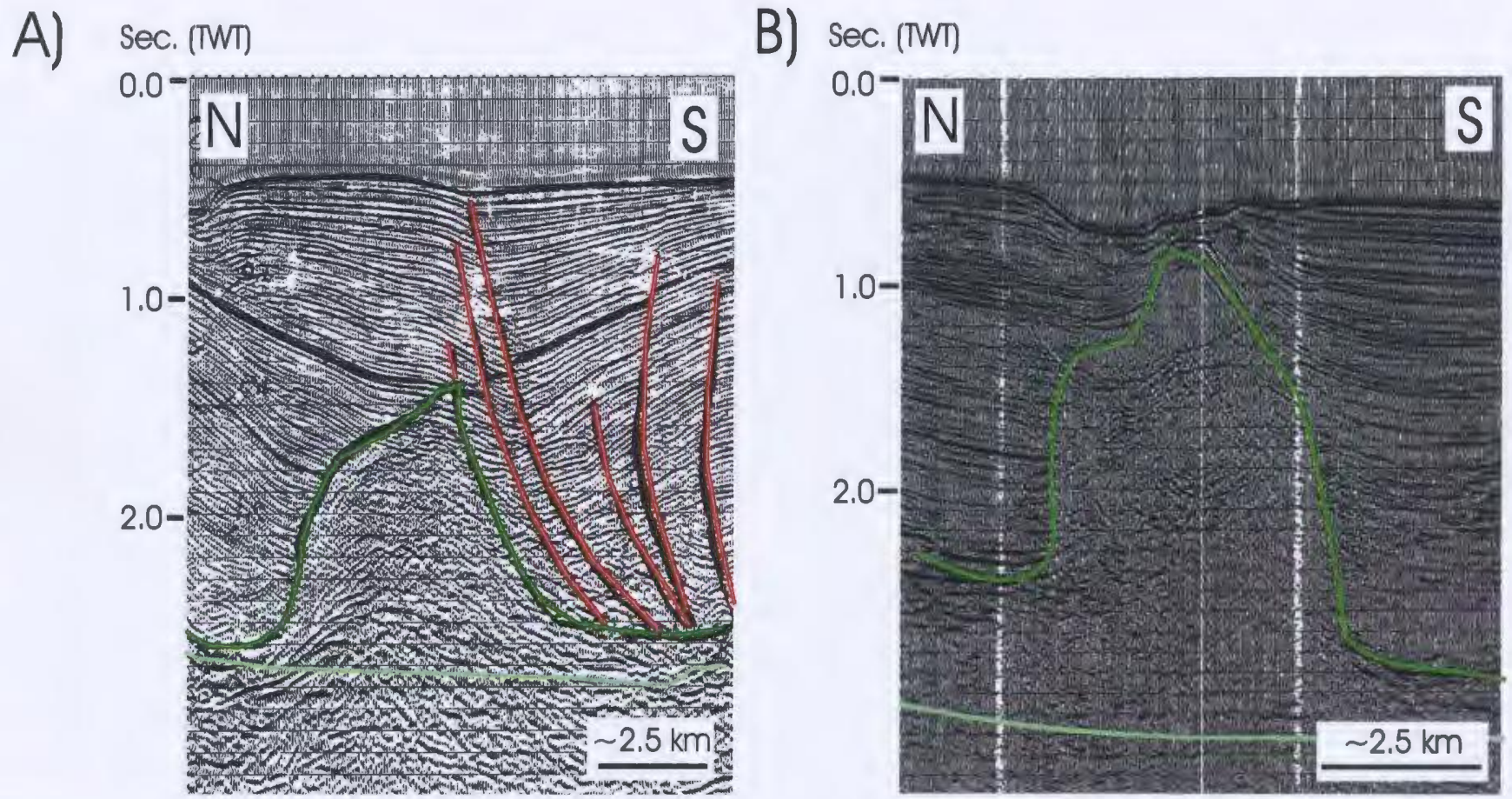

Figure 5-17: The more northerly of the three salt structures in the boundary domain is roughly 28 km long, 7 km wide and 3.4 km high and has an approximately east-west orientation. This salt body has a pointed crest with a steep, flat to concave southern flank which is in normal fault contact with the overburden in the inner basin (A) but is concordant with the overburden in the boundary domain (B), and a northern, convex flank which is has a gentler slope than the southern flank and is concordant with the overburden in both the boundary domain and at the edge of the inner extensional domain. This salt structure is overlain by 1.5 sec (TWT) of overburden sediments at its shallowest depth in seismic sections.

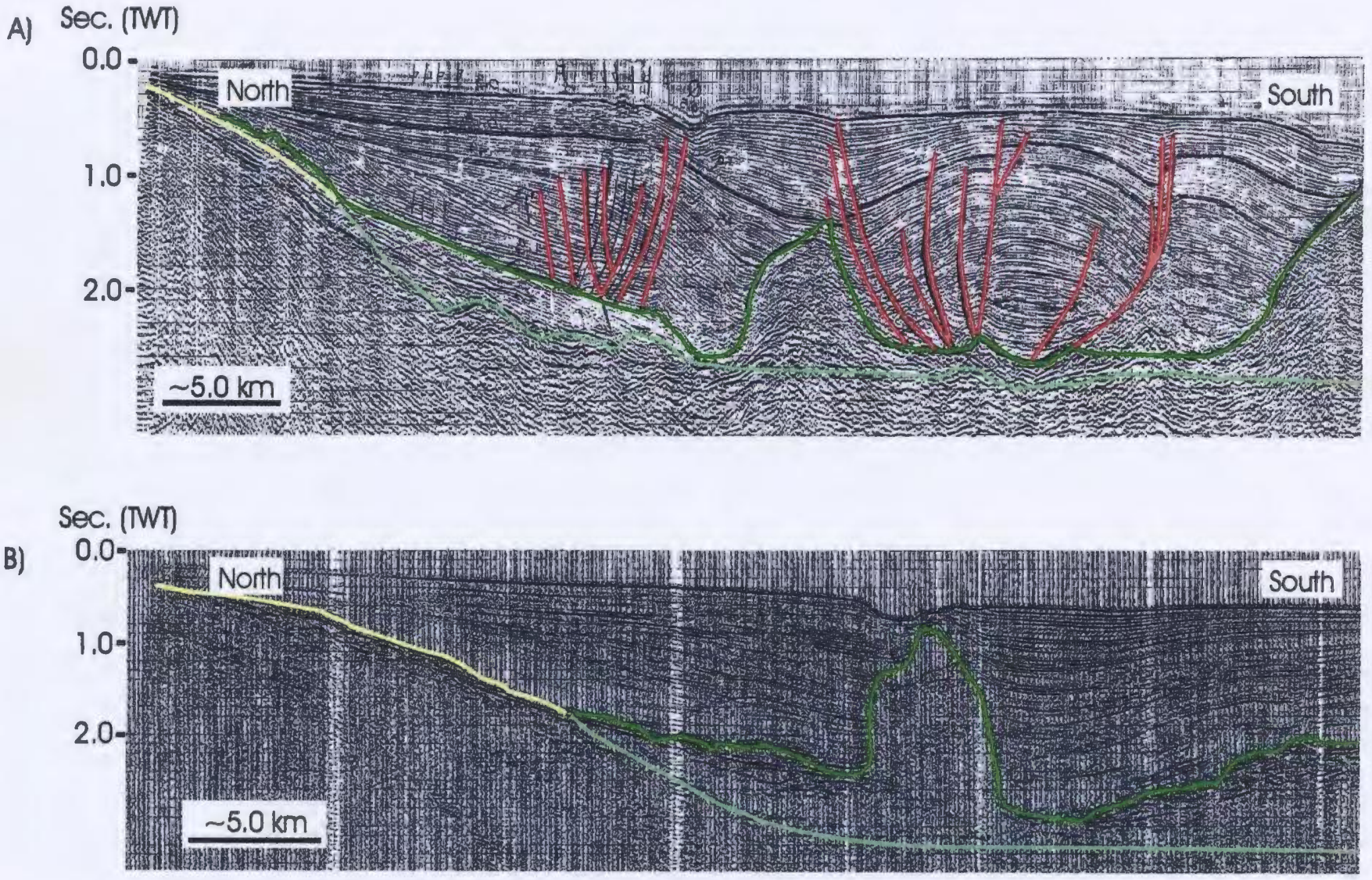

Figure 5-18: The anticline found between the north and central salt walls is faulted in the inner basin (A) but appears to have no faults in the boundary domain (B).

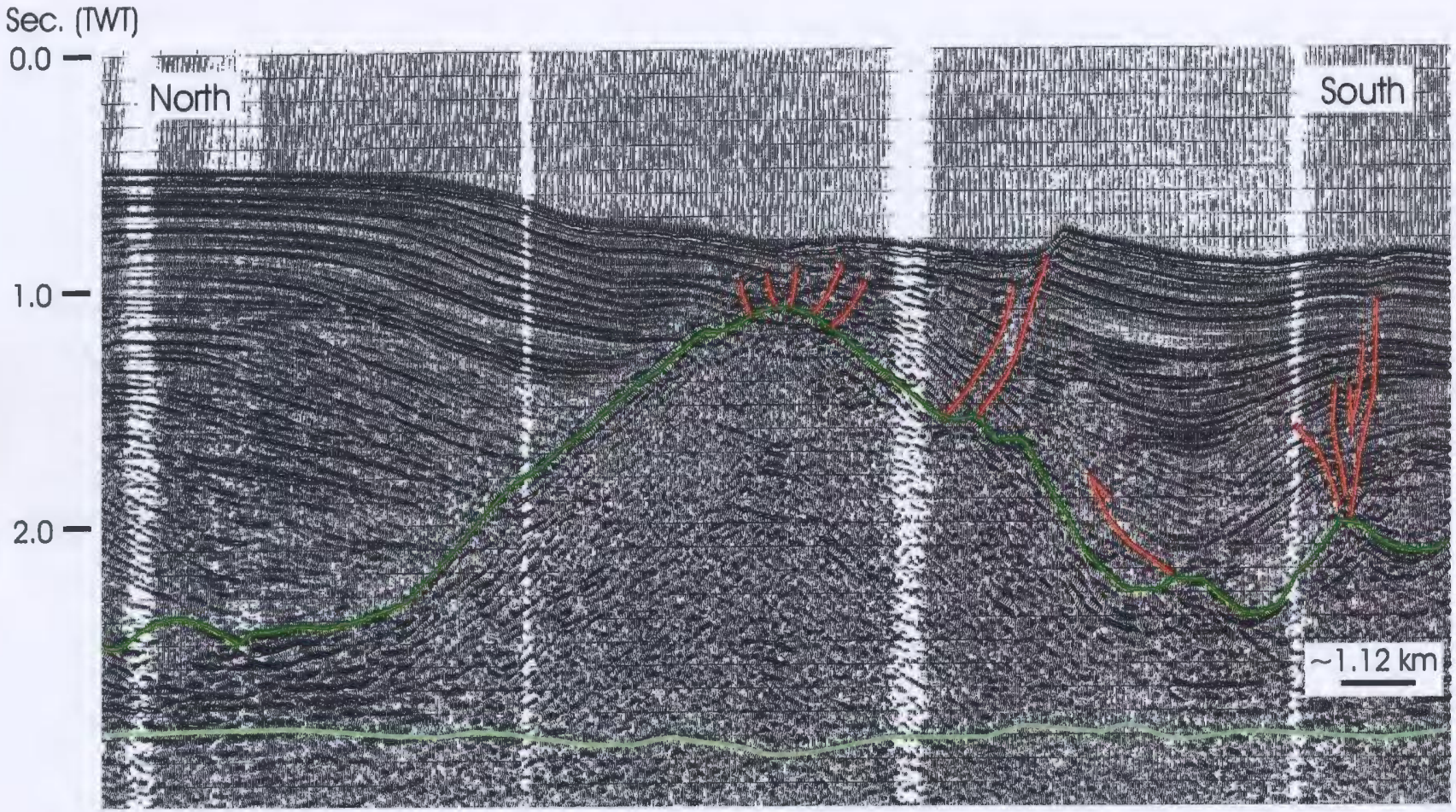

Figure 5-19: The central salt wall in the Cilicia Basin is aligned in a NW-SE direction and has maximum dimensions of 21 km long by 10 km wide; it is ~3.4 km high and is covered by as little as 0.23 seconds (TWT) of overburden sediment.

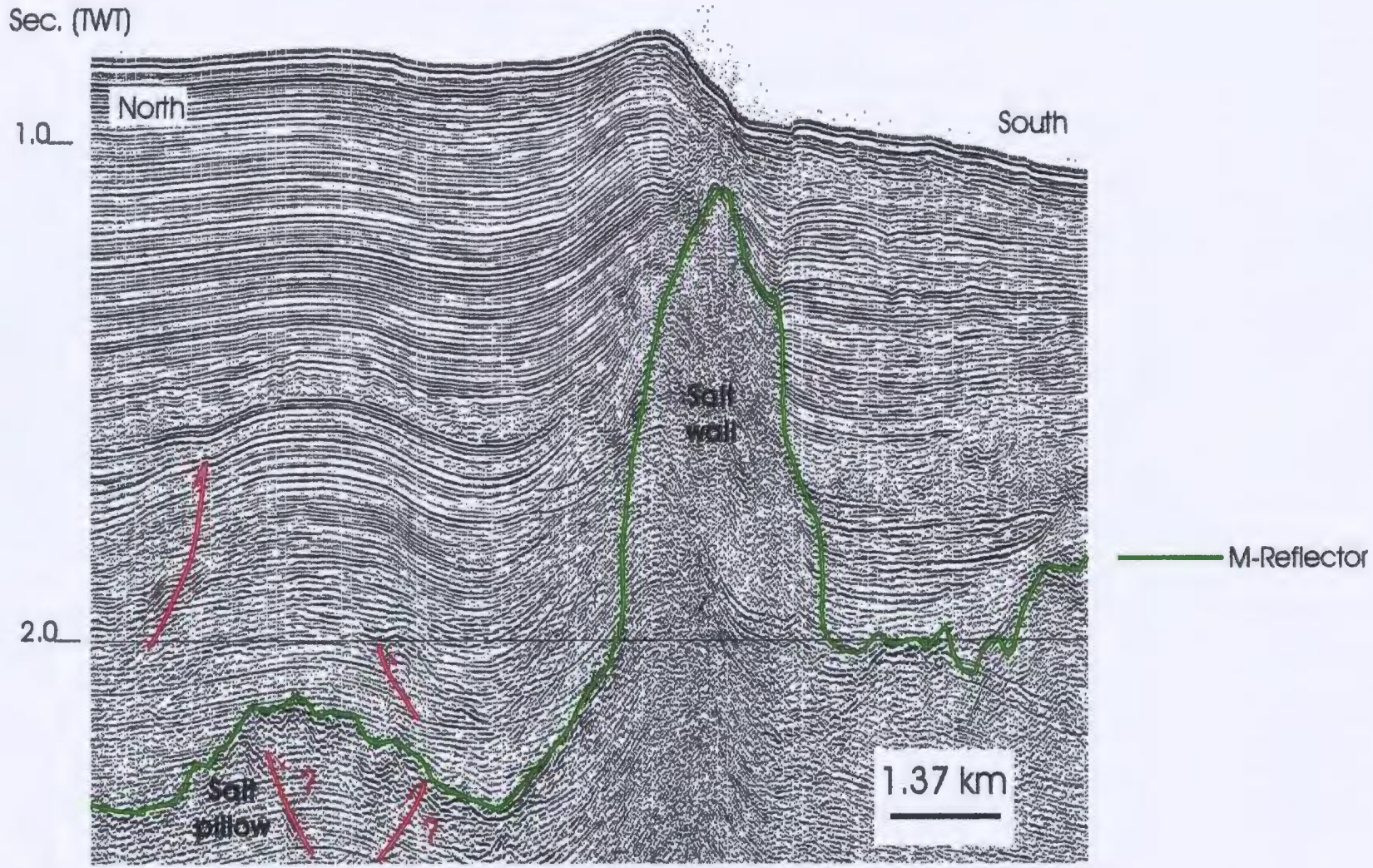

Figure 5-20: Located between the central and southern salt walls, a small salt pillow has formed. This pillow structure may be related to some thrusting ocurring in the evaporite unit which has not been imaged on seismic.

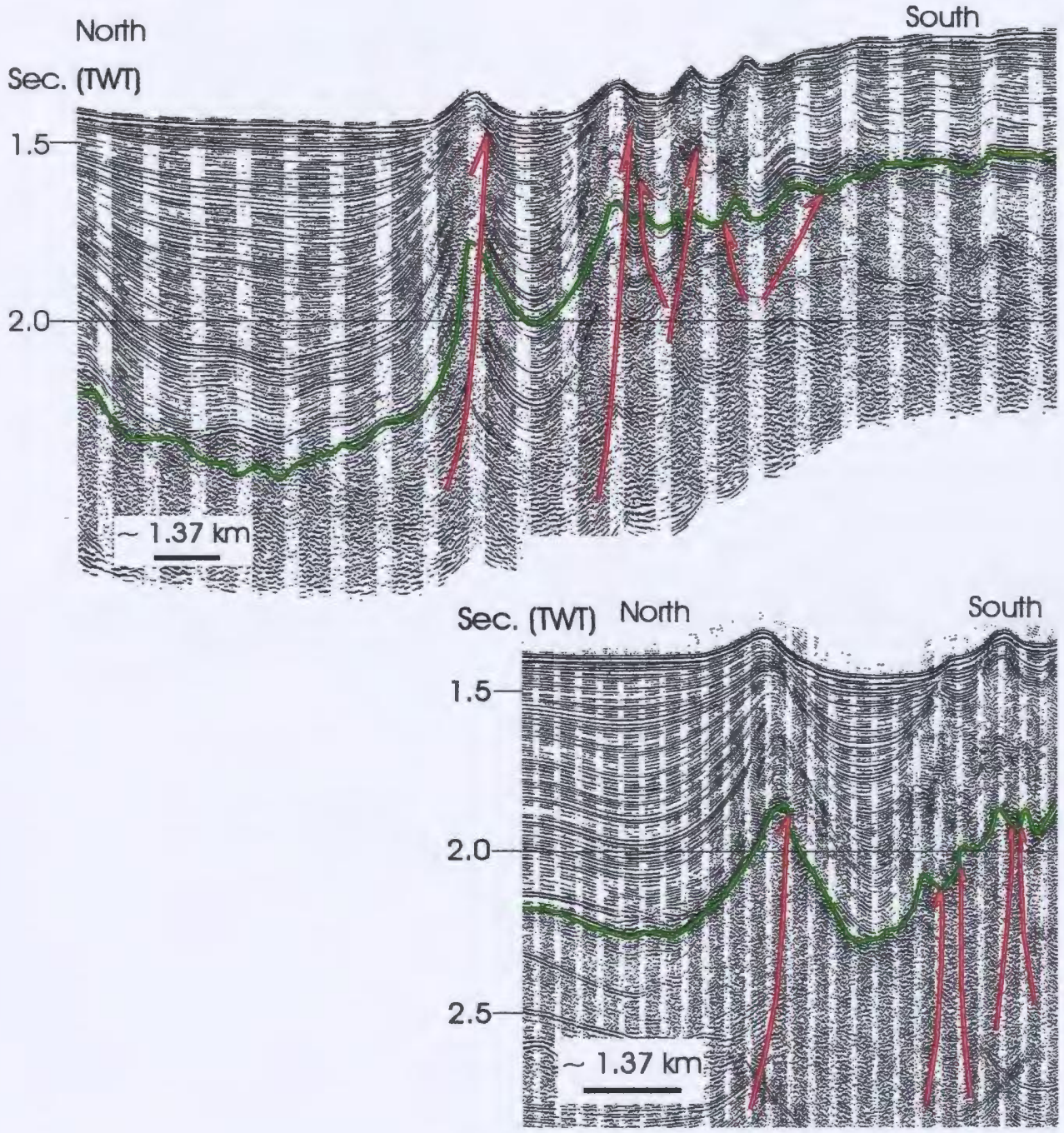

Figure 5-21: Faults of the Basin Central Fault Family display mainly south-directed vergence with faults rooting in salt and displaying a great deal of variability in shape and offset.

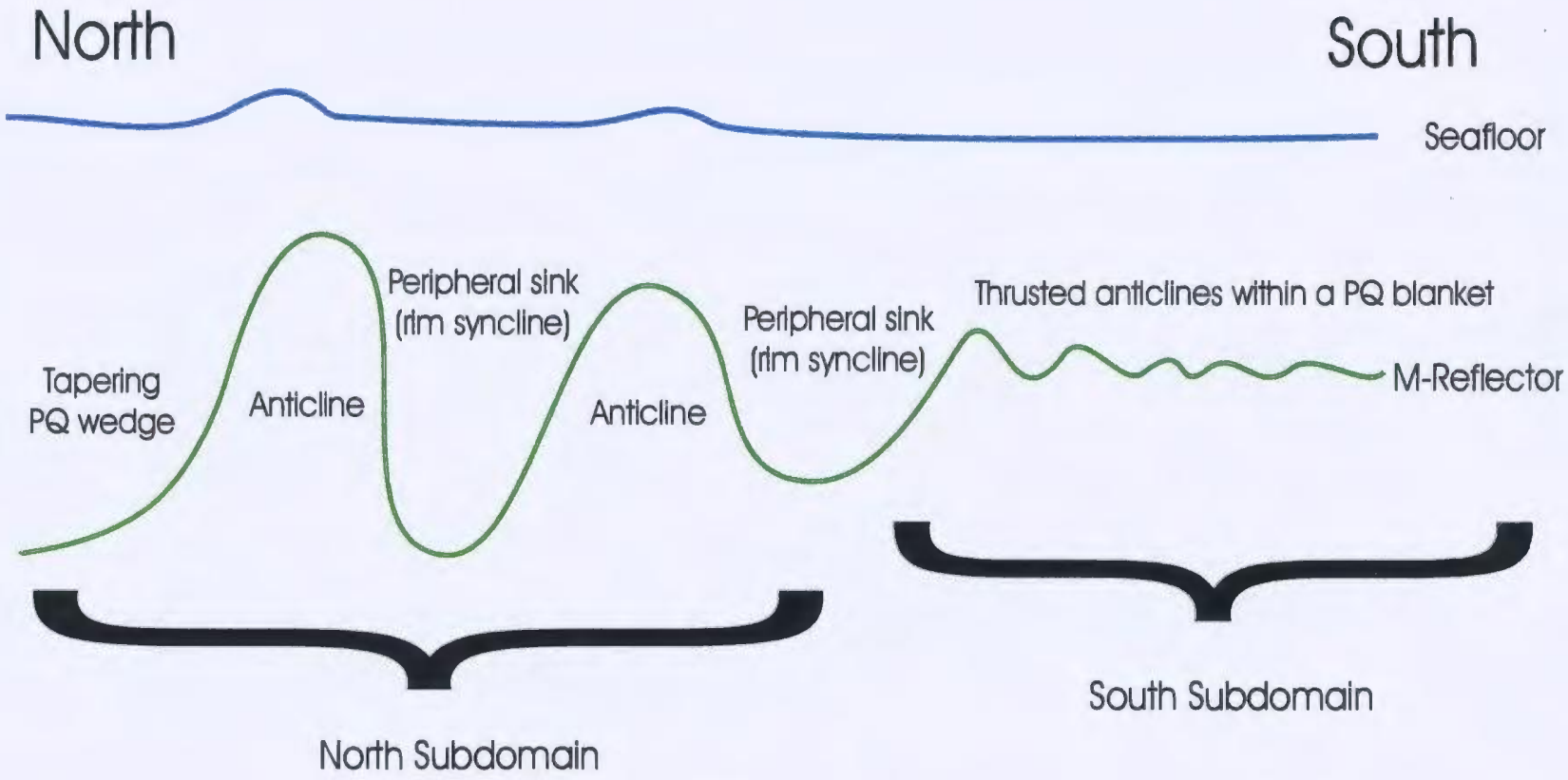

Figure 5-22: The salt structures of the Basin Central Fault Family are divided into two subdomains. In the north subdomain, there are 1-3 large salt anticlines with high structural relief, separated by large peripheral sinks. In the south subdomain, there is a series of low relief, narrowly spaced anticlines developed on the platform of the southern outer basin.

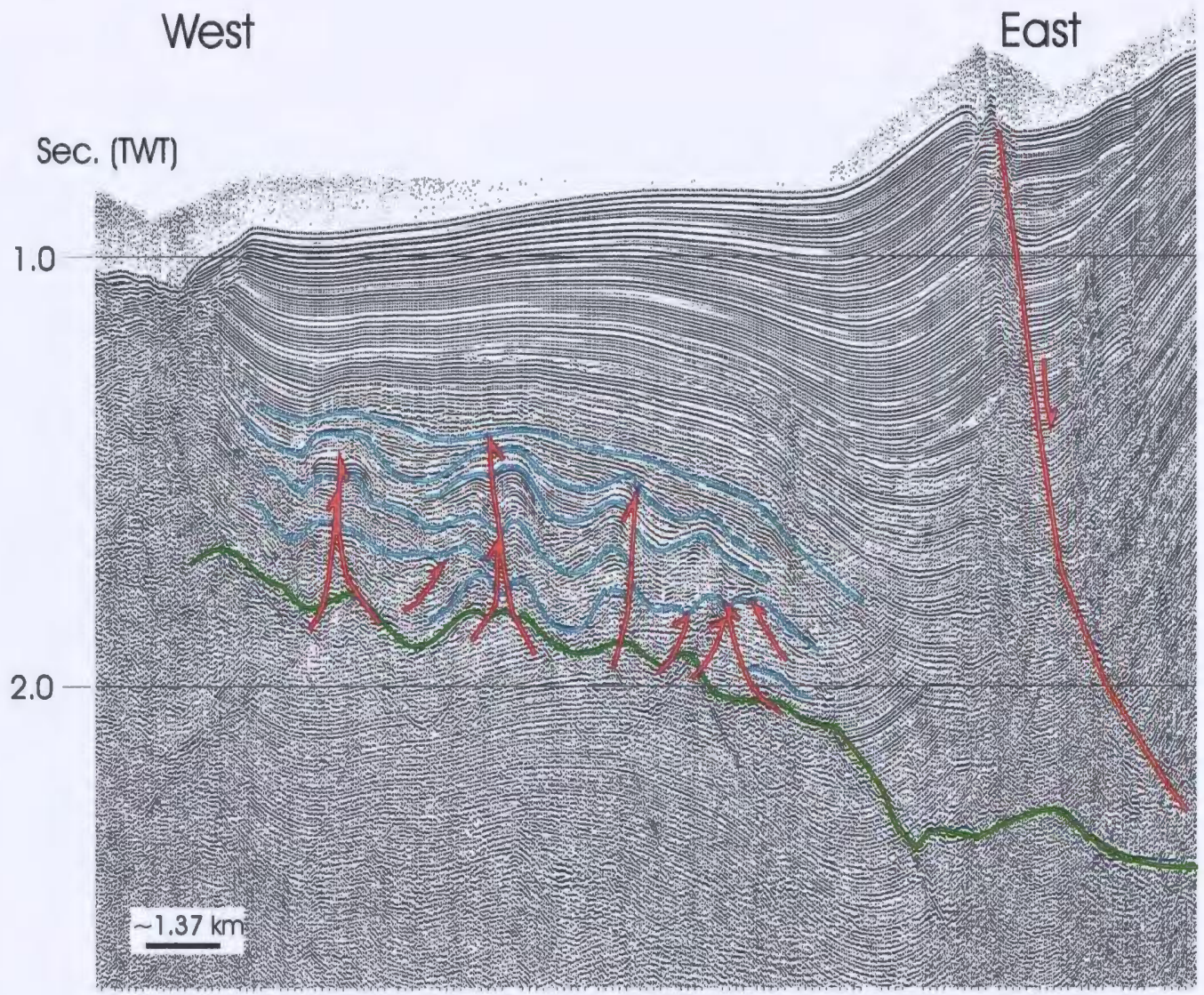

Figure 5-23: The Toe-Thrust Fault Family is a series of shallow dipping thrust faults which sole in the evaporite unit. Salt structures relating to this fault family are predominantly salt pillows or salt cored anticlines which are cut by thrust faults. Angular unconformities are common at the crests of anticlines.

6. KINEMATICS OF SALT STRUCTURES

6.1 Introduction

Kinematic indicators help establish the relative timing of localized tectonic events that have occurred in a region and may also provide limited information about the cause and direction of movement within a basin. There are three main types of kinematic indicators, microscopic, mesoscopic and macroscopic. In this chapter we look at the macroscopic kinematic indicators such as sedimentary thickening and thinning rather than microscopic or mesoscopic kinematic indicators (flow banding in salt, shearing at faults, grain rotations, etc.) which cannot be resolved on seismic sections. The study of localized kinematic indicators in the Cilicia Basin is carried further, to the interpretation of the basin-scale and regional tectonics, in order to get a wholistic basin dynamic model.

Many of the salt structures in the Cilicia basin (salt rollers and pillows in the inner basin and salt-cored anticlines in the outer basin) tell little about the large-scale movement patterns of the evaporite unit in the Cilicia Basin over a period of time. This is likely because these features display a limited set of kinematic indicators that show that a salt tectonic event has occurred but tell nothing of the relative timing of that event. The three large salt structures at the center of the Cilicia Basin are the best locations to study kinematics as they display a wide variety of kinematic indicators that can be found in the sediments surrounding the evaporite unit as well as being within the evaporite unit itself.

It is difficult to determine the timing of the movement of evaporites in the Cilicia Basin. Four factors are responsible for this difficulty. First, the presence of multiples in seismic sections frequently masks the seismic reflectors in sediments believed to be pre-

kinematic or early syn-kinematic. This masking makes it impossible to satisfactorily delineate the temporal kinematic divisions in the seismic sequence. Second, many salt structures became active quite early and do not appear to contain pre-kinematic strata. Similarly, in the outer and boundary domains some salt structures are still active today so do not display the post-kinematic division in seismic sections. The absence of these divisions makes it difficult to determine any timing relationships for the salt movement; adding to this difficulty is the absence of well data and the lack of a record of the rate of sedimentation in various regions within the basin. Further, in a limited number of seismic lines there are several episodes of rise and/or sagging at a salt body, and these are interrupted by periods of no apparent salt tectonic activity. Sediments considered post-kinematic to one episode of rise or sagging may be pre-kinematic to another episode of rise or sagging. This makes it quite difficult to clearly correlate between divisions of pre-, syn-, and post- kinematic sediments across different salt structures in the Cilicia Basin. For simplicity, these pre-kinematic/syn-kinematic strata will be referred to as non-kinematic strata because their most important property is that they represent a pause in salt tectonic activity. Another problem with the timing of salt movements in the Cilicia Basin is the inability to determine the absolute timing of the movement of evaporites in the basin. The absence of well data over most of the study area means that the correlation between biostratigraphic data from wells and seismic units is only possible in the innermost inner Cilicia Basin in an area where large gaps in the seismic grid make for poor correlation with regions in the outer basin.

6.2 Salt Structures in the Extensional Domain

The extensional domain in the inner Cilicia Basin contains numerous kinematic indicators. Salt rollers, the triangular prismatic salt bodies in the footwalls of extensional faults, salt welds alongside these salt rollers and at the basin flanks, thickness variations in sediments above and beside salt structures as well as the presence of turtle structures and intervening synclines in the basin all disclose information about the complex movements which occurred in the extensional domain of the Cilicia Basin. Unfortunately, although these kinematic indicators tell a lot about localized evaporite movement, they generally do not provide a great deal of information about the large-scale basin-wide salt tectonics, making a wholistic basin model tectonic analysis quite difficult.

6.2.1 The Salt Rollers

Salt rollers are quite abundant in the extensional domain of the Cilicia Basin. These features, described in section 5.3.2, are located in the footwall region of extensional faults throughout the extensional domain. Since a great deal of information is known about the formation and development of salt rollers, the recognition of the geometry of the salt structures in the inner Cilicia Basin can be viewed as a kinematic indicator in itself. These features immediately tell the seismic interpreter that they formed as a result of gravitational gliding on a decollement surface during extensional faulting.

Variation in the height of the salt rollers along strike can also be used as a kinematic indicator. In this case, the height variations along the salt rollers indicate that there is the potential for various types of evaporite movement related to the salt rollers.

Lateral movement of salt within the length of the salt roller may have occurred creating highs where salt moved into an area and lows where salt had evacuated. Alternatively, lateral movement may have occurred between salt rollers in regions where they were not completely isolated from each other by salt welds. In this case salt would withdraw from one roller (creating a low region in the roller) to feed another roller (creating a high in that roller) without any along strike movement of salt occurring. A combination of along strike and strike-perpendicular evaporite flow may also have occurred at the salt rollers in the inner basin.

The thickening and or thinning of strata above a salt structure can also be a kinematic indicator. Numerous examples of thinning and thickening of sediments are observed above the salt rollers in the extensional domain of the Cilicia Basin. These thickness variations are related to the growth or rise of a structure (thinning of sediments observed), the subsidence or sagging of a structure (thickening of sediments observed), or a combination of successive stages of both growth and subsidence indicative of structural inversion.

Structural inversion, in a regional tectonic sense is observed in a basin where the sense of vertical movement on a fault or other tectonic feature is reversed. The reversal of vertical movements causes the thinning of strata where there was formerly stratal thickening (eg. when an extensional fault becomes a reverse fault) or the thickening of strata where there was initial thinning (a thrust structure becomes extensional). Structural inversion also occurs in a localized salt tectonics sense. Thinning and thickening strata can be observed stacked above a salt body that has been undergoing successive episodes

of growth and subsidence, respectively.

The distinction between purely tectonic (fault-controlled) thickening or thinning and salt tectonic thickening or thinning is sometimes difficult to make. For example, listric extensional faulting in the inner Cilicia Basin clearly resulted in the thickening of sediments above salt rollers in the hanging wall region. The formation of these thickened 'growth strata' is related to rotation that occurred during the listric extensional faulting (purely tectonic thickening). Salt rollers, by definition, have a listric fault on their hanging wall flank. The migration of salt from one salt roller to a neighbouring salt roller (strike perpendicular movement of salt when no weld exists between rollers) or from one part of a salt roller to another part of the same roller (along strike salt migration) will cause subsidence of a portion of the salt roller. This subsidence at the salt roller will intensify the growth observed in the hanging wall of the fault. The thickening of sediments in the hanging wall of the listric fault would be the product of both the rotation and growth of sediments of the fault block (purely tectonic thickening) and the salt withdrawal and subsidence at the salt roller (salt tectonic thickening). Similarly, the growth of a salt roller and associated thinning of strata (salt tectonic thinning) may mask all or part of the stratal thickening and growth observed at an extensional fault (purely tectonic thickening). The inability to determine if growth observed above a salt roller at a listric normal growth fault is entirely related to faulting (purely tectonic thickening) or if it is influenced by salt growth and/or sagging (salt tectonic thickening) can create problems when interpreting the salt tectonic history of the salt rollers. This is especially problematic when studying an evolved form of salt rollers, namely the salt walls (see section 6.3).

6.2.2 Salt Welds and Fault Welds

Fault welds are commonly found between adjacent salt rollers in the listric fault fan in the inner Cilicia Basin. Salt welds are observed at the basin edges, just upslope of the present-day edge of salt. These fault welds and salt welds are regions of evacuated salt that show up on seismic sections as a series of high amplitude reflectors underlain by sub-salt basement sediments. Although the two types of welds are quite similar in appearance, their formation resulted from entirely different kinematic processes.

In the case of salt rollers, the presence of fault welds indicates that hanging wall fault blocks grounded on the base of the evaporite unit during extension. Salt evacuated from beneath the sinking hanging wall fault blocks and moved into the footwall area as a salt roller. Alternatively, salt moved out of the plane of seismic line and into neighbouring salt rollers or into the salt walls. The region from which the salt evacuated has salt remnants that result in a high amplitude seismic response at the boundary between the overburden and subsalt sediments.

The presence of salt welds at the basin margins suggests that the edge of evaporite deposition was initially further landward than the present-day edge of salt. After evaporite deposition, salt structures in the basin began to grow by salt withdrawal from the source layer salt. These evaporites were drawn away from the basin margins towards the more centralized salt structures. Some relict pods of salt may exist landward of the present-day edge of salt, elsewhere the salt evacuation left behind thin salt remnants that create high amplitude reflectors on seismic sections that look similar to the fault welds described above. The areas of salt withdrawal at the basin edge often create apparent

downlap patterns. At basin margins, the lower Pliocene strata, which directly overlie the evaporite unit and originally onlapped the M-Reflector unconformity, show a slight downwarping where evaporites were drawn to the centralized portions of the basin creating a salt withdrawal basin above the salt weld.

6.2.3 Turtle Structures Associated With Salt Rollers

The extensional faults in the inner Cilicia Basin form distinct anticlinal structures in the sediments above the salt rollers (Fig. 6-1). Two of these anticlinal structures have been delineated in the inner Cilicia Basin; however the MUN seismic sections do not image to the base of the evaporite unit below these anticlinal structures and therefore do not provide a complete representation of the anticlinal structure. The more westerly of the two anticlinal structures is imaged to the base of the evaporite unit and is therefore used in this analysis. The anticlinal structure observed in the western part of the inner Cilicia Basin occurs above an area where the faults in the listric fault fan change vergence. The listric fault fan controlling this anticline takes up a very symmetrical form, and it becomes impossible to determine which faults are the synthetic faults (the main extensional faults) and which faults are antithetic faults (secondary extensional faults which form after the synthetic faults). The symmetrical anticlinal structure appears, at a first glance, to be a turtle anticline or mock turtle anticline structure as described by Vendeville and Jackson (1992). These workers describe a turtle structure as a characteristic effect of source layer depletion and indicate that there are four ways in which a turtle structure can form. In all four mechanisms for turtle structure formation the

core of the anticline maintains its height while the flanks of the anticline subside from different causes (Vendeville and Jackson, 1992).

Classic Turtle Structure Anticline of Trusheim (1960)

The first of the four ways in which a turtle structure can form is the classic turtle structure anticline of Trusheim (1960). According to Vendeville and Jackson (1992) these structures form when "*a non-piercing salt pillow* (i.e. reactive diapirism) *transforms to a piercing salt diapir* (i.e.active diapirism). *The periphery of a salt pillow subsides as it contracts inwards into a piercing salt diapir. The subsiding flanks of adjacent pillows form the sagging limbs of the turtle structure anticline. The anticline forms during early diapirism* (early active diapirism), *when the secondary peripheral sink* (salt withdrawal basin) *deepens. This type of turtle structure has never been envisaged as resulting from regional extension.*" This definition does not really fit what is observed in the inner Cilicia Basin. In the definition of Vendeville and Jackson (above) active salt diapirs are growing from previously reactive diapirs. In the Cilicia Basin the salt rollers are still in a stage of reactive diapirism, only the main salt wall to the west of the turtle structure has become an active diapir. Vendeville and Jackson describe the turtle structure as forming '*when the secondary peripheral sink deepens*'. Secondary peripheral sinks are not observed in the region of the turtle structure in the Cilicia Basin. Furthermore, Vendeville and Jackson indicate that turtle structures of Trusheim (1960) have '*never been envisaged as resulting from regional extension*' however; the turtle structure observed in the Cilicia Basin is intrinsically linked to extensional faulting in the

basin.

Turtle Structure Horst

A turtle structure horst is another form of a turtle structure; it was first identified and defined by Vendeville and Jackson (1992). A turtle structure horst "*forms by regional extension by the reactive rise of diapirs...a diapir rises reactively through a graben thinned by regional extension. Bridging two such* (adjacent) *grabens is a residual horst formed by the downfaulting of its margins. The horst resembles a turtle structure anticline in its humped shape and because it can be cored by a lens of sediment or salt. However, it differs* from other turtle structures *because its flanks are downfaulted rather than downfolded; it is a horst rather than an anticline*" (Vendeville and Jackson, 1992). The turtle structure in the Cilicia Basin is not a turtle structure horst because its margins are not downfaulted by graben formation during regional extension; furthermore, it is not located between two grabens created by the reactive rise of a diapir.

Turtle Structure Anticline of Vendeville and Jackson (1992)

The turtle structure anticline defined by Vendeville and Jackson (1992) is the second example of a turtle structure formed by regional extension. According to Vendeville and Jackson (1992), a turtle structure anticline is "A broad, gentle antiform between two diapirs. Although the source layer is still abundant, strata between diapirs either have a flat base or are even slightly synformal. Once the source layer becomes depleted during continued extension, the diapir sags. Intervening strata flex down toward

the sagging diapirs to become the limbs of gentle anticlines. This causes the upper strata of the fold hinge to be extended, forming grabens or distributed normal faults in the crests of the anticlines. If synforms separated reactive diapirs the resulting turtle structure contains a lens of thickened sediments deposited during the reactive stage.... in brief, this type of turtle structure anticline forms next to a mature diapir sagging by regional extension. This type differs from Trusheim's turtle structure anticline because it is unrelated to the transformation of salt pillows and because it forms late in a diapirs evolution rather than early like the classic turtle structure." Again, this description of a turtle structure does not fit what is observed in the Cilicia Basin. Vendeville and Jackson's turtle structure anticline forms by the sagging of mature diapirs at the ends of the turtle structure anticline. The salt rollers in the Cilicia Basin do not display any evidence of sagging and they are still immature salt rollers that have not reached the mature diapir stage. The salt structures in the inner Cilicia Basin are still in a very early stage of their evolution, and therefore would not display this late evolving type of turtle structure anticline.

Mock Turtle Anticline

The final turtle structure described by Vendeville and Jackson (1992) is a mock turtle anticline. This type of turtle structure forms when a syncline is inverted to an anticline as the result of extreme extension. "A mock turtle anticline forms on the crest of a subsiding diapir that has separated into two remnants. The indenting synformal graben sinks until it grounds onto basement; its flanks subside further with continued extension

until they also begin to ground. The graben is inverted into an arched mock turtle anticline. This process of inversion can result entirely from extreme extension but will be accelerated by the flow of salt out of the plane of section. Excellent examples of mock turtle structures are the depocenters between extensional rafts in Angola. During inversion the outer arc of the mock turtle anticline is extended by a fan of normal faults. The best documented example of this faulting is the oil-rich Quenguela anticline in the Kwanza Basin, Angola " (Vendeville and Jackson, 1992). The examples that are given by Vendeville and Jackson (Fig. 6-2) are very similar in appearance to those observed in the Cilicia Basin. It is important to note that the mock turtle anticlines described by Vendeville and Jackson formed on the crest of a subsiding diapir that had separated into two remnants. The turtle structures in the Cilicia Basin do not subside into a diapir but subside into the source layer of salt. Additionally, unlike the mock turtle anticlines observed in Angola, the turtle structures in the Cilicia Basin do not form in depocenters between rafts because the overburden in the Cilicia Basin is still in a pre-raft stage.

Turtle-Back Growth Anticlines

The turtle structure anticline in the Cilicia Basin seems to belong to yet another group of turtle structures. These features are known as 'turtle-back growth anticlines' and are described by Mauduit et al. (1998). 'Turtle-back growth anticlines' form where two facing (oppositely dipping, or verging) listric extensional faults experience growth with strata that thin toward the anticlinal axis and thicken away from the axis. These structures, like the turtle structures described by Vendeville and Jackson (1992), form in

such a way that the core of the anticline maintains its height while the flanks of the anticline progressively rotate and subside. The growth strata at the listric faults thicken away from the central axis of the anticline creating a distinct humped appearance that is a consistently observed trait of turtle structures. In Vendeville and Jackson's examples the flanks of the anticlines generally subside as the result of one of two processes: i) the sagging of pre-existing salt structures, and ii) the downfaulting of the flanks of the anticline. In the Cilicia Basin, the flanks of the turtle-back growth anticline are curved downwards as a result of extensional growth faulting on oppositely dipping listric faults rather than being downfaulted. The growth strata at the listric faults thicken away from the central axis of the anticline creating the distinctive humped appearance.

Turtle structures are a characteristic effect of source layer depletion (Vendeville and Jackson, 1992). The growth on the extensional faults in the inner Cilicia Basin is accommodated by subsidence of hanging wall fault blocks into the salt source layer. The subsidence of these hanging wall fault blocks would not be possible without source layer depletion. In the case of the Cilicia Basin salt depletion occurred as salt from the source layer was drawn into salt rollers and other salt structures (such as the salt walls) in the early salt tectonic evolution of the basin.

The turtle-back growth anticline observed in the Cilicia Basin has a symmetrical external shape. This external symmetry is typical of turtle-back growth anticlines and is observed in similar turtle structures from the Kwanza Basin, Angola and Campos Basin, Brazil (Fig. 6-3). The internal structure of these externally symmetrical turtles is demonstrably asymmetric in seismic sections (Fig. 6-4). This asymmetry is indicative of

uneven extension and growth along the opposing listric faults of the anticline. The turtle-back growth anticlines of Mauduit et al. (1998) form between two salt rollers or salt pillows, and infrequently show a single salt pillow near the center of the anticline. The central part of their turtle-back growth anticline is a typical keystone graben as defined by McClay and Ellis (1987) or Vendeville and Jackson (1992 b). The turtle-back growth anticlines in the Cilicia Basin differ from these turtle structures in that the Cilicia Basin turtles have numerous full listric faults which do not form in a keystone graben between two salt rollers but instead form as two facing fans of listric faults, each listric fault having a salt roller in its footwall. Mauduit et al. (1998) indicate that factors like the dip of the detachment surface, the coupling of overburden and basement after salt evacuation, and the rates of sedimentation and extension can all influence the geometry of the turtle-back growth anticline, and may be able to account for the differences in natural examples (such as the Cilicia Basin) and experimental results.

6.3 Kinematic Interpretations of Salt Structures in the Boundary Domain

The Boundary Domain, located at the boundary between the inner Cilicia Basin and the outer Cilicia Basin is home to the three large salt walls and their intervening salt withdrawal basins. This area exhibits an assortment of kinematic indicators, both associated with the salt and with the sediments above and at the sides of the salt walls. The three salt walls are studied individually in order to determine the differences in the manner and relative timing of their initial development, the events of growth and sagging which have occurred since that time, and the relationships between each individual salt

wall and its surrounding sediments.

6.3.1 North Salt Wall in the Boundary Domain

The northernmost salt structure within the Cilicia Basin (described in section 6.3) has an approximately east-west orientation. To the north and south an extensional fault fan borders this salt wall. The east and west margins of this salt wall pinch out into the extensional and contractional domains, respectively. This salt wall is observed in four different seismic lines in the data set.

Northern Flank

In the three, northwest-southeast oriented seismic lines (Figs. 6-5, 6-6 and 6-7) and the northeast-southwest oriented line (Fig. 6-8), pre-kinematic reflectors to the north of, and near the base of the salt wall are folded and are truncated by Sequence Boundary 1. The folding of the pre-kinematic sediments likely occurred at the sides of the evolving salt wall as it underwent active diapirism. During active diapirism, the salt punched through the overburden, bending it back out of the way during further growth of the salt wall. Truncation of pre-kinematic reflectors at the northern edge of the north salt wall is observed on three of these seismic lines (Figs. 6-5, 6-6 and 6-8) and is related to an erosional event which is marked by Sequence Boundary 1. Several syn-kinematic reflectors may have been removed during this erosional event. Immediately above Sequence Boundary 1, seismic reflectors converge towards the salt (thinning of sediments) suggesting growth of the salt wall during a period of active and/or passive

diapirism. Above this region, there is a thick seismic reflection package with reflectors that diverge near the salt (sediment thickening). These divergent reflectors are indicative of subsidence at the northern margin of the salt wall. This subsidence is due to the withdrawal of source-layer salt from the outer, northern edge of the salt wall creating a depression that is known as a salt withdrawal basin or secondary peripheral sink (Fig. 6-7).

The most westerly of the four seismic lines crossing the north salt wall displays convergent (thinning) reflectors at the top of the salt wall. This thinning is indicative of growth at this portion of the salt wall. The remaining three seismic lines show signs of sagging above the salt wall; the easternmost of these three lines has a thick zone of post-kinematic reflectors directly above the salt wall indicating that the eastern part of the salt wall is undergoing neither growth nor sagging at present. The simplest interpretation of this arrangement is a situation in which the southwestern end of the salt wall is growing at the expense of the eastern and northeastern portion of the salt wall (ie. salt is flowing from northeast to southwest).

Southern Flank

The southern edge of the north salt wall is also observed in the same four seismic lines. Unfortunately, an extensional fault lies along the southern boundary of the north salt wall in all but the westernmost seismic line. Thickening of sediments along the south part of the salt wall can be attributed to the growth that occurs along the extensional fault. The westernmost seismic line shows a relatively constant thickness for a pre-kinematic

seismic package below Sequence Boundary 1. This package is relatively thin (0.6 seconds) compared to the thickness of the syn-kinematic sediments (1.6 seconds). In the two westernmost seismic lines (Figs. 6-6 and 6-7), seismic reflectors above Sequence Boundary 1 diverge as they approach the salt wall and then converge just above and at the sides of the salt wall. These reflectors indicate the creation of a secondary peripheral sink as sediments subside into a salt withdrawal basin (diverging reflectors) resulting in growth near the top of the salt wall (converging reflectors).

The kinematic indicators that can be observed at the southern edge of the north salt wall do not contradict the observations made at the northern edge of the salt wall. The easternmost seismic line crossing the southern edge of the north salt wall (Fig. 6-8) contains a thick upper post-kinematic sequence suggesting that movement at this portion of the salt wall has ceased. Growth at the southern margin of the salt wall in the two westernmost seismic lines (Figs. 6-6 and 6-7) may be due to a process of salt evacuation from the eastern end of the salt wall to the western end. This conclusion is similar to the one reached for the evolution of the northern flank of the salt wall.

The region of present-day growth at the northern salt wall is indicated on the fault map for the Cilicia Basin (Fig. 5-3 [insert 1]). This region of growth is a direct result of a northeast to southwest (or east to west) migration of salt that was interpreted from kinematic indicators at the northern salt wall.

6.3.2 Central Salt Wall in the Boundary Domain

The central salt wall in the boundary domain of the Cilicia Basin (described in

section 6.3) has a roughly northwest-southeast orientation. Parts of this salt wall can be observed in six different seismic lines (Figs. 6-9 thru 6-14) in the basin. To the north and east of this salt wall, the extensional fault fan of the inner Cilicia Basin can be found. South and west of the salt wall lie the contractional faults of the Toe-Thrust Fault Family (Fig. 5-3 [insert 1]).

Practically all of the lines that cross the central salt walls have very low amplitude reflectors near the base of the salt wall. This is a characteristic of the oldest overburden sediments that was described in the seismic stratigraphy of Depositional Sequence A. These low amplitude reflectors cause problems when trying to determine if the sediments near the base of the salt wall are folded or truncated, and whether they are pre-kinematic or syn-kinematic. Other complications arise where normal faults exist at the flanks of the salt wall. These normal faults make the interpretation of diverging reflectors difficult because it is impossible to determine if all of the thickening of sediments at the margins of the salt wall is due to growth on the listric growth faults (purely tectonic thickening) or if it is partially related to sagging of the salt wall or subsidence during the formation of a salt withdrawal basin (salt tectonic thickening). Interpretations in the area of the central salt wall place greater importance on seismic sections which do not have the above noted problems; less merit is given to lines with these problems.

The central salt wall is a very complex salt structure. Seismic lines crossing this salt wall indicate that it has a multi-stage movement history involving a period of initial growth of the salt wall followed by various stages of growth and subsidence (attributed to salt migration) distributed in a varied manner, both temporally and spatially, over the salt

wall.

In order to best analyze the salt tectonic activity at the central salt wall, each seismic line was broken into two segments, one on each side of the salt diapir. These segments were arranged on a map of the salt diapir so that they lie in the correct location along the flanks of the salt wall. The resulting map (Fig. 6-15 [insert 2] made it relatively easy to construct a salt tectonic history for the salt wall. Lines that are located close to each other can be grouped in support of a single explanation for what is happening at a particular region of the salt wall.

Northern and Eastern Flanks

Kinematic indicators located along the northern flank of the central salt wall can be observed in six different seismic lines. From west to east these seismic lines are labeled as Figures 6-9, 6-10, 6-11, 6-12, 6-13 and 6-14 (locations shown in Fig. 5-3 [insert 1]).

Figure 6-9 shows the gently dipping north flank of the central salt wall with ~500 ms of pre-kinematic overburden. Approximately 800 ms of syn-kinematic sediments overlie these pre-kinematic strata. The syn-kinematic strata thin towards the salt wall, and generally this would indicate that the salt wall is growing; however, in this instance the thinning of strata may be related to salt withdrawal indicated by a salt withdrawal basin occurring at the adjacent northern salt wall (Figs. 6-6 and 6-7).

In Figure 6-10, the central salt wall has a normal fault at its crest which influences the sedimentation observed at the north flank of the salt wall. The extension on this

normal fault seems to be confined to the upper 700 ms of the overburden sediments. An approximately 300 ms thick pre-kinematic unit is overlain by over 1400 ms of syn-kinematic sediments. Sequence Boundary 1 truncates the pre-kinematic strata and the lowermost portion of the syn-kinematic sediments. The truncated syn-kinematic sediments record greater than 300 ms of growth at the diapir as indicated by thinning of sediments towards the salt wall. The growth at this salt wall continued for an undeterminable amount of time; as a result, sediments of depositional sequence A were eroded and truncated by Sequence Boundary 1. Above this erosional and truncating unconformity, the thinning of sediments related to the growth of the salt wall continued, producing another 300 ms thick package of thinning sediments. The uppermost 7 ms of sedimentation record a thickening of sediments which may represent sagging and subsidence of the salt wall, or may be attributed to normal faulting and associated sediment growth near the top of the salt wall.

The north flank of the central salt wall is observed to have a very complicated kinematic history in Figure 6-11. The kinematic indicators at this part of the salt wall are distributed over two fault blocks. To assist in the description and interpretation of these kinematic indicators, the fault blocks have been labeled FB1 and FB2 (FB1 being the fault block closest to the salt wall; Fig. 6-11). The lowermost reflectors in FB1 are masked by multiples in the seismic data. This area is interpreted as having originally been the location of a small salt structure that subsided during the development of the salt wall as suggested by a minor folding of the lowermost strata in FB2. The base of FB2 has a 300 ms thick unit of pre-kinematic strata that terminate against the normal fault that is

located between FB1 and FB2. These pre-kinematic strata were likely pushed away from the margins of the small salt structure during reactive and active diapirism. Directly overlying the pre-kinematic strata in FB2 is a 700 ms thick unit of syn-kinematic strata that thin towards the small salt structure in FB1. These thinning strata record the active growth stage in the evolution of the small salt body. An approximately 300 ms thick unit of constant thickness non-kinematic strata can be observed in both fault blocks. Above this non-kinematic unit a 400 ms syn-kinematic unit in FB1 records the initial stage of diapir subsidence at the smaller salt structure. These sediments show thickening of strata above the area of the small salt body accompanied by a thinning of strata over the large salt wall. This pattern of thickening and thinning in adjacent domains shows that the small salt body was subsiding while the salt wall was growing. FB2 records nearly 200 ms of growth at the smaller salt structure before recording the withdrawal of salt. The delay observed between withdrawal of salt from FB1 and FB2 is probably related to the way in which the central salt wall withdrew the salt from the smaller salt body. It appears as if salt was partially withdrawn from the area closest to the salt wall first (without formation of a salt/fault weld) and then it was withdrawn from the end of the smaller salt body that was near FB2. The uppermost 700-800 ms of sediments in both FB1 and FB2 display stratal thickening that suggests that one or both of the salt structures were subsiding. Normal faulting in the region makes it impossible to determine if the thickening is due to subsidence of the salt structures, to extensional growth faulting or to a combination of both processes

Figure 6-12 shows a >600 ms package of pre-kinematic strata that are eroded at

Sequence Boundary 1 (SB1). The erosional unconformity at SB1 is overlain by 400 ms of syn-kinematic strata that thin towards the salt wall and record a stage of reactive and/or active diapirism. A 300 ms non-kinematic unit overlies these syn-kinematic sediments, indicating a period of interruption of the growth of the salt wall. Thinning of strata occurs over a thickness of 100 ms before a pronounced thickening of strata is observed in the upper 500 ms of overburden. These uppermost, thickening strata are again bounded by an extensional fault which makes it difficult to determine whether the salt wall is actually subsiding or if normal growth faulting is to blame for the thickening strata. In this case, thinning strata are observed at the crest of the salt wall suggesting that thickening of the sediments can be attributed to growth faulting.

In Figure 6-13 the central salt wall has three pinnacles; a broadly curved crest is located above the largest part of the salt wall and two smaller peaks are located low along the southern margin of the salt wall. North of the salt wall a salt withdrawal basin is observed at the base of the structure. It separates the salt wall from an elevated salt body that is cut off at the end of the seismic line. This salt body may actually represent the average salt elevation in this area of the basin or may be the base of another small salt structure situated between the northern and central salt walls in the Cilicia Basin. The kinematic indicators at the north flank of the central salt wall concern only the broad crest of the salt wall and the elevated salt body that is terminated at the end of the seismic line. This seismic line (Fig. 6-13) begins with a 500 ms section of pre-kinematic strata alongside the lower flank of the main salt wall. These sediments are pre-kinematic to the salt wall but display notable thickness variations above the elevated salt body, where they

display a 100 ms thick section of thinning sediments indicating that the elevated structure began to grow prior to the formation of the main salt wall. A 600 ms section of thinned sediments lies directly above the thinned section and represent subsidence of the elevated salt body to its current level. The upper 400 ms of this syn-kinematic unit corresponds to significant thinning of strata at the north flank of the salt wall. This arrangement suggests that the subsidence of the elevated salt body was due to salt withdrawal in order to feed the salt wall. A 300 ms thick unit of non-kinematic sediments overlies these pre-kinematic sediments and represents a pause in salt tectonic activity at this side of the salt wall. Approximately 600 ms of syn-kinematic sediments overlie these non-kinematic sediments. The syn-kinematic sediments thicken towards the salt wall and partially represent the withdrawal of salt at the side of the salt wall (the salt withdrawal basin) but may also represent subsidence of the broadly curved crest of the salt wall in order to feed other (growing) parts of the salt wall.

The line in Figure 6-14 is located along the northeast part of the salt wall and is included in the analysis of the northern flank. This seismic line crosses a part of the salt wall where a normal fault has dominant control over the thickness variations in the sedimentary sequence. Growth along the normal fault, manifested as thickening and rotationof strata towards the salt wall, is the only kinematic indicator observed along this portion of the central salt wall.

The kinematic activity observed in all six seismic lines at the north flank of the central salt wall recount similar salt tectonic events. After a brief period of sediment deposition (represented by the early pre-kinematic strata) the northern flank of the salt

wall underwent a period of reactive and active diapirism related to extension in the Cilicia Basin. The salt wall grew by salt withdrawal from the source layer in the immediate vicinity of its base (producing salt withdrawal basins) and also by salt withdrawal from neighbouring salt bodies (resulting in thickened strata above previously elevated, but now depleted, salt structures). During or immediately following this period of growth of the salt wall, a period of erosion (indicated by the unconformity at Sequence Boundary 1) or halted kinematic activity (indicated by non-kinematic units) occurred. A period of sagging most likely followed the period of interrupted growth. Most kinematic indicators along the northern flank of this salt wall show a thickening of sediments towards the salt wall that is often accompanied by downward extensional curvature (half graben formation?) above the salt walls. Figure 6-9 is the only exception to the observation of sediments which thicken towards the salt wall, but, thinning at the margin of the central salt wall can be attributed to salt withdrawal into the northern salt wall. Caution must be expressed regarding the interpretation of subsidence and sagging at the north flank of the central salt wall. This caution is rooted in the observation that most of the seismic lines crossing the northern flank of this salt wall show signs of extension-related growth or thickening of the overburden strata which can be easily mistaken for stratal thickening related to subsidence.

Southern Flank

Kinematic indicators at the southern flank of the central salt wall can be observed on three seismic lines. These lines, labeled Figure 6-13, 6-12 and 6-14 (from east to west)

record the thickness changes, onlap, offlap and truncations related to salt tectonic activity occurring at the southern flank of the central salt wall.

Figure 6-13, located near the easternmost point of the central salt wall has a complicated assemblage of kinematic indicators. This part of the salt wall consists of two small peaks that form along the flank of a large, broad crested portion of the salt wall (previously described in section 7.2.2.1 at Fig. 6-13). The kinematic indicators described here are found in the sediments at the southern side of the large broad portion of the salt wall and in the sediments surrounding the two smaller peaks. To simplify the description and interpretation of the kinematic indicators, the crests of the salt wall are labeled A, B and C from north to south (Fig. 6-13; A is largest, B central and C southern). The southernmost part of the salt wall observed in this line (that is, the southern flank of crest C) shows no obvious pre-kinematic strata in the immediate vicinity of the salt wall. Approximately 400 ms (TWT) of syn-kinematic strata in this area record growth due to the withdrawal of salt from the margin of the salt wall creating a salt withdrawal basin. These syn-kinematic sediments are overlain by a 100 ms thick non-kinematic unit which is in turn overlain by nearly 700 ms of syn-kinematic sediments which record a small amount of growth at crest C (thickening is quite subtle). The growth at crest C is recorded up to the level of the seafloor suggesting that this part of the salt wall is still (slowly) growing today. This growth possibly takes place at the expense of the larger part of the salt wall (crest A). The two smaller peaks (B and C) at the side of the larger portion of the salt wall display indications of growth at their crests with subsidence (thickening) being observed in the trough between these crests. Kinematic indicators at

the south side of the large, broad part of the salt wall show that Crest A was onlapped by approximately 500 ms of constant thickness non-kinematic sediments near its base (between crests A and B). The onlap relationship shows that crest A was elevated at the time these sediments were deposited and may have reached the seafloor level. This relationship would show the change from active to passive diapirism at crest A. Above these non-kinematic sediments a 200 ms unit of syn-kinematic sediments appears to downlap the broad crest of the salt wall. These syn-kinematic strata record a thickening of sediments (subsidence of salt) directly above the trough that divides crests A and B. The thinning strata over crest B indicate that the crest is undergoing growth. The thickening between the crests formed when the growing salt wall (crest A) withdrew sediments from its southern flank. The apparent downlap observed in these syn-kinematic sediments was originally an offlap that was rotated when crest A of the salt wall began to subside. Evidence for this proposed subsidence is exhibited in 600 ms of thickened syn-kinematic sediments that overlie the 'rotated downlap' section at crest A.

Kinematic indicators along the line in Figure 6-12 show the formation of a salt withdrawal basin at the southern margin of the salt wall. In this seismic line, pre-kinematic strata are masked by multiples in the data set. These pre-kinematic strata are probably no more than 400 ms thick. Sediments above the pre-kinematic strata thicken towards the salt wall indicating the formation of a salt withdrawal basin at the southern margin of the salt wall during a stage of active or passive diapirism. The salt withdrawn from the southern flank of the salt wall was feeding the growing central portion of the salt wall. An approximately 400 ms thick unit of sediments thins and onlaps the crestal

region of the diapir. This thinning of sediments records the growth of the salt wall that was associated with the withdrawal of salt from the salt withdrawal basin. This thinning and salt wall growth continues to the level of the seafloor suggesting that growth along this part of the salt wall continues today.

Figure 6-14 shows approximately 300 ms of pre-kinematic strata which seem to downlap a southwest facing portion of the southern flank of the central salt wall. These pre-kinematic strata are overlain by 900 ms of syn-kinematic strata. The syn-kinematic strata are observed to thicken towards the salt wall. The thickening of these strata coupled with the apparent downlap of pre-kinematic strata suggests that the salt wall was growing as a result of salt withdrawal from beneath the pre-kinematic strata at the edge of the salt wall. This process continues to the present as indicated by the barely perceptible thinning of strata that is observed just beneath the seafloor, above the salt wall as wll as by the presence of a fault scarp at the seafloor in the same area.

The combined kinematic indicators in seismic sections in Figures 6-13, 6-12 and 6-14 indicate that the south flank of the central salt wall underwent an initial period of growth associated with the thinning of sediments at the salt wall. Further growth occurred as the result of withdrawal of salt from a salt withdrawal basin at the southernmost part of the salt wall. In the east, this growth was interrupted by a period of no salt tectonic activity that is not observed in the other two lines crossing this part of the salt wall. The eastern seismic line (Fig. 6-13) displays sagging of the broader part of the salt wall in favour of growth of two smaller crests along the same salt wall. The other seismic lines (Figs. 6-12 and 6-14) show growth at a single crest that continues to the present. At the

point of intersection of these lines growth of the salt body is suggested by the thinning of the overburden strata at the crest of the diapirs. Seismic lines in figures 6-13 and 6-14 cross at a region undergoing thickening of sediment due to growth on normal faults. This thickening is likely the same as that observed in Figure 6-13 at the sediment trough between crests A and B of the salt wall.

Western Flank

The western flank of the central salt wall is imaged in seismic lines in Figures 6-9 and 6-10. In Figure 6-9 the salt wall forms a double crested portion and a separate single crested portion. The seismic line in Fig. 6-9 is practically tangential to the western flank of the central salt wall and cuts the protruding ends of the salt wall before they die out to the west. The crests of these protrusions are labeled A, B and C from south to north.

The kinematic indicators at the southwestern corner of the central salt wall (crest A) in Figure 6-9 are very difficult to see because of poor imaging in this part of the seismic section. Kinematic indicators in the sediments directly above crest A and crest B record a thin section (100- 200 ms) of thinned strata which indicate that a period of growth has occurred at the western flank of the salt wall. These sediments are immediately overlain by approximately 500 ms of thickened sediments indicating subsidence at these crests (crests A and B) that continues to the present. A trough located between crests A and B may represent the development of a salt withdrawal basin that fed the early stages of growth at the salt wall. Crest C of the western flank of the central salt wall has 300 ms of pre-kinematic overburden. Approximately 800-1000 ms of syn-

kinematic sediments overlie the pre-kinematic sediments. The lower 200 ms of syn-kinematic sediments record a period of growth at the salt wall. The upper 600-800 ms of the syn-kinematic strata thicken towards the salt wall. Normal faulting above the fault wall makes it impossible to determine how much of this thickening is due to sedimentary growth at the normal fault and/or to subsidence of crest C of the salt wall.

A 200 ms section of pre-kinematic sediments overlie the evaporite unit in Figure 6-10. Directly above these pre-kinematic sediments are 800 ms of syn-kinematic sediments. The lowermost 200 ms of these syn-kinematic sediments records a period of growth at crest C of the salt wall as indicated by strata that thin towards the salt wall. Above this thinned section, 600 ms of thickened strata are observed at crest C. This thickened unit is unaccompanied by the characteristic downwarping of a salt withdrawal basin and is therefore interpreted to mark a period of subsidence and sagging at crest C.

The observations made at the western flank of the central salt wall indicate that an initial period of growth in this region was immediately followed by a period of subsidence accompanied by extensional growth faulting.

After evaporite deposition in the region of the central salt wall, a thin unit of overburden sediments was deposited. Extension in the region resulted in graben formation and reactive diapirism. A salt structure began to form and eventually withdrew salt from its flanks as it developed into a salt wall. The western and northeastern flanks of the salt wall were drawn further inwards as the salt wall grew. Most portions of the salt wall experienced subsidence with the exception of the central portions of the salt wall observed in Figure 6-12 which continue to grow today. The area of salt growth is

indicated on the fault map for the Cilicia Basin (Fig. 5-3 [insert 1]).

6.3.3 South Salt Wall in the Boundary Domain

Two seismic lines in Figures 6-16 and 6-17 cut the southern salt wall in the boundary domain of the Cilicia Basin (salt wall description in section 6.3). Because of the poor seismic coverage of this salt wall, it is difficult to determine just how extensive the salt wall is. An outline of the minimum extent of the salt wall has been calculated for mapping purposes. The mapped portion of the south salt wall has a north-south orientation. The extensional fault fan of the inner Cilicia Basin is located to the northeast of this salt wall; contractional faults of the Toe-Thrust Fault Family lie to the southwest.

Seismic lines crossing the south salt wall show the crest of the salt wall to be within 200-300 ms of the present day seafloor. Thinning at the margins and the crest of the salt wall indicate that the salt wall is still growing, and it is in the advanced stages of active diapirism. A minor salt withdrawal basin has formed at the northern and western margins of the salt wall. The formation of this depression is evident in diverging reflectors located in the lowermost 500 ms of sediment at the base of the south salt wall, just off its north and west flanks.

Just north of this salt wall there is a small salt pillow with a reflector configuration that suggests a period of early growth as indicated by slightly thinning reflectors in the lowermost 200 ms of sediment above the pillow. Diverging reflectors located directly above the thinned sequence suggest that a 'sag basin' formed when the small salt body subsided after the initial period of growth. This sagging may have been

due to salt withdrawal at the salt structure that occurred in order to feed the southern salt wall. Sediments within the 'sag basin' are arched upwards and sediments above the sag basin are slightly thinned suggesting that growth was re-established at this salt structure for a brief period after the thickening (i.e. sagging of the salt) occurred. This section is overlain by relatively flat-lying post-kinematic sediments.

6.4 Kinematic Interpretations of Salt Structures in the Contractional Domain

Many kinematic indicators are displayed around the salt structures in the outer Cilicia Basin. These kinematic indicators have little diversity and indicate similar movements for all of the faults within the Basement-Linked Fault Family as well as similar movements for all faults within the Toe-Thrust Fault Family. The Intra-Salt Fold/Thrust Fault Family has different kinematics than these two families.

6.4.1 Salt Structures in the Basement-Linked and Toe-Thrust Fault Families

The salt anticlines associated with both the Basement-Linked and Toe-Thrust Fault Families (described in sections 6.4 and 6.5) display thinning sediments at their crests with intervening synclines being filled by thickened sedimentary packages. The backlimbs of thrusted anticlines in both fault families are commonly onlapped by the overlying sediments indicating that the crests of these thrusts were elevated above the level of the seafloor during subsequent sediment deposition. These relationships are generally indicative of folding and thrusting that has kept pace with the sedimentation in a basin.

Most of the thrusted anticlines at the northern edge of the central fold and thrust belt (Basement-Linked Fault Family) have kept up with sediment deposition, constantly keeping the thrust culminations elevated above the seafloor. The folds at the southern edge of the belt form very low amplitude salt pillows that are associated with the youngest thrusts at the toe of the fold and thrust belt. These salt pillows, located in the frontal portion of the fold belt are overlain by concordant, unfaulted, constant thickness strata that gently fold over the top of the salt pillows. This salt-sediment relationship suggests that these folds have only recently developed whereas the more northerly faults have been active for quite some time.

The type of folding observed at the salt pillows and salt anticlines of the Basement-Linked Fault Family is known as fault propagation folding. This type of folding occurs when the sediments above a propagating fault are folded over the tip point of the fault. These faults continue to propagate from their tips during the formation of the fold belt making it relatively easy for the tip points of the faults to keep up with sedimentation in the region.

The sediments and faults at the Toe-Thrust Fault Family indicate that salt-cored anticlines in this region are much better developed than the salt structures of the Basement Linked Fault Family. Practically every salt anticline in this region displays thrusting of one, and sometimes both limbs. Because the leading thrusts of this fault family merge with thrusts of the Basement-Linked Fault Family, no poorly developed structures such as low amplitude salt pillows or salt anticlines are observed in the leading edge of this belt. The merging pattern of the Toe-Thrust Fault Family with the Basement-

Linked Fault Family suggests that the two families of salt structures and associated faults developed almost simultaneously in the region.

The salt structures associated with the faults of both the Basement-Linked Fault Family and the Toe-Thrust Fault Family are reactive-type structures which form in response to salt detached folding in the outer Cilicia Basin. These salt structures simply fill in the space created beneath folded sediments and do not appear to grow of their own accord.

6.4.2 Salt Structures in the Intra-Salt Fold/Thrust Family

Evaporites related to the Intra-Salt Fold/Thrust Family (described in section 6.2) commonly display internal reflectors that appear to repeat in a single seismic section. The repetitive appearance of these seismic reflectors has been interpreted as a series of low angle thrusts that cut the internal evaporite markers and sole onto a near-horizontal detachment surface within the salt. The thrusts in the evaporite sequence show a north vergence across the entire sequence of north-south oriented seismic lines in the outer Cilicia Basin. Davis and Engelder (1995) indicated that a fold and thrust belt which is underlain by an evaporite detachment should show no consistent vergence of thrusts. Their finding effectively eliminates the interpretation of these structures as fold and thrust belt related structures as they obviously sole onto a detachment surface within the salt yet they display a pervasive northward vergence. The thrusts in the evaporite unit are observed to both the north and the south of the central fold and thrust belt in the outer Cilicia Basin but appear to be absent or overprinted in the region of the fold and thrust

belt itself. It is quite likely that the intra-salt faults have been overprinted by a younger episode of thrusting occurring in the central fold and thrust belt of the Basement-Linked Fault Family.

The evaporite unit is notably thicker in the southern part of the outer basin than in the northern end of the basin. This observed thickness variation suggests that when the evaporites in the outer portion of the Cilicia Basin were deposited the basin likely had a south dipping tilt that caused evaporites to pool in that part of the basin. The evaporites were later thrusted toward the northern part of the basin producing the low-angle fault structures that were noted in north-south oriented seismic lines in the outer basin

Evaporite bulges in the northern part of the basin suggest that the thrusting of the evaporites occurred in response to some kind of north directed compressional force in the basin. These evaporite bulges developed as the north directed thrusting of salt was obstructed by a thick package of Pliocene and Quaternary sediments that were being deposited in a large anticline in the northern end of the outer basin. This package of sediments is thickest in the northern part of the basin and notably thins towards and onlaps the evaporite unit at the south end of the outer Cilicia Basin. The thickness variations observed in this sedimentary sequence records a north dipping tilt in the basin. The tilting of the basin probably began shortly after the initial deposition of evaporites in the outer Cilicia Basin and continued up until the Pliocene-Pleistocene (M-Reflector unconformity). This north-dipping basin geometry could explain the northward directed thrusting observed in the evaporite unit. The configuration of evaporites and overlying sediments therefore should reflect a northward directed gravitational gliding tectonic

system in the outer Cilicia Basin. Extensional faults that are commonly observed upslope of a gravitational gliding system are not immediately apparent in the southern part of the outer Cilicia Basin. Upon closer analysis it is concluded that the upslope extensional faulting expected in the evaporite unit may have been overprinted by early tectonic activity along the seaward faults of the Basin Forming Fault at the southernmost part of the outer Cilicia Basin (an alternative interpretation is that these thrusts are simply backthrusts related to compressional activity in Northern Cyprus).

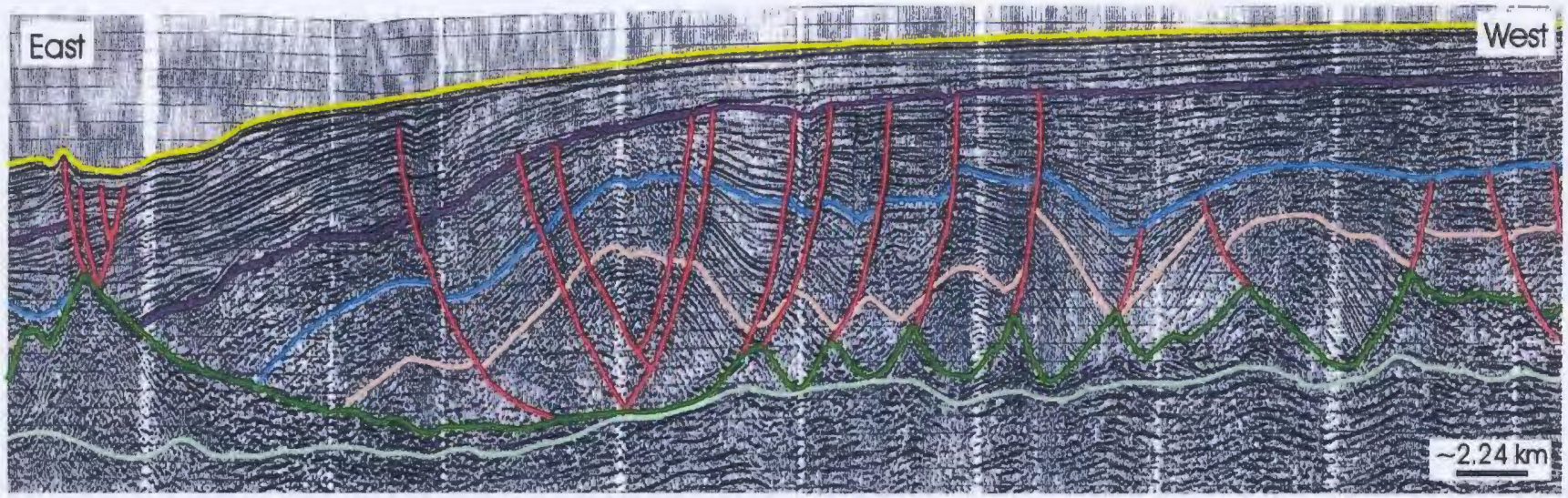

Figure 6-1: The extensional faults in the inner Cilicia Basin form distinct anticlinal structures in the sediments above the salt rollers.

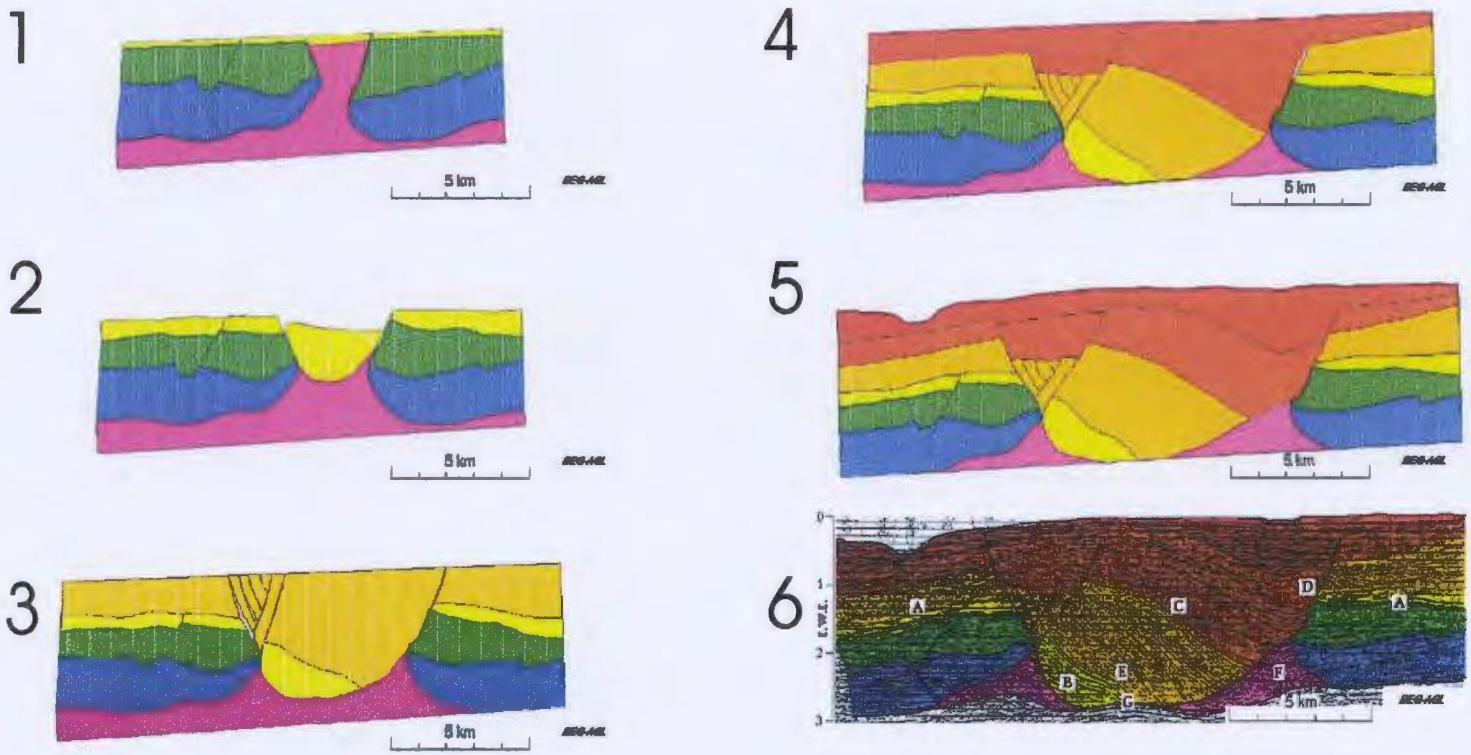

Figure 6-2: Selected shots of an animation showing a palinspastic reconstruction of a seismic section from the Kwanza Basin, Angola, illustrates the evolution of a mock turtle structure. These structures appear to be the same as those in the Cilicia Basin (Fig. 6-1) however, as demonstrated in the above example, they are different from Cilicia structures because they form as a result of extreme extension causing overburden sediments to subside into the crest of a sagging diapir and eventually ground-out creating a turtle structure. The Cilicia Basin examples do not form from sediments sinking into a pre-existing diapir, but rather, form when the sedimentary overburden subsides into the source-layer salt as a result of salt withdrawal to feed growing diapirs elsewhere in the basin. (Animation source: Guglielmo, Giovanni, Jr., D. D. Schultz-Ela, and M. P. A. Jackson 1997, Raft tectonics in the Kwanza Basin, Angola: an animation. A BEG hypertext multimedia publication on the Internet at: http://www.beg.utexas.edu/indassoc/agl/animations/AGL96-MM-003/index.html.)

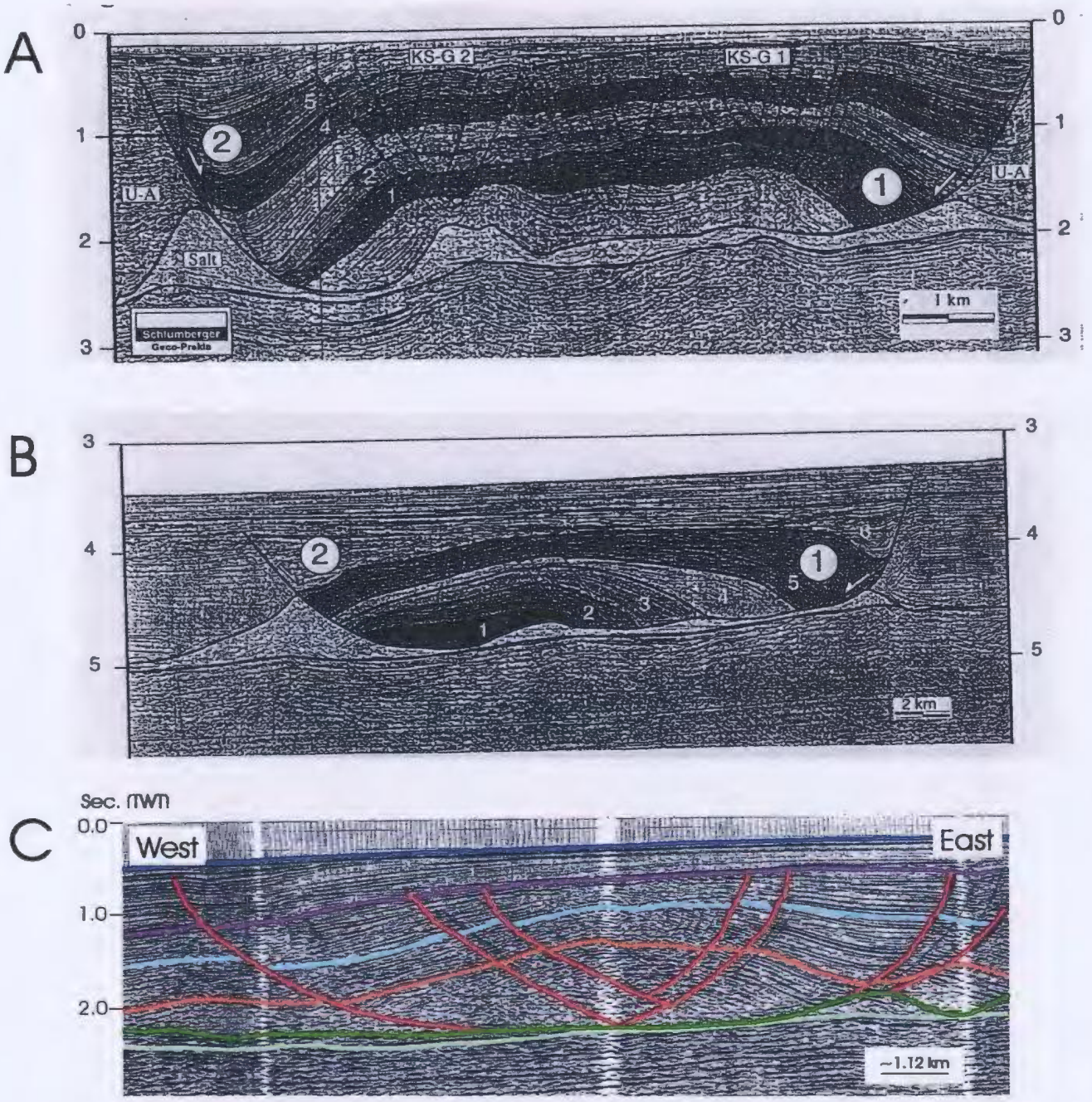

Figure 6-3: Turtle-back growth anticlines observed in the Kwanza Basin, Angola (A) and Campos Basin, Brazil (B) show a remarkable resemblance to those in the Cilicia Basin. Internal reflector asymmetry arises when the extension on one side of the structure progresses at a rate faster than that at the other side of the structure. This is particularly evident in the example from the Campos Basin, Brazil (B). Note that the structures are quite symmetrical externally despite internal asymmetries (Modified from Mauduit et al., 1997).

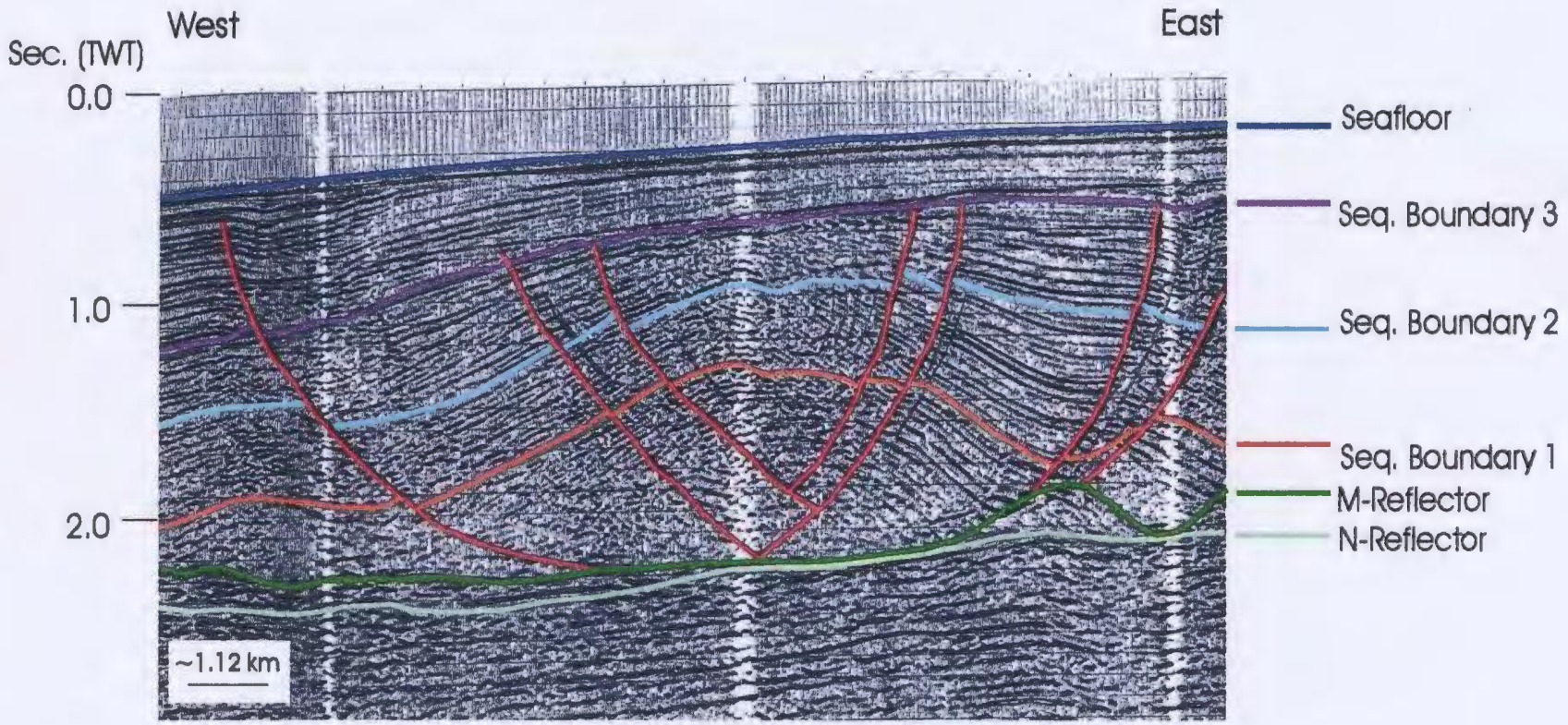

Figure 6-4: Turtles in the Cilicia Basin often have a more or less external symmetry with a distinct asymmetry observed in the growth strata on each side of the turtle.

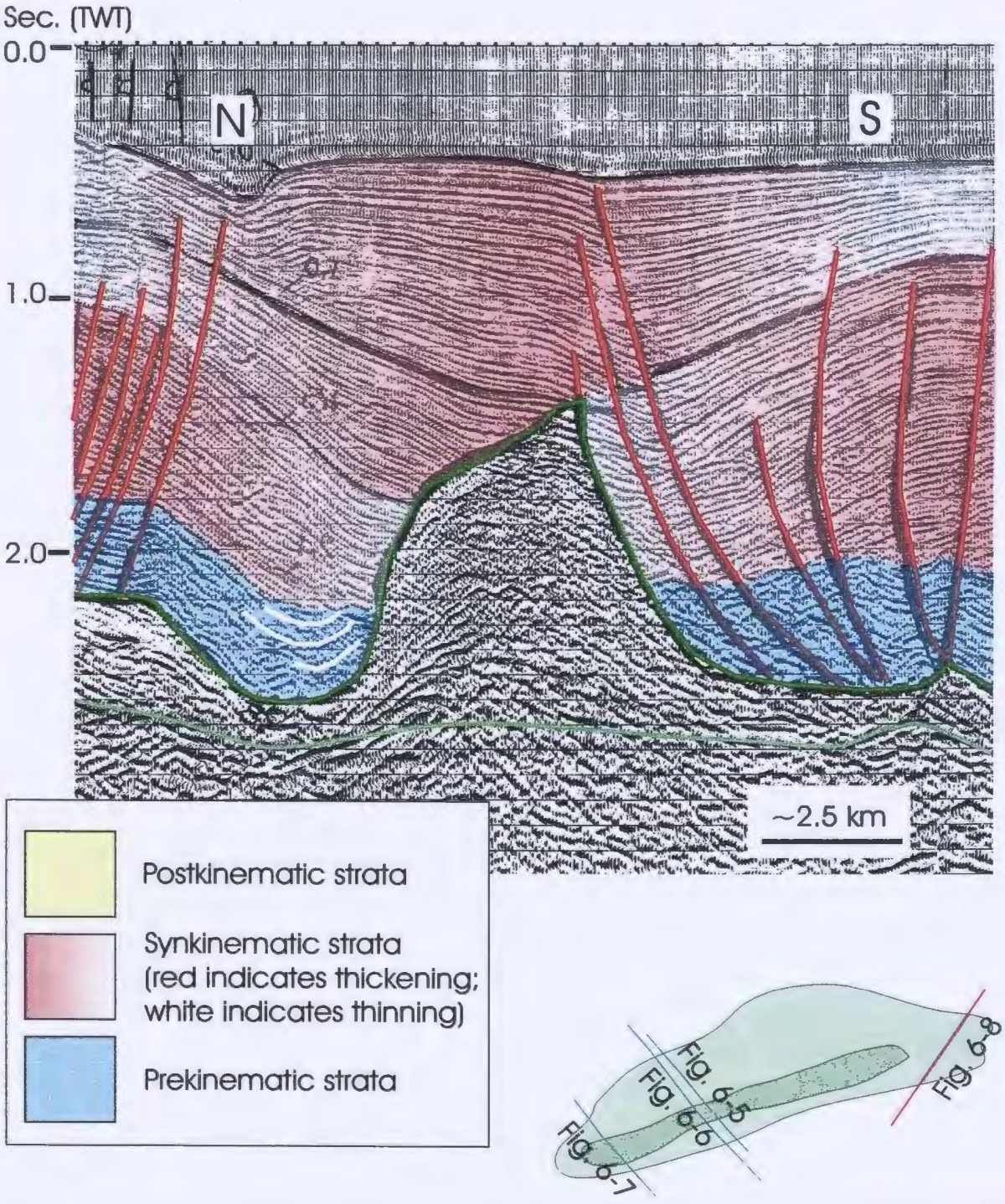

Figure 6-5: North-South seismic section near the center of the northern salt wall displaying kinematic stages and thinning and thickening of sediments.

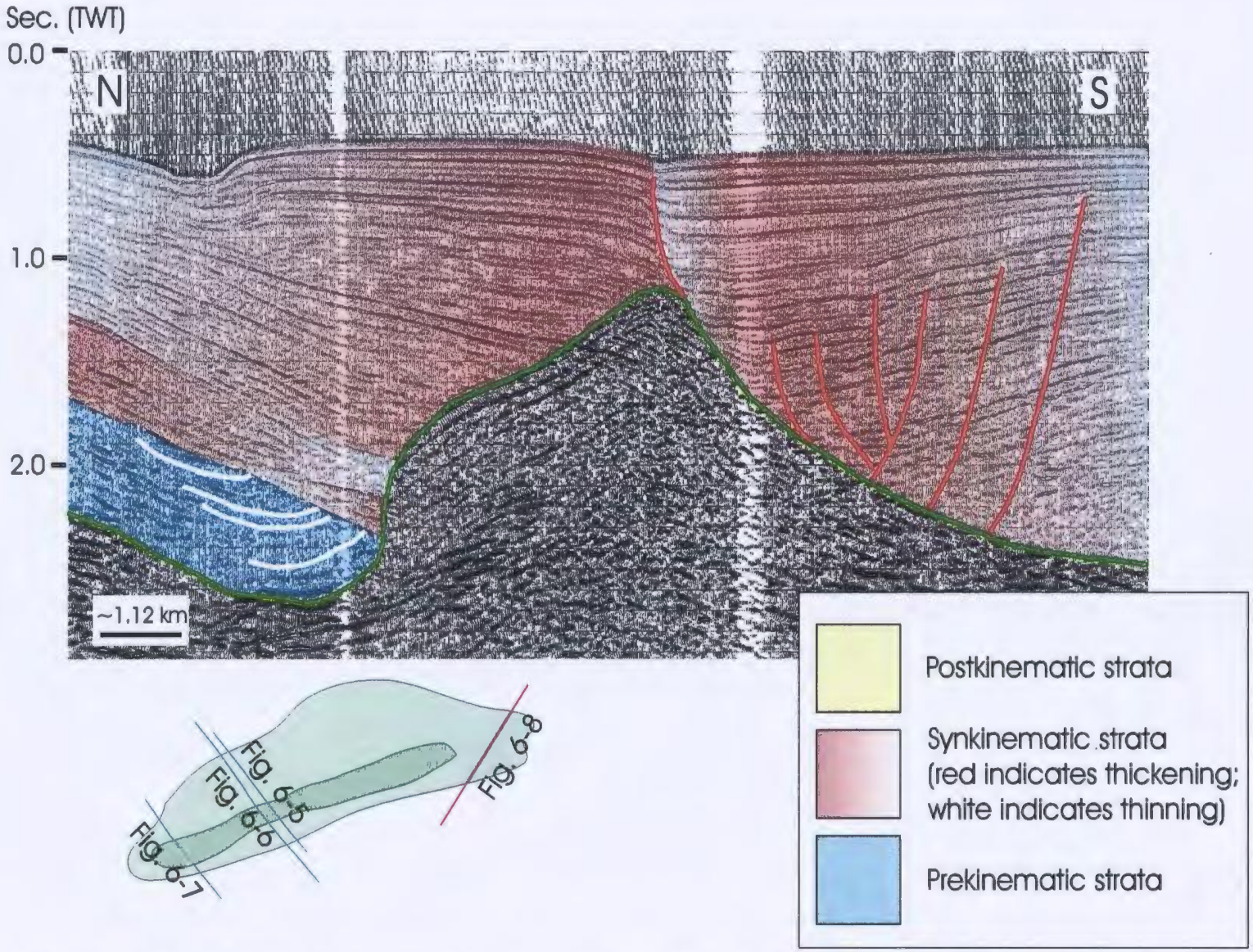

Figure 6-6: Another North-South seismic section near the center of the Northern salt wall displaying kinematic stages and thinning and thickening of sediments.

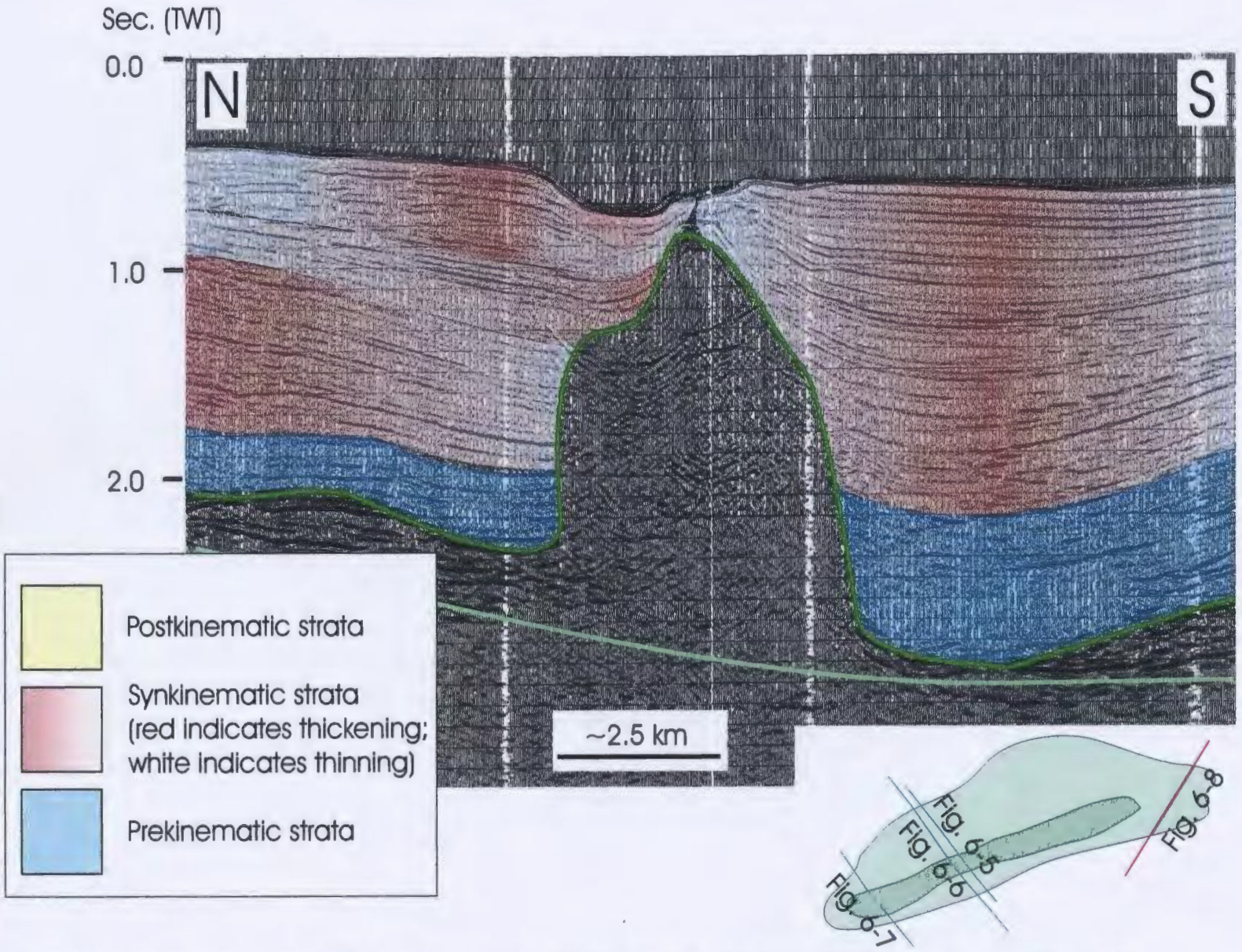

Figure 6-7: Western end of the northern salt wall displaying kinematic stages and thinning and thickening of sediments.

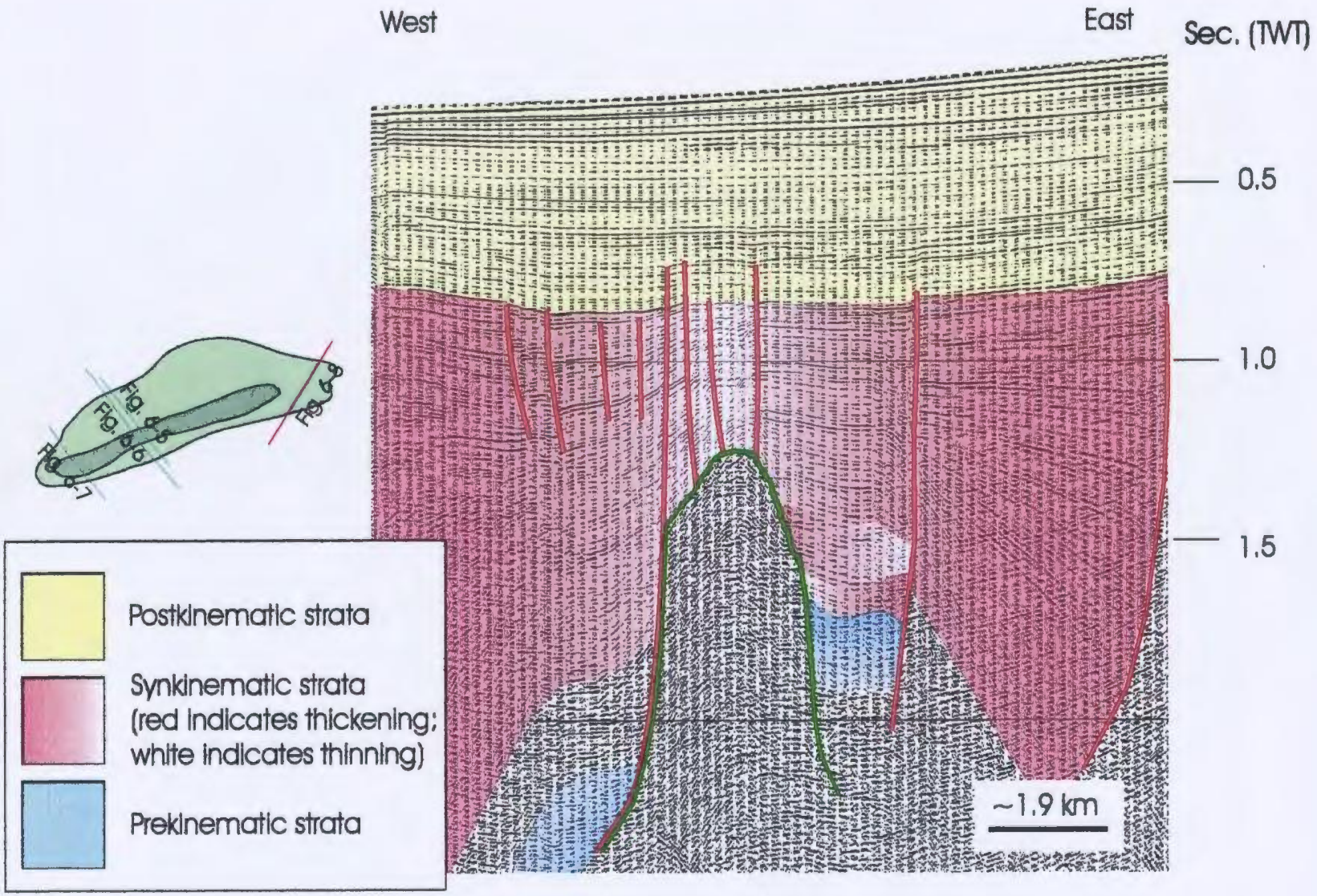

Figure 6-8: A west-east seismic section at the Northern salt wall displaying kinematic stages and thinning and thickening of sediments.

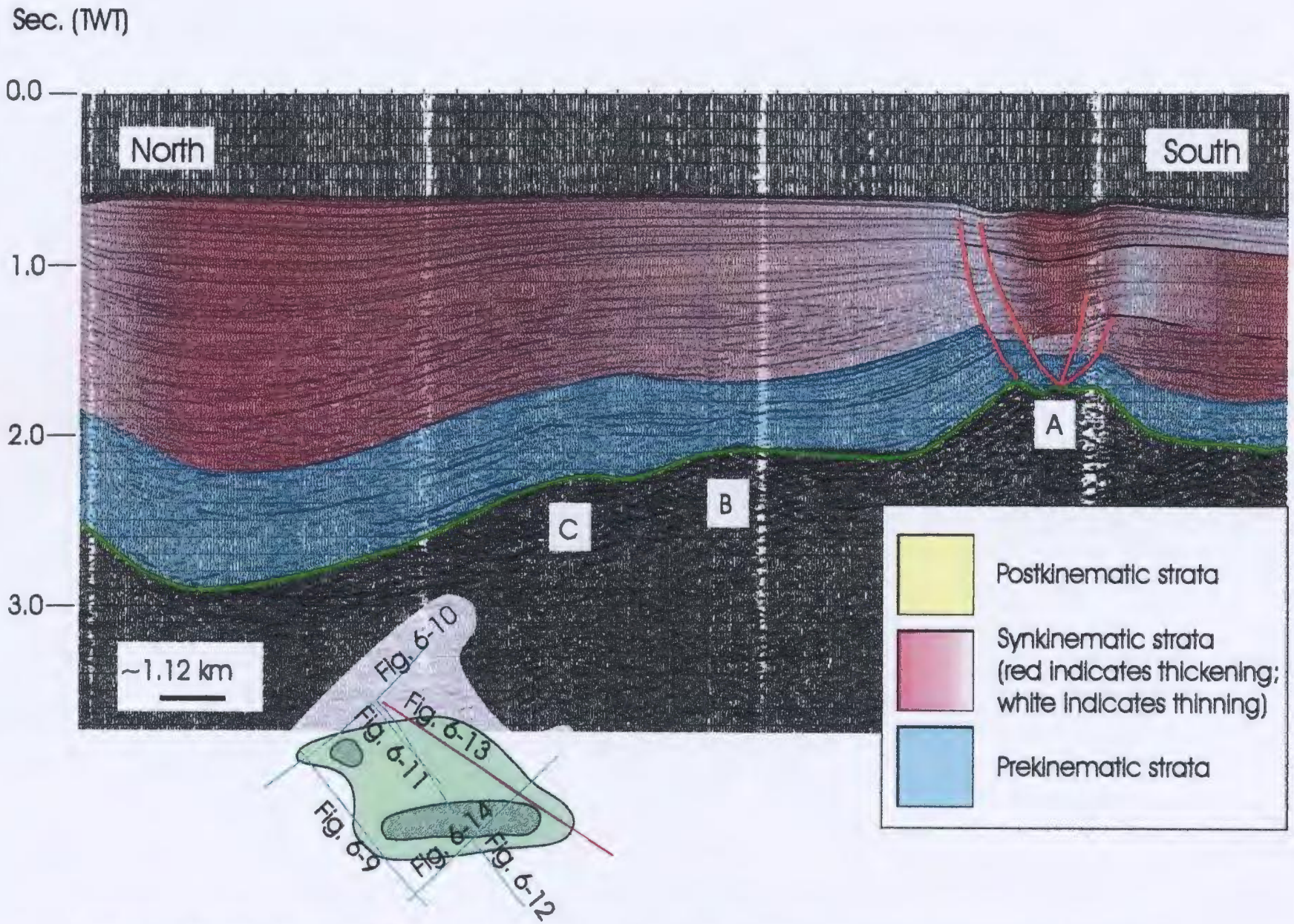

Figure 6-9: Central salt wall displaying kinematic stages and thinning and thickening of sediments.

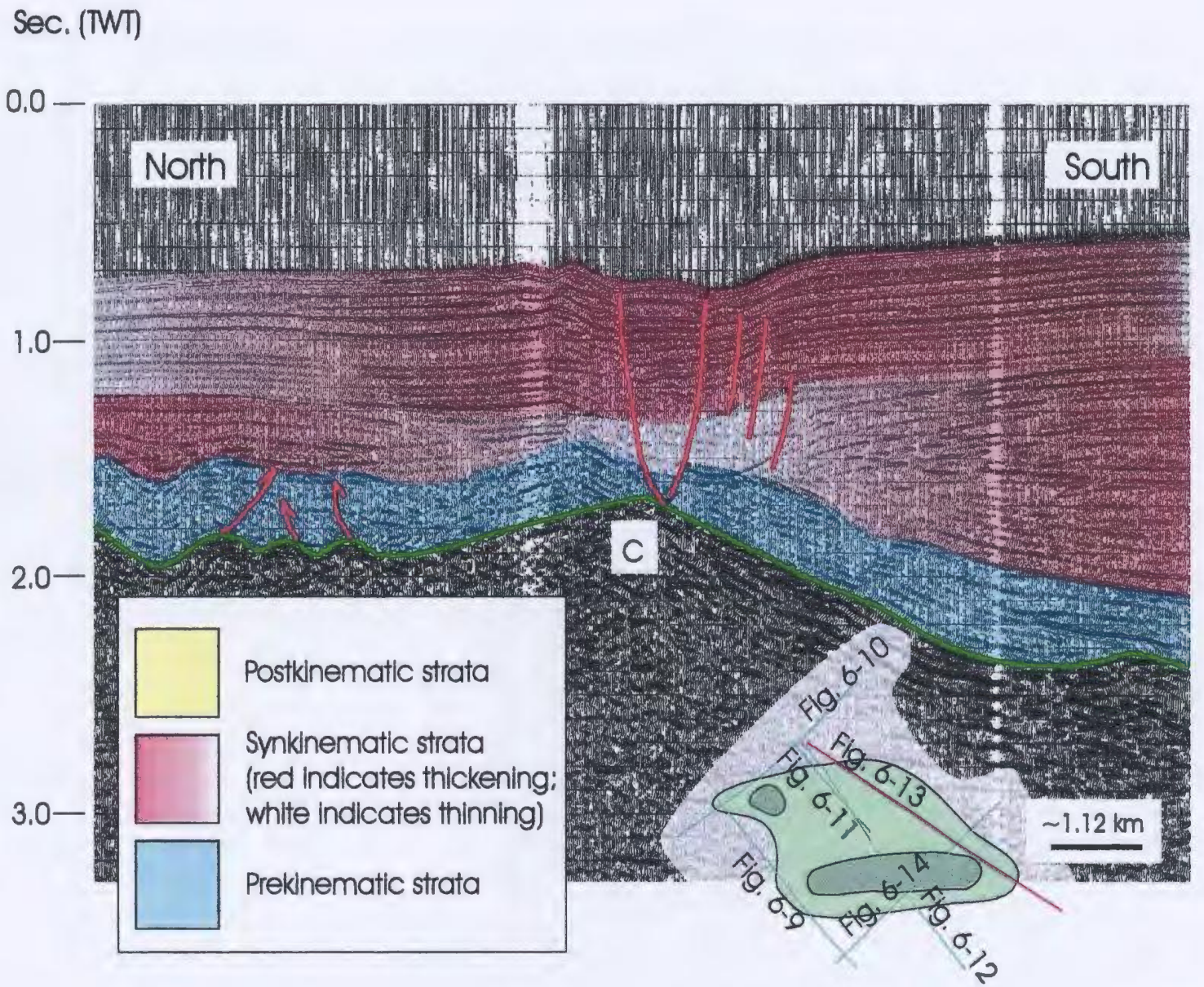

Figure 6-10: Central salt wall displaying kinematic stages and thinning and thickening of sediments.

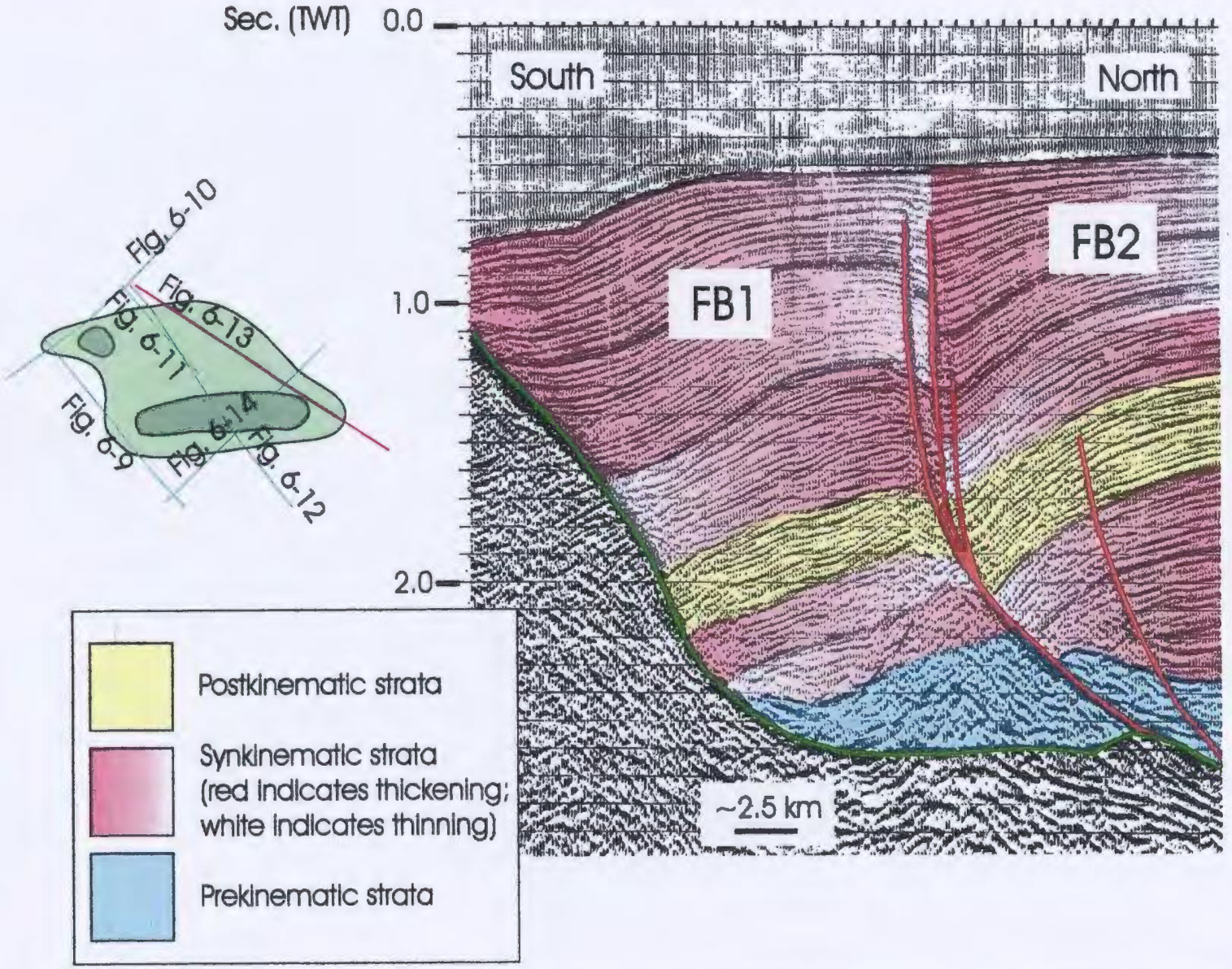

Figure 6-11: Central salt wall displaying kinematic stages and thinning and thickening of sediments.

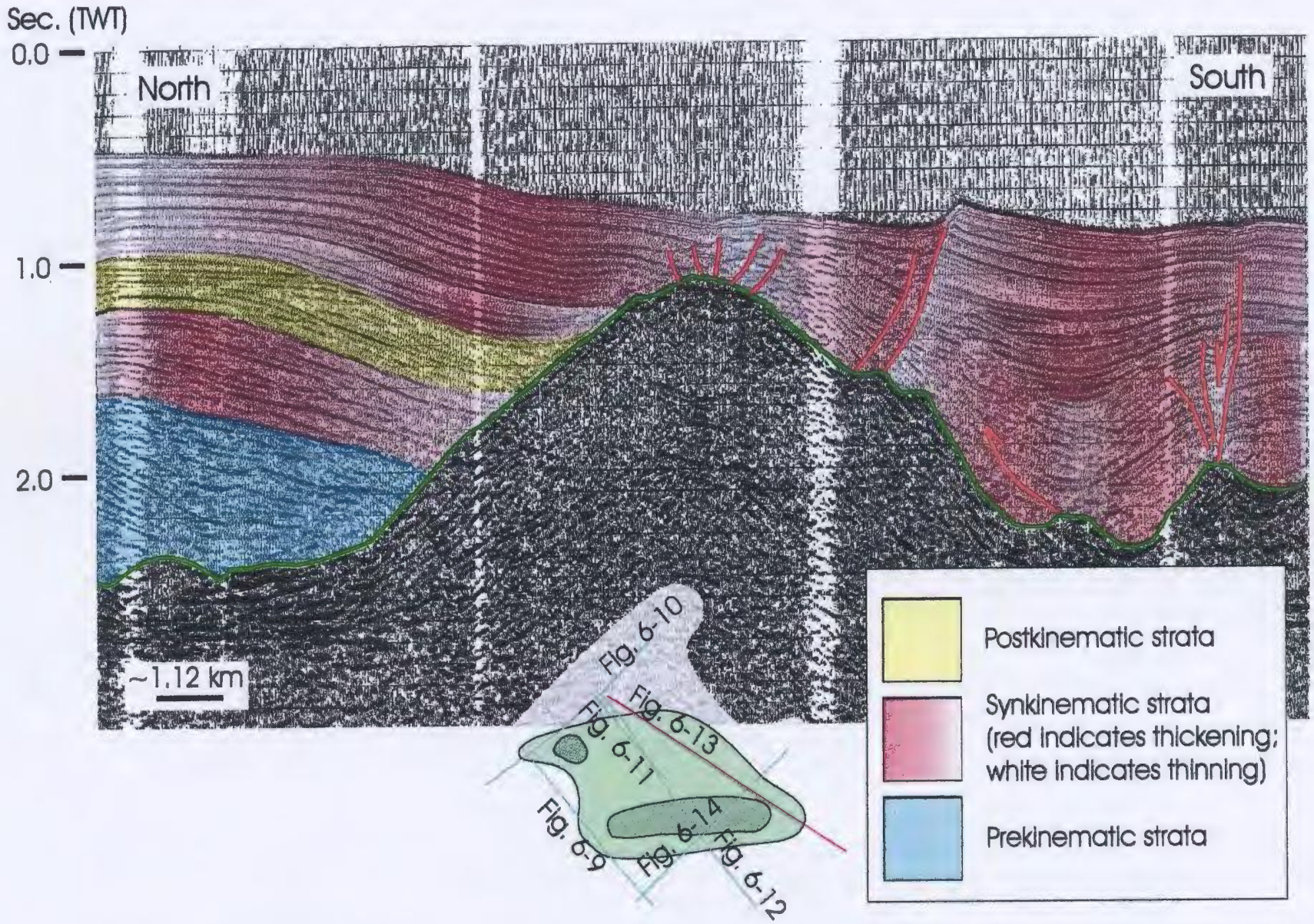

Figure 6-12: Central salt wall displaying kinematic stages and thinning and thickening of sediments.

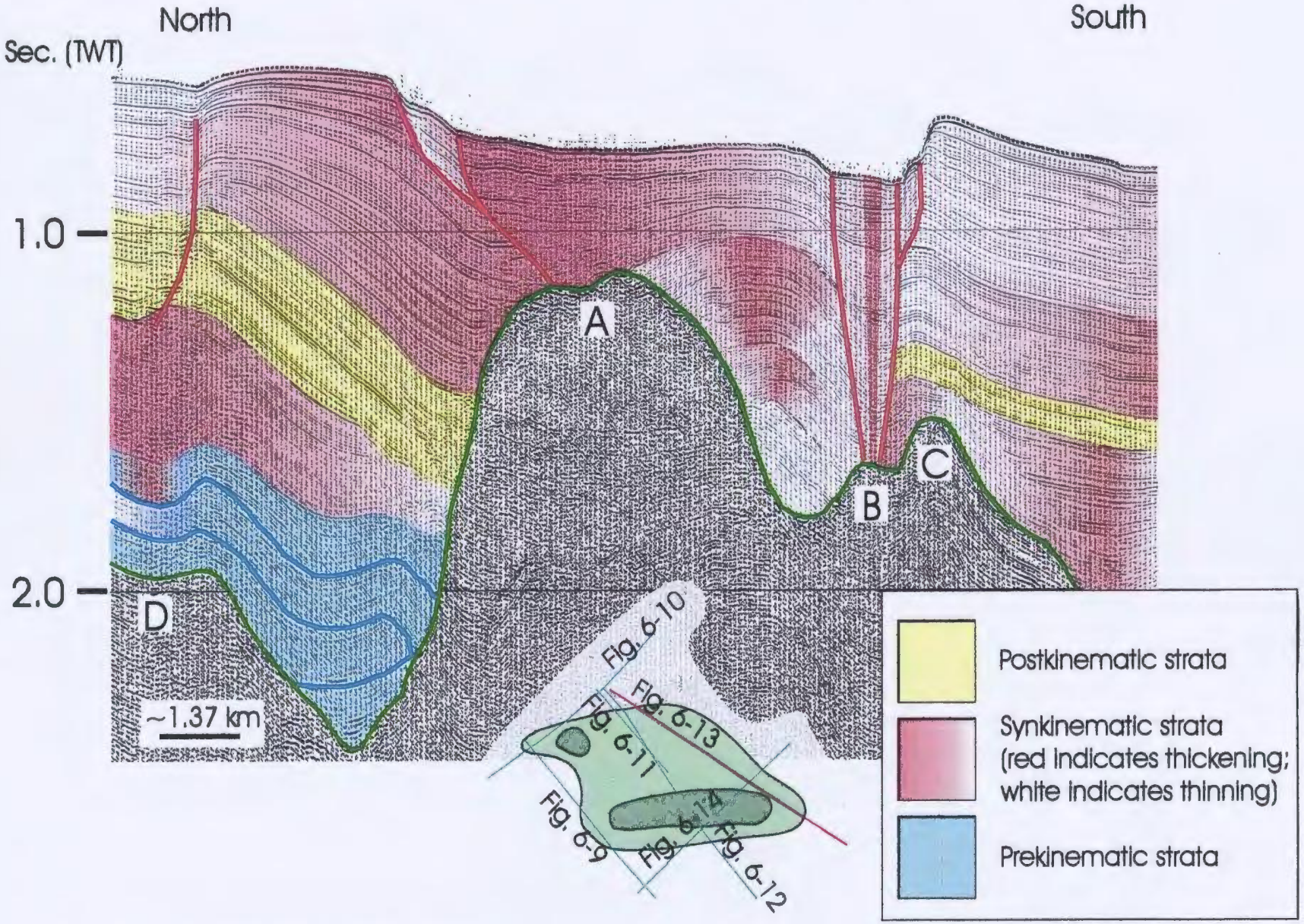

Figure 6-13: Central salt wall displaying kinematic stages and thinning and thickening of sediments.

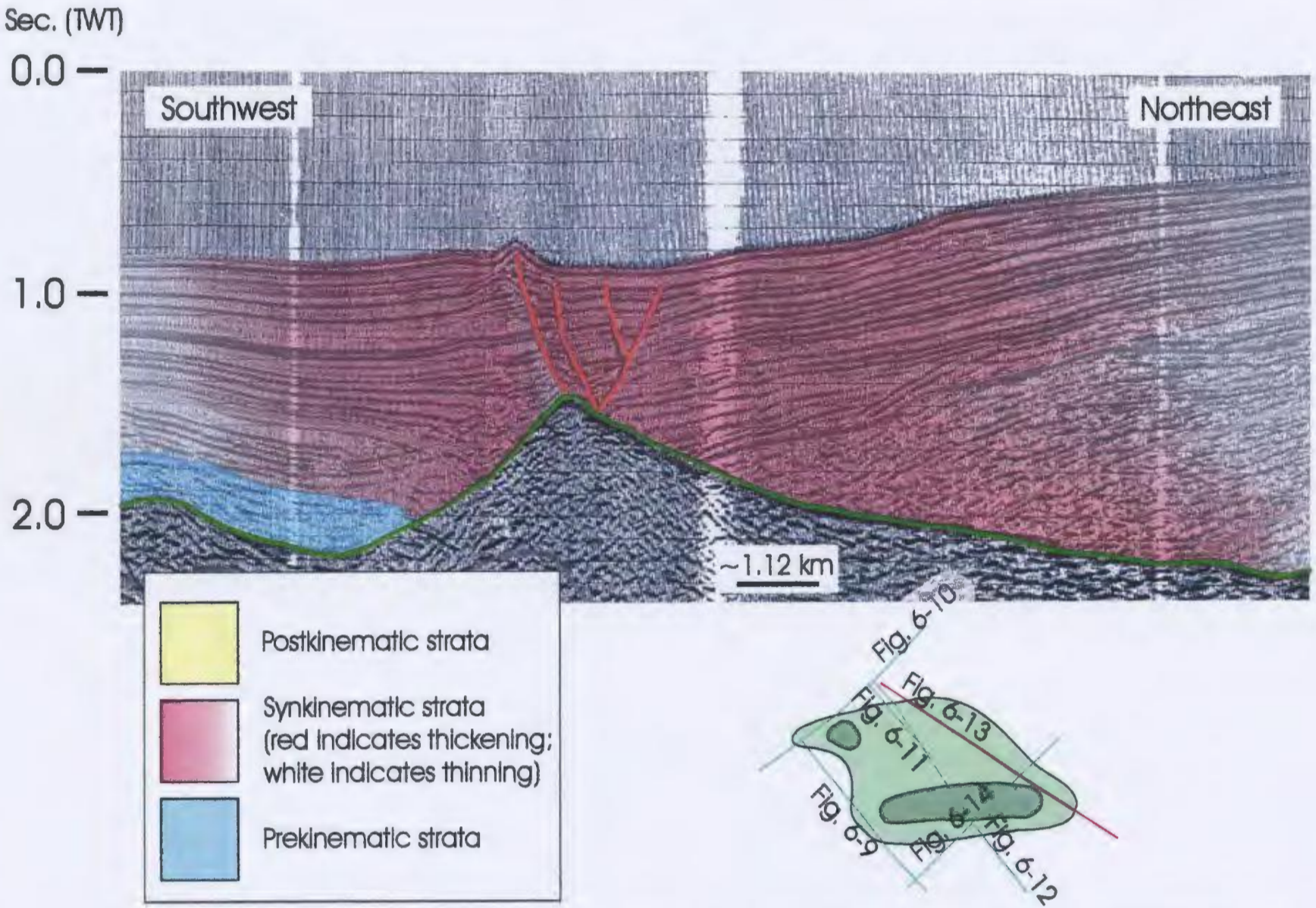

Figure 6-14: Central salt wall displaying kinematic stages and thinning and thickening of sediments.

Figure located in back pocket.
INSERT 2

Figure 6-15: Compilation diagram showing location, kinematic stages, as well as the thinning and thickening of sediments at the central salt wall.

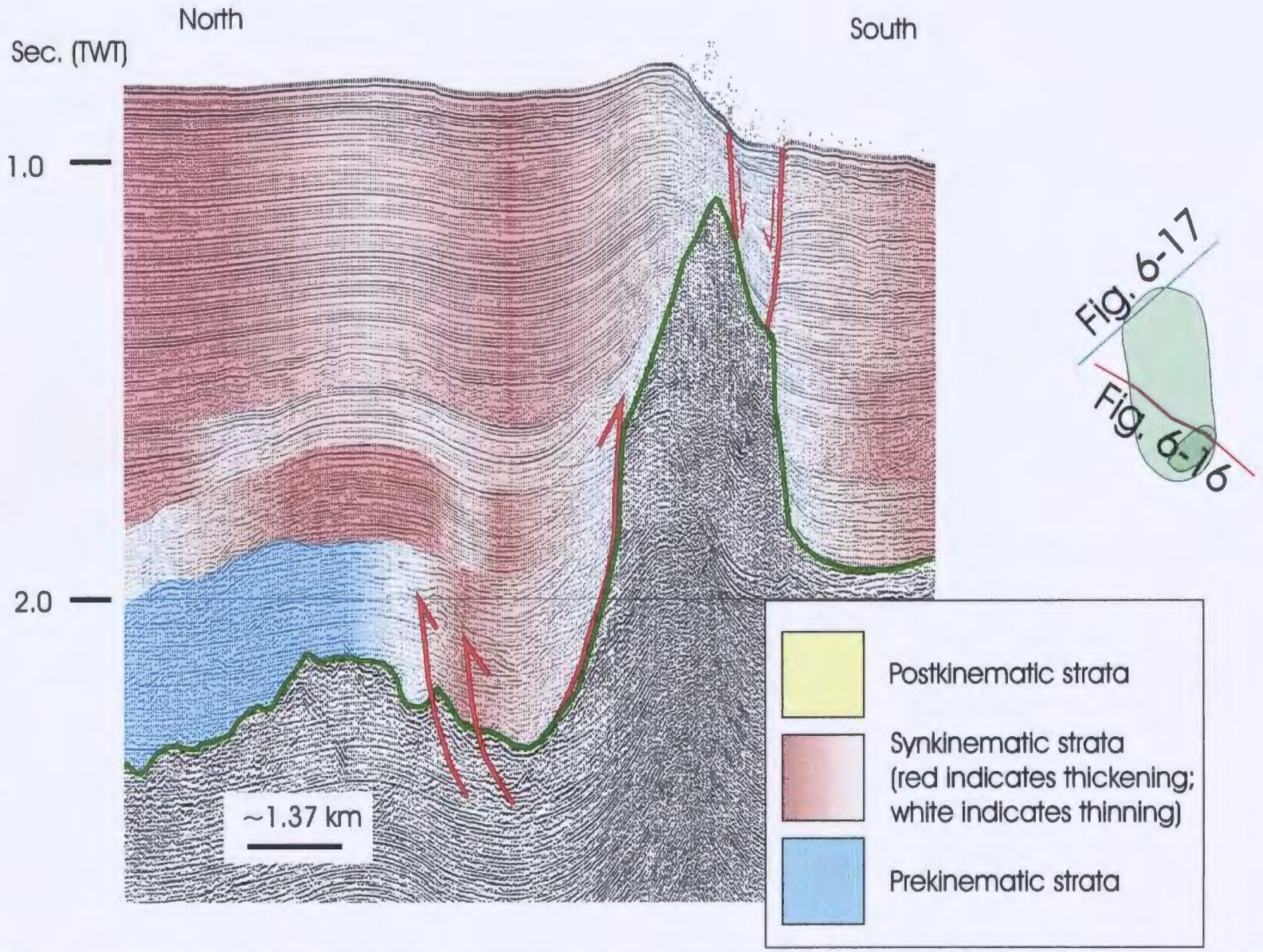

Figure 6-16: North-South seismic section across the southern salt wall displaying kinematic stages and thinning and thickening of sediments.

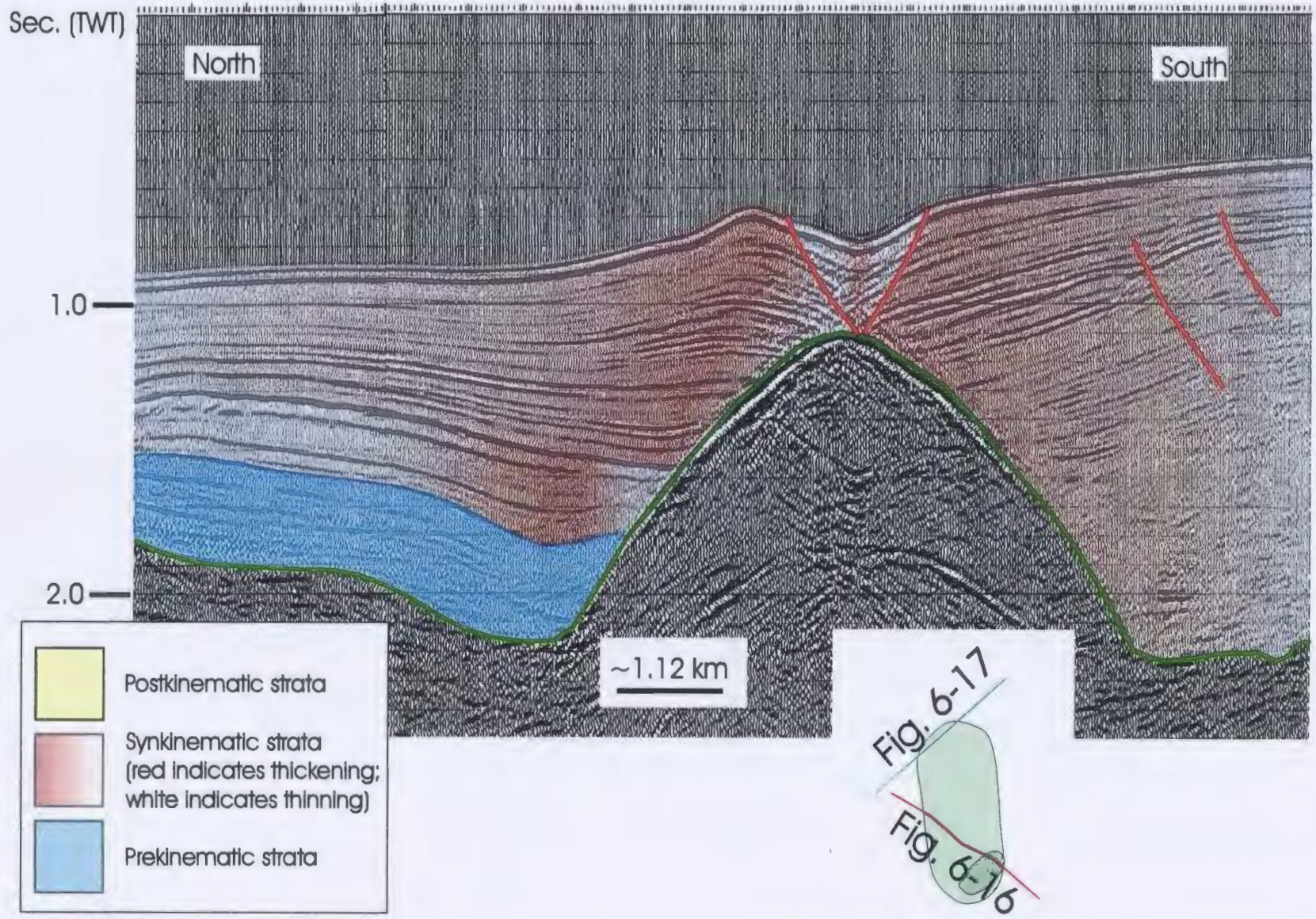

Figure 6-17: Seismic from the tip of the southern salt wall displaying kinematic stages and thinning and thickening of sediments.

7. DISCUSSION

7.1 Pre-Messinian Tectonic Evolution of Eastern Mediterranean Region

The easternmost end of the Mediterranean Sea formed as a part of a linked system of opening and closing seas known as the Tethyan Evolution. The Tethyan Evolution opened a sea between the former Laurasia and Gondwanaland plate margins. This process occurred in two distinct and separate events: a Cimmeridian Episode and an Alpine Episode (Görür et al., 1998).

During the Cimmeridian Episode the closing of the Palaeo-Tethys ocean near the end of the Triassic indirectly resulted in the formation of the Karakaya suture in northern Turkey (Görür et al., 1998).

The Alpine Episode includes the formation of the Neo-Tethys Ocean along a northern branch and a southern branch. The northern branch includes ocean segments represented by the Intra-Pontide suture, the Izmir-Ankara-Erzincan Suture and the Intra-Tauride Suture of central Turkey. The southern branch consists of the Antalya (Pamphylian) and Bitlis Ocean segments of the Neo-Tethys (Görür et al., 1998). These two branches of the Neo-Tethys Ocean divided Turkey into six geologically distinct tectonic terranes. (Şengör and Yılmaz, 1981, Okay, 1989). These tectonic terranes are grouped as having either Laurasian (North America, Greenland, Europe and Asia) or Gondwanaland (South America, Africa, India, Australia and Antarctica) Plate origins.

The Laurasian Plate margin in Turkey consists of three tectonic terranes. From north to south these terranes are the Strandja Massif, the Istanbul Zone and the Sakarya

Zone (Fig. 7-1). The three remaining tectonic terranes in Turkey belong to the Gondwanaland Plate margin: the Kırşehir Block of central Anatolia, the Menderes-Taurus Platform of western and central Anatolia and the Arabian Platform (Syrian-Arabian Microplate) of southeastern Turkey (Fig. 7-1).

Cyprus also formed from a grouping of tectonic terranes; all were individual fragments with Gondwanaland Plate affinity. The tectonic terranes of Cyprus are: the Kyrenia Terrane in northern Cyprus, the Troodos Terrane in central Cyprus and the Mamonia Terrane in southeastern Cyprus (Fig. 7-1; Robertson, 1990).

7.1.1 Triassic Period

The Triassic Period in the Eastern Mediterranean region had two main highlights: the closing of the Palaeo-Tethys and the opening of the Neo-Tethys. A south dipping subduction zone known as the Palaeo-Tethyan Arc was located at the southern margin of Gondwanaland and consumed the oceanic crust of the Palaeo-Tethys. This subduction zone was probably active since the latest Cretaceous and facilitated the development of a back-arc extensional magmatic arc in Turkey, near the northern margin of Gondwanaland (Dewey et al., 1980). Back-arc regions in Gondwanaland underwent rifting and extension resulting in the formation of a branching system of oceanic segments, the future Neo-Tethys Ocean. All branches of this ocean with the exception of the Intra-Pontide Ocean began to rift in the early Triassic Period (Görür et al., 1983). The Kırşehir Block and the Menderes-Taurus Platform were completely isolated from each other and from other terranes as the northern branches of the Neo-Tethys opened. The southern Laurasian

Margin, consisting of the Strandja Zone, the Istanbul Zone and the basement of the Sakarya Zone, faced the Palaeo-Tethys Ocean (Görür et al., 1998). The end of the Triassic closed the more easterly portion of the Palaeo-Tethys Ocean and the Karakaya Complex (fore-arc origins) was thrust onto the basement of the Sakarya Zone during the Karakaya Orogeny.

During the Triassic, Cyprus formed part of an unstable shelf consisting of the Kyrenia Terrane. This shelf area was fringed by continental slivers and atolls of the Mamonia and Troodos Terranes (Robertson, 1990).

7.1.2 Jurassic Period

During the early Jurassic (Liassic) the southern Laurasian margin experienced an episode of rifting which separated the Sakarya Zone from the Strandja and Istanbul Zones. The Intra-Pontide Ocean formed in the gap created by this rifting (Okay, 1989). The remnants of the Palaeo-Tethys Ocean, north of the Intra-Pontide Ocean, continued to close until the middle Jurassic (Şengör et al., 1984). The Laurasian Plate separated into North American and Eurasian plates in the late Jurassic at approximately 150 Ma. By this time, the entire Palaeo-Tethys Ocean had been eliminated and the Strandja Nappe became part of the Strandja Zone (Şengör et al., 1984). The Jurassic period in Cyprus saw the Kyrenia Terrane as a subsiding passive continental margin bordered by a small ocean basin, the Mamonia Terrane (Robertson, 1990). Throughout the entire Jurassic, platformal carbonates grew on the margins of the tectonic terranes.

7.1.3 Cretaceous to Middle Eocene

By the Cretaceous Period Palaeo-Tethyan tectonics had significantly abated and the Neo-Tethyan evolution neared its climax. Passive continental margins surrounding the Neo-Tethys Ocean were converted to active subduction zones in the early Cretaceous (ie. Albian to Aptian; Görür, 1988). Locally, subduction related extension occurred and continents above the subduction zones became rimmed by magmatic arcs. The presence of these magmatic arcs changed the sedimentation on the margins of the tectonic terranes from shallow water carbonate deposition in a shelf environment to predominantly siliciclastic deposition in a deeper fore-arc setting (Görür, 1988). A melange wedge began to form above the subduction zones.

Extension on the Laurasian margin followed shortly thereafter. During Albian-Aptian the Istanbul Zone underwent extension. This zone then moved south along two transform faults to form the western Black Sea Basin. The eastern Black Sea Basin formed shortly thereafter through counter-clockwise motion of a large tectonic block, the Eastern Black Sea Block (Görür, 1988; Okay et al., 1994).

During the middle to late Cretaceous large ophiolite nappes were emplaced upon the Kırşehir Block (Albian or Aptian), Menderes-Taurus Platform (late Campanian to early Maastrichtian) and Arabian Platform (early Campanian to early Maastrichtian) as part of the final stages of subduction of Palaeo-Tethyan crust (Şengör and Yılmaz, 1981; Özgül et al., 1981; Pişkin and Delaloye, 1983; Yılmaz, 1985). Studies by Delaune-Mayer et al. (1977) established that the emplacement of these ophiolitic nappes resulted in the large scale, collective subsidence of the tectonic terranes. They showed that following the

nappe emplacements almost all neritic (shallow water) depositional domains were invaded by pelagic (open sea) sedimentation confirming a deepening of the basins.

In the late Cretaceous the Troodos ophiolite of Cyprus formed above an intra-oceanic subduction zone. The Troodos Microplate then underwent approximately 90° of counterclockwise rotation that lasted throughout the Paleocene and into the early Eocene (Okay et al., 1994).

The Intra-Pontide Ocean in northern Turkey (formed during Jurassic rifting events which separated the Sakarya Zone from the Strandja and Istanbul Zones) may have closed by the late Cretaceous; however, the timing of this closure is much debated. Şengör and Yılmaz (1981) suggest a pre-Maastrichtian closure of the Intra-Pontide Ocean. Okay and Tansell (1994) claim that the closure of the Intra-Pontide was during the early Eocene. Görür and Okay (1996) consider the closing of the Intra-Pontide to have been a diachronous event that began in the early Eocene in the eastern portion of the ocean while the western portion of the Intra-Pontide Ocean remained open until the late Oligocene. Whatever the timing, the closure of this ocean halted the opening of the western Black Sea as the Istanbul Zone collided with the Sakarya Zone (Okay et al., 1994).

The westernmost segment of the Izmir-Ankara-Erzincan Ocean closed during the Palaeocene to Lutetian (Şengör and Yılmaz, 1981), whereas the eastern portion of the Ocean along with the Intra-Tauride Ocean closed during the late Cretaceous to early Eocene (Görür et al., 1984; Okay 1989).

The Troodos and Mamonia terranes of Cyprus are believed to have converged before the middle Eocene. The boundary between these two units is sealed by a distinct

marker horizon composed of chalk, limestone, marl and chert that is a part of the Lefkara Formation (Robertson, 1990).

7.1.4 Late Eocene to Middle Miocene

The late Eocene saw a north-south shortening in the Eastern Mediterranean region that continued until at least the Pliocene. This shortening affected both the Kyrenia Terrane of Cyprus and numerous tectonic terranes of Turkey (Robertson, 1990, Görür et al., 1998). The Kyrenia Terrane underwent south directed thrusting, finally amalgamating with the Troodos and Mamonia Terranes of Cyprus by the late Eocene to early Oligocene (Robertson, 1990). The late Oligocene to late Miocene saw drastic subsidence of the Kyrenia Terrane that was buried under over two kilometers of deep water turbidites. In the late Miocene (Tortonian) southeast directed thrusting facilitated the development of the Misis-Kyrenia Lineament between Cyprus and southeast Turkey. Imbrication in southern and eastern Turkey lead to the formation a large orogenic belt, the Anatolian Orogenic Collage. This orogenic collage consists of numerous nappe complexes of the Menderes-Taurus Platform and many metamorphic massifs such as the Menderes Massif in southwestern Turkey (Görür et al., 1998). The north-south shortening had resulted in the formation of the Taurus Mountains in southern Turkey by the Oligocene (Rögl et al., 1978). This shortening affected regions so far north as the Kırşehir Block where the result was the creation of north verging basement thrusts.

The same north-south contractional deformation event that caused imbrication and nappe formation in Turkey and Cyprus was also the cause for the convergence of Eurasia

and the Arabian Platform (Görür et al., 1998). Eventually, the north-south shortening had advanced the collision of Eurasia with the African Plate and Syrian-Arabian Microplate such that the Bitlis Ocean was completely eliminated resulting in the development of a suture zone, known as the Bitlis-Zagros Suture Zone. This suture zone consists of thrust slices of disrupted ophiolite, ophiolitic melange and arc volcanics with ages ranging from late Triassic to late Eocene (Yılmaz et al., 1993b). The majority of the Neo-Tethys had closed by the middle Miocene with the exception of a part of the southern branch of the Neo-Tethys; the present-day Eastern Mediterranean Sea (Şengör et al., 1985).

The continued squeezing of the Aegean-Anatolian Microplate between the Syrian-Arabian Microplate and the Eurasian Plate caused a gradual west directed escape of the Aegean-Anatolian Microplate along the North Anatolian and East Anatolian transform faults, away from high strain areas in the east (Şengör, 1979; Dewey et al., 1986). Şengör et al. (1985) indicate that this 'escape tectonics' represents the neo-tectonic regime of the Eastern Mediterranean.

7.2 The Cilicia Basin in the Eastern Mediterranean Tectonic Framework

In order to place the Cilicia Basin in the context of the Eastern Mediterranean tectonic framework it is necessary to look at the formation and development of its ancestor basin.

7.2.1 The Cilicia Basin Ancestor

In front of the thrust front of the Taurus Mountains, a foredeep or foreland basin

developed during the Oligocene to early Miocene. This arcuate basin contained the Cilicia Basin, the Adana Basin and a southern basinal region that later became the Mesaoria Basin of Cyprus. This foreland basin developed in response to differential slip rates on major faults in the eastern Mediterranean Region (Şengör et al., 1985).

A simplified tectonic map for the Eastern Mediterranean (Fig. 7-2) shows the main tectonic elements involved in the evolution of the ancestor basin. Şengör et al. identified what they called a 'quadruple junction' (labeled KM) at the meeting point of three continental blocks and one oceanic plate (Fig. 7-3). The margins of these features meet in the region of Kahramanmaraş along the East Anatolian Fault Zone (a sinistral transtensional fault zone that forms the plate boundary between the Syrian-Arabian and Aegean-Anatolian microplates), the Dead Sea Fault Zone (a major sinistral fault zone forming the plate boundary between the Syrian-Arabian Microplate and the African Plate) and the Southeast Taurus Boundary Thrust Zone (a southward directed collection of thrusts within the northern part of the Arabian Plate). Şengör et al. analyzed the major tectonic elements and their interactions and determined that the Southeast Taurus Boundary Thrust Zone absorbed a great deal of northward directed movement of the Syrian-Arabian Plate. This northward movement would not be focused along boundary between the Syrian-Arabian and Anatolian Plates at the East Anatolian Transform Fault but would be spread over the Southeast Taurus Boundary Thrust Zone as well as the East Anatolian Transform Zone. The reduction in northward-directed movement at the northwestern Syrian-Arabian and Anatolian segment of the East Anatolian Transform Zone requires transtensional activity along the southern African and Anatolian segment of

the East Anatolian Transform Zone. Şengör et al. calculated two possible extension rates along the southern segment of the East Anatolian Transform Zone based on the amount of north-south movement absorbed by the Southeast Taurus Boundary Thrust Zone. They calculated an extension rate of 0.41 cm/year if the Southeast Taurus Boundary Thrust Zone absorbed 3.16 of the 3.5 cm/year African-Arabian motion or 0.42 cm/year if the Southeast Taurus Boundary Thrust Zone absorbed 3.4 cm/year of the African-Arabian motion. The orientation of this extension is also dependant on the amount of north-south movement absorbed by the Southeast Taurus Boundary Thrust Zone, as indicated in Figure 7-4. Şengör et al. went on to say that the buoyant nature of continental lithosphere might cause further incompatibilities at strike-slip fault intersections that generate complex basin types.

Exhumation of the Misis-Kyrenia Lineament at the center of the ancestor basin began during the late Eocene and was coupled with extension and subsidence of the sediments along the flanks of the lineament. These combined tectonic processes continued into the Quaternary and partitioned the large ancestor basin into a northern Cilicia-Adana Basin and a southern Mesaoria Basin. The elongate Cilicia-Adana Basin was filled from the northeast by sediments from the Ceyhan, Seyhan, Tarsus and Göksu rivers. These sediments were eroded from parts of the Taurus Mountains and it's surrounding landmass at the southern and southeastern coasts of Turkey.

7.2.2 Size and Morphology of the Cilicia Basin During the Messinian

The present-day Cilicia Basin has significantly evolved since its original

formation during the Oligocene to early Miocene. The present day distribution of evaporites in the Cilicia Basin gives some indication of what the basin looked like in the Messinian.

The Cilicia Basin evolved as a small part of its broader ancestral foreland basin at the base of the Tauride Mountains. Forming as a small part of an extensive basin, the Cilicia Basin probably exhibited southwards tilting of its seafloor that was retained during the latest Miocene and early Messinian (Fig. 7-5). The southward tilting of the seafloor was probably more pronounced in the outer Cilicia Basin where the ancestor basin would have been deepest. The presence of a southward tilt in the outer Cilicia Basin is confirmed by a thicker accumulation of evaporites in the south end of the outer basin than that observed in the north (especially considering that the thickness of evaporites observed in the northern basin has been considerably thickened by the Intra-Salt Fold and Thrust Family). The southward tilt of the seafloor of the basin controlled the northern limit of evaporite deposition in the outer basin. In the inner Cilicia Basin the slope of the southern Turkish continental shelf probably controlled the northern limit of evaporite deposition.

Deformation at the Misis-Kyrenia Lineament had begun as early as the late Cretaceous. According to Robertson (1980), the Kyrenia Range in Cyprus was uplifted, deformed and thrust southwards in the Late Eocene to Early Oligocene then underwent a period of subsidence from the Oligocene to late Miocene. Late Miocene (Tortonian) thrusting established an elevated ridge at the Kyrenia Terrane (the Kyrenia Range) and caused the growth of the Misis-Kyrenia Lineament. These raised features controlled the

southward limit of deposition of Messinian evaporites.

The Cilicia Basin, like its ancestor basin, shallowed to the east at the Adana Basin. The gradual shallowing at the eastern end of the basin produced a gentle slope that controlled the eastward limit of evaporite distribution.

In its western end, the Cilicia Basin remains open to the Antalya Basin. The Anamur Kormakiti High to the north and the Aksu-Kyrenia Lineament to the south restrict this opening. Evaporites in this part of the basin are observed in the gap between these bathymetric highs and likely continue westward into the Antalya Basin.

A map of present-day evaporite distribution in the Cilicia Basin approximates the shape and minimum size of the Messinian Cilicia Basin (Fig. 4-7). The presence of salt welds at the margins of the evaporite unit suggest that the basin may have occupied a much larger area than that outlined on the map.

Fault mapping from seismic sections shows that the basement is most likely normal faulted in the central portion of the outer basin. The offset at these normal faults may have placed further restrictions on the distribution of evaporites in the outer Cilicia Basin.

7.3 Developmental Maturity of Salt Structures in the Cilicia Basin

The development of salt structures in the Cilicia Basin is at a relatively immature stage compared to salt tectonic basins such as the Gulf of Mexico and the North Sea, which display allochthonous layering of evaporites or salt structures in the advanced diapiric stages. This immaturity comes as no surprise since the Mediterranean evaporites

are found in one of the youngest salt basins in the world.

The most developed salt structures in the Cilicia Basin are the salt walls that are located at the boundary between the inner and outer basins. Most of the salt that has migrated throughout the Cilicia Basin has fed into these three large salt walls. The kinematic indicators in the sediments above the salt walls tell of a complex salt tectonic history that involves early reactive diapirism in response to extension in the Cilicia Basin followed by an active diapirism stage where the diapir punches through the sediment cover in an attempt to reach the seafloor. Some parts of the salt walls appear to have reached the seafloor experienced growth by passive diapirism before becoming buried by sediments again.

The thrusted salt anticlines in the outer Cilicia Basin are immature forms of salt structures. These features do not go through reactive, active and passive diapir stages but grow by the tightening and amplification of folds in the contractional domain at the outer Cilicia Basin. The most immature of these contractional salt structures are the salt pillows that form at the leading edge of the fold belts. These salt structures increase in maturity from salt pillows, to low-amplitude salt anticlines, to high-amplitude salt anticlines, to faulted high-amplitude salt anticlines and finally to faulted salt anticlines with pop-up structures. All of these salt structures can be observed in the thrusted fold belts of the outer Cilicia Basin (Basement-Linked Fault Family and Toe-Thrust Fault Family).

The remaining salt structures in the Cilicia Basin, the salt rollers, are less mature than the salt walls, salt pillows and salt anticlines; most of them never get beyond the reactive stage of diapir growth. The salt rollers represent the most immature group of salt

structures that arise from a line source. The salt walls in the boundary domain of the Cilicia Basin evolved from immature salt rollers such as those in the inner basin.

7.4 Tectonic Systems Identified in the Cilicia Basin

Five different fault families and three distinct salt tectonic styles are delineated in the three domains of the Cilicia Basin. These different components form localized tectonic systems that constitute the regional tectonics of the Cilicia Basin. These tectonic systems include a basin forming system, two gravitational gliding systems, and a convergent fold belt system.

7.4.1 Basin-Forming Tectonic System

A series of extensional and transtensional faults were identified in the Cilicia Basin in the north and south coastal regions and in the center of the outer basin. The faults at the north margin of the Cilicia Basin have a different history than those at the south or center of the basin; those in the inner basin are different than those in the outer basin, yet all of the faults of the Basin-Forming Fault Family are an integral part of the tectonic system that is responsible for the formation of the Cilicia Basin.

The Basin-Forming Tectonic System consists of two main extensional/sinistral-transtensional fault zones at the margins of the basin and one or more deeply buried extensional (or transtensional) faults in the central portion of the basin. Extension along these faults allowed the Cilicia Basin to subside and become a part of the Eastern Mediterranean Sea. These faults roughly correlate with the Kozan Fault Zone in southern

Turkey and the Misis-Kyrenia Fault Zone in northern Cyprus; two sinistral transtensional branches of the East Anatolian Fault Zone. The different rates of extension along the various branches of the East Anatolian Fault Zone coupled with different rates of northward advance of the African and Syrian-Arabian plates favoured the formation of the Cilicia Basin ancestor in the Oligocene.

7.4.2 Intra-Salt Gravitational Gliding Tectonic System

The Intra-Salt Fold/Thrust Family, described in section 5.2, is a series of northward-directed thrust faults which are located within the evaporite unit. These thrusts likely formed as a result of post-Messinian growth of the Kyrenia Range in Cyprus. When the growth at the Kyrenia Range disturbed the recently deposited evaporites, they began to glide off the rising slope. Upslope extension was balanced by contraction in the lower parts of the gravitational gliding system. The upslope extensional component of the Intra-Salt Gravitational Gliding Tectonic System was overprinted by early tectonic activity along the older seaward faults of the Basin Forming Fault at the southernmost part of the outer Cilicia Basin. The contractional part of the system is preserved in the north and south parts of the basin but has been overprinted in the region of the Basement-Linked Fault Family. This compression was in the form of low-angle, north directed, salt-detached thrusts of the Intra-Salt Fold/Thrust Family.

The Intra-Salt Gravitational Gliding Tectonic System developed in response to a major change in the tilt of the Cilicia Basin seafloor from a south-dipping tilt in the Early Messinian (during the deposition of the evaporite unit) to a north-dipping tilt in the late

Messinian (before the Miocene-Pliocene erosional event at the M-Reflector).

7.4.3 Convergent Fold and Thrust Belt Tectonic System

A narrow fold and thrust belt occupies the central portion of the outer Cilicia Basin. This fold and thrust belt is formed predominantly of the faults of the Basement-Linked Fault Family and the surrounding folded reflector packages. The thrusts in this fold and thrust belt have a south directed vergence; however, a less frequent and apparently random placement of subdued northward directed thrusts is sometimes observed. The faults of this fold and thrust belt do not detach along a salt décollement but are commonly traced into areas below the evaporite unit and into the pre-Messinian basement. It is likely that these faults extend as deep as the pre-Miocene basement high that is believed to be partially responsible for their formation. Faults toward the north edge of this belt are stronger and more pervasive than those at the southern margin of the belt indicating the influence of a southward-directed compressional tectonic system. Southward compressional forces in the Cilicia Basin propelled sediments into the pre-Miocene basement high causing them to thrust upwards over the basement escarpment. This process may have resembled that in a figure by Cooper et al. (1989) that shows the buttressing effect of the footwall block of a normal fault undergoing inversion. Alternatively, inversion may not be required in the basin; the central basement fault may simply act as a ramp over which the Miocene to Recent sediments are projected during contraction.

7.4.4 Supra-Salt Gravitational Gliding Tectonic System

The style and placement of tectonic elements in the inner Cilicia Basin suggest that the region is controlled by a gravitational gliding tectonic system. Sediments prograding from the northeastern end of the Cilicia-Adana Basin loaded the eastern edge of the evaporite unit and forced the evaporites basinward. Continued delta loading in the inner basin resulted in gravity driven extension of the overburden sediments. A series of extensional faults developed in the inner Cilicia Basin forming a fault fan that extended from the west end of the Adana Basin to a region just northeast of the eastern tip of Cyprus. Salt rollers began to develop in the footwall regions of these extensional faults. Extension and sedimentation continued throughout the Plio-Quaternary as indicated by the presence of growth strata in the hanging walls of the extensional faults of the fault fan. The evaporites, which were being driven basinward by progradational loading, began to well up into salt walls in front of the extensional system. The faults of the Listric Extensional Fault Family terminated against the flanks of these salt walls.

In the outer Cilicia Basin, a broad zone of thrust faults with a northwest-southeast orientation is observed at the seaward flanks of the three salt walls. These faults belong to the Toe-Thrust Fault Family. In plan view, the arcuate trace of these thrust faults follows the trend of the more central of the three salt walls. This tightly folded region of thrust faults balances the extension observed in the inner Cilicia Basin. Prograding sediments at the north edge of the Cilicia Basin rotated the north salt wall into an east-west orientation, offsetting this salt wall from the northwest-southeast alignment observed at the central salt wall.

Gravitational gliding tectonic systems similar to this one from the Cilicia Basin have been created in sandbox model experiments (Cobbold et al., 1989; Cobbold and Szatmari, 1991; Koyi, 1996; Ge et al., 1997; Guglielmo, 1998) and have been observed in seismic studies of the Campos and Santos Basins, offshore Brazil (Demercian et al., 1993) and in the Gulf of Mexico (Diegel et al., 1995).

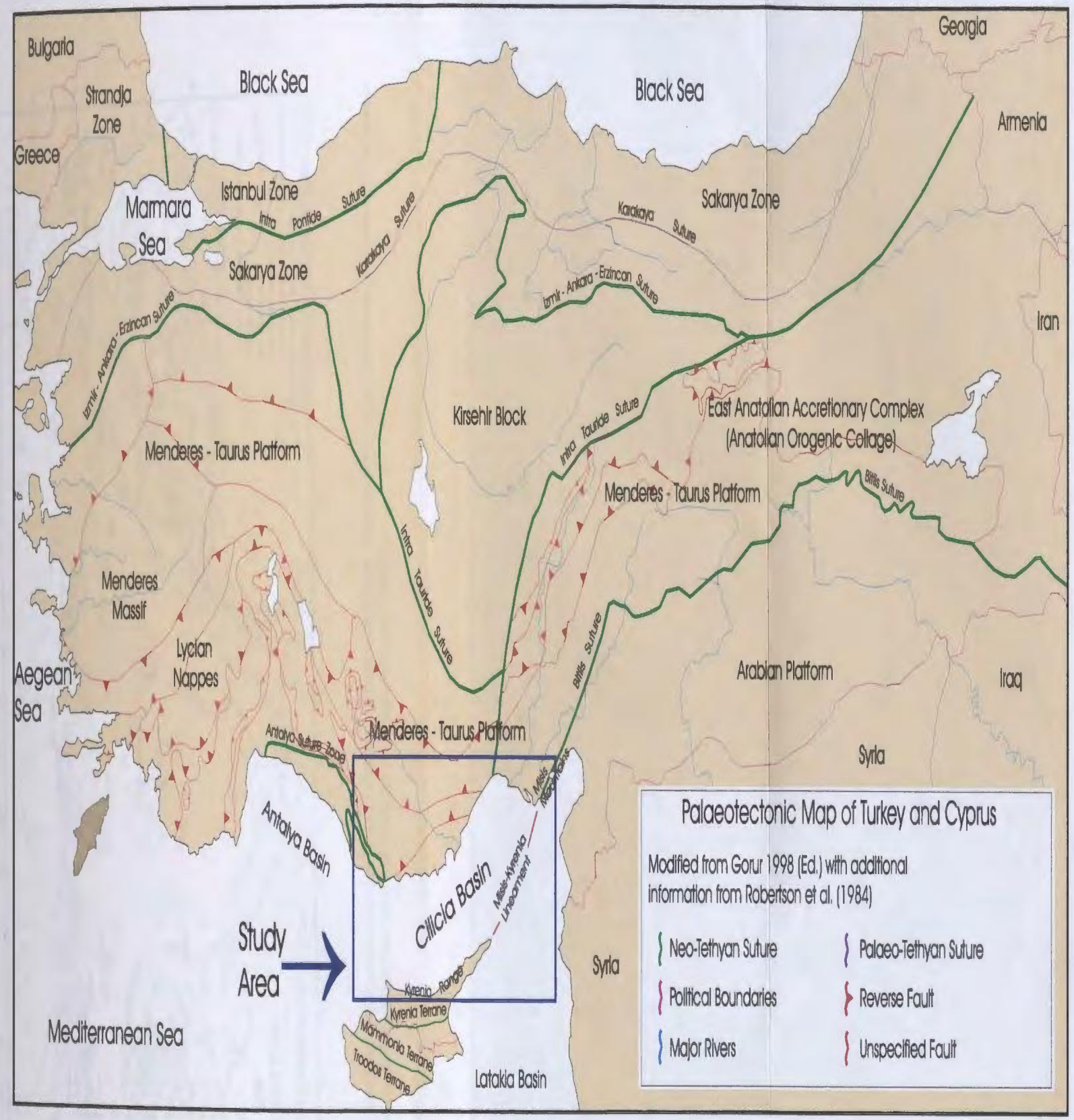

Figure 7-1: Paleotectonic Map of Turkey and Cyprus showing tectonic terranes, suture zones and major thrust structures

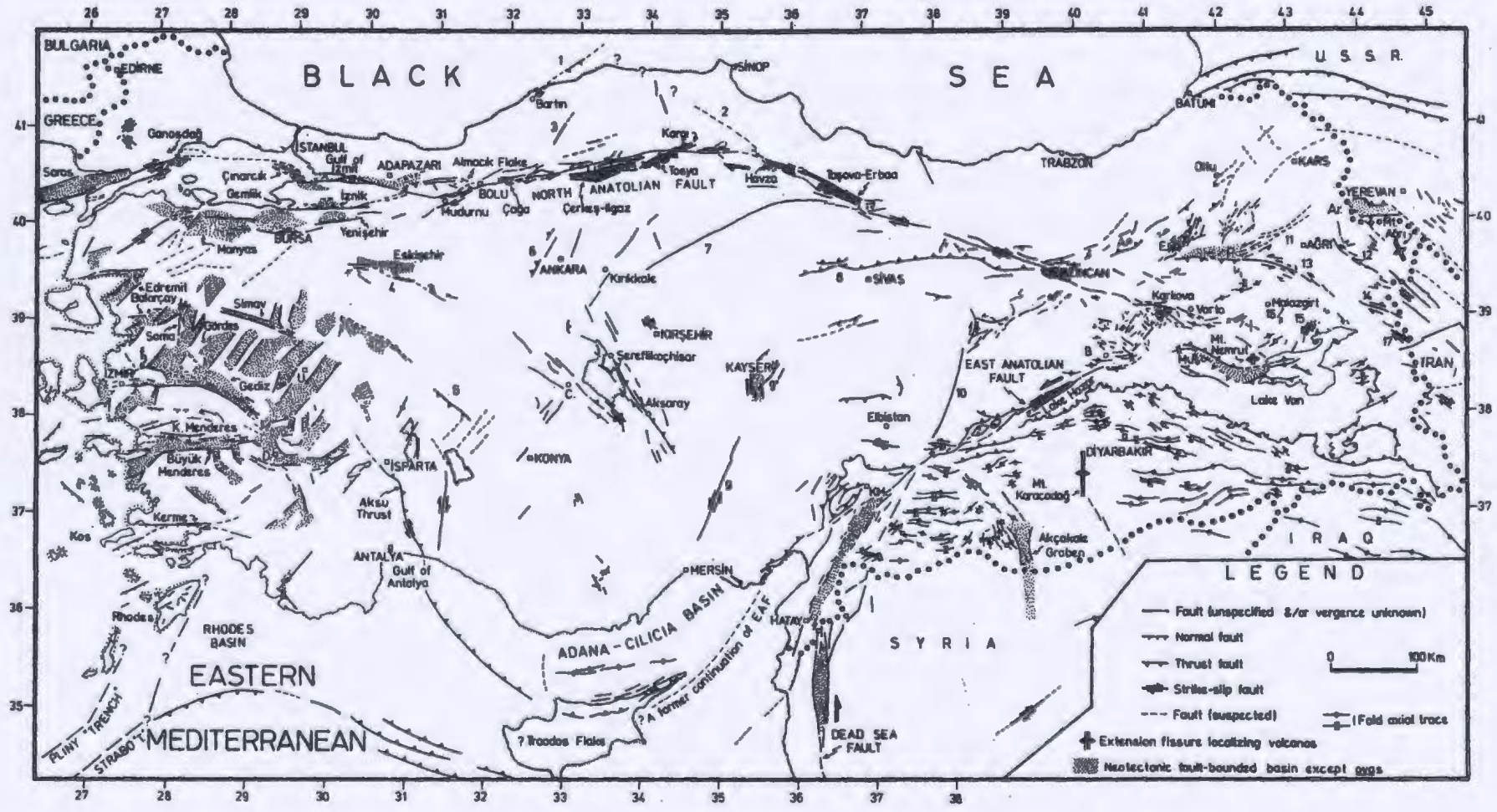

Figure 7-2: A simplified tectonic map for the Eastern Mediterranean shows the main tectonic elements involved in the evolution of the ancestor basin (Sengor et al., 1985).

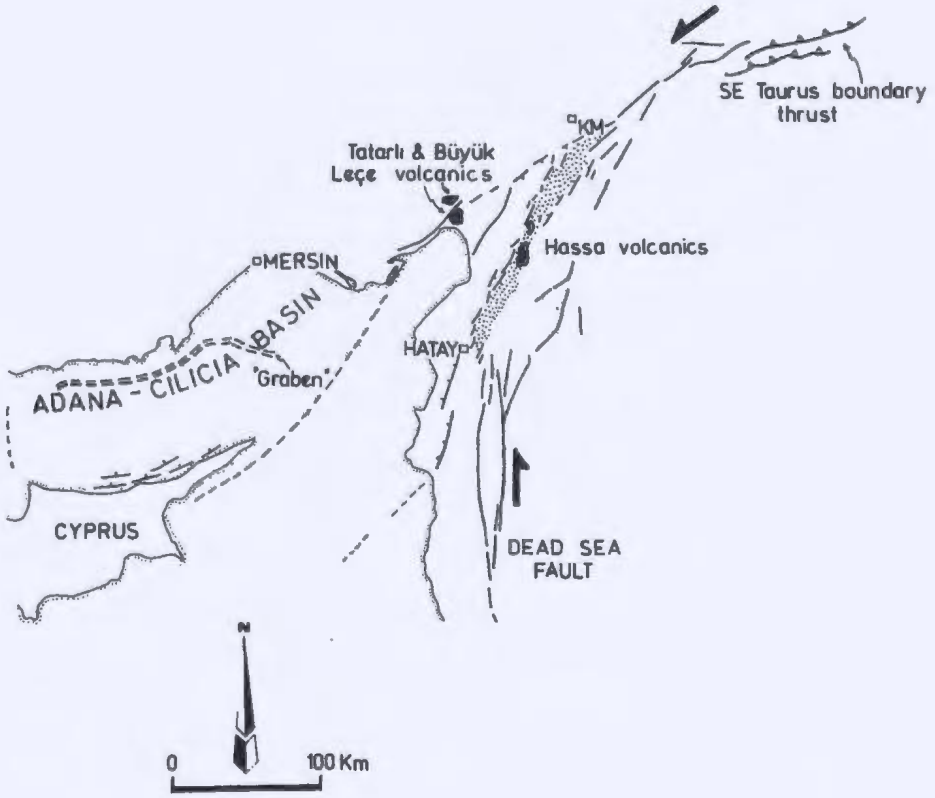

Figure 7-3: A 'quadruple junction' has been identified at the meeting point of three continental blocks and one oceanic plate.. The margins of these features meet in the region of Kahramanmaras along the East Anatolian Fault Zone (a sinistral transtensional fault zone that forms the plate boundary between the Syrian-Arabian and Aegean-Anatolian microplates), the Dead Sea Fault Zone (a major sinistral fault zone forming the plate boundary between the Syrian-Arabian Microplate and the African Plate) and the Southeast Taurus Boundary Thrust Zone (a southward directed collection of thrusts within the northern part of the Arabian Plate) (from Sengor et al., 1985).

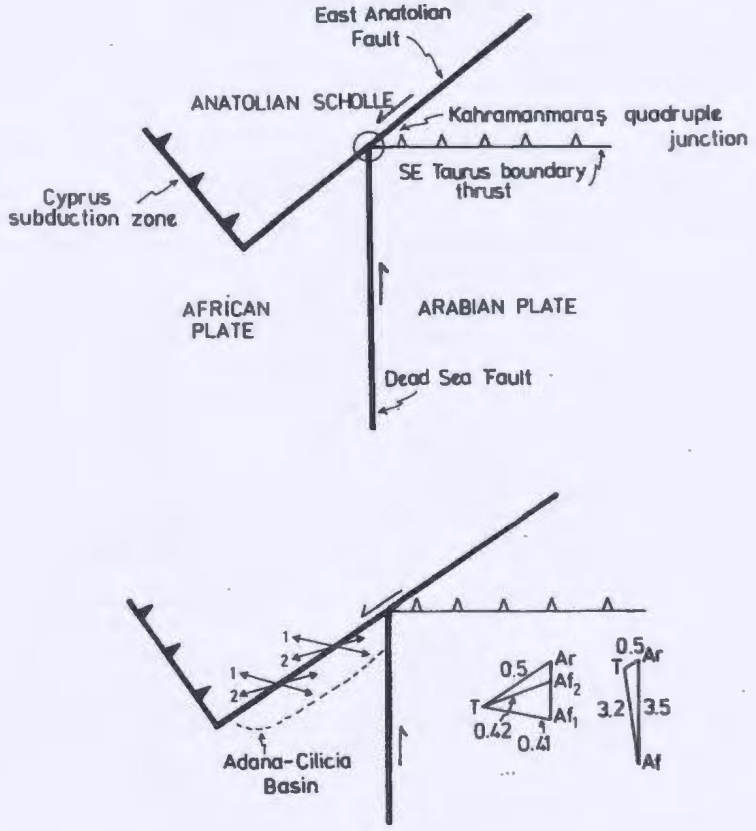

Figure 7-4: Analysis of the major tectonic elements by Sengor et al. (1985) found that the Southeast Taurus Boundary Thrust Zone absorbed a great deal of northward directed movement of the Syrian-Arabian Plate. This movement would not be focused along boundary between the Syrian-Arabian and Anatolian Plates at the East Anatolian Transform Fault but would be spread over the Southeast Taurus Boundary Thrust Zone as well as the East Anatolian Transform Zone. The reduction in northward-directed movement at the northwestern Syrian-Arabian and Anatolian segment of the East Anatolian Transform Zone requires transtensional activity along the southern African and Anatolian segment of the East Anatolian Transform Zone. Sengör et al. calculated two possible extension rates along the southern segment of the East Anatolian Transform Zone (shown in triangle diagrams) based on the amount of north-south movement absorbed by the Southeast Taurus Boundary Thrust Zone. They calculated an extension rate of 0.41cm/year if the Southeast Taurus Boundary Thrust Zone absorbed 3.16 of the 3.5 cm/year African-Arabian motion or 0.42 cm/year if the\ Southeast Taurus Boundary Thrust Zone absorbed 3.4 cm/year of the African-Arabian motion. The orientation of this extension is also dependant on the amount of north-south movement absorbed by the Southeast Taurus Boundary Thrust Zone (Sengor et al., 1985).

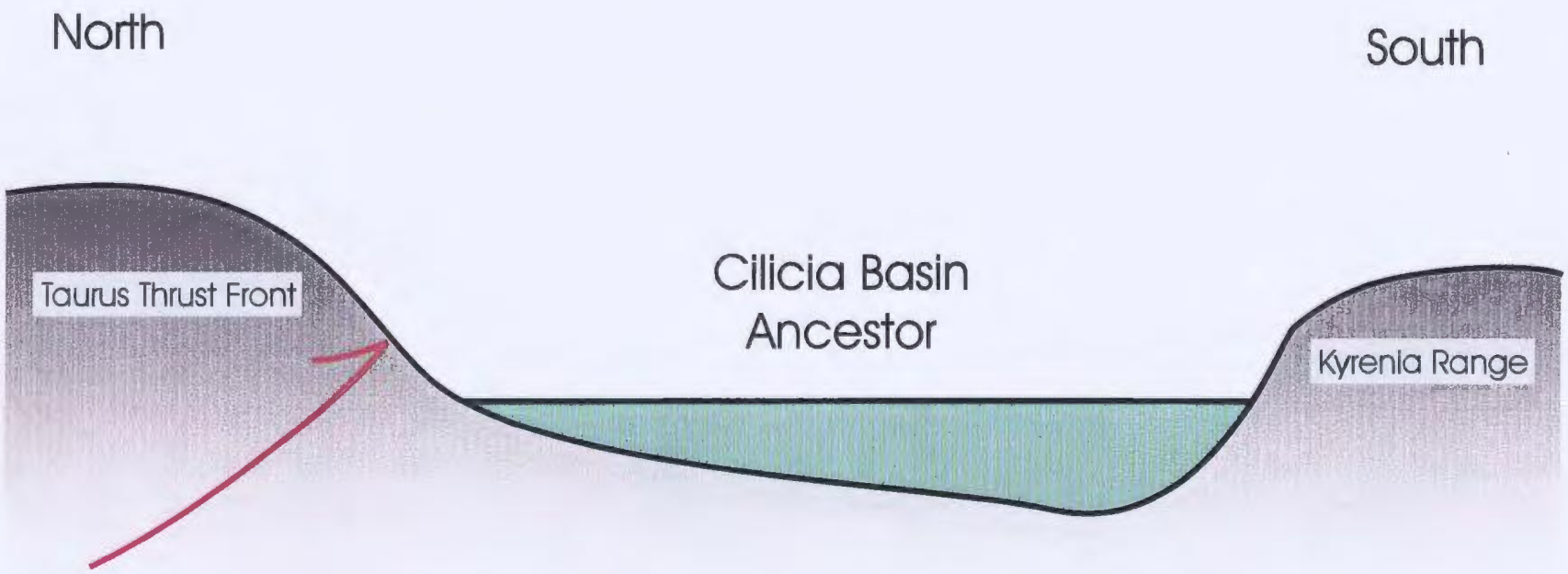

Figure 7-5: The Cilicia Basin Ancestor likely tilted to the south as suggested by a thicker accumulation of evaporites in the southern portion of the present-day outer Cilicia Basin.

8. CONCLUSIONS

Through an in-depth analysis of seismic data in the Cilicia Basin it has been determined that the evaporite distribution in the Cilicia Basin is directly related to the regional tectonics in the Eastern Mediterranean. The structural and salt tectonic activity that have occurred since the development of the basin forms a complex network of tectonic systems in the Cilicia Basin, some of which are extinct or dormant and others which are still active in the basin today. The following is a list of the interpretations and conclusions relating to the development of the Cilicia Basin:

1. The Cilicia Basin evolved from an extensive foreland ancestor basin during the Oligocene to Late Miocene to become a shallow, elongate and arcuate basin that had a southern basin seafloor tilt during the deposition of evaporites in the Messinian (~5.32-7.12 Ma).
2. The Cilicia Basin is a relatively young salt tectonic basin which displays relatively immature salt structures in a tectonically active and complex basin.
3. The southern basin tilt of the Cilicia Basin reversed to a northward basin tilt upon the exhumation of the Kyrenia Terrain of Cyprus (Kyrenia Range) and the Misis-Kyrenia Lineament during the Miocene to Pliocene interval; gravitational instability occurred along the margins of these elevated features as a result of their rapid uplift.
4. Delta progradation in the neighbouring Adana Basin loaded the evaporite unit in the Cilicia Basin producing a gravitational collapse of the evaporite overburden

and a build up of evaporites in the distal portions of the delta succession.

5. North-South contraction in the Cilicia Basin produced a number of contractional features in the region between Cyprus and southern Turkey but seemed to have little effect on the evaporite overburden in the inner Cilicia Basin.

6. The Cilicia Basin can be divided into five fault families within four tectonic systems:

    A) The Basin-Forming Tectonic System - composed of the faults of the Basin-Forming Fault Family; namely the Kozan Fault Zone and the Misis-Kyrenia Fault Zone; partially responsible for the formation of the Cilicia Basin.

    B) Intra-Salt Gravitational Gliding Tectonic System - composed of the faults of the Intra-Salt Fold/Thrust Family; records the change from a south tilted Cilicia Basin to a north tilting Cilicia Basin.

    C) Convergent Fold and Thrust Belt Tectonic System - composed of the faults of the Basement-Linked Fault Family; coincides with the hypothesized presence of a basin central extensional fault (Basin-Forming Fault Family) near the central part of the Cilicia Basin, having a large offset and acting as a buttress to southward moving sediments.

    D) Supra-Salt Gravitational Gliding Tectonic System - composed of the faults of the Listric Extensional Fault Family and the Toe-Thrust Fault Family; records extension related to delta progradation from the northeastern portion of the basin and the counterbalancing contraction

at the toe of the gravitationally controlled tectonic system.

7. The Cilicia Basin can be divided into three thin-skinned salt tectonic domains based on the classification and tectonic expression of salt structures:

   A) The Inner Cilicia Basin Domain - a zone of salt rollers controlled by extensional growth faulting at a listric fault fan.

   B) The Cilicia Basin Boundary Domain - a zone of salt walls at the boundary between the extensional and contractional domains.

   C) The Outer Cilicia Basin Domain - a zone of thrusted and non-thrusted salt anticlines and salt pillows controlled by contractional tectonics.

8. The migration of evaporites in the Cilicia Basin are dynamically linked to the tectonic elements internal to the basin but are also strongly linked to large-scale regional tectonic activity of the Eastern Mediterranean.

REFERENCES

Aksu, A.E., Calon, T.J., Piper, D.J.W., Turgut, S., Izdar, E., 1992a. Architecture of late orogenic Quaternary basins in northeastern Mediterranean Sea. Tectonophysics, v. 210: p.191-213.

Aksu, A.E., Ulug, A., Piper, D.J.W., Konuk, Y.T., Turgut, S., 1992 b. Quaternary Sedimentary History of Adana, Cilicia and Iskenderun Basins: Northeast Mediterranean Sea. Marine Geology, v.104: p.55-71.

Aksu, A.E., Calon, T.J. and Hall, J., in prep. The Cilicia-Adana Basin Complex, Eastern Mediterranean: Neogene Evolution of and Active Fore-Arc Basin in an Obliquely Convergent Margin.

Aleria, 1979. The Messinian of the Corsican channel and the North Tyrrhenian basins. Comptes Rendus Hebdomadaires des Seances de l'Academie des Sciences, Serie D: Sciences Naturelles. V.288, no.20: p.1521-1524.

Bagnall, P.S., 1960. The geology and mineral resources of the Pano Lefkara-Larnaca area. Cyprus, Geological Survey Dept., Memoir 5. 116p.

Balk, R., 1947. Project 9: Salt Flowage, mapping the flow structure in the interior of salt mines, Texas and Louisiana. AAPG Research Comm. 1946-47, Reports on Projects, v.1-12: p.140-148.

Balk, R., 1936. Structural Elements of Domes. AAPG Bulletin, v.33, no.11: p. 51-67.

Balk, R., 1949. Structure of Grand Saline salt dome, Van Zandt County, Texas. AAPG Bulletin, v. 33, no.11: p.1791-1829.

Bally, A.W. (Ed.) 1987. Atlas of seismic stratigraphy. AAPG Studies in Geology. v.27; no.1.

Barber, P. M., 1981. Messinian subaerial erosion of the proto-Nile Delta. Marine Geology. v.44; no.3-4: p. 253-272.

Barton, D.C., 1933. Mechanics of formation of salt domes with special reference to Gulf Coast salt domes of Texas and Louisiana. AAPG Bulletin, v.17: p.1025-1083.

Ben-Avraham, Z., Tibor, G., Limonov, A.F., Leybov, M.K., Tokarev, M.Yu., Woodside, J.M., 1995. Structure and Tectonics of the Eastern Cyprean Arc. Marine and Petroleum Geology, v.12, no.3: p. 263-271.

Biju-Duval , B., Letouzey, J., and Montadert, L., 1978. Structure and Evolution of the Mediterranean Sea Basins. *In:* Hsu, K.J., Montadert, L. et al., Initial Reports of the Deep Sea Drilling Project, Volume 42: Washington, U.S. Government Printing Office, p. 951-984.

Biju-Duval , B., Letouzey, J., and Montadert, L., 1979. Variety of margins and deep basins in the Mediterranean. *In:* Watkins, J.S., Montadert L., Dickerson P.W. (Eds.). Geological and geophysical investigations of continental margins. American Association of Petroleum Geologists Memoir 29, p.293-317.

Bishop, 1978. Mechanism for emplacement of piercement diapirs. AAPG Bulletin. v.62, no.9: p.1561-1583.

Calon, T.J., Hall, J. and Aksu, A.E., in prep. Salt tectonics in Two Convergent Margin Basins of the Cyprean Arc, Eastern Mediterranean.

Chapple, W.M., 1978. Mechanics of thin-skinned fold-and-thrust belts. Geological Society of America Bulletin, v.89: p.1189-1198.

Chumakov, 1973. Geological history of the Mediterranean at the end of the Miocene--the beginning of the Pliocene according to new data. *In:* Initial reports of the Deep Sea Drilling Project, Leg 13 (2): p.1241-1242.Clauzon, G., 1978. The Messinian Var Canyon (Provence, southern France); paleogeographic implications. *In:* Cita, M., Ryan, W.(Eds.) Messinian erosional surfaces in the Mediterranean. Marine Geology. v.27; no.3-4, p. 231-246.

Clauzon, G., Suc, J.P., Gautier, F., Loutre, M.F., 1996. Alternate interpretation of the Messinian salinity crisis; controversy resolved? Geology, v.24: p.363-366.

Clauzon, G., 1982. The Messinian Canyon of the Rhone; a decisive proof of a "desiccated deep-basin model" (Hsu, Cita and Ryan, 1973). *In:* Oceans paleo-oceans; special session of the Geological Society of France. : Bulletin de la Societe Geologique de France. v.24; no.3, p.597-610.

Cobbold, P., Rossello, E., Vendeville, B., 1989. Some experiments on interacting sedimentation and deformation above salt horizons. Bull. Soc. Geol. France, v.8, no. 3: p.453-460.

Cobbold and Szatmari, 1991. Radial gravitational gliding on passive margins. Tectonophysics. v.188; no.3-4: p.249-289.

Cooper M.A., Williams G. D., de Graciansky P.C., Murphy R.W., Needham T., De Paor Declan G., Stoneley R., Todd S.P., Turner J.P., Ziegler P.A. Inversion tectonics; a discussion. *In:* Cooper M.A., Williams G.D. (Eds.) Inversion tectonics meeting - Geological Society Special Publications. No.44; p.335-347.

Davis, D., and Engelder, T., 1985. The role of salt in fold-and-thrust belts. Tectonophysics, v.119: p.67-88.

Davis, D.M., Suppe, J., and Dahlen, F.A., 1983. Mechanics of fold-and-thrust belts and accretionary wedges. Journal of Geophysical Research, v.88: p.1153-1172.

Delaune-Mayer, M., Marcoux, J., Parrot, J.F. and Poisson, A., 1977. Modele d'evolution mesozoique de la paleo-marge tethysienne au niveau des nappes radiolaritiques et ophiolitiques du Taurus Lycien, d'Antalya et du Baer-Bassit. *In:* Technip (Ed.), International Symposium on the structural history of the Mediterranean basins, p.79-94.

Delrieu, B., Rouchy J.M., Foucault A., 1993. The uppermost Messinian erosional surface in central Crete (Greece) and around the Mediterranean; relationship to the Mediterranean salinity crisis. Comptes Rendus de l'Academie des Sciences, Series 2, v.316, no.4: p.527-533.

Demercian, S., Szatmari, P., Cobbold, P.R., 1993. Style and pattern of salt diapirs due to thin-skinned gravitational gliding, Campos and Santos basins, offshore Brazil. *In:* Cobbold, P.R. (Ed.), New insights into salt tectonics; collection of invited papers reflecting the recent developments in the field of salt tectonics. Tectonophysics v.228; no.3-4, p.393-433.

Dewey, J.F., Hempton, M.R., Kidd, W.S.F., Saroglu, F. and Segnor, A.M.C., 1986. Shortening of Continental Lithosphere: The Neotectonics of Eastern Anatolia - A Young Collision Zone. *In:* Coward, M.P. and Reis, A.C.(eds), Collision Tectonics. Geological Society of London Special Publication, v.19: p.3-36.

Dewey, J.F., Kidd, W., Sengor, A., Saroglu, F., 1980. Neotectonics of eastern Anatolia. Eos, Transactions, American Geophysical Union. v.61; no.46, p.1107-1108.

Diegel, F.A., Karlo, J.F., Schuster, D.C., Shoup, R.C., Tauvers, P.R., 1995. Cenozoic structural evolution and tectono-stratigraphic framework of the northern Gulf Coast continental margin. *In:* Jackson, M.P.A., Roberts, D.G., Snelson, S. Salt tectonics; a global perspective. AAPG Memoir 65; p.109-151.

Duval, B.C., Cramez, C., Jackson, M.P.A., 1992. Raft tectonics in the Kwanza Basin, Angola. Marine and Petroleum Geology, v.9: p.389-404.

EIE, Elektrik Isleri Etud Idaresi Genel Direktorlugu, 1982. Sediment Data and Sediment Transport Amount For Surface Water in Turkey. Publ. 82-22, 283 pp.

Evans, G., Morgan, P., Evans, W.E., Evans, T.R., Woodside J.M., 1978. Faulting and Halokinetics in the Northeastern Mediterranean between Cyprus and Turkey. Geology, v.6: p.392-396.

Fails, T.G., 1990. Variation in salt dome faulting, Coastal Salt Basin. Transactions - Gulf Coast Association of Geological Societies, v.40: p.181-193.

Fischer, M., Woodward, N., and Mitchell, M., 1992. The kinematics of break-thrust folds. Journal of Structural Geology, v.14: p.451-460.

Fontes, J.C., Letolle, R., Nesteroff, W.D., 1972. Deep Sea Drilling Program Traverses in the Mediterranean Sea (Leg 13); reconnaissance of isotopes. *In:* Stanley, D.J. (Ed.), The Mediterranean Sea ; A Natural Sedimentation Laboratory. Symposium on Sedimentation in the Mediterranean Sea. p. 671-680.

Garrison, R.E., Schreiber, B.C., Bernouilli, D., Fabricius, F.H., Kidd, R.B. and Meliere, F., 1978. Sedimentary petrology and structures of Messinian evaporitic sediments in the Mediterranean Sea, Leg 42A, Deep Sea Drilling Project. *In:* Hsu, K., Montadert, L. et al. (Eds.), Initial Reports of the Deep Sea Drilling Project, v.42(1): p.571-611, U.S. Government Printing Office, Washington.

Garrison, R.E., Schreiber, C., Bernouilli, D., Fabricius, F.H., Kidd, R.B., Melieres, F., 1978. Sedimentary Petrology and Structures of Messinian Evaporitic Sediments in the Mediterranean Sea, Leg 42A, Mediterranean Sea. *In:* Hsu, K., Montadert, L, et al., 1978. Initial reports of the Deep Sea Drilling Project, v.42(1): p.571-611, U.S. Government Printing Office, Washington.

Ge, H., Jackson, M.P.A., and Vendeville, M.P.A., 1997. Kinematics and dynamics of salt tectonics driven by progradation. AAPG Bulletin, v.81: p.398-423.

Gorur, N., Oktay, F.Y., Seymen, I., Sengor, A.M.C., 1984. Paleotectonic evolution of the Tuzgolu basin complex, Central Turkey: sedimentary record of a Neo-Tethyan closure. *In:* Dixon, J.E. and Robertson, A.H.F. (Eds.), The Geological Evolution of the Eastern Mediterranean, Geological Society of London, Special Publication 17, p. 467-482.

Gorur, N., 1988. Timing of the opening of the Black Sea basin. Tectonophysics, v.14: p.247-262.

Gorur, N., Sengor, A.M.C., Akkok, R., Yilmaz, Y., 1983. Pontidlerde Neo-Tetis'in kuzey kolunun acilmasina iliskin sedimentolojik veriler (Sedimentologic evidence for the opening of the northern branch of the Neo-Tethys in the Pontides). Turkiye Jeoloji Kurumu Buelteni (Bulletin of the Geological Society of Turkey), v.26: p.11-20.

Gorur, N. and Okay, A.I., 1996. A fore-arc origin for the Thrace Basin, Northwest Turkey. Geol. Rundsch, v.85: p.662-668.

Gorur, N., Tuysuz, O., Sengor, A.M.C., 1998. Tectonic evolution of the central Anatolian basins. International Geology Review. v.40; no.9, p.831-850.

Guglielmo, G., Jackson, M.P.A., Vendeville, B., 1998. Three-dimensional visualization of salt walls and associated fault systems. AAPG Bulletin v.81; no.1, p.46-61.

Harrison, J.C., and Bally A.W., 1988. Cross-sections of the Parry Islands fold belt on Melville Island, Canadian Arctic Islands; implications for the timing and kinematic history of some thin-skinned decollement systems. Bulletin of Canadian Petroleum Geology v.36, no.3, p. 311-332.

Hsu, K.J., Ryan, W.B.F., Cita, M.B., 1973. Late Miocene Desiccation of the Mediterranean. Nature, v.242: p.240-244.

Hsu, K., Montadert, L. et al., 1978. Initial Reports of the Deep Sea Drilling Project, v.42(1): p.571-611, U.S. Government Printing Office, Washington.

Hsu, K., 1978. The Messinian Salinity Crisis: Evidence of Late Miocene Eustatic Changes in the World Ocean. Naturwissenschaften, v.65: p.151.

Jackson, M.P.A. and Cramez, Carlos, 1989. Seismic recognition of salt welds in salt tectonic regimes (extended abstract). Houston, Gulf Coast Section of the Society of Economic Paleontologists and Mineralogists Foundation, Tenth Annual Research Conference Program and Extended Abstracts, p.66-71.

Jackson, M.P.A. and Talbot, C.J., 1991. A Glossary of Salt Tectonics. The University of Texas at Austin, Bureau of Economic Geology Circular No. 91-4, 44p.

Jackson, M.P.A., and Vendeville, B.C., 1994. Regional extension as a geologic trigger for diapirism. Geological Society of America Bulletin, v.106: p.57-73.

Jackson, M.P.A., Vendeville, B.C., and Schultz-Ela, D.D., 1994. Structural dynamics of salt systems. Annual Reviews of Earth and Planetary Science, v.22: p.93-117.

Jaume, S.C., and Lillie, R.J., 1988. Mechanics of the Salt Range - Potwar Plateau, Pakistan: a fold-and-thrust belt underlain by evaporites. Tectonics, v.7: p.57-71.

Jenyon, M.K., 1986. Salt tectonics. Elsevier Science: New York. 191 p.

Kelling, G., Gokcen, S.L., Floyd, P.A. and Gokcen, N., 1987. Neogene tectonics and plate convergence in the eastern Mediterranean: new data from southern Turkey. Geology, v.15: p.425-429.

Kempler, D. and Garfunkel, Z., 1991. The Northeast Mediterranean Triple Junction From A Plate Kinematic Point of View. Bulletin of the Technical University of Istanbul, v.34, no. 3-4: p.425-454.

Kolarsky, R.A., 1997. Interaction between salt diapir growth and sedimentation; an example from Cote Blanche Island Field, Louisiana. AAPG Gulf Coast Association of Geological Societies Section Meeting; Abstracts. AAPG Bulletin, v.81 no.9: p.1589.

Koyi, H., 1996. Salt flow by aggrading and prograding overburdens. *In:* Alsop, G.I., Blundell, D.J. and Davidson, I. (eds.), Salt Tectonics, Geological Society Special Publication No. 100, p. 243-258.

Letouzey, J., Colletta, B., Vially, R., Chermette, J.C., 1995. Evolution of salt-related structures in compressional settings. *In:* Jackson, M.P.A., Roberts, D.G., and Snelson, S. (Eds.), Salt Tectonics: A Global Prespective. AAPG Memoir 65, p.41-60.

Mauduit, T., Brun, J.P., 1998. Growth fault/ rollover systems; birth, growth, and decay. Journal of Geophysical Research, B, Solid Earth and Planets v.103; no.8, p.18,119-18,136.

McClay, K.R. and Ellis, P.G. 1987. Geometries of extension fault systems developed in model experiments. Geology v.15; no.4, p.341-344.

McClay, K.R., Dooley, T., Lewis, G., 1998. Analog modeling of progradational delta systems. Geology v.26, no.9, p.771-774.

Mitchum, R.M. Jr., Vail, P.R., Thompson, S. III., 1977. Seismic Stratigraphy and Global Changes of Sea Level, Part 2: The Depositional Sequence as a Basic Unit for Stratigraphic Analysis. Seismic Stratigraphy - Applications to Hydrocarbon Exploration: AAPG Memoir 26: p.53-62.

Mulder C.J., Lehner, P., Allen, D.C.K., 1975. Structural evolution of the Neogene salt basins in the eastern Mediterranean and the Red Sea. Geologie en Mijnbouw. V.54, no.3-4, p.208-221.

Mulder, C.J., 1973. Tectonic framework and distribution of Miocene evaporites in the Mediterranean. *In:* Drooger, C.W. (Ed.), Messinian events in the Mediterranean. p.44-59

Myers, K.J. and Milton, N.J., 1996. Concepts and Principles of Sequence Stratigraphy. *In:* Sequence Stratigraphy. Editors: Emery, D. and Myers, K.J. p. 11-41.

Nalpas, T., and Brun, J. -P., 1993. Salt flow and diapirism related to extension at crustal scale. Tectonophysics, v.228: p.349-362.

Nesteroff, W.D., 1973. A model for the Messinian evaporites of the Mediterranean; very deep basins with lagoonal evaporite deposits. *In:* Drooger, C.W. (Ed.) Messinian events in the Mediterranean. p.68-81.

Okay, A.I. and Tansell, I., 1994. Pontid-ici okyanusunun ust yasi hakkinda Sarkoy kuzeyinden (Trakya) yeni bir bulgu (New data on the uper age of the Intra-Pontide ocean from north of Sarkoy in Thrace) . Bulletin of Mineral Resources Exploration, v.114: p.23-26.

Okay, A.I., 1989. Tectonic units and structures in the Pontides, Northern Turkey. *In:* Sengor, A.M.C. (Ed.), Tectonic Evolution of Tethyan Region. Nato ASI Series, Kluwer Academic Publishers, 109-116.

Okay, A.I., Sengor, A.M.C. and Gorur, N., 1994. Kinematic history of the opening of the Black Sea and its effect on the surrounding regions. Geology, v.22: p.267-270.

Orszag-Sperber, F., Rouchy, J.M., Elion, P., 1989. The sedimentary expression of regional tectonic events during the Miocene-Pliocene transition in the southern Cyprus basins. Geological Magazine. v.126; no.3, p.291-299.

Ozgul, N., Tursucu, A., Ozyardimici, N., Senol, M., Bingol, I., Uysal, S., 1981. Munzur Daglari'nin jeolojisi. M.T.A Report, No. 6995, 136p.

Perinçek, D., and Çemen, I., 1990. The structural relationship between the East Anatolian and Dead Sea fault zones in southeastern Turkey. Tectonophysics. v.172; no.3-4, p.331-340.

Pişkin, O. and Delaloye, M., 1983. Consequenses geolotectoniques de l'etudie des roches vertes a l'est de Marmaris (SW Anatolie). Schweizeriche Mineralogische Petrographische Mittalungen, 63: 129-148.

Remmelts, G., 1995. Fault-related salt tectonics in the southern North Sea, the Netherlands. *In:* Jackson, M.P.A., Roberts, D.G., Snelson, S. (Eds.), Salt Tectonics: A Global Perspective, AAPG Memoir 65, p. 261-272.

Robertson, A.H.F. and Woodcock, N.H., 1986. The role of the Kyrenia Range Lineament, Cyprus, in the geological evolution of the eastern Mediterranean area. *In*: Reading, H.G., Watterson, J., White, S.H. (Eds.). Major crustal lineaments and their influence on the geological history of the continental lithosphere. Philosophical Transactions of the Royal Society of London, Series A: Mathematical and Physical Sciences. V.317; no.1539, p.141-177.

Robertson, A.H.F., Emeis, K.-C, Richter, C. and Camerlenghi, A. (Eds.), 1998. Proceedings of the Ocean Drilling Program, Scientific Results, v.160.

Robertson, A.H.F., 1998. Tectonic Significance of the Eratosthenes Seamount: A Continental Fragment in the Process of Collision with a Subduction Zone in the Eastern Mediterranean. Tectonophysics, v.298: p.63-82.

Robertson, A.H.F., 1990. Tectonic Evolution of Cyprus. *In*: Malpas, J., Moores, E.M., Panayiotou, A., and Xenophontos, C. (Eds.), Ophiolites: Oceanic Crustal Analogues. Proceedings of the symposium "Troodos 1987", Nicosa, Cyprus, p.235-250.

Rőgl, F., Steininger, F., Muller, C., 1978. Middle Miocene salinity crisis and paleogeography of the Paratethys (middle and eastern Europe). In: Hsu, K., et al. Initial Reports of the Deep Sea Drilling Project. Leg 42, Part 1; p.985-990.

Rouchy, J.M., Orszag-Sperber, F., Bizon, G., Bizon, J.J., 1980. Evidence of a late Messinian emersion phase in the Pissouri Basin (Cyprus); one aspect of the Miocene-Pliocene boundary in the eastern Mediterranean. Comptes Rendus Hebdomadaires des Seances de l'Academie des Sciences, Serie D: Sciences Naturelles. v.291; no.9, p.729-732.

Rouchy, J.M., and Saint-Martin, J.P., 1992. Late Miocene events in the Mediterranean as recorded by carbonate-evaporite relations. Geology v.20; no.7, p.629-632.

Rowan, M., 1999. Practical Salt Tectonics. Notes distributed at AAPG Short Course: Houston, Texas.Ryan W.B.F., 1969. The floor of the Mediterranean. Part I: Structure and Evolution and Part II: The stratigraphy of the eastern Mediterranean: Ph.D. thesis, Columbia University, New York.

Ryan, W.B.F, Hsu, K.J. et al., 1973. Initial Reports of the Deep Sea Drilling Project, Volume 13: Washington, U.S. Government Printing Office.

Schmalz, R.F., 1969. Deep-water evaporite deposition: a genetic model. AAPG Bulletin, v.53: p.798-823.

Selley, R.C., 1998. Diapiric Traps. Elements of Petroleum Geology. Toronto : Academic Press.

Sengor, A.M.C., 1979. The North Anatolian Transform Fault: Its Age, Offset and Tectonic Significance. Journal of the Geological Society of London, v.136: p.269-282.

Sengor, A.M.C. and Yilmaz, Y., 1981. Tethyan evolution of Turkey: A plate tectonic approach. Tectonophysics, v.75: p.181-241.

Sengor, A.M.C., Yilmas, Y.; Sungurlu, O., 1984. Tectonics of the Mediterranean Cimmerides; nature and evolution of the western termination of Palaeo-Tethys. *In:* Dixon J.E.; Robertson A.H.F. (Eds.) The geological evolution of the eastern Mediterranean. Geological Society Special Publications. v.17; p.77-112.

Sengor, A.M.C., Gorur, N., and Saroglu, F., 1985. Strike-slip faulting and related basin formation in zones of tectonic escape :Turkey as a case study. *In:* Biddle, K.D. and Christie-Blick, N. (Eds.), Strike-Slip Deformation , Basin Formation and Sedimentation, Society of Economic Paleontologists and Mineralogists, Special Publication 7, p.227-264.

Smith, S.G., 1977. Diapiric structures in the eastern Mediterranean Cilicia Basin. Geology. v.5; no.11, p.705-707.

Trusheim, F., 1960. Mechanism of salt migration in northern Germany. AAPG Bulletin, v.44: p.1519-1540.

Vendeville, B.C., and Jackson, M.P.A., 1992c. The rise and fall of diapirs during thin-skinned extension. Bureaul of Economic Geology (UT Austin) Report of investigations No. 209, 60p.

Vendeville, B.C., and Jackson, M.P.A., 1992b. The fall of diapirs during thin-skinned extension. Marine and Petroleum Geology, v.9: p.354-371.

Vendeville, B.C., and Jackson, M.P.A., 1992a. The rise of diapirs during thin-skinned extension. Marine and Petroleum Geology, v.9: p.331-353.

Woodside, J.M., 1976. Regional vertical tectonics in the eastern Mediterranean. The Geophysical Journal of the Royal Astronomical Society. v.47; no.3, p.493-514.

Woodside, 1977. Tectonic elements and crust of the eastern Mediterranean Sea. Marine Geophysical Researches. v.3; no.3, p.317-354.

Yalcin, M.N., and Gorur, N., 1984. Sedimentological evolution of the Adana Basin. *In:* Tekeli, O. and Goncuoglu, M.C. (Eds.) Geology of the Taurus Belt, International Symposium Proceedings, Maden Tetkik ve Arama Enstitusu, Ankara, p.165-172.

Yilmaz, Y., Yigitbas, E. and Genc, S.C., 1993b. Different ophiolitic and metamorphic assemblages of southeast Anatolia and their significance in the geologic evolution of the orogenic belt. Tectonics, v.12: p.1280-1297.

Yilmaz, Y., 1985. Geology of the Cilo Ophiolite: An ancient island arc fragment on the Arabian Platform, Southeast Turkey. *In:* Desmons, J. (ed) Ophiolites Through Time, Conference Proceedings.Ofioliti, v.10: p.457-483.

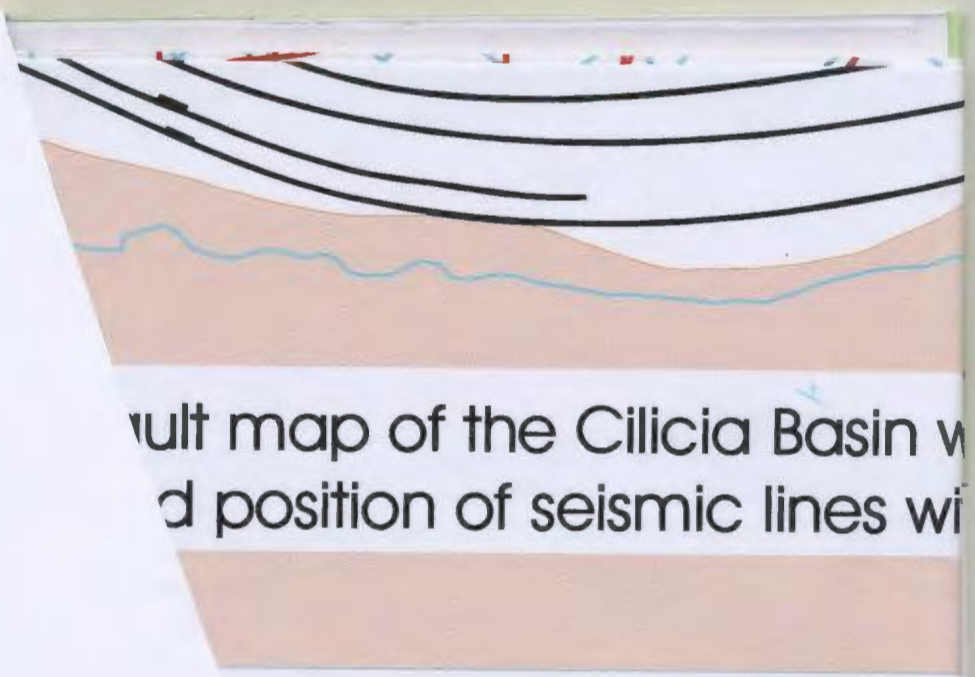

ult map of the Cilicia Basin w
d position of seismic lines wi